

837

Two and three dimensional flows in the non-Newtonian fluids



By

Muhammad Qasim

Department of Mathematics
Quaid-I-Azam University
Islamabad, Pakistan
2011

Two and three dimensional flows in the non-Newtonian fluids



By

Muhammad Qasim

Supervised By

Prof. Dr. Tasawar Hayat

Department of Mathematics
Quaid-I-Azam University
Islamabad, Pakistan
2011

Two and three dimensional flows in the non-Newtonian fluids



By

Muhammad Qasim

A THESIS SUBMITTED IN THE PARTIAL FULFILLMENT OF THE REQUIREMENTS FOR THE
DEGREE OF
DOCTOR OF PHILOSOPHY
IN
MATHEMATICS

Supervised By

Prof. Dr. Tasawar Hayat

Department of Mathematics
Quaid-I-Azam University
Islamabad, Pakistan
2011

CERTIFICATE

Two and three dimensional flows in the non-Newtonian fluids

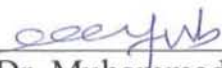
By

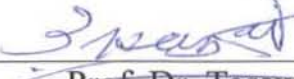
Muhammad Qasim

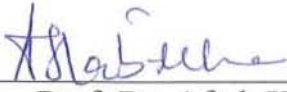



A THESIS SUBMITTED IN THE PARTIAL FULFILMENT OF THE
REQUIREMENTS FOR THE DEGREE OF THE DOCTOR OF PHILOSOPHY

We accept this dissertation as conforming to the required standard

1. 
Prof. Dr. Muhammad Ayub
(Chairman)

2.  19/4/11
Prof. Dr. Tasawar Hayat
(Supervisor)

3. 
Prof. Dr. Aftab Khan
(External Examiner)

4. 
Prof. Dr. Akhtar Hussain
(External Examiner)

**Department of Mathematics
Quaid-i-Azam University
Islamabad, Pakistan
2011**

CERTIFICATE

Two and three dimensional flows in the non-Newtonian fluids

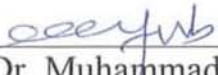
By

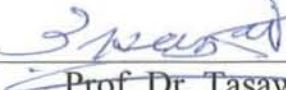
Muhammad Qasim

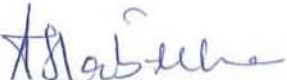



A THESIS SUBMITTED IN THE PARTIAL FULFILMENT OF THE
REQUIREMENTS FOR THE DEGREE OF THE DOCTOR OF PHILOSOPHY

We accept this dissertation as conforming to the required standard

1. 
Prof. Dr. Muhammad Ayub
(Chairman)

2.  19/4/11
Prof. Dr. Tasawar Hayat
(Supervisor)

3. 
Prof. Dr. Aftab Khan
(External Examiner)

4. 
Prof. Dr. Akhtar Hussain
(External Examiner)

**Department of Mathematics
Quaid-i-Azam University
Islamabad, Pakistan
2011**

Dedicated to

My Parents

and

Prof. Dr. Tasawar Hayat

Acknowledgements

I bow my head with deep gratitude to Almighty ALLAH Who bestowed upon me the courage and steadfastness to accomplish my Ph. D studies. He is the most powerful, compassionate, kind and merciful. All respects and affection to the Holy Prophet MUHAMMAD (Peace be upon Him) who is mercy for the mankind and enabled us to recognize us our creators.

I express my deepest gratitude to my supervisor **Prof. Dr. Tasawar Hayat**, whose guidance, devotion and keen interest enabled me to complete this task. It is a matter of pride and privilege for me to be his Ph. D student. His sober, graceful and elegant personality will always remain a source of inspiration for me. He is in fact chief architect of all my achievements. What I think, these few words do not do justice to his contribution. May Allah bless him with his best.

I am also thankful to my respected teachers Prof. Dr. Muhammad Ayub, Dr. Qari Naseer Ahmad, Dr. Muhammad Zakaullah, Dr. Sohail Nadeem, Dr. Masood Khan, Dr. Rahmat Ellahi and Dr. Malik Yousuf whose teaching have brought me to this stage.

I would like to extend my gratitude to all members of the Fluid Mechanics Group (FMG). I always feel honor to be the part of the group. I would like to thank my friends and colleagues especially M. Nawaz, Zahid Iqbal, Sabir Ali, Fahad Abbasi, Majid Hussain, Zafar Ali, Muhammad Afzal, Rizwan-ul-Haq, Raja Rashid, Salman Saleem, Hafiz Obaid, Muhammad Faheem, Rai Sajjad, Tayyab Hussain, Malik Tariq Hussain, Rabnawaz and Syed Aziz Rasool. Their helping attitude in my academic and social life encouraged me in difficult times.

Words are vane in expressing my veneration for my sweet mother and caring father, who scarified their desires over mine, prayed for my edification, endeavored for my betterment, and faced all the vexations moments that come with courage and cheerfully took the burden of my prodigious studies. I would also like to express my sincerest thanks to my sisters, brothers and brother in law, who constantly provide emotional support and took care of me in many aspects.

Last but not the least; I am thankful to someone who is very special for me.

Muhammad Qasim

Preface

The non-Newtonian fluids find increasing practical applications in the recent years. It is due to the fact that many of the fluids used in industry and engineering are significantly non-Newtonian. The flows of such fluids have special relevance in oil and gas well drilling to well completion operations from industrial processes involving waste fluids, synthetic fibers, foodstuffs to extrusion of molten plastic and polymer solutions. The expression between shear stress and shear rate in the non-Newtonian fluids is non-linear. A distinct feature of non-Newtonian fluids from Newtonian fluid is that these cannot be described by a single constitutive equation. Mathematical systems in the non-Newtonian fluids are of higher order and in general more complicated in comparison to the Newtonian fluids. These systems need additional initial/boundary conditions for a unique solution.

The boundary layer flows of non-Newtonian fluids over a stretching sheet is important in a variety of contexts including extrusion process, glass fiber and paper production, hot rolling, wire drawing, crystal growing in food processing and movements of biological fluids. Such flows add complexities to the governing equations for the dependence of physical quantities in the two and three dimensions. The heat transfer analysis in boundary layer flow with radiation is further important in electrical power generation, astrophysical flows, solar power technology, space vehicle reentry and other industrial areas. Mass transfer in such flows is inspired for an interest in membrane separation process, microfiltration, and reverse osmosis, in electrochemistry and fiber industries. There are transport processes in industrial applications in which heat and mass transfer is a consequence of buoyancy effects caused by thermal and mass diffusion in the presence of chemical reaction. Such interaction is significant in the design of chemical processing equipment, nuclear reactor safety, combustion of solar system equipment etc. Motivated by such practical applications, the present thesis is structured as follows.

Chapter one provides the background and boundary layer equations for some models of non-Newtonian fluids namely second grade, Maxwell, Jeffrey and micropolar fluids. Brief idea of homotopy analysis method (HAM) is also given.

The unsteady mixed convection boundary layer magnetohydrodynamic (MHD) flow of a second grade fluid bounded by a stretching surface has been addressed in chapter two. Both the

stretching velocity and the surface temperature are taken time-dependent. Problem formulation is developed in the presence of thermal radiation. Governing nonlinear problem is solved by a homotopy analysis method. Convergence of derived solution is studied. The dependence of velocity and temperature profiles on various quantities is shown and discussed by plotting graphs. Numerical values of skin friction coefficient and local Nusselt number are tabulated. It is noticed that velocity profiles are increasing functions of second grade parameter. The local Nusselt number also increases when the value of Prandtl number is increased. **These observations have been published in "International Journal for Numerical Methods in Fluids, DOI: 10.100/fld.2285".**

Chapter three investigates the unsteady three-dimensional flow of an elastico-viscous fluid over a stretching sheet. The mass transfer analysis is also studied. The governing boundary layer equations are reduced into the partial differential equations by similarity transformation. The effects of embedded parameters in the considered problem are examined in detail. Numerical data for surface shear stresses and surface mass transfer in steady case are also tabulated. Both cases of destructive/generative chemical reactions are analyzed. It is found that the influence of viscoelastic parameter and the Hartman number on the shear stresses are quantitatively similar. **Such results are published in "International Journal for Numerical Methods in Fluids, DOI: 10.100/fld.2252".**

The joule heating and thermophoresis effects on MHD flow of a Maxwell fluid in the presence of thermal radiation are studied in chapter four. The nonlinear ordinary differential systems obtained after employing similarity transformations have been solved and series solutions are constructed. The local Nusselt and Sherwood numbers are further computed. The thermal boundary layer thickness increases with increase in the Prandtl number. The local Nusselt and Sherwood number increases when porosity parameter is increased. **These conclusions have been published in "International Journal of Heat and Mass Transfer, 53 (2010) 4780-4788".**

The influence of heat transfer on the boundary layer flow of a Maxwell fluid over a moving permeable surface in a parallel free stream is argued in chapter five. Solution of the governing problem is developed by homotopy analysis method. The results of velocity, temperature and Nusselt number are presented and discussed for various emerging parameters. A comparative

study is seen with the known numerical solution in a limiting sense and an excellent agreement is noted. It is also found that velocity in the Maxwell fluid is less than the viscous fluid. It is revealed that the boundary layer thickness decreases with the increasing values of Deborah number. The thermal boundary layer thickness decreases by increasing suction parameter. **This research is submitted for publication in "Chinese Journal of Mechanics-Series A".**

In chapter six, we perform a study for heat and mass transfer analysis in the presence of thermal radiation on the unsteady MHD flow of a micropolar fluid. Series solutions for velocity, temperature and concentration fields are derived and discussed. Plots for various interesting parameters are reported and analyzed. Numerical data for surface shear stress, Nusselt number and Sherwood numbers in steady cases are also computed. Comparison between the present and previous limiting results is shown. **The results of this chapter have been published in "Zeitschrift Naturforschung A, 64 (2010) 950-960".**

Chapter seven is prepared to analyze the heat and mass transfer characteristics for the steady mixed convection flow of an incompressible micropolar fluid. The relevant system of the partial differential equations has been reduced into ordinary differential equations by employing similarity transformation. Series solutions for velocity, temperature and concentration fields are developed by using homotopy analysis method (HAM). Effects of various parameters on velocity, temperature and concentration fields are discussed by displaying graphs. Numerical values of skin friction coefficient, Nusselt number and Sherwood numbers are worked out. A comparison between the available numerical solutions in a limiting situation is seen. The velocity profile is found to decrease when the Prandtl number increases. Moreover, the buoyancy parameter decreases the thickness of thermal boundary layer. **These conclusions have been accepted for publication in "International Journal for Numerical Methods in Fluids, DOI: 10.1002/flid.2424".**

Chapter eight examines the MHD flow and mass transfer characteristics in a Jeffrey fluid bounded by a non-linearly stretching surface. The velocity and concentration fields are derived. Homotopy analysis procedure is adopted for computations of a set of coupled nonlinear ordinary differential equations. Effects of involved parameters on the velocity and concentrations fields are examined carefully. Numerical values of mass transfer coefficient are first tabulated and then investigated. As expected the concentration fields decreases by

increasing the Schmidt number. The surface mass transfer decreases when the Hartman number increases. **The observations of this problem have been published in "Zeitschrift Naturforschung A, 64 (2010) 1111 – 1120".**

In chapter nine, we have considered the effect of mass transfer on stagnation point flow of a Jeffrey fluid bounded by a stretching surface. Similarity transformations reduce the partial differential equations into the ordinary differential equations. Homotopy analysis method (HAM) is invoked for the development of solutions. Plots are prepared to illustrate the flow and mass transfer characteristics and their dependence on the physical parameters. The values of surface mass transfer and gradient of mass transfer are computed and analyzed. It is observed that velocity field and boundary layer thickness are increasing functions of Deborah number. The fluid concentration increases with an increase in generative chemical reaction parameter and has opposite behavior for destructive chemical reaction when compared with the situation in case of generative chemical reaction parameter. **Such contexts have been submitted for publication in "Asia-Pacific Journal of Chemical Engineering".**

The unsteady stagnation point flow of a second grade fluid with heat transfer is discussed in chapter ten. The time-dependent free stream is considered. The equations of motion and energy are transformed into the ordinary differential equations by similarity transformations. Homotopy analysis method is used to find the solution of the governing problem. Graphical results are given in order to illustrate the details of flow and heat transfer characteristics and their dependence upon the embedded parameters. Numerical values of skin- friction coefficients and Nusselt number are given and examined carefully. It is seen that velocity is greater for second grade fluid when compared with a Newtonian fluid. The velocity and boundary layer thickness increases in both cases of suction and injection as second grade parameter increases. However, in injection case such increase is larger than that of suction. We further found that for fixed values of other parameters, the local Nusselt number increases when there is an increase in the second grade parameter. **The findings of this chapter have been submitted for publication in "International Journal of Heat and Mass Transfer".**

Chapter eleven discusses the steady mixed convection stagnation point flow of a micropolar flow towards a stretching sheet. Governing problems of flow, heat and mass transfer are solved by employing homotopy analysis method (HAM). The skin friction coefficients, local Nusselt

number and Sherwood number are computed. Comparison of the present solution series solution is given to the corresponding numerical solution. A good agreement is achieved. When the stretching velocity of the surface is greater than the stagnation velocity of the external stream the flow has inverted boundary layer structure. The effect of the local buoyancy parameter on the velocity is found similar to the material parameter. **These observations have been submitted for publication in "Central European Journal of Physics".**

Contents

1	Background and boundary layer analysis	5
1.1	Review of literature	5
1.2	Basic equations	9
1.2.1	The continuity equation	9
1.2.2	The momentum equation	9
1.2.3	The energy equation	9
1.2.4	The concentration equation	9
1.2.5	Maxwell's equations	10
1.3	Constitutive expressions and boundary layer equations in the non-Newtonian fluids	11
1.3.1	Boundary layer equation in a second grade fluid	11
1.3.2	Boundary layer equation in a Maxwell fluid	13
1.3.3	Boundary layer equation in a Jeffrey fluid	14
1.3.4	Boundary layer equation in a micropolar fluid	15
1.4	Homotopy analysis method	17
2	Unsteady MHD mixed convection flow of second grade fluid over a stretching surface with thermal radiation	19
2.1	Mathematical formulation	20
2.2	Analytic solutions	23

2.3	Convergence of the series solutions	27
2.4	Results and discussion	29
2.5	Concluding remarks	30
3	Unsteady three-dimensional flow of an elasto-viscous fluid in the presence of mass transfer	41
3.1	Problem statement	41
3.2	Homotopy analysis solutions	45
3.3	Convergence of the homotopy solutions	50
3.4	Results and discussion	52
3.5	Final remarks	53
4	Thermal Radiation and Joule heating effects on MHD flow of a Maxwell fluid with thermophoresis	66
4.1	Problem description	66
4.2	Solutions by homotopy analysis method (HAM)	70
4.3	Convergence of the series solutions	75
4.4	Discussion of results	76
4.5	Concluding remarks	77
5	Influence of thermal radiation on the steady flow of a Maxwell fluid over a moving permeable surface in a parallel free stream	88
5.1	Problem development	89
5.2	Homotopy analysis solutions	91
5.3	Convergence of the homotopy solution	94
5.4	Results and discussion	95
6	Effects of thermal radiation on unsteady MHD flow of a Micropolar fluid	

with heat and mass transfer	105
6.1 Mathematical formulation	105
6.2 Homotopy analysis solutions	110
6.3 Convergence of the homotopy solutions	115
6.4 Results and discussion	116
6.5 Closing remarks	118
7 Mixed convection flow of a micropolar fluid in the presence of radiation and chemical reaction	130
7.1 Mathematical formulation	130
7.2 Homotopy analysis solutions	134
7.3 Convergence of the homotopy solutions	139
7.4 Results and discussion	140
7.5 Conclusions	142
8 MHD steady flow and mass transfer of Jeffrey fluid over a non-linear stretch- ing surface with mass transfer	156
8.1 Mathematical formulation	157
8.2 Homotopy analysis solutions	159
8.3 Convergence of homotopy solutions	165
8.4 Results and discussion	167
8.5 Closing remarks	168
9 Stagnation point flow of a Jeffrey fluid with mass transfer	180
9.1 Problem formulation	180
9.2 Homotopy solutions	182
9.3 Convergence of homotopy solutions	186

9.4	Results and discussion	188
9.5	Closing remarks	189
10	Unsteady stagnation point flow of a second grade fluid with heat transfer	197
10.1	Definition of the problem	197
10.2	Solution expressions	200
10.3	Convergence of the derived solution expressions	204
10.4	Results and discussion	205
10.5	Concluding remarks	206
11	Mixed convection stagnation point flow of a micropolar fluid towards a stretch-	
	ing surface with thermal radiation	214
11.1	Mathematical formulation	215
11.2	Homotopy analysis solutions	218
11.3	Convergence of the series solutions	223
11.4	Results and discussion	225
11.5	Conclusions	226

Chapter 1

Background and boundary layer analysis

1.1 Review of literature

The non-Newtonian fluids are quite prevalent in industry and engineering. Examples of such fluids include polymer solutions, paints, certain oils, exotic lubricants, colloidal and suspension solutions, clay coatings and cosmetic products etc. As a consequence of diverse physical structure of such fluids there is not a single model which can predict all the salient features of non-Newtonian fluids. The non-Newtonian fluids are in general classified into three categories known as (i) the differential type (ii) the rate type and (iii) the integral type. The detailed discussion of the relevant issue is found in the literature by Rajagopal [1] and Rajagopal and Kaloni [2]. The differential type fluids have received much attention in the past. Dunn and Rajagopal [3] discussed interesting features of differential type fluids. There is a simplest subclass of differential type fluids which is known as second grade fluid. This fluid model has an ability to describe normal stress differences and does not exhibit the shear thinning/shear thickening effects. The thermodynamical compatibility of second grade fluid model has been taken into

account by Fosdick and Rajagopal [4]. It was revealed that Clausius-Duhem inequality should hold together with the helmholtz free energy being at its minimum whenever the fluid is locally at rest. Later various investigators including Rajagopal [5], Siddiqui and Kaloni [6], Siddiqui and Benharbit [7], Fetecau and Fetecau [8], Fetecau and Zierep [9], Asghar et. al [10], Erdogan and Imark [11], Tan and Masuoka [12], Tan and Xu [13] and Hayat et al. [14 – 16] discussed the steady and unsteady flows of second grade fluid under various aspects.

There is a simplest subclass of the rate type fluids known as the Maxwell. This model can easily describe the characteristics of the relaxation time. Bhatnagar et al. [17] reported the pioneering works on the flow analysis of rate type fluids. They considered the two-dimensional flow of an oldroyd-B fluid over a stretching surface in the presence of variable free stream velocity. Choi et al. [18] considered the channel flow of an upper convected Maxwell (UCM) fluid induced by suction. Numerical and analytical solutions of the resulting differential system were obtained. The analytical solution was derived by power series method and numerical solutions was obtained by Runge-Kutta method. The unsteady flow of a Maxwell fluid between two side walls due to a suddenly moved plate was examined by Hayat et al. [19]. Zierep et al. [20] discussed the numerical results for the energy conservation of Maxwell media for Stokes' first problem. Haitao and Mingyu [21] addressed the unsteady flow of fractional Maxwell fluid in a channel. Fetecau et. al [22, 23] studied the unsteady flows in Maxwell fluids respectively. In these studies, the flows have been induced by the oscillating/accelerated rigid plate. The MHD unsteady flow of a Maxwell fluid in a rotating frame of reference and porous medium has been reported by Hayat et al. [24]. Tan and Masuoka [25] analyzed linear convective stability of a Maxwell fluid layer in a porous medium. The theory of micropolar fluid was initiated by Eringen [26, 27]. The equations governing the flow of a micropolar fluid involve a microrotation vector and a gyration parameter in addition to the classical velocity vector field. Interesting features and applications of micropolar fluids are described in the books by Eringen [28] and Lukaszewicz [29]. This fluid model has special relevance in blood flows, suspension solutions,

liquid crystals, fluids with additives, flow of colloidal solutions etc.

The boundary layer flow [30] on a moving surface are very important because of their relevance in a number of engineering processes. Sakiadis [31] initiated the seminal work on this topic. The work of Sakiadis was subsequently extended by many authors for boundary layer flows in viscous and non-Newtonian fluids under various conditions. Crane [32] investigated the viscous flow over a sheet with linear surface velocity. In this attempt, the similarity solution was given. Vleggar [33] and Gupta and Gupta [34] have investigated the stretching problem with constant surface temperature while Soundalgekar and Ramana Myrty [35] analyzed constant surface velocity case with power-law temperature variation. Chen and Char [36] extended the works of Gupta and Gupta [34] for non-isothermal stretching sheet. The non-Newtonian boundary layer flow by a stretching sheet was examined by Siddappa and Khapate [37] and Rajagopal et al. [38]. Lawrence and Rao [39] discussed the uniqueness of the solution obtained Rajagopal et al. [38]. Troy et al. [40] constructed the uniqueness of the steady flow of an incompressible second-order fluid over a stretching sheet. Andersson et al. [41] investigated the stretching flow of a power-law fluid. Few investigations dealing with non-Newtonian flow problems over stretching/shrinking sheet has been presented by Cortell [42, 43], Hayat et al. [44 – 49], Ariel [50, 51], Mushtaq et al. [52] and A. Ishak [53]. All the aforementioned attempts takes into account a constant value of velocity wall or linearly stretching sheet problem. The flow of non-linearly stretching sheet was investigated by Vajravelu [54, 55], Cortell [56, 57] and Hayat et al [58]. Raptis and Perdikis [59] have examined the MHD viscous flow over a non-linear stretching sheet in the presence of a chemical reaction. The works on unsteady boundary layer viscous and non-Newtonian fluids flow by an impulsively stretching surface have been discussed by Pop and Na [60], Wang et al. [61], Liao [62, 63], Pahlavan and Sadeghy [64] and Sajid et al. [65]. Nazar et al. [66] argued at the unsteady flow over a stretching sheet in a micropolar fluid. Liquid film flow on an unsteady stretching surface was first considered by Wang [67]. Few more contributions regarding the time-dependent stretching flows have been presented in

the references [68 – 74]. All the above mentioned studies were concerned the two-dimensional flows induced by a stretching surface. Three-dimensional boundary layer flow over a stretched surface has been investigated by Wang [75]. Devi et al. [76] studied the problem of unsteady three-dimensional flow over a stretching surface. Lakshmisha et al. [77] presented the numerical solution for unsteady three-dimensional flow induced by a stretching surface with heat and mass transfer. Chamkha [78] examined the hydromagnetic steady three-dimensional viscous flow over a stretching surface with heat generation absorption. Exact and perturbation solutions for the problem arising in the three dimensional flow of a viscous fluid over a stretching surface have been derived by Ariel [79]. The other investigations for three-dimensional stretching flow has been examined by Aboeldahab [80], Aboeldahab and Azzam [81] and Xu et al. [82]. Hayat et al. [83] firstly studied the problem of three-dimensional boundary layer flow of a viscoelastic fluid by a stretching surface via homotopy analysis method (HAM). Roslinda and Norfaizin [84] numerically examined the three-dimensional flow due to a stretching surface.

The stagnation point flow of a fluid past a stretching sheet has been given much attention in the recent times. This is in view of their importance in many industrial applications, such as extrusion, paper production, insulating materials, glass drawing, continuous casting etc. Chiam [85] investigated the steady two dimensional stagnation point flow of a viscous fluid towards a stretching sheet. Bhatangar et al. [17] obtained solution for the flow of an Oldroyd-B fluid over a stretching sheet in the presence of constant free stream. Mahapatra and Gupta [86] analyzed the heat transfer in the stagnation point flow towards a stretching surface. The steady stagnation point flow of an incompressible micropolar fluid over a stretching surface is studied by Nazar et al. [87]. Sadeghy et al. [88] numerically studied the stagnation point flow of an upper convected Maxwell fluid. Ishak et al. [89] investigated the mixed convection stagnation point flow of an incompressible viscous fluid towards a vertical permeable stretching sheet. The effect of thermal radiation on the mixed convection boundary layer magnetohydrodynamic stagnation point flow in a porous space has been investigated by Hayat et al. [90]. Mahapatra et al. [91] discussed

the steady two-dimensional oblique stagnation point flow of an incompressible viscoelastic fluid towards a stretching sheet. Labropulu and D. Li examined [92] the steady two dimensional stagnation point flow with partial slip. Nazar et al. [93] described the steady stagnation point flow of an incompressible micropolar fluid by a stretched sheet.

1.2 Basic equations

The following laws have been used for the problems formulation in this thesis.

1.2.1 The continuity equation

$$\operatorname{div} \mathbf{V} = 0. \quad (1.1)$$

1.2.2 The momentum equation

$$\rho \frac{d\mathbf{V}}{dt} = \operatorname{div} \tilde{\mathbf{T}} + \rho \mathbf{b}, \quad (1.2)$$

$$\tilde{\mathbf{T}} = -p\mathbf{I} + \tilde{\mathbf{S}}. \quad (1.3)$$

1.2.3 The energy equation

$$\rho c_p \frac{dT}{dt} = k \nabla^2 T + \tilde{\mathbf{T}} \cdot \mathbf{L}. \quad (1.4)$$

1.2.4 The concentration equation

$$\frac{dC}{dt} = D \nabla^2 C - RC. \quad (1.5)$$

In above equations \mathbf{V} is the velocity, $\tilde{\mathbf{T}}$ is the Cauchy stress tensor, $\tilde{\mathbf{S}}$ is the extra stress tensor, \mathbf{b} is the body force per unit mass, ρ the density, p is the pressure, \mathbf{I} is the identity tensor, c_p is the specific heat, k the thermal conductivity, \mathbf{L} is the velocity gradient, T the temperature of fluid, D is coefficient of mass diffusivity, R is the chemical reaction and C is the concentration of fluid.

1.2.5 Maxwell's equations

(a) Gauss's law

$$\nabla \cdot \mathbf{E} = \frac{\rho_c}{\epsilon_0}. \quad (1.6)$$

(b) Gauss's law for magnetism

$$\nabla \cdot \mathbf{B} = 0. \quad (1.7)$$

(c) Faraday's law

$$\nabla \times \mathbf{E} = -\frac{\partial \mathbf{B}}{\partial t}. \quad (1.8)$$

(d) Amperes law

$$\nabla \times \mathbf{B} = \mu_0 \mathbf{J} + \mu_0 \epsilon_0 \frac{\partial \mathbf{E}}{\partial t}. \quad (1.9)$$

(e) Ohms' law

$$\mathbf{J} = \sigma (\mathbf{E} + \mathbf{V} \times \mathbf{B}). \quad (1.10)$$

where ρ_c is the charge density, \mathbf{E} is the electric field, \mathbf{B} is the magnetic field, μ_0 is the magnetic constant, ϵ_0 is the electric constant, \mathbf{J} is the current density and σ is the electrical conductivity of the fluid.

1.3 Constitutive expressions and boundary layer equations in the non-Newtonian fluids

This thesis will be based upon the boundary layer flows in second grade, Maxwell, Jeffrey and micropolar fluids. Hence, we briefly describe the relevant equations here for the convenience of readers.

1.3.1 Boundary layer equation in a second grade fluid

Extra stress tensor in a second grade fluid is

$$\tilde{\mathbf{S}} = \mu \mathbf{A}_1 + \alpha_1 \mathbf{A}_2 + \alpha_2 \mathbf{A}_1^2 \quad (1.11)$$

in which μ is the dynamic viscosity and the material parameters $\alpha_i (i = 1, 2)$ satisfy the following constraints:

$$\mu \geq 0, \quad \alpha_1 \geq 0, \quad \alpha_1 + \alpha_2 = 0. \quad (1.12)$$

The definitions of the first two Rivlin-Ericksen tensors \mathbf{A}_1 and \mathbf{A}_2 are

$$\mathbf{A}_1 = \mathbf{L} + \mathbf{L}^T, \quad (1.13)$$

$$\mathbf{A}_2 = \frac{d\mathbf{A}_1}{dt} + \mathbf{A}_1 \mathbf{L} + \mathbf{L}^T \mathbf{A}_1, \quad (1.14)$$

where $\mathbf{L}^T = (\text{grad } \mathbf{V})^T$ and d/dt is used for the material derivative. The two-dimensional flow field requires that

$$\mathbf{V} = [u(x, y, t), v(x, y, t), 0], \quad (1.15)$$

in which u and v are the respective components of velocity parallel to the x - and y -axes, respectively.

In view of Eqs. (1.11) – (1.15) and (1.3) we have the following components of the Cauchy stress tensor

$$\begin{aligned}
T_{xx} = & -p + 2\mu \left(\frac{\partial u}{\partial x} \right) + \alpha_1 \left[2 \left(\frac{\partial^2 u}{\partial x \partial t} + u \frac{\partial^2 u}{\partial x^2} + v \frac{\partial^2 u}{\partial x \partial y} \right) + \right. \\
& \left. 4 \left(\frac{\partial u}{\partial x} \right)^2 + 2 \left(\frac{\partial v}{\partial x} \right)^2 + 2 \frac{\partial u}{\partial y} \frac{\partial v}{\partial x} \right] \\
& + \alpha_2 \left[4 \left(\frac{\partial u}{\partial x} \right)^2 + \left(\frac{\partial u}{\partial y} \right)^2 + \left(\frac{\partial v}{\partial x} \right)^2 + 2 \frac{\partial u}{\partial y} \frac{\partial v}{\partial x} \right], \tag{1.16}
\end{aligned}$$

$$\begin{aligned}
T_{yy} = & -p + 2\mu \left(\frac{\partial v}{\partial y} \right) + \alpha_1 \left[2 \left(\frac{\partial^2 v}{\partial y \partial t} + v \frac{\partial^2 v}{\partial y^2} + u \frac{\partial^2 v}{\partial x \partial y} \right) + \right. \\
& \left. 4 \left(\frac{\partial v}{\partial y} \right)^2 + 2 \left(\frac{\partial u}{\partial y} \right)^2 + 2 \frac{\partial u}{\partial y} \frac{\partial v}{\partial x} \right] \\
& + \alpha_2 \left[4 \left(\frac{\partial v}{\partial y} \right)^2 + \left(\frac{\partial u}{\partial y} \right)^2 + \left(\frac{\partial v}{\partial x} \right)^2 + 2 \frac{\partial u}{\partial y} \frac{\partial v}{\partial x} \right], \tag{1.17}
\end{aligned}$$

$$\begin{aligned}
T_{xy} = T_{yx} = & \mu \left(\frac{\partial u}{\partial y} + \frac{\partial v}{\partial x} \right) + \alpha_1 \left[\begin{array}{l} \frac{\partial^2 u}{\partial y \partial t} + \frac{\partial^2 u}{\partial x \partial y} + v \frac{\partial^2 u}{\partial y^2} + \frac{\partial^2 v}{\partial x \partial t} + \\ u \frac{\partial^2 v}{\partial x^2} + v \frac{\partial^2 v}{\partial x \partial y} + 3 \frac{\partial u}{\partial x} \frac{\partial u}{\partial y} + \\ 3 \frac{\partial v}{\partial x} \frac{\partial v}{\partial y} + \frac{\partial u}{\partial x} \frac{\partial v}{\partial x} + \frac{\partial u}{\partial y} \frac{\partial v}{\partial y} \end{array} \right] \\
& + \alpha_2 \left[\frac{\partial u}{\partial x} \frac{\partial u}{\partial y} + \frac{\partial u}{\partial x} \frac{\partial v}{\partial x} + \frac{\partial u}{\partial y} \frac{\partial v}{\partial y} + \frac{\partial v}{\partial x} \frac{\partial v}{\partial y} \right], \tag{1.18}
\end{aligned}$$

$$T_{zz} = -p, \quad T_{xz} = T_{yz} = 0. \tag{1.19}$$

Substituting the above equations along with the continuity equation the x - and y -components

of equation of motion become

$$\rho \left(\frac{\partial u}{\partial t} + u \frac{\partial u}{\partial x} + v \frac{\partial u}{\partial y} \right) = -\frac{\partial p}{\partial x} + \mu \left(\frac{\partial^2 u}{\partial x^2} + \frac{\partial^2 u}{\partial y^2} \right) + \alpha_1 \left[\begin{array}{l} \frac{\partial^3 u}{\partial y^2 \partial t} + u \frac{\partial^3 u}{\partial x \partial y^2} + \frac{\partial u}{\partial x} \frac{\partial^2 u}{\partial y^2} + \frac{\partial u}{\partial y} \frac{\partial x \partial y}{\partial y^2} \\ \frac{\partial^3 u}{\partial y^2 \partial t} + u \frac{\partial^3 u}{\partial x \partial y^2} + \frac{\partial u}{\partial x} \frac{\partial^2 u}{\partial y^2} + \frac{\partial u}{\partial y} \frac{\partial x \partial y}{\partial y^2} \\ v \frac{\partial^3 u}{\partial x^2 \partial y} + 4 \frac{\partial v}{\partial x} \frac{\partial^2 u}{\partial x \partial y} + \frac{\partial u}{\partial y} \frac{\partial^2 v}{\partial x^2} + 2 \frac{\partial v}{\partial x} \frac{\partial^2 v}{\partial x^2} \end{array} \right], \quad (1.20)$$

$$\rho \left(\frac{\partial v}{\partial t} + u \frac{\partial v}{\partial x} + v \frac{\partial v}{\partial y} \right) = -\frac{\partial p}{\partial y} + \mu \left(\frac{\partial^2 v}{\partial x^2} + \frac{\partial^2 v}{\partial y^2} \right) + \alpha_1 \left[\begin{array}{l} \frac{\partial^3 v}{\partial x^2 \partial t} + u \frac{\partial^3 v}{\partial x \partial y^2} + \frac{\partial v}{\partial x} \frac{\partial^2 u}{\partial y^2} + \frac{\partial u}{\partial y} \frac{\partial^2 v}{\partial x \partial y} \\ \frac{\partial^3 v}{\partial y^2 \partial t} + u \frac{\partial^3 v}{\partial x^3} + v \frac{\partial^3 v}{\partial y^3} + 4 \frac{\partial v}{\partial y} \frac{\partial^2 v}{\partial y^2} \\ \frac{\partial v}{\partial x} \frac{\partial^2 v}{\partial x \partial y} + 2 \frac{\partial u}{\partial y} \frac{\partial^2 u}{\partial y^2} + 2 \frac{\partial v}{\partial y} \frac{\partial^2 v}{\partial x^2} \end{array} \right], \quad (1.21)$$

The above equations after employing the usual boundary layer assumptions [30]

$$u = O(1), \quad v = O(\delta), \quad x = O(1), \quad y = O(\delta), \quad (1.22)$$

$$\frac{Txx}{\rho} = O(1), \quad \frac{Txy}{\rho} = O(\delta), \quad \frac{Tyy}{\rho} = O(\delta^2), \quad (1.23)$$

gives

$$\frac{\partial u}{\partial t} + u \frac{\partial u}{\partial x} + v \frac{\partial u}{\partial y} = \nu \frac{\partial^2 u}{\partial y^2} + \frac{\alpha_1}{\rho} \left[\frac{\partial^3 u}{\partial y^2 \partial t} + u \frac{\partial^3 u}{\partial x \partial y^2} + \frac{\partial u}{\partial x} \frac{\partial^2 u}{\partial y^2} + v \frac{\partial^3 u}{\partial y^3} \right] \quad (1.24)$$

1.3.2 Boundary layer equation in a Maxwell fluid

In this section the relevant equations are [18]

$$\begin{aligned}
\rho \left(u \frac{\partial u}{\partial x} + v \frac{\partial u}{\partial y} \right) &= -\frac{\partial \bar{p}}{\partial x} + \frac{\partial S_{xx}}{\partial x} + \frac{\partial S_{xy}}{\partial y}, \\
\rho \left(u \frac{\partial v}{\partial x} + v \frac{\partial v}{\partial y} \right) &= -\frac{\partial \bar{p}}{\partial y} + \frac{\partial S_{yx}}{\partial x} + \frac{\partial S_{yy}}{\partial y},
\end{aligned} \tag{1.25}$$

$$\begin{aligned}
S_{xx} + \lambda_1 \left[u \frac{\partial S_{xx}}{\partial x} + v \frac{\partial S_{xx}}{\partial y} - S_{xx} \frac{\partial u}{\partial x} - S_{xy} \frac{\partial u}{\partial y} - S_{xx} \frac{\partial u}{\partial x} - S_{xy} \frac{\partial u}{\partial y} \right] &= 2\mu \frac{\partial u}{\partial x}, \\
S_{xy} + \lambda_1 \left[u \frac{\partial S_{xy}}{\partial x} + v \frac{\partial S_{xy}}{\partial y} - S_{xy} \frac{\partial u}{\partial x} - S_{yy} \frac{\partial v}{\partial y} - S_{xx} \frac{\partial v}{\partial x} - S_{xy} \frac{\partial v}{\partial y} \right] &= \mu \left(\frac{\partial u}{\partial x} + \frac{\partial v}{\partial y} \right), \\
S_{yy} + \lambda_1 \left[u \frac{\partial S_{yy}}{\partial x} + v \frac{\partial S_{yy}}{\partial y} - S_{xy} \frac{\partial v}{\partial x} - S_{yy} \frac{\partial v}{\partial y} - S_{yx} \frac{\partial v}{\partial x} - S_{yy} \frac{\partial v}{\partial y} \right] &= 2\mu \frac{\partial v}{\partial y}.
\end{aligned} \tag{1.26}$$

The boundary layer flow equation is

$$u \frac{\partial u}{\partial x} + v \frac{\partial u}{\partial y} + \lambda_1 \left[u^2 \frac{\partial^2 u}{\partial x^2} + v^2 \frac{\partial^2 u}{\partial y^2} + 2uv \frac{\partial^2 u}{\partial x \partial y} \right] = -\frac{1}{\rho} \frac{\partial \bar{p}}{\partial x} + \nu \frac{\partial^2 u}{\partial y^2}.$$

1.3.3 Boundary layer equation in a Jeffrey fluid

The extra stress tensor $\bar{\mathbf{S}}$ in a Jeffrey fluid is

$$\bar{\mathbf{S}} = \frac{\mu}{1 + \lambda_1} \left[\mathbf{A}_1 + \lambda_2 \frac{d\mathbf{A}_1}{dt} \right], \tag{1.27}$$

where λ_1 is the ratio of relaxation to retardation times and λ_2 is the retardation time and the stress components are

$$T_{xx} = -p + \left(\frac{2\mu}{1 + \lambda_1} \right) \left[\frac{\partial u}{\partial x} + \lambda_2 \left(u \frac{\partial^2 u}{\partial x^2} + v \frac{\partial^2 u}{\partial y \partial x} \right) \right], \tag{1.28}$$

$$T_{xy} = T_{yx} = \left(\frac{\mu}{1 + \lambda_1} \right) \left[\frac{\partial u}{\partial y} + \frac{\partial v}{\partial x} + \lambda_2 \left(u \frac{\partial^2 u}{\partial y \partial x} + v \frac{\partial^2 u}{\partial y^2} + u \frac{\partial^2 v}{\partial x^2} + v \frac{\partial^2 v}{\partial y \partial x} \right) \right], \tag{1.29}$$

$$T_{yy} = -p + \left(\frac{2\mu}{1 + \lambda_1} \right) \left[\frac{\partial v}{\partial y} + \lambda_2 \left(u \frac{\partial^2 v}{\partial y \partial x} + v \frac{\partial^2 v}{\partial y^2} \right) \right], \tag{1.30}$$

$$T_{zz} = -p, \quad T_{zz} = T_{yz} = T_{zx} = T_{zy} = 0. \quad (1.31)$$

The two-dimensional equations are

$$\begin{aligned} \rho \left(u \frac{\partial u}{\partial x} + v \frac{\partial u}{\partial y} \right) &= -\frac{\partial p}{\partial x} + \left(\frac{\mu}{1 + \lambda_1} \right) \left(\frac{\partial^2 u}{\partial x^2} + \frac{\partial^2 u}{\partial y^2} \right) \\ &+ \left(\frac{\mu \lambda_2}{1 + \lambda_1} \right) \left[\begin{aligned} &2 \frac{\partial u}{\partial x} \frac{\partial^2 u}{\partial x^2} + u \frac{\partial^3 u}{\partial x^3} + 2 \frac{\partial v}{\partial x} \frac{\partial^2 u}{\partial y \partial x} \\ &+ v \frac{\partial^3 u}{\partial y \partial x^2} + \frac{\partial u}{\partial y} \frac{\partial^2 u}{\partial y \partial x} + u \frac{\partial^3 u}{\partial y^2 \partial x} \\ &+ \frac{\partial v}{\partial y} \frac{\partial^2 u}{\partial y^2} + v \frac{\partial^3 u}{\partial y^3} + \frac{\partial u}{\partial y} \frac{\partial^2 v}{\partial x^2} + \frac{\partial v}{\partial y} \frac{\partial^2 v}{\partial y \partial x} \end{aligned} \right], \end{aligned} \quad (1.32)$$

$$\begin{aligned} \rho \left(u \frac{\partial u}{\partial x} + v \frac{\partial u}{\partial y} \right) &= -\frac{\partial p}{\partial y} + \left(\frac{\mu}{1 + \lambda_1} \right) \left(\frac{\partial^2 v}{\partial x^2} + \frac{\partial^2 v}{\partial y^2} \right) \\ &+ \left(\frac{\mu \lambda_2}{1 + \lambda_1} \right) \left[\begin{aligned} &\frac{\partial u}{\partial x} \frac{\partial^2 u}{\partial x \partial y} + \frac{\partial v}{\partial x} \frac{\partial^2 u}{\partial y^2} + \frac{\partial u}{\partial x} \frac{\partial^2 v}{\partial x^2} \\ &+ u \frac{\partial^3 v}{\partial x^3} + \frac{\partial v}{\partial x} \frac{\partial^2 v}{\partial y \partial x} + v \frac{\partial^3 v}{\partial y \partial x^2} \\ &+ u \frac{\partial^3 v}{\partial y^2 \partial x} + 2 \frac{\partial u}{\partial y} \frac{\partial^2 v}{\partial x \partial y} + 2 \frac{\partial v}{\partial y} \frac{\partial^2 v}{\partial y^2} + v \frac{\partial^2 v}{\partial y^2} \end{aligned} \right]. \end{aligned} \quad (1.33)$$

The above expressions under usual boundary layer assumptions reduce to

$$\begin{aligned} u \frac{\partial u}{\partial x} + v \frac{\partial u}{\partial y} &= -\frac{\partial p}{\partial x} + \frac{v}{1 + \lambda_1} \frac{\partial^2 u}{\partial y^2} \\ &+ \left(\frac{v \lambda_2}{1 + \lambda_1} \right) \left[\frac{\partial u}{\partial y} \frac{\partial^2 u}{\partial y \partial x} + u \frac{\partial^3 u}{\partial y^2 \partial x} + \frac{\partial v}{\partial y} \frac{\partial^2 u}{\partial y^2} + v \frac{\partial^3 u}{\partial y^3} \right]. \end{aligned} \quad (1.34)$$

1.3.4 Boundary layer equation in a micropolar fluid

For micropolar fluid, the momentum Eq. (1.2) along with the law of angular momentum in the absence of body forces and body couple are given by

$$\begin{aligned}
\rho \frac{d\mathbf{V}}{dt} &= -\nabla \tilde{p} + (\mu + \kappa) \nabla^2 \mathbf{V} + \kappa \nabla \times \mathbf{N}, \\
\rho j \frac{d\mathbf{N}}{dt} &= \gamma^* \nabla (\nabla \cdot \mathbf{N}) - \gamma^* \nabla \times (\nabla \times \mathbf{N}) + \kappa \nabla \times \mathbf{N} - 2\kappa \mathbf{N}.
\end{aligned} \tag{1.35}$$

In above equations \mathbf{V} and \mathbf{N} are the velocity and microrotation vectors, j denotes the gyration parameters of the fluid, γ^* and κ are the spin gradient viscosity and vortex viscosity, respectively.

Microrotation vector \mathbf{N} for two-dimensional flow is

$$\mathbf{N} = [0, 0, \mathbf{N}(x, y)]. \tag{1.36}$$

The scalar equations are

$$u \frac{\partial u}{\partial x} + v \frac{\partial u}{\partial y} = -\frac{1}{\rho} \frac{\partial \tilde{p}}{\partial x} + \frac{(\mu + \kappa)}{\rho} \left(\frac{\partial^2 u}{\partial x^2} + \frac{\partial^2 u}{\partial y^2} \right) + \frac{\kappa}{\rho} \frac{\partial N}{\partial y}, \tag{1.37}$$

$$u \frac{\partial v}{\partial x} + v \frac{\partial v}{\partial y} = -\frac{1}{\rho} \frac{\partial \tilde{p}}{\partial y} + \frac{(\mu + \kappa)}{\rho} \left(\frac{\partial^2 v}{\partial x^2} + \frac{\partial^2 v}{\partial y^2} \right) + \frac{\kappa}{\rho} \frac{\partial N}{\partial x}, \tag{1.38}$$

$$u \frac{\partial N}{\partial x} + v \frac{\partial N}{\partial y} = \frac{\gamma_1}{\rho j} \left(\frac{\partial^2 N}{\partial x^2} + v \frac{\partial^2 N}{\partial y^2} \right) + \frac{k}{\rho j} \left(\frac{\partial v}{\partial x} - \frac{\partial v}{\partial y} \right) - \frac{2\kappa}{\rho j} N, \tag{1.39}$$

in which the Eq. (1.39) suggests that $o(N) \sim o\left(\frac{\partial u}{\partial y}\right) \sim o\left(\frac{\partial v}{\partial x}\right)$.

The subjected boundary layer flow equations are given by

$$\begin{aligned}
u \frac{\partial u}{\partial x} + v \frac{\partial u}{\partial y} &= -\frac{1}{\rho} \frac{\partial \tilde{p}}{\partial x} + \left(v + \frac{k}{\rho} \right) \frac{\partial^2 u}{\partial y^2} + \frac{k}{\rho} \frac{\partial N}{\partial y}, \\
u \frac{\partial N}{\partial x} + v \frac{\partial N}{\partial y} &= \frac{\gamma^*}{\rho j} \frac{\partial^2 N}{\partial y^2} - \frac{k}{\rho j} \left(2N + \frac{\partial v}{\partial y} \right).
\end{aligned}$$

1.4 Homotopy analysis method

The method is proposed by Liao [94, 95] and is very useful for the development of series solutions especially to nonlinear problems [96 – 125]. We choose a nonlinear equation

Let us consider a nonlinear equation governed by

$$N(v) + f(x) = 0, \quad (1.40)$$

in which N is a nonlinear operator, $f(x)$ is a known function and v is an unknown function.

We now write

$$(1 - p)\mathcal{L}[\widehat{v}(x, p) - v_0(x)] = p\hbar \{N[\widehat{v}(x, p) - f(x)]\}. \quad (1.41)$$

where $v_0(x)$ denotes the initial approximation, \mathcal{L} is an auxiliary linear operator, $p \in [0, 1]$ is an embedding parameter, \hbar is an auxiliary parameter, $\widehat{v}(x, p)$ is an unknown function of x and p .

Obviously for $p = 0$ and $p = 1$ we have

$$\begin{aligned} \widehat{v}(x, 0) &= v_0(x) \\ \widehat{v}(x, 1) &= v(x) \end{aligned} \quad (1.42)$$

respectively. and for p variation from 0 to 1, the solution $\widehat{v}(x, p)$ approaches from the initial approximation $v_0(x)$ to the desired solution $v(x)$.

Taylor series gives

$$\widehat{v}(x, p) = v_0(x) + \sum_{m=1}^{\infty} v_m(x) p^m, \quad (1.43)$$

$$v_m(x) = \frac{1}{m!} \left. \frac{\partial^m \widehat{v}(x, p)}{\partial p^m} \right|_{p=0}. \quad (1.44)$$

in which the auxiliary parameter is responsible for the series convergence and for $p = 1$ one

obtains

$$v(x) = v_0(x) + \sum_{m=1}^{\infty} v_m(x). \quad (1.45)$$

The m th-order deformation problems are

$$\mathcal{L}[v_m(x) - \chi_m v_{m-1}(x)] = \hbar \mathcal{R}_m(x), \quad (1.46)$$

$$\chi_m = \begin{cases} 0, & m \leq 1, \\ 1, & m > 1, \end{cases} \quad (1.47)$$

$$\mathcal{R}_m(x) = \frac{1}{(m-1)!} \times \left\{ \frac{d^{m-1}}{dp^{m-1}} A \left[v_0(x) + \sum_{m=1}^{\infty} v_m(x) p^m \right] \right\} \Big|_{p=0}. \quad (1.48)$$

MAPLE or MATHEMATICA can solve the resulted problems.

Chapter 2

Unsteady MHD mixed convection flow of second grade fluid over a stretching surface with thermal radiation

This chapter investigates the mixed convection flow of a magnetohydrodynamic (MHD) second grade fluid over an unsteady permeable stretching sheet. Boundary layer assumptions are used in the problem statement. The stretching velocity and the surface temperature are time-dependent. Series solutions of the governing boundary value problems are obtained by employing homotopy analysis method (HAM). Convergence of the obtained solution is explicitly discussed. The dependence of velocity and temperature profiles on the various embedded parameters is shown and discussed by plotting graphs. Skin friction coefficient and the local Nusselt number are tabulated and analyzed.

2.1 Mathematical formulation

Consider the unsteady flow of an incompressible MHD second grade fluid over a porous stretching surface. The fluid is electrically conducting under the influence of a time dependent magnetic field $B(t)$ applied in a direction normal to the stretching surface. The induced magnetic field is negligible under the assumption of a small magnetic Reynolds number. In addition, heat transfer process is considered. Under these assumptions and Boussineq's approximation, the governing boundary layer equations are

$$\frac{\partial u}{\partial x} + \frac{\partial v}{\partial y} = 0, \quad (2.1)$$

$$\begin{aligned} \frac{\partial u}{\partial t} + u \frac{\partial u}{\partial x} + v \frac{\partial u}{\partial y} = \nu \frac{\partial^2 u}{\partial y^2} + \frac{\alpha_1}{\rho} \left[\frac{\partial^3 u}{\partial t \partial y^2} + u \frac{\partial^3 u}{\partial x \partial y^2} + \frac{\partial u}{\partial x} \frac{\partial^2 u}{\partial y^2} + \frac{\partial u}{\partial y} \frac{\partial^2 v}{\partial y^2} + v \frac{\partial^3 u}{\partial y^3} \right] \\ + g\beta_T(T - T_\infty) - \frac{\sigma B^2(t)}{\rho} u, \end{aligned} \quad (2.2)$$

$$\begin{aligned} \rho c_p \left[\frac{\partial T}{\partial t} + u \frac{\partial T}{\partial x} + v \frac{\partial T}{\partial y} \right] = \alpha_1 \left[\frac{\partial^2 u}{\partial y \partial t} \frac{\partial u}{\partial y} + u \frac{\partial^2 u}{\partial x \partial y} \frac{\partial u}{\partial y} + v \frac{\partial^2 u}{\partial y^2} \frac{\partial u}{\partial y} \right] \\ + k \frac{\partial^2 T}{\partial y^2} + \mu \left(\frac{\partial u}{\partial y} \right)^2 - \frac{\partial q_r}{\partial y}. \end{aligned} \quad (2.3)$$

By using Rosseland approximation [136] for radiation we have

$$q_r = -\frac{4\sigma^*}{3k^*} \frac{\partial T^4}{\partial y} \quad (2.4)$$

in which σ^* is the Stefan–Boltzmann constant, q_r is the radiative heat flux in the y -direction, T is the fluid temperature, g is gravitational acceleration, ν is the kinematic viscosity, σ is the electrical conductivity, ρ is fluid density, β_T is thermal expansion coefficients of temperature, c_p is specific heat and k^* the mean absorption coefficient. The fluid is compatible with the thermo-

dynamics in the sense that the specific Helmholtz free energy is a minimum when the fluid is in equilibrium when $\mu \geq 0$, $\alpha_1 \geq 0$, $\alpha_1 + \alpha_2 = 0$ (α_i ($i = 1, 2$) are the material parameters of second grade fluid). We express the term T^4 as the linear function of temperature into a Taylor series about T_∞ by neglecting higher terms and write

$$T^4 \cong 4T_\infty^3 T - 3T_\infty^4. \quad (2.5)$$

Now Eq. (2.3) becomes

$$\begin{aligned} \rho c_p \left[\frac{\partial T}{\partial t} + u \frac{\partial T}{\partial x} + v \frac{\partial T}{\partial y} \right] &= \alpha_1 \left[\frac{\partial^2 u}{\partial y \partial t} \frac{\partial u}{\partial y} + u \frac{\partial^2 u}{\partial x \partial y} \frac{\partial u}{\partial y} + v \frac{\partial^2 u}{\partial y^2} \frac{\partial u}{\partial y} \right] \\ &+ \frac{\partial}{\partial y} \left[\left(\frac{16\sigma^* T_\infty^3}{3k^*} + k \right) \frac{\partial T}{\partial y} \right] + \mu \left(\frac{\partial u}{\partial y} \right)^2 \end{aligned} \quad (2.6)$$

The associated boundary conditions are presented in the following forms

$$u = U_w, \quad v = V_w, \quad T = T_w, \quad \text{at } y = 0, \quad (2.7)$$

$$u \rightarrow 0, \quad T \rightarrow T_\infty, \quad \text{as } y \rightarrow \infty. \quad (2.8)$$

where V_w given by

$$V_w = -\frac{v_0}{(1 - \varepsilon t)^{1/2}} \quad (2.9)$$

represents the mass transfer at surface with $V_w > 0$ for injection and $V_w < 0$ for suction.

Further the stretching velocity $U_w(x, t)$ and surface temperature $T_w(x, t)$ are taken as

$$U_w(x, t) = \frac{ax}{1 - \varepsilon t}, \quad T_w(x, t) = T_\infty + T_0 \frac{ax}{2\nu} (1 - \varepsilon t)^{-2}, \quad (2.10)$$

in which a and ε are the constants with $a > 0$ and $\varepsilon \geq 0$ (with $\varepsilon t < 1$), and both a and ε have dimension time⁻¹. We choose time dependent magnetic field of the form $B(t) = B_0(1 - \varepsilon t)^{-1/2}$

[126 – 130].

Writing

$$\eta = \sqrt{\frac{U_w}{\nu x}} y, \quad \psi = \sqrt{\nu x U_w} f(\eta), \quad \theta(\eta) = \frac{T - T_\infty}{T_w - T_\infty} \quad (2.11)$$

and the velocity components

$$u = \frac{\partial \psi}{\partial y}, \quad v = -\frac{\partial \psi}{\partial x}, \quad (2.12)$$

where ψ is a stream function, the continuity equation is identically satisfied and the resulting problems for f and θ are given by

$$f''' - f'^2 + f f'' - A \left(f' + \frac{1}{2} \eta f'' \right) - M^2 f' + \lambda \theta + \alpha \left[\begin{array}{l} 2f' f''' - f''^2 - f f'''' \\ + A (2f''' + \frac{1}{2} \eta f'''') \end{array} \right] = 0, \quad (2.13)$$

$$\begin{aligned} (1 + \frac{4}{3} R_d) \theta'' + \text{Pr} (f \theta' - f' \theta) - \text{Pr} Ec (f'')^2 - \text{Pr} A (\eta \theta' + 4\theta) \\ - \text{Pr} Ec \alpha \left[\begin{array}{l} f' f''^2 - f f'' f''' \\ + \frac{1}{2} A (3f''^2 + \eta f'' f''') \end{array} \right] = 0, \end{aligned} \quad (2.14)$$

$$\begin{aligned} f(0) &= S, \quad f'(0) = 1, \quad f'(\infty) \rightarrow 0, \\ f''(\infty) &\rightarrow 0, \quad \theta(0) = 1, \quad \theta(\infty) \rightarrow 0. \end{aligned} \quad (2.15)$$

Here $A = \varepsilon/a$ is the unsteadiness parameter, $\alpha = a\alpha_1/\mu(1 - \varepsilon t)$ (with $\varepsilon t < 1$) is the dimensionless second grade parameter, $\lambda = \frac{Gr_x}{Re_x^2}$ is mixed convection parameter, $Gr_x (= \frac{g\beta(T_w - T_\infty)x^3/\nu^2}{u_w^2 x^2/\nu^2})$ is the local Grashof number, $Re_x = U_w x/\nu$ is the local Reynolds number, $\text{Pr} = \frac{\mu c_p}{k}$ is the Prandtl number, $R_d (= \frac{4\sigma^* T_\infty^3}{k^* k})$ is the radiation parameter, $Ec (= \frac{u_w^2}{c_p(T_w - T_\infty)})$ is the Eckert number and primes indicate the differentiation with respect to η .

Expressions of the skin friction coefficient C_f and local Nusselt number Nu_x are given by

$$C_f = \frac{\tau_w}{\rho u_w^2}, \quad (2.16)$$

$$Nu_x = \frac{xq_w}{k(T_w - T_\infty)} \quad (2.17)$$

where the skin-friction τ_w and wall heat flux q_w are

$$\tau_w = \left[\mu \frac{\partial u}{\partial y} + \alpha_1 \left(\frac{\partial^2 u}{\partial y \partial t} + 2 \frac{\partial u}{\partial x} \frac{\partial u}{\partial y} + u \frac{\partial^2 u}{\partial x \partial y} + v \frac{\partial^2 u}{\partial y^2} \right) \right]_{y=0}, \quad (2.18)$$

$$q_w = -k \left(\frac{\partial T}{\partial y} \right)_{y=0}. \quad (2.19)$$

From Eqs. (2.3) – (2.5) one can write

$$R_{e_x}^{1/2} C_f = \left[f''(\eta) + \alpha \left(3f'(\eta)f''(\eta) - f(\eta)f'''(\eta) + \frac{A}{2} (3f''(\eta) + \eta f'''(\eta)) \right) \right]_{\eta=0}, \quad (2.20)$$

$$R_{e_x}^{-1/2} Nu_x = -\theta'(0). \quad (2.21)$$

2.2 Analytic solutions

The velocity $f(\eta)$ and temperature $\theta(\eta)$ for HAM solutions can be expressed in the set of base functions

$$\left\{ \eta^k \exp(-n\eta) \mid k \geq 0, n \geq 0 \right\} \quad (2.22)$$

as follows

$$f(\eta) = a_{0,0}^0 + \sum_{n=0}^{\infty} \sum_{k=0}^{\infty} a_{m,n}^k \eta^k \exp(-n\eta), \quad (2.23)$$

$$\theta(\eta) = \sum_{n=0}^{\infty} \sum_{k=0}^{\infty} b_{m,n}^k \eta^k \exp(-n\eta), \quad (2.24)$$

where $a_{m,n}$ and $b_{m,n}$ are the coefficients.

The initial guesses f_0 and θ_0 of $f(\eta)$ and $\theta(\eta)$ are

$$f_0(\eta) = S + 1 - \exp(-\eta), \quad (2.25)$$

$$\theta_0(\eta) = \exp(-\eta). \quad (2.26)$$

The auxiliary linear operators are chosen as

$$\mathcal{L}_f = \frac{d^3 f}{d\eta^3} - \frac{df}{d\eta}, \quad (2.27)$$

$$\mathcal{L}_\theta = \frac{d^2 \theta}{d\eta^2} - \theta. \quad (2.28)$$

Above operators have the following properties

$$\mathcal{L}_f [C_1 + C_2 \exp(\eta) + C_3 \exp(-\eta)] = 0, \quad (2.29)$$

$$\mathcal{L}_\theta [C_4 \exp(\eta) + C_5 \exp(-\eta)] = 0, \quad (2.30)$$

in which C_i ($i = 1 - 5$) are the arbitrary constants.

If $p \in [0, 1]$ is an embedding parameter, \hbar_f and \hbar_θ the non-zero auxiliary parameters then we construct the following zeroth-order deformation problems as

$$(1 - p)\mathcal{L}_f[\hat{f}(\eta, p) - f_0(\eta)] = p\hbar_f \mathcal{N}_f [\hat{f}(\eta, p), \hat{\theta}(\eta, p)], \quad (2.31)$$

$$(1 - p)\mathcal{L}_\theta[\hat{\theta}(\eta, p) - \theta_0(\eta)] = p\hbar_\theta \mathcal{N}_\theta [\hat{f}(\eta, p), \hat{\theta}(\eta, p)], \quad (2.32)$$

$$\hat{f}(\eta; p)\Big|_{\eta=0} = S, \quad \frac{\partial \hat{f}(\eta; p)}{\partial \eta}\Big|_{\eta=0} = 1, \quad \frac{\partial \hat{f}(\eta; p)}{\partial \eta}\Big|_{\eta=\infty} = 0, \quad (2.33)$$

$$\hat{\theta}(\eta; p)\Big|_{\eta=0} = 1, \quad \hat{\theta}(\eta; p)\Big|_{\eta=\infty} = 0, \quad (2.34)$$

$$\begin{aligned}
\mathcal{N}_f [\hat{f}(\eta; p), \hat{\theta}(\eta; p)] &= \frac{\partial^3 \hat{f}(\eta; p)}{\partial \eta^3} - \left(\frac{\partial \hat{f}(\eta; p)}{\partial \eta} \right)^2 + \hat{f}(\eta; p) \frac{\partial^2 \hat{f}(\eta; p)}{\partial \eta^2} - M^2 \frac{\partial \hat{f}(\eta; p)}{\partial \eta} \\
&\quad + \lambda \hat{\theta}(\eta; p) - A \left(\frac{\eta \partial^2 \hat{f}(\eta; p)}{2 \partial \eta^2} + \frac{\partial \hat{f}(\eta; p)}{\partial \eta} \right) \\
&\quad + \alpha \left[- \left(\frac{\partial^2 \hat{f}(\eta; p)}{\partial \eta^2} \right)^2 - A \left(2 \frac{\partial^3 \hat{f}(\eta; p)}{\partial \eta^3} + \frac{1}{2} \eta \frac{\partial^4 \hat{f}(\eta; p)}{\partial \eta^4} \right) \right. \\
&\quad \left. + 2 \frac{\partial \hat{f}(\eta; p)}{\partial \eta} \frac{\partial^3 \hat{f}(\eta; p)}{\partial \eta^3} - \frac{\partial \hat{f}(\eta; p)}{\partial \eta} \frac{\partial^4 \hat{f}(\eta; p)}{\partial \eta^4} \right], \tag{2.35}
\end{aligned}$$

$$\begin{aligned}
\mathcal{N}_\theta [\hat{f}(\eta; p), \hat{\theta}(\eta; p)] &= (1 + \frac{4}{3} R_d) \frac{\partial^2 \hat{\theta}(\eta; p)}{\partial \eta^2} + \Pr \left(\hat{f}(\eta; p) \frac{\partial \hat{\theta}(\eta; p)}{\partial \eta} - \hat{\theta}(\eta; p) \frac{\partial \hat{f}(\eta; p)}{\partial \eta} \right) \\
&\quad - \Pr Ec \left(\frac{\partial^2 \hat{f}(\eta; p)}{\partial \eta^2} \right)^2 - \Pr \frac{A}{2} \left[\eta \frac{\partial \hat{\theta}(\eta; p)}{\partial \eta} + 4 \hat{\theta}(\eta; p) \right] \\
&\quad - \alpha \Pr Ec \left[\frac{3}{2} A \left(\frac{\partial^2 \hat{f}(\eta; p)}{\partial \eta^2} \right)^2 + \frac{1}{2} \eta \frac{\partial^2 \hat{f}(\eta; p)}{\partial \eta^2} \frac{\partial^3 \hat{f}(\eta; p)}{\partial \eta^3} \right. \\
&\quad \left. + \frac{\partial \hat{f}(\eta; p)}{\partial \eta} \frac{\partial^2 \hat{f}(\eta; p)}{\partial \eta^2} - \frac{\partial \hat{f}(\eta; p)}{\partial \eta} \frac{\partial^2 \hat{f}(\eta; p)}{\partial \eta^2} \frac{\partial^3 \hat{f}(\eta; p)}{\partial \eta^3} \right]. \tag{2.36}
\end{aligned}$$

For $p = 0$ and $p = 1$, we have

$$\hat{f}(\eta; 0) = f_0(\eta), \quad \hat{f}(\eta; 1) = f(\eta), \tag{2.37}$$

$$\hat{\theta}(\eta; 0) = \theta_0(\eta), \quad \hat{\theta}(\eta; 1) = \theta(\eta) \tag{2.38}$$

and when p increases from 0 to 1, $\hat{f}(\eta; p)$ and $\hat{\theta}(\eta; p)$ deforms from $f_0(\eta)$ and $\theta_0(\eta)$ to $f(\eta)$ and $\theta(\eta)$ respectively. Expanding $\hat{f}(\eta; p)$ and $\hat{\theta}(\eta; p)$ we have

$$\hat{f}(\eta; p) = f_0(\eta) + \sum_{m=1}^{\infty} f_m(\eta) p^m, \tag{2.39}$$

$$\hat{\theta}(\eta; p) = \theta_0(\eta) + \sum_{m=1}^{\infty} \theta_m(\eta) p^m, \tag{2.40}$$

$$f_m(\eta) = \frac{1}{m!} \left. \frac{\partial^m \widehat{f}(\eta; p)}{\partial p^m} \right|_{p=0}, \quad \theta_m(\eta) = \frac{1}{m!} \left. \frac{\partial^m \widehat{\theta}(\eta; p)}{\partial p^m} \right|_{p=0} \quad (2.41)$$

and the auxiliary parameters \hbar_f and \hbar_θ are selected in such a way that the series (2.39) and (2.40) converge at $p = 1$. Therefore

$$f(\eta) = f_0(\eta) + \sum_{m=1}^{\infty} f_m(\eta), \quad (2.42)$$

$$\theta(\eta) = \theta_0(\eta) + \sum_{m=1}^{\infty} \theta_m(\eta). \quad (2.43)$$

The m th order deformation problems are

$$\mathcal{L}_f [f_m(\eta) - \chi_m f_{m-1}(\eta)] = \hbar_f \mathcal{R}_m^f(\eta), \quad (2.44)$$

$$\mathcal{L}_\theta [\theta_m(\eta) - \chi_m \theta_{m-1}(\eta)] = \hbar_\theta \mathcal{R}_m^\theta(\eta), \quad (2.45)$$

$$\begin{aligned} f_m(0) = 0, \quad f'_m(0) = 0, \quad f'_m(\infty) = 0, \quad \theta_m(0) = 0, \quad \theta_m(\infty) = 0, \\ \phi_m(0) = 0, \quad \phi_m(\infty) = 0, \end{aligned} \quad (2.46)$$

where

$$\begin{aligned} \mathcal{R}_m^f(\eta) = & f'''_{m-1} - A(f'_{m-1} + \frac{1}{2}\eta f''_{m-1}) + \alpha A(2f'''_{m-1} + \frac{1}{2}\eta f''''_{m-1}) - M^2 f'_{m-1} \\ & + \lambda \theta_{m-1-k} + \sum_{k=0}^{m-1} \left[\begin{aligned} & f_{m-1-k} f''_k - f'_{m-1-k} f'_k \\ & + \alpha (2f_{m-1-k} f'''_k - f''_{m-1-k} f''_k - f_{m-1-k} f''''_k) \end{aligned} \right], \end{aligned} \quad (2.47)$$

$$\mathcal{R}_m^\theta(\eta) = \left(1 + \frac{4}{3}R_d\right)\theta''_{m-1} - \Pr \frac{A}{2} (\eta\theta'_{m-1} + 4\theta_{m-1}) + \Pr \sum_{k=0}^{m-1} (f_{m-1-k}\theta'_k - f'_{m-1-k}\theta_k) - \Pr Ec \left[\sum_{k=0}^{m-1} \left[f''_{m-1-k}f''_k + \alpha \left(\frac{A}{2} (3f''_{m-1-k}f''_k + \eta f''_{m-1-k}f''_k) + f'_{m-1-k} \sum_{l=0}^k f''_{k-l}f''_l - f_{m-1-k} \sum_{l=0}^k f''_{k-l}f'''_l \right) \right] \right], \quad (2.48)$$

$$\chi_m = \begin{cases} 0, & m \leq 1, \\ 1, & m > 1. \end{cases} \quad (2.49)$$

The general solutions of Eqs. (2.44) – (2.46) are

$$f_m(\eta) = f_m^*(\eta) + C_1 + C_2 \exp(\eta) + C_3 \exp(-\eta), \quad (2.50)$$

$$\theta_m(\eta) = \theta_m^*(\eta) + C_4 \exp(\eta) + C_5 \exp(-\eta), \quad (2.51)$$

where $f_m^*(\eta)$ and $\theta_m^*(\eta)$ depict the special solutions and

$$\begin{aligned} C_2 &= C_4 = 0, \\ C_1 &= -C_3 - f_m^*(0), \quad C_3 = \left. \frac{\partial f_m^*(\eta)}{\partial \eta} \right|_{\eta=0}, \\ C_5 &= -\theta_m^*(0). \end{aligned} \quad (2.52)$$

2.3 Convergence of the series solutions

It is obvious that the series solutions (2.42) and (2.43) contain non-zero auxiliary parameters \hbar_f and \hbar_θ . Such parameters are useful in adjusting and controlling the convergence. For the allowed values of \hbar_f and \hbar_θ of the functions $f''(0)$ and $\theta'(0)$ the \hbar_f and \hbar_θ –curves are plotted for 20th-order of approximations. Fig. 2.1 depicts that the range for the admissible values of \hbar_f and \hbar_θ are $-1.1 \leq \hbar_f, \hbar_\theta \leq -0.3$. The series given by (2.42) and (2.43) converge in the whole region of η for $\hbar_f = \hbar_\theta = -0.6$. Table 2.1 elucidates the convergence of HAM solutions

for $-f''(0)$ and $-\theta'(0)$ at different order of approximations when $\alpha = 0.2$, $A = 0.2$, $S = 0.5$, $M = 1.0$, $\lambda = 1.5$, $Pr = 0.7$, $R_d = 0.3$ and $Ec = 0.5$.

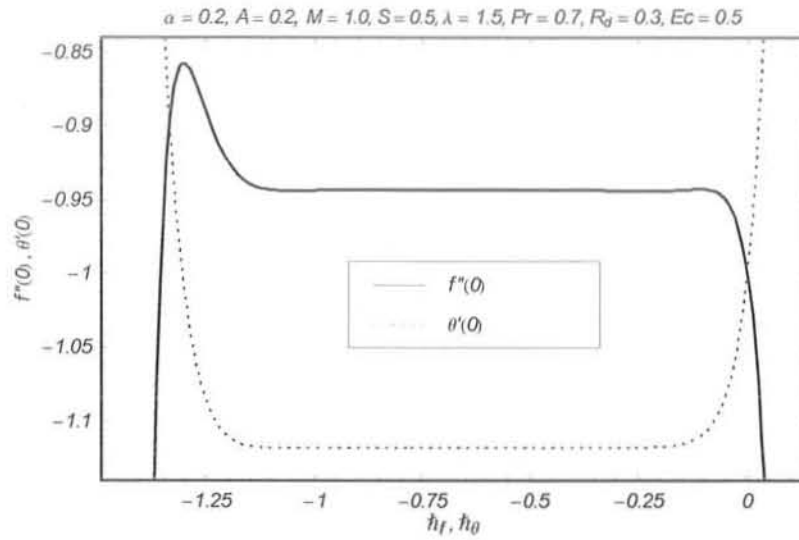


Fig. 2.1: The h -curves of the functions $f''(0)$ and $\theta'(0)$ at 20^{th} order of approximation.

Order of convergence	$-f''(0)$	$-\theta'(0)$
1	0.934000	1.062300
5	0.933202	1.072775
10	0.931987	1.071984
15	0.931871	1.071892
20	0.931861	1.071876
25	0.931861	1.071876
30	0.931861	1.071876

Table 2.1: Convergence of HAM solutions for different order of approximations when $\alpha = 0.2$, $A = 0.2$, $S = 0.5$, $M = 1.0$, $\lambda = 1.5$, $Pr = 0.7$, $R_d = 0.3$ and $Ec = 0.5$.

2.4 Results and discussion

The aim of this section is to examine the effects of second grade parameter α , unsteadiness parameter A , suction parameter S , Hartman number M , mixed convection parameter λ , Prandtl number Pr , radiation parameter R_d and Eckert number Ec on the velocity and temperature fields in Figs. 2.2 – 2.17. The variation of skin friction coefficient $Re_x^{1/2}C_f$ and the local Nusselt number $Re_x^{-1/2}Nu_x$ for different involved parameters are also computed in the Tables 2.2 and 2.3.

Figs. 2.2 and 2.3 illustrate the influence of second grade parameter α on the velocity and temperature profiles respectively. It is observed that f' is an increasing function of α whereas the temperature field θ decreases when α is increased. The effect of unsteadiness parameter A is explained in the Figs. 2.4 and 2.5. Both velocity and temperature fields decrease when unsteadiness parameter A is increased. The influence of suction parameter S is shown in Figs. 2.6 and 2.7. It is seen that velocity and boundary layer thickness are decreasing functions of S . The thermal boundary layer thickness also decreases by increasing S . Porous wall is a powerful mechanism for controlling momentum of the boundary layer regime flow in actual applications. Fig. 2.8 describes the variation of M on f' . Obviously f' is a decreasing function of M . This is in view of the fact that an increase of M signifies the increase of Lorentz force thereby decreasing the magnitude of velocity. However temperature profile increases upon increasing the Hartman number M (Fig. 2.9). The increasing frictional drag due to the Lorentz force is responsible for increasing the thermal boundary layer thickness. Magnetic field can control the flow characteristics. The influence of λ on f' (from Fig. 2.10) is similar when compared with Fig. 2.1 but the increment in f' is slightly larger in case of λ when compared with the effects of α . Infact increasing values of λ corresponds to the stronger buoyancy force which causes an increase in flow velocity. The thermal boundary layer decreases by increasing λ (Fig. 2.11). Figs. 2.12 and 2.14 describe the effects of Pr and Ec on f' respectively. Both Ec and

Pr decrease the velocity profile. Infact an increase in the Prandtl number leads to an increase in fluid viscosity which causes a decrease in the flow velocity. As expected it is found that θ is decreasing by increasing Pr (Fig.2.13). A higher Prandtl number fluid has a thinner thermal boundary layer and this increase the gradient of the temperature. Fig. 2.17 clearly indicates that an increase in the radiation parameter R_d leads to an increase of the temperature profiles and boundary layer thickness with R_d .

From Table 2.2 it is noticed that the magnitude of skin friction coefficient increases for large values of α , A , M and S . The skin friction coefficient on the wall increases with the application of magnetic field. This is because of the magnetic force acts as a retarding force and causes an increase of shear stress. We found that for a fixed values of other parameters, the local Nusselt number increases with an increase in the radiation parameter R_d . The local Nusselt number is increased as Pr increases. Table 2.3 shows that the magnitude of skin friction coefficient decreases for large values of λ and R_d while it has opposite behaviors for Pr and Ec .

2.5 Concluding remarks

Heat transfer analysis in presence of thermal radiation is discussed for an unsteady mixed convection flow of an incompressible second grade fluid. Series solutions for velocity and temperature fields are developed and discussed. The main results of the present analysis are listed below.

- The effects of M , Pr and Ec on f' are similar in a qualitative sense.
- Velocity f' is an increasing function of second grade parameter α .
- Thermal boundary layer decreases by increasing λ
- Behaviors of R_d and Pr on the temperature θ are opposite.
- Temperature θ is decreasing function of Pr.

- Skin friction coefficient decreases for large values of λ and R_d .

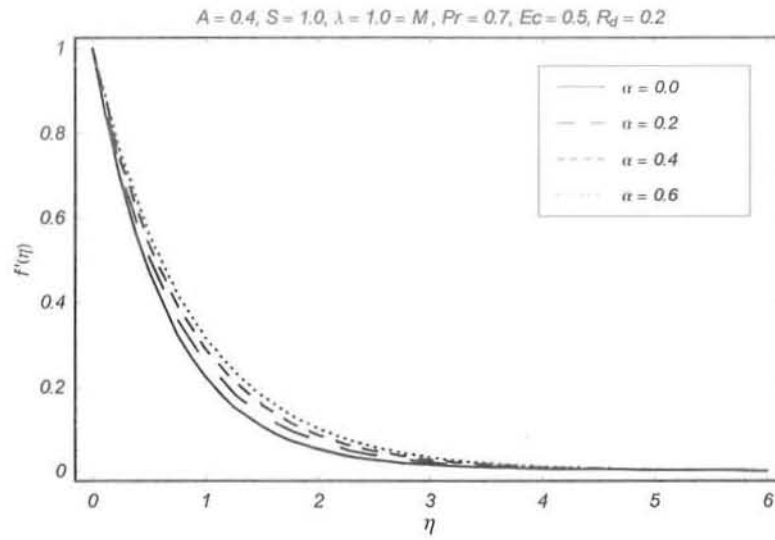


Fig. 2.2. Influence of second grade parameter α on f' .

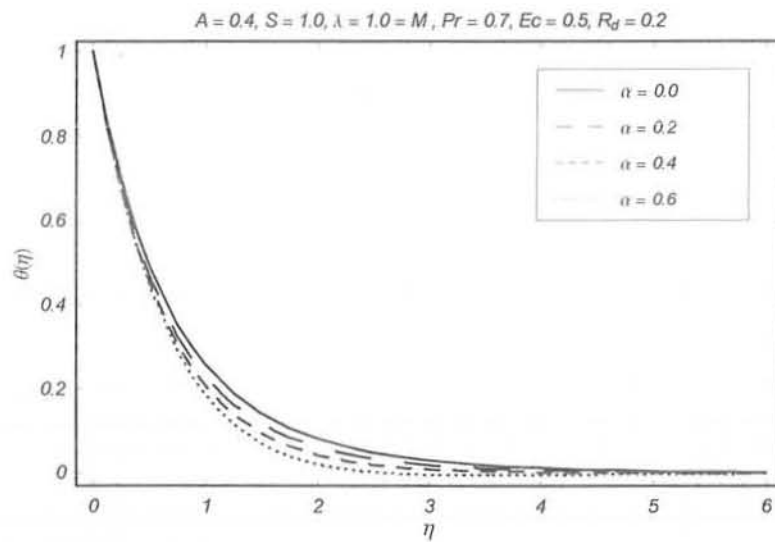


Fig. 2.3. Influence of second grade parameter α on θ .

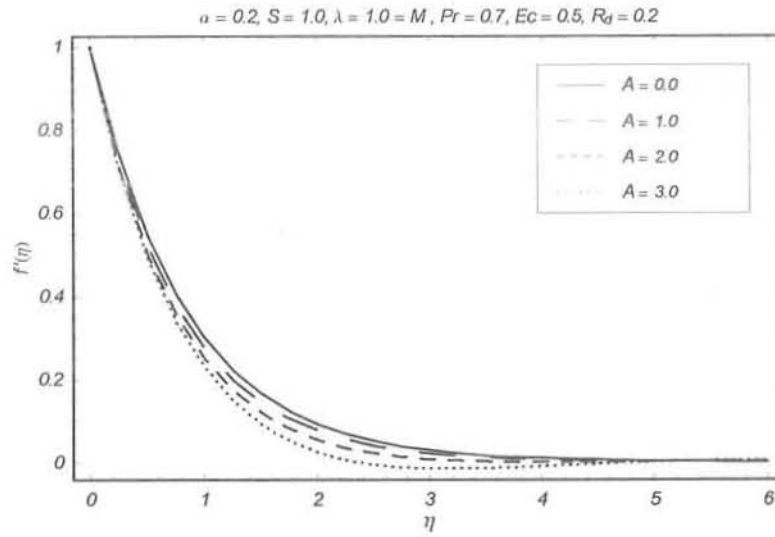


Fig. 2.4. Influence of unsteadiness parameter A on f' .

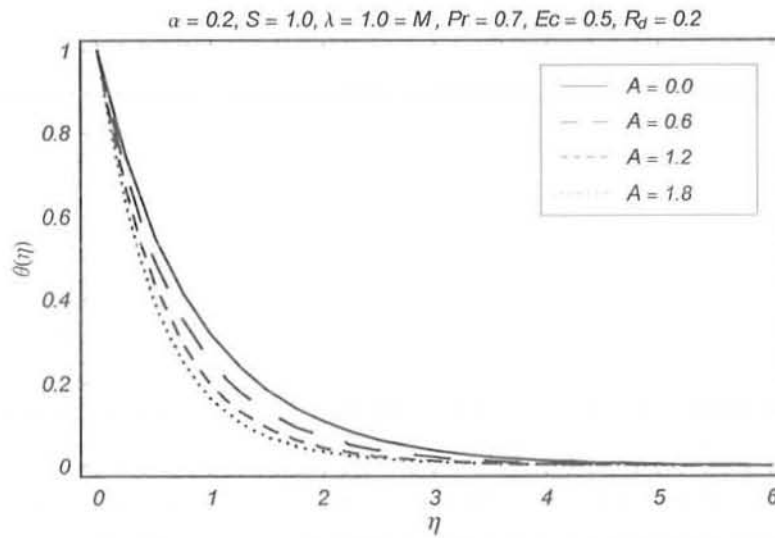


Fig. 2.5. Influence of unsteadiness parameter A on θ .

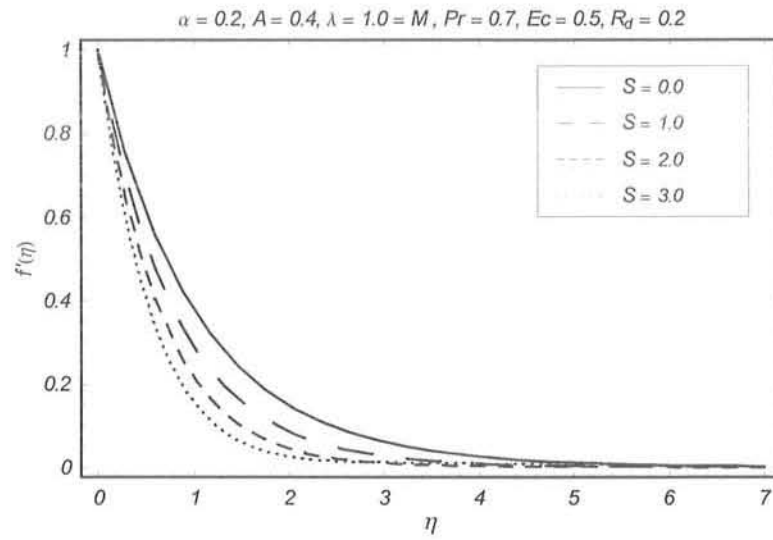


Fig. 2.6. Influence of suction parameter S on f' .

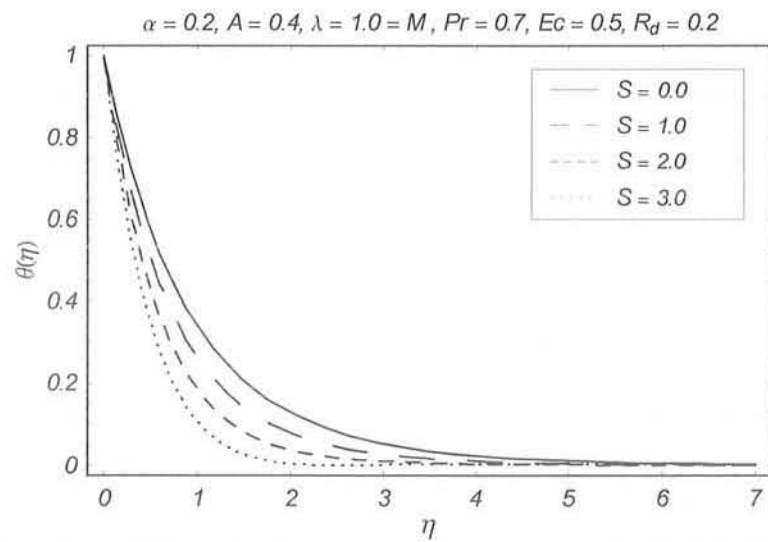


Fig. 2.7. Influence of suction parameter S on θ .

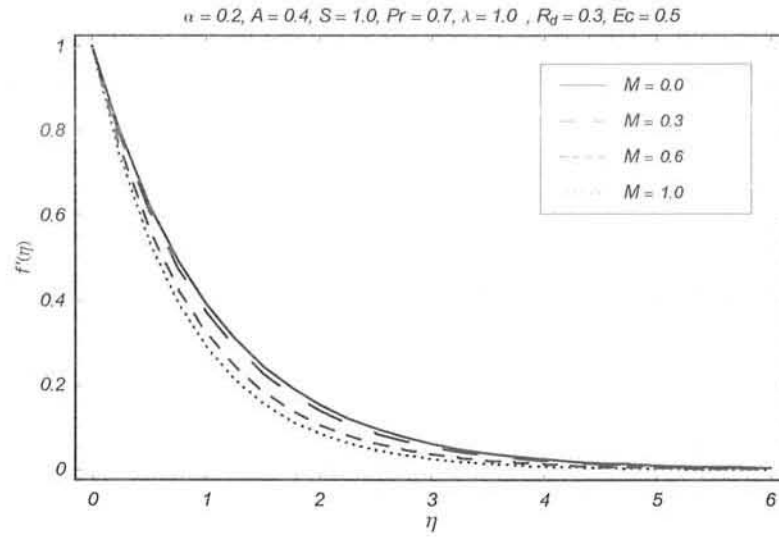


Fig. 2.8. Influence of magnetic field parameter M on f' .

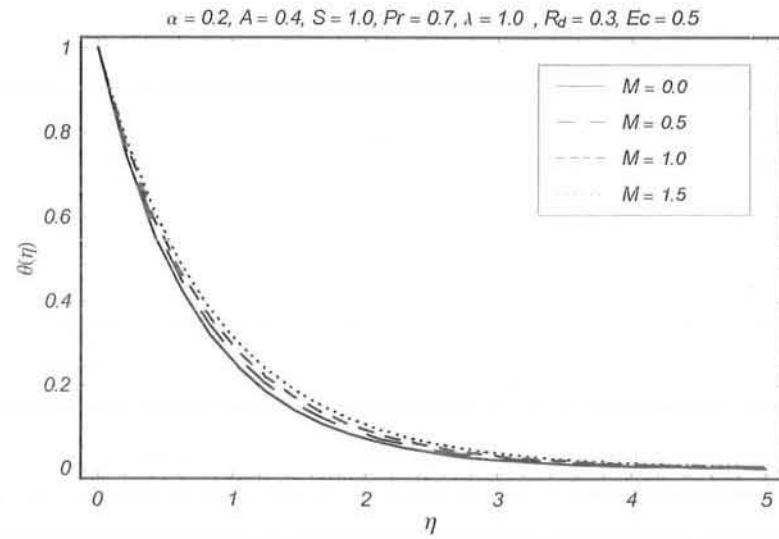


Fig. 2.9. Influence of magnetic field parameter M on θ .

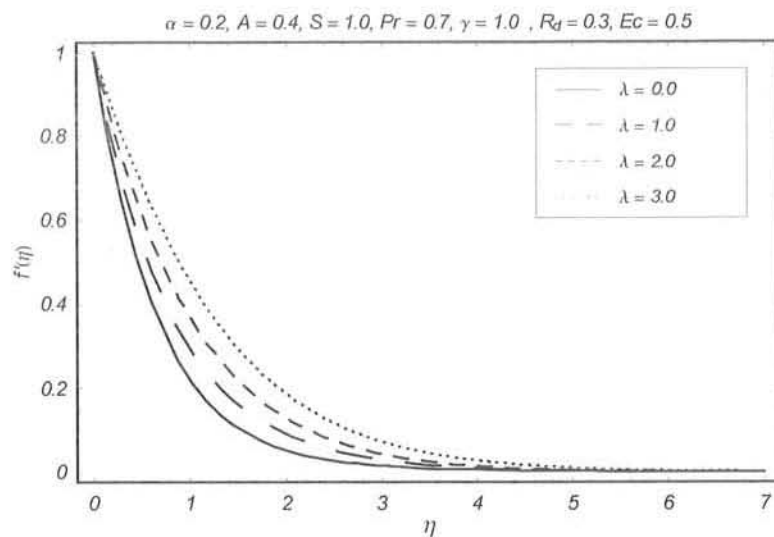


Fig. 2.10. Influence of mixed convection parameter λ on f' .

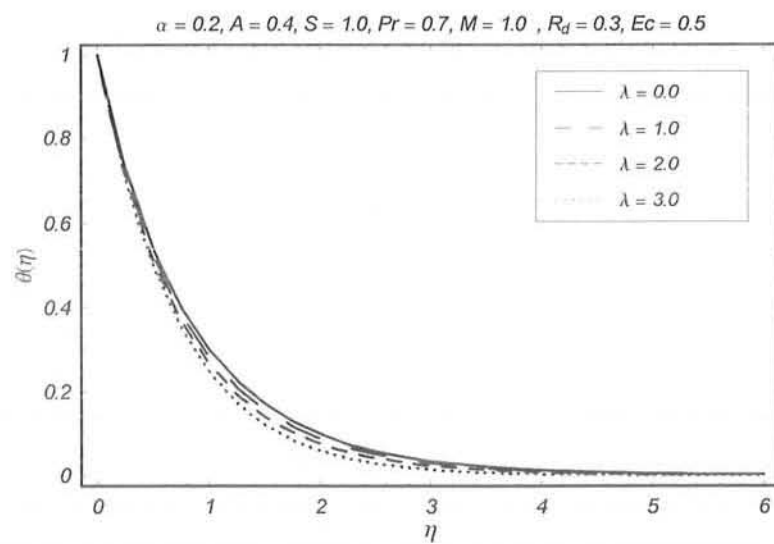


Fig. 2.11. Influence of mixed convection parameter λ on θ .

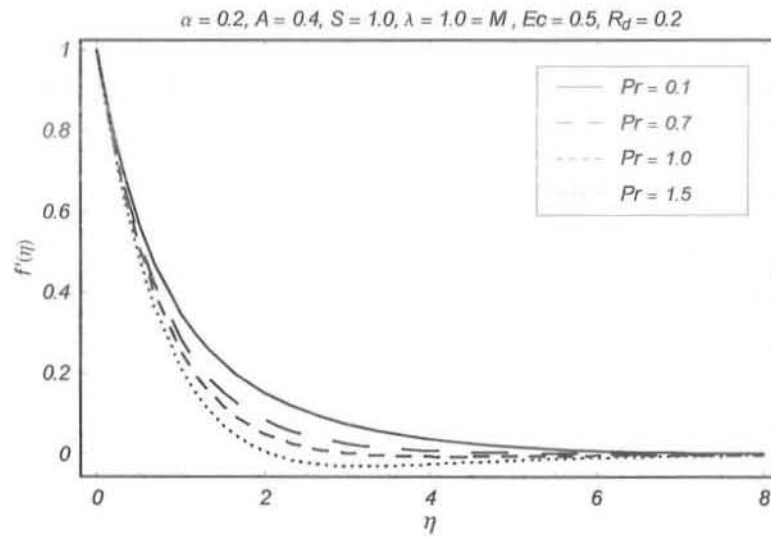


Fig. 2.12. Influence of Prandtl number Pr on f' .

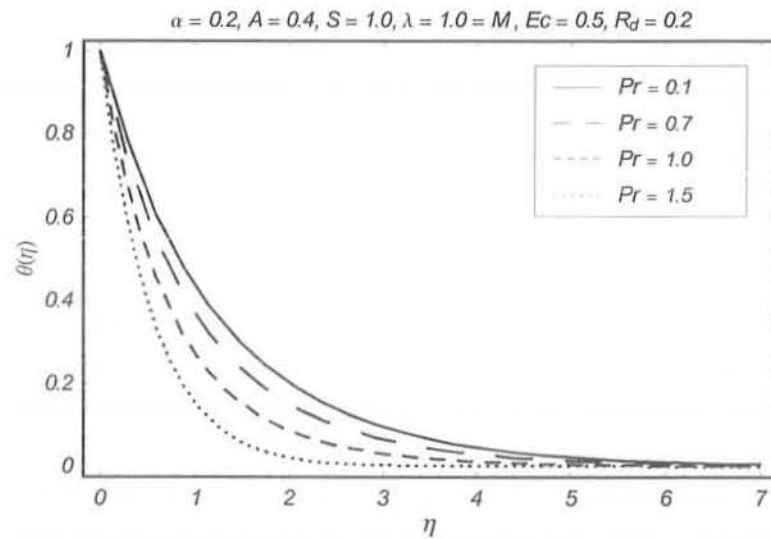


Fig. 2.13. Influence of Prandtl number Pr on θ .

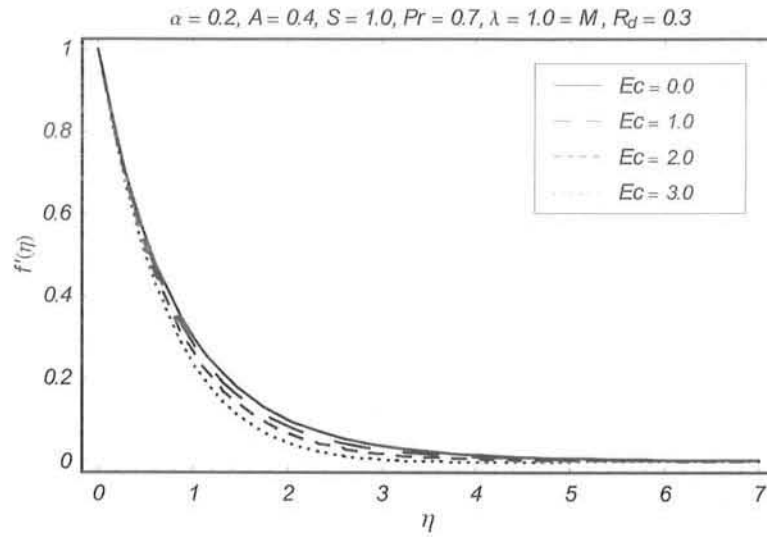


Fig. 2.14. Influence of Eckert number Ec on f' .

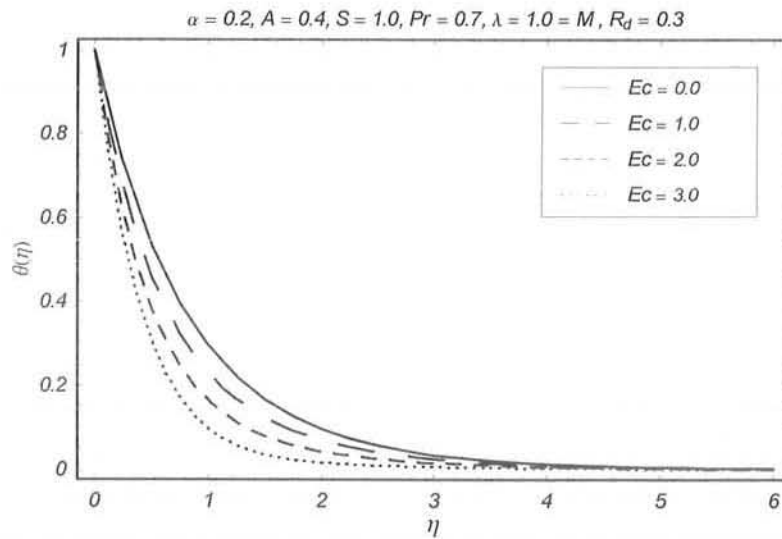


Fig. 2.15. Influence of Eckert number Ec on θ .

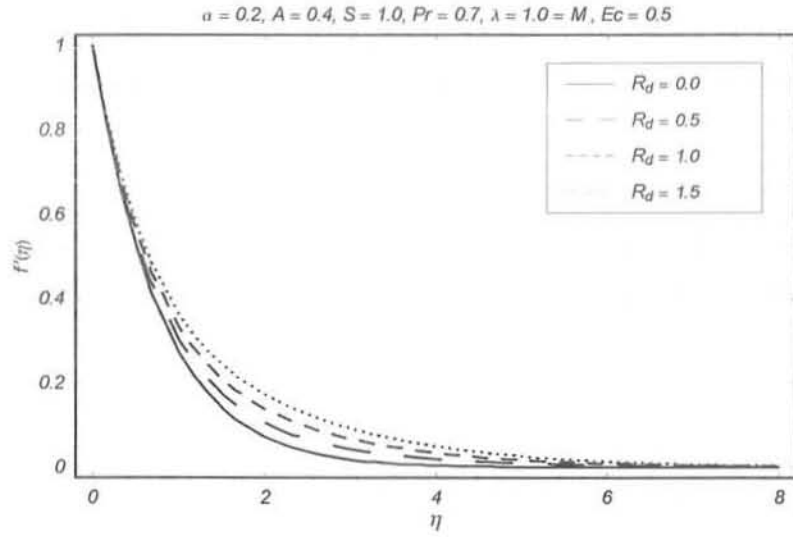


Fig. 2.16. Influence of radiation parameter R_d on f'' .

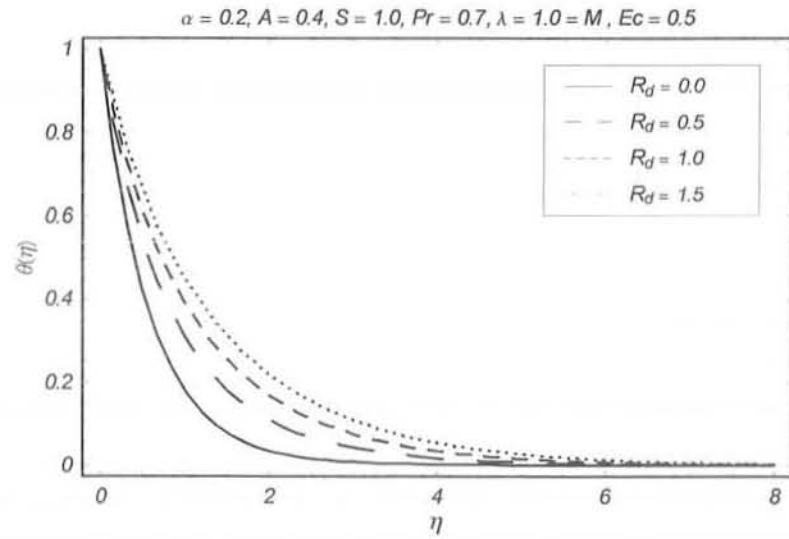


Fig. 2.17. Influence of radiation parameter R_d on θ .

α	A	S	M	$-Re_x^{-1/2} C_f$	$-Re_x^{-1/2} Nu_x$
0.0	0.3	1.0	1.0	1.410729	1.331094
0.1				1.663287	1.357985
0.2				1.915516	1.379278
0.3				2.157693	1.397342
0.1	0.0	1.0	1.0	1.473777	1.128001
	0.2			1.604252	1.287265
	0.5			1.772210	1.486206
	1.0			2.011094	1.754981
0.1	0.3	0.0	1.0	1.138991	1.021669
		0.5		1.391402	1.176773
		1.0		1.663289	1.357986
		2.0		2.195402	1.796294
0.1	0.3	1.0	0.0	1.376664	1.299427
			0.5	1.520058	1.303633
			1.0	1.893507	1.318593
			1.5	2.392306	1.347098

Table 2.2: Values of skin friction coefficient $Re_x^{-1/2} C_f$ and local Nusselt number $Re_x^{-1/2} Nu_x$ for some values of α , A , S and M when $Pr = 0.7$, $Ec = 0.5$ and $R_d = 0.2$.

λ	Pr	Ec	R_d	$-Re_x^{-1/2} C_f$	$-Re_x^{-1/2} Nu_x$
0.0	0.7	0.5	0.3	2.566913	1.360468
1.0				2.106632	1.329651
2.0				1.689495	1.309902
3.0				1.304385	1.298427
1.5	0.5	0.5	0.3	1.759576	1.029008
	0.7			1.893504	1.318593
	1.0			2.037612	1.733572
	1.4			2.168786	2.263574
1.5	0.7	0.0	0.3	1.848007	1.155598
		1.0		1.941544	1.494708
		2.0		2.046708	1.892974
		3.0		2.461445	3.609218
1.5	0.7	0.5	0.0	2.029563	1.706453
			0.5	1.823451	1.158098
			1.0	1.692786	0.908656
			1.5	1.601013	0.763227

Table 2.3: Values of skin friction coefficient $Re_x^{-1/2} C_f$ and local Nusselt number $Re_x^{-1/2} Nu_x$ for some values of λ , Pr, Ec and R_d when $\alpha = 0.2$, $A = 0.3$ and $S = M = 1.0$.

Chapter 3

Unsteady three-dimensional flow of an elasto-viscous fluid in the presence of mass transfer

The purpose of this chapter is to discuss the unsteady three-dimensional MHD flow of an elasto-viscous fluid over a stretching surface. The whole analysis is examined in the presence of mass transfer. The governing boundary layer equations are reduced into the partial differential equations by similarity transformations. The transformed system of equations is solved analytically by employing homotopy analysis method (HAM). Plots for various interesting parameters are presented and discussed. Numerical data for shear stresses and surface mass transfer in steady case is also tabulated.

3.1 Problem statement

Here we study the mass transfer effects on unsteady three-dimensional flow of an elasto-viscous fluid bounded by a stretching surface. A constant applied magnetic field \mathbf{B}_0 is exerted

in the y -direction. The magnetic Reynolds number is chosen very small and hence an induced magnetic field is not considered. No electric field is applied. Under the stated assumptions, the relevant equations are as follows:

$$\frac{\partial u}{\partial x} + \frac{\partial v}{\partial y} + \frac{\partial w}{\partial z} = 0, \quad (3.1)$$

$$\frac{\partial u}{\partial t} + u \frac{\partial u}{\partial x} + v \frac{\partial u}{\partial y} + w \frac{\partial u}{\partial z} = \nu \frac{\partial^2 u}{\partial z^2} - k_0 \left(\begin{array}{c} \left(\frac{\partial^3 u}{\partial z^2 \partial t} + u \frac{\partial^3 u}{\partial x \partial z^2} + w \frac{\partial^3 u}{\partial z^3} \right) \\ - \left(\frac{\partial u}{\partial x} \frac{\partial^2 u}{\partial z^2} + \frac{\partial u}{\partial z} \frac{\partial^2 w}{\partial z^2} \right) \\ + 2 \frac{\partial u}{\partial z} \frac{\partial^2 u}{\partial x \partial z} + 2 \frac{\partial w}{\partial z} \frac{\partial^2 u}{\partial z^2} \end{array} \right) - \frac{\sigma B_0^2}{\rho} u, \quad (3.2)$$

$$\frac{\partial v}{\partial t} + u \frac{\partial v}{\partial x} + v \frac{\partial v}{\partial y} + w \frac{\partial v}{\partial z} = \nu \frac{\partial^2 v}{\partial z^2} - k_0 \left(\begin{array}{c} \left(\frac{\partial^3 v}{\partial z^2 \partial t} + v \frac{\partial^3 v}{\partial v \partial z^2} + w \frac{\partial^3 v}{\partial z^3} \right) \\ - \left(\frac{\partial v}{\partial y} \frac{\partial^2 v}{\partial z^2} + \frac{\partial v}{\partial z} \frac{\partial^2 w}{\partial z^2} \right) \\ + 2 \frac{\partial v}{\partial z} \frac{\partial^2 v}{\partial y \partial z} + 2 \frac{\partial w}{\partial z} \frac{\partial^2 v}{\partial z^2} \end{array} \right) - \frac{\sigma B_0^2}{\rho} v, \quad (3.3)$$

$$\frac{\partial C}{\partial t} + u \frac{\partial C}{\partial x} + v \frac{\partial C}{\partial y} + w \frac{\partial C}{\partial z} = D \frac{\partial^2 C}{\partial z^2} - RC, \quad (3.4)$$

where u , v and w denote the respective velocities in the x -, y - and z -directions, ρ the fluid density, ν the kinematic viscosity, σ the electrical conductivity of the fluid, k_0 the material parameter, C the concentration species and D the diffusion coefficient of the diffusing species in the fluid and R the first -order homogeneous constant reaction rate.

The prescribed boundary conditions are

$$\begin{aligned}
u &= v = w = 0, \quad C = C_\infty, \quad t < 0, \\
u &= u_w = ax, \quad v = v_w = by, \quad w = 0, \quad C = C_w, \quad z = 0; \quad t \geq 0, \\
u &\rightarrow 0, \quad v \rightarrow 0, \quad \frac{\partial u}{\partial z} \rightarrow 0, \quad \frac{\partial v}{\partial z} \rightarrow 0, \quad C \rightarrow 0, \quad \text{as } z \rightarrow \infty; \quad t \geq 0
\end{aligned} \tag{3.5}$$

in which the constants a and b are positive.

By virtue of the following dimensionless quantities

$$\begin{aligned}
\eta &= \sqrt{\frac{a}{\nu\xi}}z, \quad u = ax \frac{\partial f(\eta, \xi)}{\partial \eta}, \quad v = ay \frac{\partial g(\eta, \xi)}{\partial \eta}, \quad w = -\sqrt{a\nu\xi} [f(\eta, \xi) + g(\eta, \xi)], \\
\xi &= 1 - \exp(-\tau), \quad \tau = at.
\end{aligned} \tag{3.6}$$

equation (3.1) is satisfied identically and Eqs. (3.2) – (3.5) take the forms given below

$$\begin{aligned}
&\xi \frac{\partial^3 f}{\partial \eta^3} + \xi^2 \left[(f + g) \frac{\partial^2 f}{\partial \eta^2} - \left(\frac{\partial f}{\partial \eta} \right)^2 - M^2 \frac{\partial f}{\partial \eta} \right] + \xi(1 - \xi) \left[\frac{\eta}{2} \frac{\partial^2 f}{\partial \eta^2} - \xi \frac{\partial^2 f}{\partial \xi \partial \eta} \right] \\
&+ K \left[\begin{aligned} &(1 - \xi) \frac{\partial^3 f}{\partial \eta^3} + \xi(f + g) \frac{\partial^4 f}{\partial \eta^4} + \xi \left(\frac{\partial^2 f}{\partial \eta^2} - \frac{\partial^2 g}{\partial \eta^2} \right) \frac{\partial^2 f}{\partial \eta^2} \\ &- 2\xi \left(\frac{\partial f}{\partial \eta} + \frac{\partial g}{\partial \eta} \right) \frac{\partial^3 f}{\partial \eta^3} + (1 - \xi) \left(\frac{\eta}{2} \frac{\partial^4 f}{\partial \eta^4} - \xi \frac{\partial^4 f}{\partial \xi \partial \eta^3} \right) \end{aligned} \right] = 0,
\end{aligned} \tag{3.7}$$

$$\begin{aligned}
&\xi \frac{\partial^3 g}{\partial \eta^3} + \xi^2 \left[(f + g) \frac{\partial^2 g}{\partial \eta^2} - \left(\frac{\partial g}{\partial \eta} \right)^2 - M^2 \frac{\partial g}{\partial \eta} \right] + \xi(1 - \xi) \left[\frac{\eta}{2} \frac{\partial^2 g}{\partial \eta^2} - \xi \frac{\partial^2 g}{\partial \xi \partial \eta} \right] \\
&+ K \left[\begin{aligned} &(1 - \xi) \frac{\partial^3 g}{\partial \eta^3} + \xi(f + g) \frac{\partial^4 g}{\partial \eta^4} + \xi \left(\frac{\partial^2 g}{\partial \eta^2} - \frac{\partial^2 f}{\partial \eta^2} \right) \frac{\partial^2 g}{\partial \eta^2} \\ &- 2\xi \left(\frac{\partial f}{\partial \eta} + \frac{\partial g}{\partial \eta} \right) \frac{\partial^3 g}{\partial \eta^3} + (1 - \xi) \left(\frac{\eta}{2} \frac{\partial^4 g}{\partial \eta^4} - \xi \frac{\partial^4 g}{\partial \xi \partial \eta^3} \right) \end{aligned} \right] = 0,
\end{aligned} \tag{3.8}$$

$$\frac{\partial^2 \phi}{\partial \eta^2} + Sc(1 - \xi) \left[\frac{\eta}{2} \frac{\partial \phi}{\partial \eta} - \xi \frac{\partial \phi}{\partial \xi} \right] + Sc\xi(f + g) \frac{\partial \phi}{\partial \eta} - \gamma Sc\xi\phi = 0. \tag{3.9}$$

$$\begin{aligned}
f(0, \xi) &= g(0, \xi) = 0, & \frac{\partial f(0, \xi)}{\partial \eta} &= \phi(0, \xi) = 1, \\
\frac{\partial g(0, \xi)}{\partial \eta} &= c, & \frac{\partial f(\infty, \xi)}{\partial \eta} &= \frac{\partial g(\infty, \xi)}{\partial \eta} = \phi(\infty, \xi) = 0, \\
\frac{\partial^2 f(\infty, \xi)}{\partial \eta^2} &= \frac{\partial^2 g(\infty, \xi)}{\partial \eta^2} = 0.
\end{aligned} \tag{3.10}$$

$$K = \frac{k_0 a}{\nu}, \quad c = \frac{b}{a}, \quad M^2 = \frac{\sigma B_0^2}{\rho a}, \quad Sc = \frac{\nu}{D}, \quad \gamma = \frac{R}{a}. \tag{3.11}$$

In the above equations $c (= b/a)$, K , M , Sc , and γ are the dimensionless stretching, viscoelastic, Hartman, Schmidt and chemical reaction parameters respectively. Obviously for $c = 0$, the problem reduces to the two-dimensional case. It should be further noted that for destructive/generative chemical reaction $\gamma > 0/\gamma < 0$ respectively and $\gamma = 0$ corresponds to non-reactive species.

Expressions of skin friction coefficients C_{fx} and C_{fy} in the x - and y -directions and local Sherwood number Sh are given by

$$C_{fx} = \frac{\tau_{wx}}{\rho u_w^2}, \quad C_{fy} = \frac{\tau_{wy}}{\rho v_w^2}, \quad Sh = \frac{x J_w}{D (C_w - C_\infty)} \tag{3.12}$$

where τ_{wx} and τ_{wy} are the skin frictions along x and y - directions and J_w is the mass flux.

From (3.6) and (3.12) we arrive at

$$\begin{aligned}
\xi^{1/2} \text{Re}_x^{1/2} C_{fx} &= \left[\frac{\partial^2 f}{\partial \eta^2} + K \left(\frac{1-\xi}{2\xi} \left(\frac{\partial f}{\partial \eta} - \eta \frac{\partial^3 f}{\partial \eta^3} \right) + (1-\xi) \frac{\partial^3 f}{\partial \xi \partial \eta^2} + \right. \right. \\
&\quad \left. \left. 3 \left(\frac{\partial f}{\partial \eta} + \frac{\partial g}{\partial \eta} \right) \frac{\partial^2 f}{\partial \eta^2} - (f+g) \frac{\partial^2 f}{\partial \eta^2} \right) \right] \Big|_{\eta=0}, \\
\xi^{1/2} \text{Re}_y^{1/2} C_{fy} &= \left[\frac{\partial^2 g}{\partial \eta^2} + K \left(\frac{1-\xi}{2\xi} \left(\frac{\partial g}{\partial \eta} - \eta \frac{\partial^3 g}{\partial \eta^3} \right) + (1-\xi) \frac{\partial^3 g}{\partial \xi \partial \eta^2} + \right. \right. \\
&\quad \left. \left. 3 \left(\frac{\partial g}{\partial \eta} + \frac{\partial f}{\partial \eta} \right) \frac{\partial^2 g}{\partial \eta^2} - (f+g) \frac{\partial^2 g}{\partial \eta^2} \right) \right] \Big|_{\eta=0}, \\
\xi^{1/2} Sh \text{Re}_x^{-1/2} &= - \frac{\partial \phi}{\partial \eta} \Big|_{\eta=0}
\end{aligned} \tag{3.13}$$

in which the local Reynolds number is $Re_x = u_w x / \nu$.

For the steady-state results ($\xi = 1$), Eqs. (3.7) – (3.9) are reduced to

$$\frac{\partial^3 f}{\partial \eta^3} + \left[(f+g) \frac{\partial^2 f}{\partial \eta^2} - \left(\frac{\partial f}{\partial \eta} \right)^2 - M^2 \frac{\partial f}{\partial \eta} \right] + K \left[\begin{array}{l} (f+g) \frac{\partial^4 f}{\partial \eta^4} + \left(\frac{\partial^2 f}{\partial \eta^2} - \frac{\partial^2 g}{\partial \eta^2} \right) \frac{\partial^2 f}{\partial \eta^2} \\ -2 \left(\frac{\partial f}{\partial \eta} + \frac{\partial g}{\partial \eta} \right) \frac{\partial^3 f}{\partial \eta^3} \end{array} \right] = 0 \quad (3.14)$$

$$\frac{\partial^3 g}{\partial \eta^3} + \left[(f+g) \frac{\partial^2 g}{\partial \eta^2} - \left(\frac{\partial g}{\partial \eta} \right)^2 - M^2 \frac{\partial g}{\partial \eta} \right] + K \left[\begin{array}{l} (f+g) \frac{\partial^4 f}{\partial \eta^4} + \left(\frac{\partial^2 g}{\partial \eta^2} - \frac{\partial^2 f}{\partial \eta^2} \right) \frac{\partial^2 g}{\partial \eta^2} \\ -2 \left(\frac{\partial f}{\partial \eta} + \frac{\partial g}{\partial \eta} \right) \frac{\partial^3 g}{\partial \eta^3} \end{array} \right] = 0 \quad (3.15)$$

$$\frac{\partial^2 \phi}{\partial \eta^2} + Sc(f+g) \frac{\partial \phi}{\partial \eta} - \gamma Sc \phi = 0. \quad (3.16)$$

3.2 Homotopy analysis solutions

For homotopy solutions, we express $f(\eta, \xi)$, $g(\eta, \xi)$ and $\phi(\eta, \xi)$ by a set of base functions

$$\left\{ \xi^k \eta^j \exp(-n\eta) \mid k \geq 0, n \geq 0, j \geq 0 \right\} \quad (3.17)$$

in the forms

$$f(\eta, \xi) = a_{0,0}^0 + \sum_{k=0}^{\infty} \sum_{j=0}^{\infty} \sum_{n=1}^{\infty} a_{j,n}^k \xi^k \eta^j \exp(-n\eta), \quad (3.18)$$

$$g(\eta, \xi) = b_{0,0}^0 + \sum_{k=0}^{\infty} \sum_{j=0}^{\infty} \sum_{n=1}^{\infty} b_{j,n}^k \xi^k \eta^j \exp(-n\eta), \quad (3.19)$$

$$\phi(\eta, \xi) = \sum_{k=0}^{\infty} \sum_{j=0}^{\infty} \sum_{n=1}^{\infty} c_{j,n}^k \xi^k \eta^j \exp(-n\eta), \quad (3.20)$$

where $a_{j,n}^k$, $b_{j,n}^k$ and $c_{j,n}^k$ are the coefficients to be determined. By the rule of solution expressions and the boundary conditions (3.10), one can choose the initial guesses f_0 , g_0 and ϕ_0 of $f(\eta, \xi)$,

$g(\eta, \xi)$ and $\phi(\eta, \xi)$ and auxiliary linear operators \mathcal{L}_f , \mathcal{L}_g and \mathcal{L}_ϕ are selected as

$$f_0(\eta, \xi) = 1 - \exp(-\eta), \quad (3.21)$$

$$g_0(\eta, \xi) = c[1 - \exp(-\eta)], \quad (3.22)$$

$$\phi_0(\eta, \xi) = \exp(-\eta), \quad (3.23)$$

$$\mathcal{L}_f = \frac{d^3 f}{d\eta^3} - \frac{df}{d\eta}, \quad (3.24)$$

$$\mathcal{L}_g = \frac{d^3 g}{d\eta^3} - \frac{dg}{d\eta}, \quad (3.25)$$

$$\mathcal{L}_\phi = \frac{d^2 \phi}{d\eta^2} - \phi. \quad (3.26)$$

Clearly the operators defined by Eqs. (3.24) – (3.26) have the following properties

$$\mathcal{L}_f [C_1 + C_2 \exp(\eta) + C_3 \exp(-\eta)] = 0, \quad (3.27)$$

$$\mathcal{L}_g [C_4 + C_5 \exp(\eta) + C_6 \exp(-\eta)] = 0, \quad (3.28)$$

$$\mathcal{L}_\phi [C_7 \exp(\eta) + C_8 \exp(-\eta)] = 0, \quad (3.29)$$

in which $C_i (i = 1 - 8)$ are the arbitrary constants.

If $p \in [0, 1]$ and \hbar_f , \hbar_g and \hbar_ϕ depict the respective embedding and non-zero auxiliary parameters then the deformation problems at the zeroth order satisfy the following equations and boundary conditions

$$(1 - p)\mathcal{L}_f[\hat{f}(\eta, \xi; p) - f_0(\eta, \xi)] = p\hbar_f \mathcal{N}_f [\hat{f}(\eta, \xi; p)], \quad (3.30)$$

$$(1 - p)\mathcal{L}_g[\hat{g}(\eta, \xi; p) - g_0(\eta, \xi)] = p\hbar_g \mathcal{N}_g [\hat{f}(\eta, \xi; p), \hat{g}(\eta, \xi; p)], \quad (3.31)$$

$$(1-p) \mathcal{L}_\phi [\hat{\phi}(\eta, \xi; p) - \phi_0(\eta, \xi)] = p \hbar_\phi \mathcal{N}_\phi [\hat{f}(\eta, \xi; p), \hat{\phi}(\eta, \xi; p)], \quad (3.32)$$

$$\begin{aligned} \hat{f}(\eta; \xi) \Big|_{\eta=0} &= 0 = \hat{g}(\eta; \xi) \Big|_{\eta=0}, \quad \hat{\phi}(\eta; \xi) \Big|_{\eta=0} = \frac{\partial \hat{f}(\eta; \xi)}{\partial \eta} \Big|_{\eta=0} = 1, \\ \frac{\partial \hat{g}(\eta; \xi)}{\partial \eta} \Big|_{\eta=\infty} &= c, \quad \frac{\partial \hat{f}(\eta; \xi)}{\partial \eta} \Big|_{\eta=\infty} = \frac{\partial \hat{f}(\eta; \xi)}{\partial \eta} \Big|_{\eta=\infty} = \hat{\phi}(\eta; \xi) \Big|_{\eta=\infty} = 0, \end{aligned} \quad (3.33)$$

and the values of non-linear operators \mathcal{N}_f , \mathcal{N}_g , \mathcal{N}_θ and \mathcal{N}_ϕ are

$$\begin{aligned} \mathcal{N}_f [\hat{f}(\eta, \xi; p), \hat{g}(\eta, \xi; p)] &= \xi \frac{\partial^3 \hat{f}}{\partial \eta^3} + \xi(1-\xi) \left[\frac{\eta}{2} \frac{\partial^2 \hat{f}}{\partial \eta^2} - \xi \frac{\partial^2 \hat{f}}{\partial \eta \partial \xi} \right] \\ &\quad + \xi^2 \left[(\hat{f} + \hat{g}) \frac{\partial^2 \hat{f}}{\partial \eta^2} - \left(\frac{\partial \hat{f}}{\partial \eta} \right)^2 - M^2 \frac{\partial \hat{f}}{\partial \eta} \right] \\ &\quad + K \left[(1-\xi) \frac{\partial^3 \hat{f}}{\partial \eta^3} + \xi (\hat{f} + \hat{g}) \frac{\partial^4 \hat{f}}{\partial \eta^4} + \xi \left(\frac{\partial^2 \hat{f}}{\partial \eta^2} - \frac{\partial^2 \hat{g}}{\partial \eta^2} \right) \frac{\partial^2 \hat{f}}{\partial \eta^2} \right. \\ &\quad \left. - 2\xi \left(\frac{\partial \hat{f}}{\partial \eta} + \frac{\partial \hat{g}}{\partial \eta} \right) \frac{\partial^3 \hat{f}}{\partial \eta^3} + (1-\xi) \left(\frac{\eta}{2} \frac{\partial^4 \hat{f}}{\partial \eta^4} - \xi \frac{\partial^4 \hat{f}}{\partial \xi \partial \eta^3} \right) \right], \end{aligned} \quad (3.34)$$

$$\begin{aligned} \mathcal{N}_g [\hat{f}(\eta, \xi; p), \hat{g}(\eta, \xi; p)] &= \xi \frac{\partial^3 \hat{g}}{\partial \eta^3} + \xi(1-\xi) \left[\frac{\eta}{2} \frac{\partial^2 \hat{g}}{\partial \eta^2} - \xi \frac{\partial^2 \hat{g}}{\partial \eta \partial \xi} \right] \\ &\quad + \xi^2 \left[(\hat{f} + \hat{g}) \frac{\partial^2 \hat{g}}{\partial \eta^2} - \left(\frac{\partial \hat{g}}{\partial \eta} \right)^2 - M^2 \frac{\partial \hat{g}}{\partial \eta} \right] \\ &\quad + K \left[(1-\xi) \frac{\partial^3 \hat{g}}{\partial \eta^3} + \xi (\hat{f} + \hat{g}) \frac{\partial^4 \hat{g}}{\partial \eta^4} + \xi \left(\frac{\partial^2 \hat{g}}{\partial \eta^2} - \frac{\partial^2 \hat{f}}{\partial \eta^2} \right) \frac{\partial^2 \hat{g}}{\partial \eta^2} \right. \\ &\quad \left. - 2\xi \left(\frac{\partial \hat{f}}{\partial \eta} + \frac{\partial \hat{g}}{\partial \eta} \right) \frac{\partial^3 \hat{g}}{\partial \eta^3} + (1-\xi) \left(\frac{\eta}{2} \frac{\partial^4 \hat{g}}{\partial \eta^4} - \xi \frac{\partial^4 \hat{g}}{\partial \xi \partial \eta^3} \right) \right], \end{aligned} \quad (3.35)$$

$$\begin{aligned} \mathcal{N}_\phi [\hat{\phi}(\eta, \xi; p), \hat{f}(\eta, \xi; p), \hat{g}(\eta, \xi; p)] &= \frac{\partial^2 \hat{\phi}}{\partial \eta^2} + Sc(1-\xi) \left(\frac{\eta}{2} \frac{\partial \hat{\phi}}{\partial \eta} - \xi \frac{\partial \hat{\phi}}{\partial \xi} \right) + Sc\xi (\hat{f} + \hat{g}) \frac{\partial \hat{\phi}}{\partial \eta} \\ &\quad - \gamma Sc\xi \hat{\phi}. \end{aligned} \quad (3.36)$$

When $p = 0$ and $p = 1$ then

$$\hat{f}(\eta, \xi; 0) = f_0(\eta, \xi), \quad \hat{f}(\eta, \xi; 1) = f(\eta, \xi), \quad (3.37)$$

$$\hat{g}(\eta, \xi; 0) = g_0(\eta, \xi), \quad \hat{g}(\eta, \xi; 1) = g(\eta, \xi), \quad (3.38)$$

$$\hat{\phi}(\eta, \xi; 0) = \phi_0(\eta, \xi), \quad \hat{\phi}(\eta, \xi; 1) = \phi(\eta, \xi). \quad (3.39)$$

and Taylor's series gives

$$\hat{f}(\eta, \xi; p) = f_0(\eta, \xi) + \sum_{m=1}^{\infty} f_m(\eta, \xi) p^m, \quad (3.40)$$

$$\hat{g}(\eta, \xi; p) = g_0(\eta, \xi) + \sum_{m=1}^{\infty} g_m(\eta, \xi) p^m, \quad (3.41)$$

$$\hat{\phi}(\eta, \xi; p) = \phi_0(\eta, \xi) + \sum_{m=1}^{\infty} \phi_m(\eta, \xi) p^m, \quad (3.42)$$

$$\begin{aligned} f_m(\eta) &= \frac{1}{m!} \left. \frac{\partial^m f(\eta, \xi; p)}{\partial \eta^m} \right|_{p=0}, \quad g_m(\eta) = \frac{1}{m!} \left. \frac{\partial^m g(\eta, \xi; p)}{\partial \eta^m} \right|_{p=0} \\ \phi_m(\eta) &= \frac{1}{m!} \left. \frac{\partial^m \phi(\eta, \xi; p)}{\partial \eta^m} \right|_{p=0}. \end{aligned} \quad (3.43)$$

We select the auxiliary parameters in such a way that the series (3.40) – (3.42) converge at $p = 1$ and we have

$$f(\eta, \xi) = f_0(\eta, \xi) + \sum_{m=1}^{\infty} f_m(\eta, \xi), \quad (3.44)$$

$$g(\eta, \xi) = g_0(\eta, \xi) + \sum_{m=1}^{\infty} g_m(\eta, \xi), \quad (3.45)$$

$$\phi(\eta, \xi) = \phi_0(\eta, \xi) + \sum_{m=1}^{\infty} \phi_m(\eta, \xi). \quad (3.46)$$

The m th- order deformation problems are

$$\mathcal{L}_f [f_m(\eta, \xi) - \chi_m f_{m-1}(\eta, \xi)] = \hbar_f \mathcal{R}_m^f(\eta, \xi), \quad (3.47)$$

$$\mathcal{L}_g [g_m(\eta, \xi) - \chi_m g_{m-1}(\eta, \xi)] = \hbar_g \mathcal{R}_m^g(\eta, \xi), \quad (3.48)$$

$$\mathcal{L}_\phi [\phi_m(\eta, \xi) - \chi_m \phi_{m-1}(\eta, \xi)] = \hbar_\phi \mathcal{R}_m^\phi(\eta, \xi), \quad (3.49)$$

$$\begin{aligned} f_m(0, \xi) &= g_m(0, \xi) = \frac{\partial f_m(0, \xi)}{\partial \eta} = \frac{\partial g_m(0, \xi)}{\partial \eta} = \phi_m(0, \xi) = 0, \\ \frac{\partial f_m(\infty, \xi)}{\partial \eta} &= \frac{\partial g_m(\infty, \xi)}{\partial \eta} = \phi_m(\infty, \xi) = \frac{\partial^2 f_m(\infty, \xi)}{\partial \eta^2} = \frac{\partial^2 g_m(\infty, \xi)}{\partial \eta^2} = 0, \end{aligned} \quad (3.50)$$

where

$$\begin{aligned} \mathcal{R}_m^f(\eta) &= \xi \frac{\partial^3 f_{m-1}}{\partial \eta^3} + \xi(1-\xi) \left[\frac{\eta}{2} \frac{\partial^2 f_{m-1}}{\partial \eta^2} - \xi \frac{\partial^2 f_{m-1}}{\partial \xi \partial \eta} \right] - \xi^2 M^2 \frac{\partial f_{m-1}}{\partial \eta} \\ &+ K \left[(1-\xi) \frac{\partial^3 f_{m-1}}{\partial \eta^3} + (1-\xi) \left(\frac{\eta}{2} \frac{\partial^4 f_{m-1}}{\partial \eta^4} - \xi \frac{\partial^3 f_{m-1}}{\partial \xi \partial \eta^3} \right) \right] \\ &+ \sum_{k=0}^{m-1} \left[K \xi \left[\begin{aligned} &\xi^2 \left[(f_k + g_k) \frac{\partial^2 f_{m-1-k}}{\partial \eta^2} - \frac{\partial f_k}{\partial \eta} \frac{\partial f_{m-1-k}}{\partial \eta} \right] + \\ &(f_k + g_k) \frac{\partial^4 f_{m-1-k}}{\partial \eta^4} + \left(\frac{\partial^2 f_k}{\partial \eta^2} - \frac{\partial^2 g_k}{\partial \eta^2} \right) \frac{\partial^2 f_{m-1-k}}{\partial \eta^2} \\ &- 2 \left(\frac{\partial f_k}{\partial \eta} + \frac{\partial g_k}{\partial \eta} \right) \frac{\partial^3 f_{m-1-k}}{\partial \eta^3} \end{aligned} \right] \right], \end{aligned} \quad (3.51)$$

$$\begin{aligned} \mathcal{R}_m^g(\eta) &= \xi \frac{\partial^3 g_{m-1}}{\partial \eta^3} + \xi(1-\xi) \left[\frac{\eta}{2} \frac{\partial^2 g_{m-1}}{\partial \eta^2} - \xi \frac{\partial^2 g_{m-1}}{\partial \xi \partial \eta} \right] - \xi^2 M^2 \frac{\partial g_{m-1}}{\partial \eta} \\ &+ K \left[(1-\xi) \frac{\partial^3 g_{m-1}}{\partial \eta^3} + (1-\xi) \left(\frac{\eta}{2} \frac{\partial^4 g_{m-1}}{\partial \eta^4} - \xi \frac{\partial^3 g_{m-1}}{\partial \xi \partial \eta^3} \right) \right] \\ &+ \sum_{k=0}^{m-1} \left[K \xi \left[\begin{aligned} &\xi^2 \left[(f_k + g_k) \frac{\partial^2 g_{m-1-k}}{\partial \eta^2} - \frac{\partial g_k}{\partial \eta} \frac{\partial g_{m-1-k}}{\partial \eta} \right] + \\ &(f_k + g_k) \frac{\partial^4 g_{m-1-k}}{\partial \eta^4} + \left(\frac{\partial^2 g_k}{\partial \eta^2} - \frac{\partial^2 f_k}{\partial \eta^2} \right) \frac{\partial^2 g_{m-1-k}}{\partial \eta^2} \\ &- 2 \left(\frac{\partial f_k}{\partial \eta} + \frac{\partial g_k}{\partial \eta} \right) \frac{\partial^3 g_{m-1-k}}{\partial \eta^3} \end{aligned} \right] \right], \end{aligned} \quad (3.52)$$

$$\begin{aligned} \mathcal{R}_m^\phi(\eta) &= \frac{\partial^2 \phi_{m-1}}{\partial \eta^2} - Sc(1-\xi) \left(\frac{\eta}{2} \frac{\partial \phi_{m-1}}{\partial \eta} - \xi \frac{\partial \phi_{m-1}}{\partial \xi} \right) \\ &+ \xi Sc \sum_{k=0}^{m-1} \left[f_k \frac{\partial \phi_{m-1-k}}{\partial \eta} + g_k \frac{\partial \phi_{m-1-k}}{\partial \eta} \right] - \gamma Sc \xi \phi, \end{aligned} \quad (3.53)$$

$$\chi_m = \begin{cases} 0, & m \leq 1, \\ 1, & m > 1. \end{cases} \quad (3.54)$$

The general solutions of Eqs (3.47) – (3.49) can be written as

$$f_m(\eta, \xi) = f_m^*(\eta, \xi) + C_1 + C_2 \exp(\eta) + C_3 \exp(-\eta), \quad (3.55)$$

$$g_m(\eta, \xi) = g_m^*(\eta, \xi) + C_4 + C_5 \exp(\eta) + C_6 \exp(-\eta), \quad (3.56)$$

$$\phi_m(\eta, \xi) = \phi_m^*(\eta, \xi) + C_7 \exp(\eta) + C_8 \exp(-\eta), \quad (3.57)$$

where $f_m^*(\eta, \xi)$, $g_m^*(\eta, \xi)$, $\phi_m^*(\eta, \xi)$ are the particular solutions of the Eqs (3.47) – (3.47) and the coefficients $C_i (i = 1 - 8)$ are determined by the boundary conditions (3.50).

$$\begin{aligned} C_2 &= C_5 = C_7 = 0, \\ C_1 &= -C_3 - f_m^*(0, \xi), \quad C_3 = \left. \frac{\partial f_m^*(\eta, \xi)}{\partial \eta} \right|_{\eta=0}, \quad C_6 = \left. \frac{\partial g_m^*(\eta, \xi)}{\partial \eta} \right|_{\eta=0}, \\ C_4 &= -C_6 - g_m^*(0, \xi), \quad C_8 = -\phi_m^*(0, \xi), \end{aligned} \quad (3.58)$$

3.3 Convergence of the homotopy solutions

It is known that the auxiliary parameters \hbar_f , \hbar_g and \hbar_ϕ play an important role in adjusting and controlling the convergence of the series solutions (3.44) and (3.46). Hence to find the admissible values of \hbar_f , \hbar_g and \hbar_ϕ , the \hbar -curves are plotted for the 14th-order of approximations. Fig. 3.1 elucidates that the range for the admissible values of \hbar_f , \hbar_g and \hbar_ϕ are $-1.5 \leq \hbar_f \leq -0.5$,

$-1.3 \leq \hbar_g \leq -0.5$ and $-1.4 \leq \hbar_\phi \leq -0.8$. The performed calculations indicates that the series given by (3.44) and (3.46) converge in the whole region of η when $\hbar_f = \hbar_g = -0.8$ and $\hbar_\phi = -0.6$.

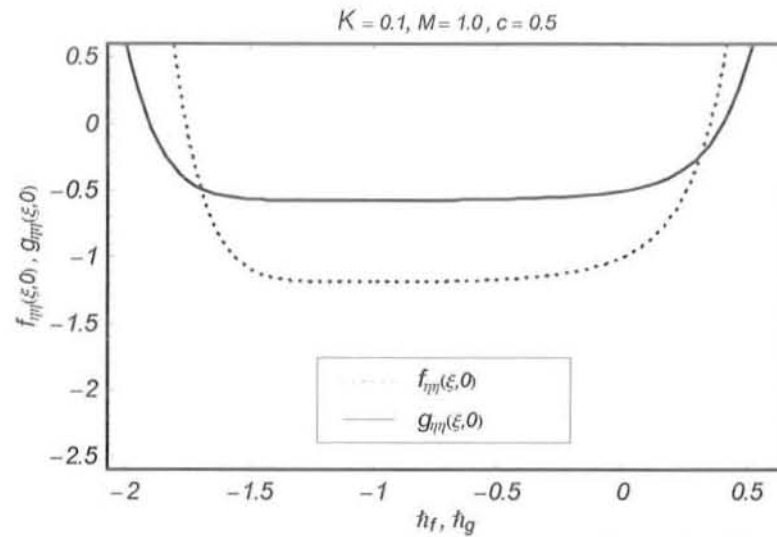


Fig. 3.1. The \hbar -curves of $f_{\eta}(\xi, 0)$ and $g_{\eta}(\xi, 0)$ at the 14th-order of approximations when $\xi = 0.5$.

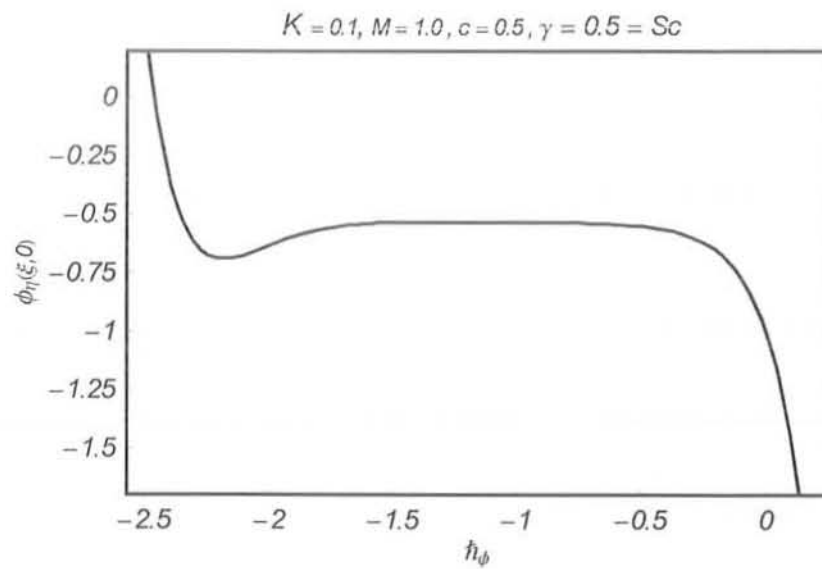


Fig. 3.2. The \hbar -curve of $\phi_{\eta}(\xi, 0)$ at the 14th-order of approximations when $\xi = 0.5$.

3.4 Results and discussion

In this section, our main interest is to discuss the variations of emerging parameters such as viscoelastic parameter K , Hartman number M , dimensionless time τ , Schmidt number Sc and chemical reaction parameter γ on the velocity components, concentration field, skin friction coefficients and the surface mass transfer. The analysis of such variations is made through Figs. 3.3 – 3.19. Figs. 3.3 – 3.12 display the effects of viscoelastic parameter K , Hartman number M , dimensionless time τ on the velocity components $f_\eta(\eta, \xi)$ and $g_\eta(\eta, \xi)$ and the local skin-friction coefficients $\xi^{1/2} \text{Re}_x^{1/2} C_{fx}$ and $\xi^{1/2} \text{Re}_x^{1/2} C_{fy}$. Figs. 3.3 – 3.6 give the variations of K and M on the velocity components $f_\eta(\eta, \xi)$ and $g_\eta(\eta, \xi)$. It is observed that both $f_\eta(\eta, \xi)$ and $g_\eta(\eta, \xi)$ decrease when the values of K are increased. The boundary layer thickness is also decreased when K increases. Note that this change is larger in $g_\eta(\eta, \xi)$ when compared with $f_\eta(\eta, \xi)$. The velocity components $f_\eta(\eta, \xi)$ and $g_\eta(\eta, \xi)$ are decreasing functions of M (Figs. 3.5 and 3.6). Figs. 3.7 and 3.8 indicate the effects of dimensionless time τ on the velocity components $f_\eta(\eta, \xi)$ and $g_\eta(\eta, \xi)$. Clearly the velocity components $f_\eta(\eta, \xi)$ and $g_\eta(\eta, \xi)$ increase by increasing τ . The effects of K , M and τ on the skin-friction coefficients $\xi^{1/2} \text{Re}_x^{1/2} C_{fx}$ and $\xi^{1/2} \text{Re}_x^{1/2} C_{fy}$ are shown in the Figs. 3.9 – 3.12. It is observed that the magnitude of skin friction coefficients $\xi^{1/2} \text{Re}_x^{1/2} C_{fx}$ and $\xi^{1/2} \text{Re}_x^{1/2} C_{fy}$ increase when K and M are increased.

Figs. 3.13 – 3.19. are prepared for the effects of dimensionless time τ , the Schmidt number Sc and the chemical reaction parameter γ on the concentration field $\phi(\eta, \xi)$ and the surface mass transfer $\xi^{1/2} \text{Re}_x^{-1/2} C_{fx} Sh$. Fig. 3.13 elucidates the influence of τ on the concentration field $\phi(\eta, \xi)$ in the case of destructive chemical reaction $\gamma > 0$. It is noted that concentration field $\phi(\eta, \xi)$ is an increasing function of τ and the concentration boundary layer thickness also increases for large values of τ . The variation of Sc on the concentration field is sketched in Fig. 3.14. It is observed that ϕ is a decreasing function of Sc . Fig. 3.15 gives the effects of destructive chemical reaction ($\gamma > 0$) on the concentration field. It is seen that results here are

similar to $\gamma < 0$ but change in Fig. 3.15 is slightly smaller when compared with Fig. 3.14. Fig. 3.16 illustrates the variation of generative chemical reaction ($\gamma < 0$). It has opposite results when compared with Fig. 3.15. Figs. 3.17 and 3.18 indicate the variation of γ on the surface mass transfer for both cases of destructive ($\gamma > 0$) and generative ($\gamma < 0$) chemical reactions. The surface mass transfer in case of ($\gamma > 0$) is opposite when compared with ($\gamma < 0$). The variation of Schmidt number Sc on surface mass transfer is shown in Fig. 3.19. It is observed that surface mass transfer increases by increasing Sc .

Here Tables 3.1 – 3.5 give the steady-state results ($\xi = 1$) for the surface shear stresses and surface mass transfer for different values of the emerging parameters. For the variation of stretching ratio c , the values of skin friction coefficients and mass transfer are presented in Table 3.1. It is shown that as the parameter c increases, the magnitude of the surface shear stresses and mass transfer increases. Table 3.2. presents the values of surface shear stresses and mass transfer for various values of viscoelastic parameter K and Hartman number M in the two-dimensional flow ($c = 0$). From Tables 3.3 and 3.4, one can see that the behaviors of K and M in three-dimensional and axisymmetric flows are qualitatively similar to the two-dimensional case. It is noted from these tables that by increasing K and M the skin friction coefficients increase while the surface mass transfer decreases. Table 3.5 is prepared for the variations of Sc and γ on the surface mass transfer. The magnitude of $-\phi'(0)$ increases when Sc and γ increase.

3.5 Final remarks

The series solutions of unsteady three-dimensional MHD flow of an elasto-viscous fluid with mass transfer are developed. Results of the velocity components, concentration field, skin friction coefficients and the surface mass transfer are sketched and analyzed. Main observations of the present study can be summarized in the points presented as follows.

- The behaviors of K and M on f_η and g_η are qualitatively similar.

- Boundary layer thickness is decreasing function of K and M .
- Behavior of time τ on the boundary layer thickness is quite opposite to that of K and M .
- Effects of K and M on the shear stresses are similar.
- The magnitude of surface shear stresses increases with K and M when stretching ratio is fixed.
- The concentration field has opposite effects for Sc and τ .
- The influence of the destructive ($\gamma > 0$) chemical reaction is to decrease the concentration field ϕ .
- The concentration field ϕ has opposite results for destructive ($\gamma > 0$) and generative ($\gamma < 0$) chemical reactions.

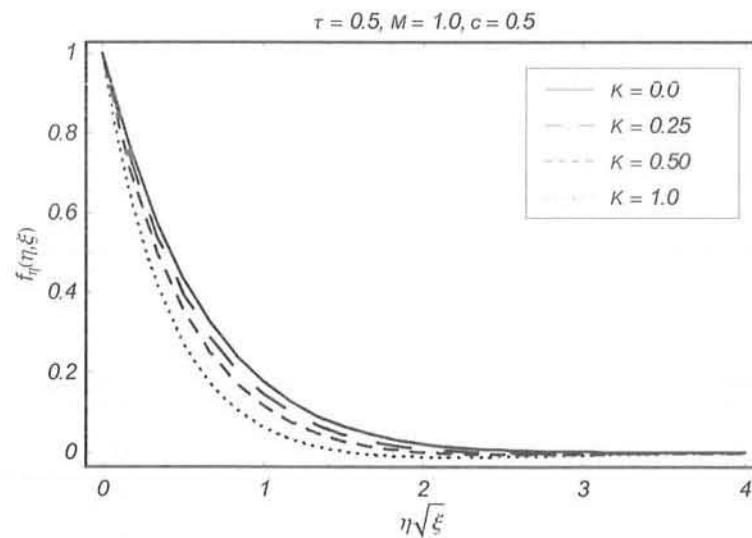


Fig. 3.3. Influence of K on $f_\eta(\eta, \xi)$.

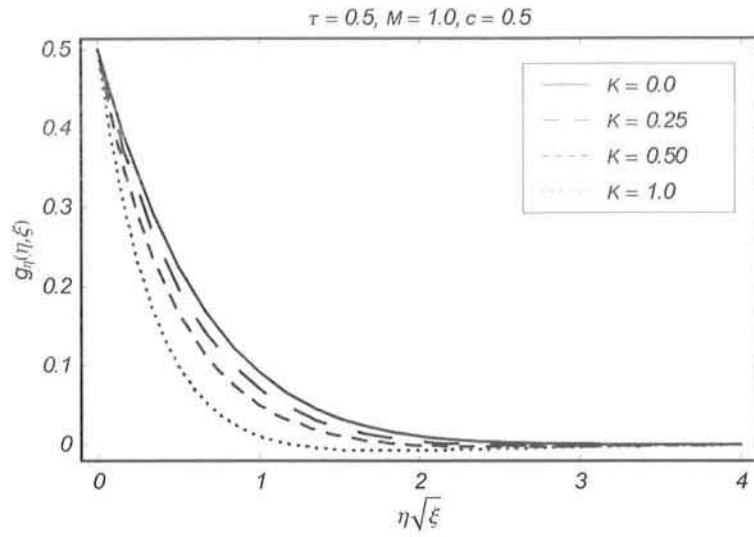


Fig. 3.4. Influence of K on $g_\eta(\eta, \xi)$.

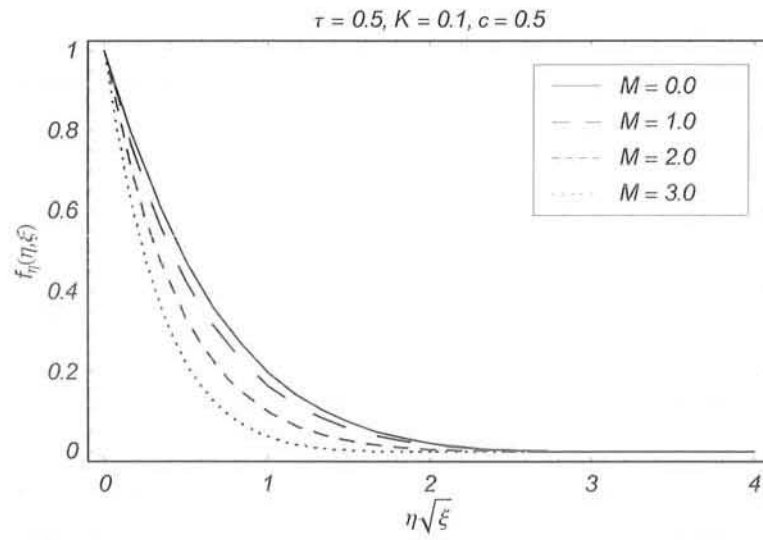


Fig. 3.5. Influence of M on $f_\eta(\eta, \xi)$.

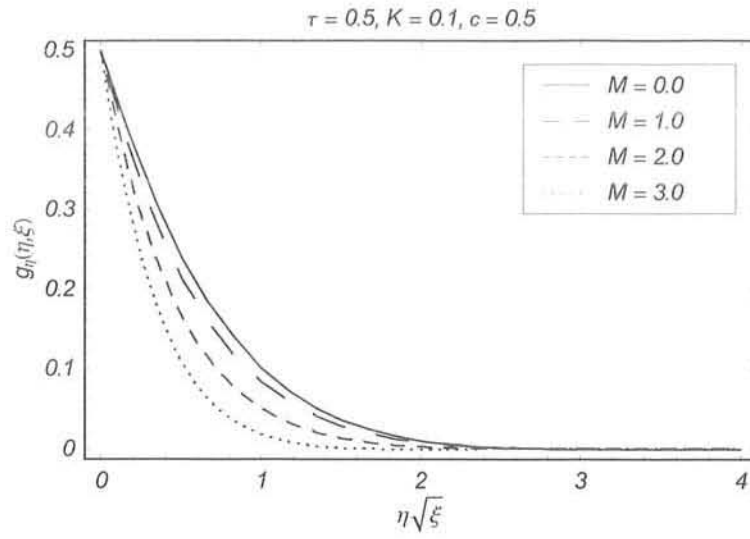


Fig. 3.6. Influence of M on $g_\eta(\eta, \xi)$.

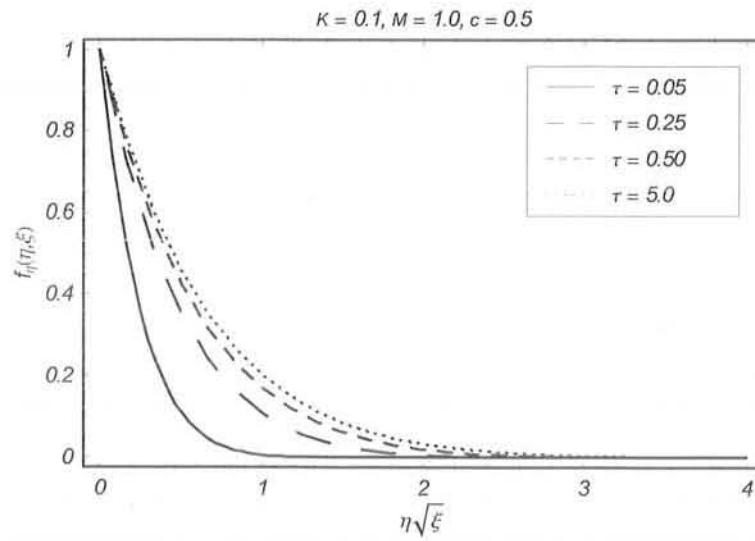


Fig. 3.7. Influence of τ on $f_\eta(\eta, \xi)$.

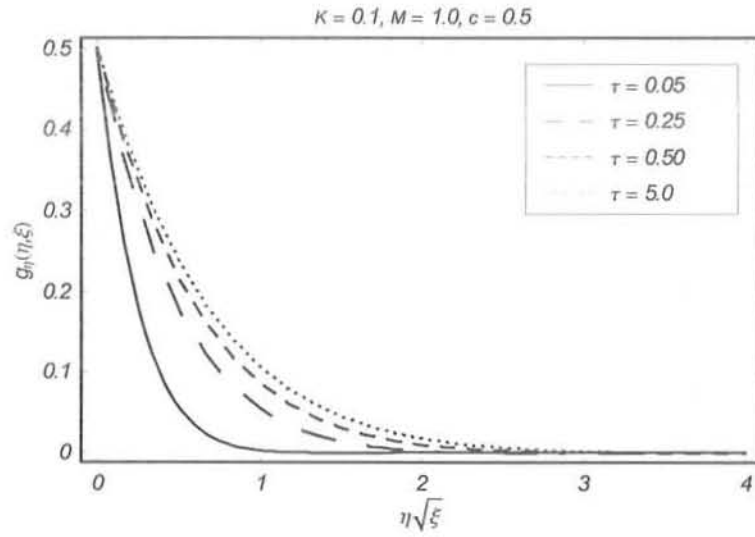


Fig. 3.8. Influence of τ on $g_\eta(\eta, \xi)$.

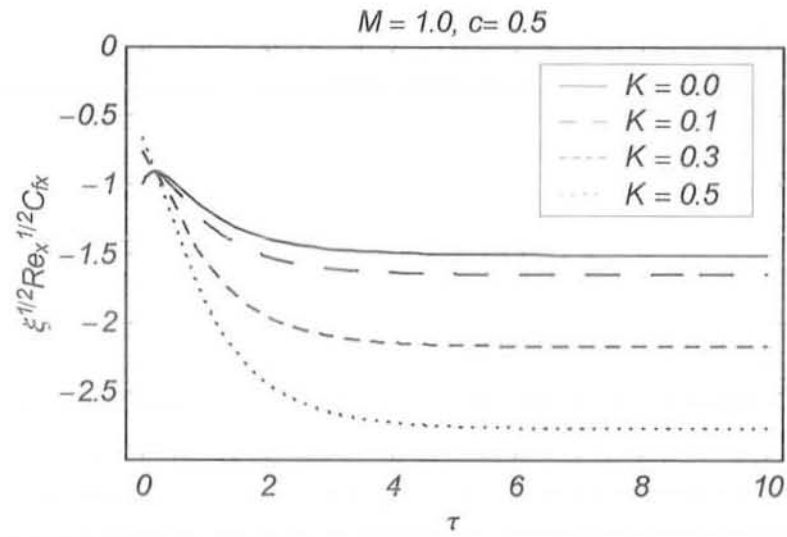


Fig. 3.9. Influence of K on $\xi^{1/2} \text{Re}_x^{1/2} C_{fx}$.

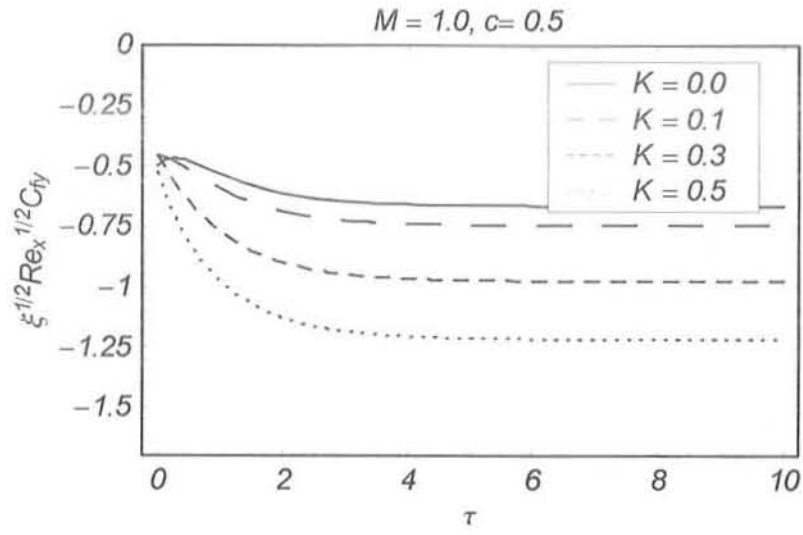


Fig. 3.10. Influence of K on $\xi^{1/2} \text{Re}_y^{1/2} C_{fy}$.

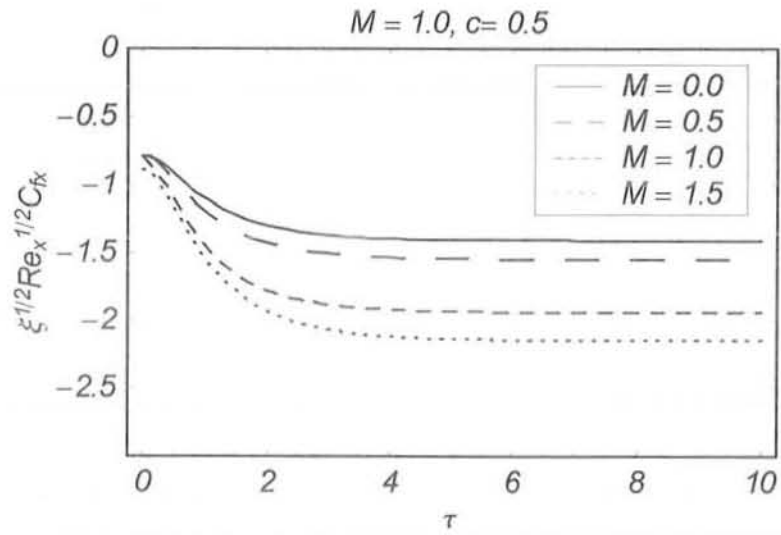


Fig. 3.11. Influence of M on $\xi^{1/2} \text{Re}_x^{1/2} C_{fx}$.

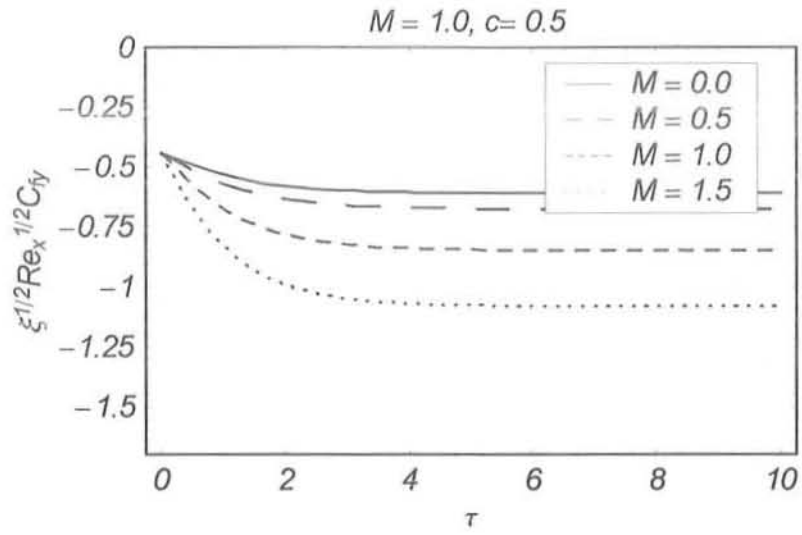


Fig. 3.12. Influence of M on $\xi^{1/2} \text{Re}_y^{1/2} C_{fy}$.

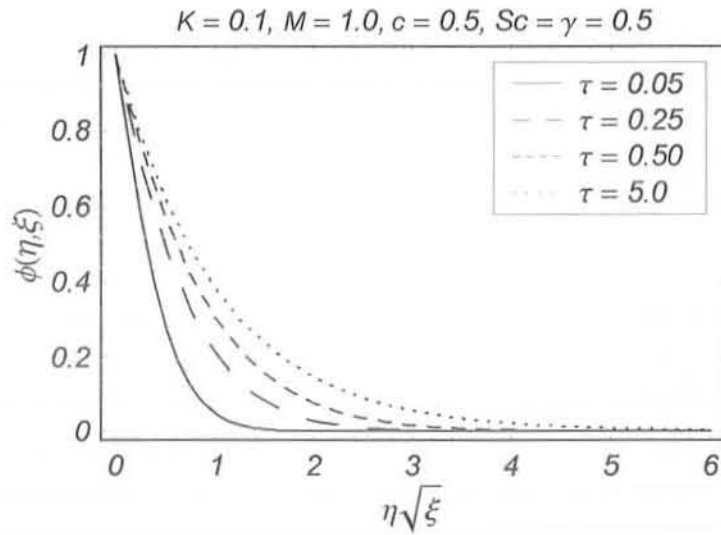


Fig. 3.13. Influence of τ on $\phi(\eta, \xi)$.

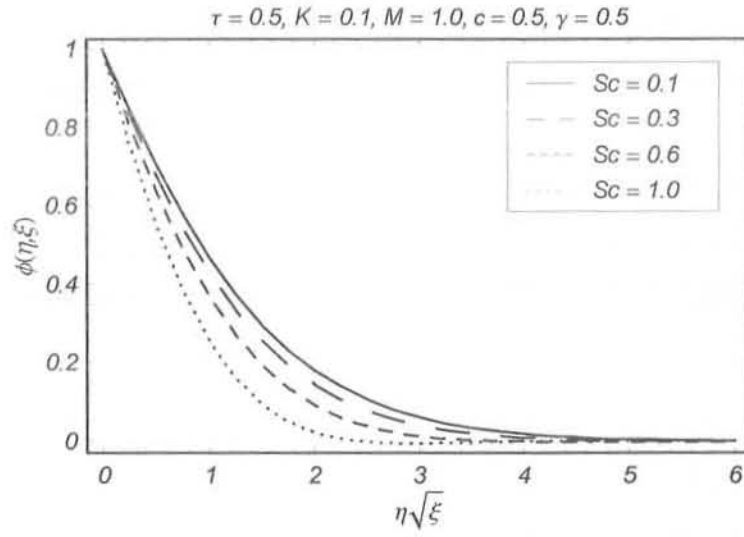


Fig. 3.14. Influence of Sc on $\phi(\eta, \xi)$.

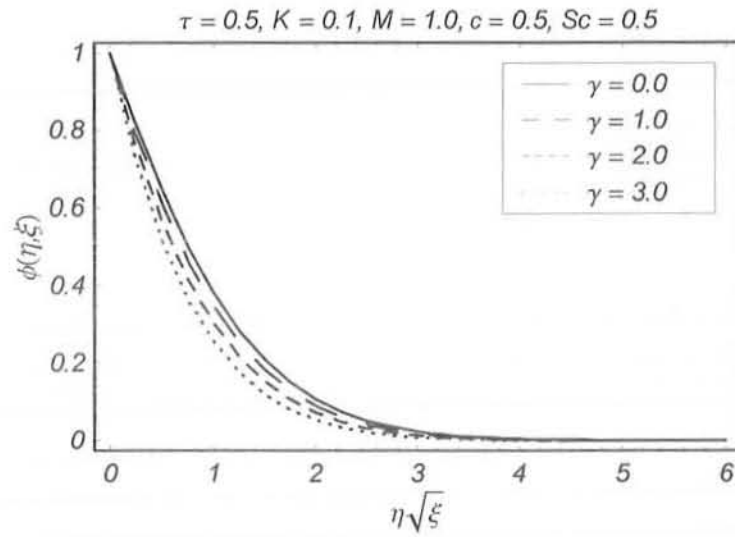


Fig. 3.15. Influence of $\gamma (> 0)$ on $\phi(\eta, \xi)$.

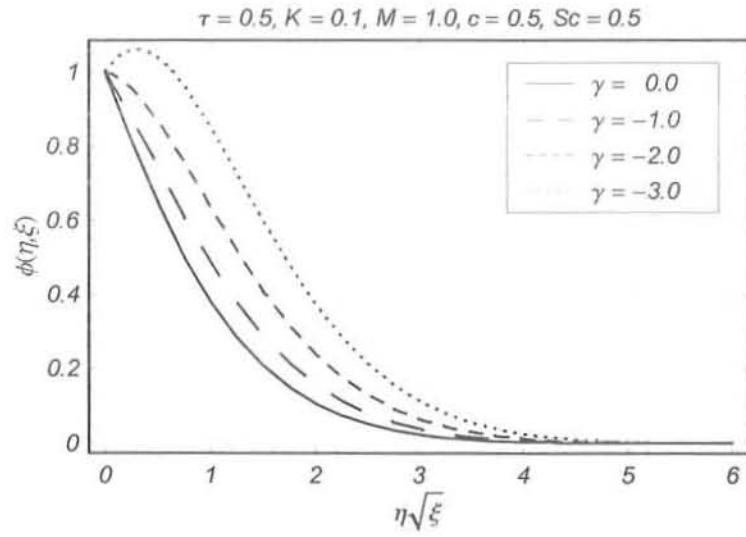


Fig. 3.16. Influence of $\gamma (< 0)$ on $\phi(\eta, \xi)$.

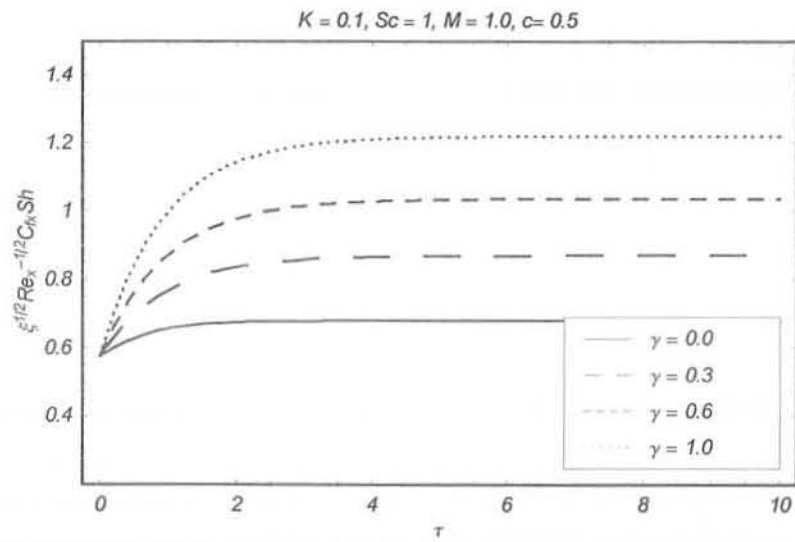


Fig. 3.17. Influence of $\gamma (> 0)$ on $\xi^{1/2} \text{Re}_x^{-1/2} C_{fx} Sh$.

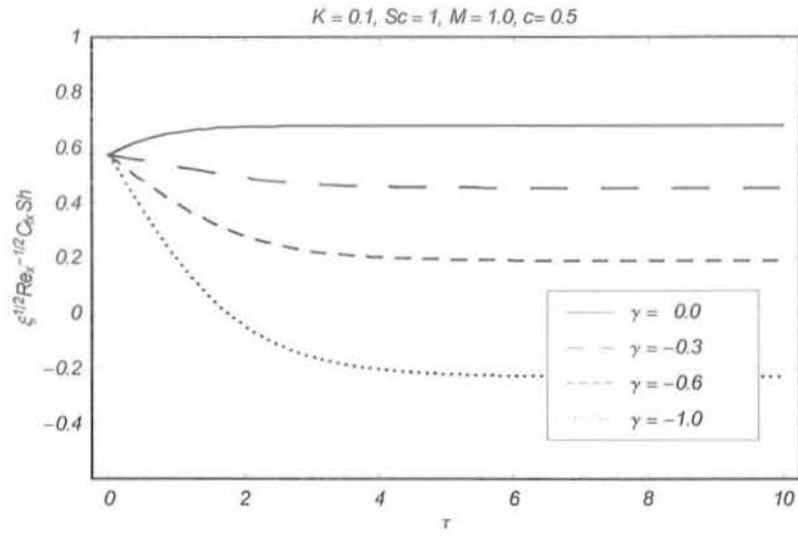


Fig. 3.18. Influence of $\gamma (< 0)$ on $\xi^{1/2} Re_x^{-1/2} C_{fx} Sh$.

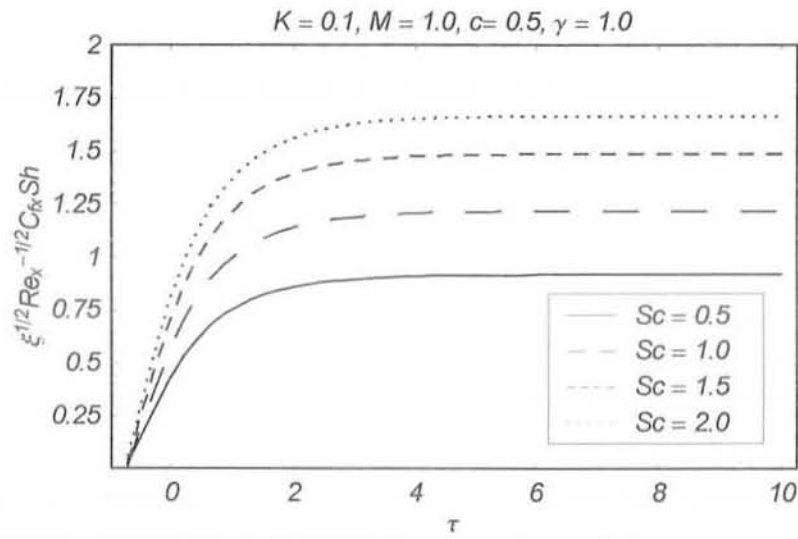


Fig. 3.19. Influence of Sc on $\xi^{1/2} Re_x^{-1/2} C_{fx} Sh$.

c	$-f_{\eta\eta}(0)$	$-g_{\eta\eta}(0)$	$-\phi_{\eta}(0)$
0	1.49071	0	0.60887
0.25	1.57275	0.36434	0.63348
0.50	1.66144	0.79772	0.65587
1.0	1.86655	1.86655	0.69511

Table 3.1: Steady state results for surface shear stresses $-f_{\eta\eta}(0)$, $-g_{\eta\eta}(0)$ and surface mass transfer $-\phi_{\eta}(0)$ when $M = 1.0$, $K = 0.1$, $Sc = \gamma = 0.5$ and $\xi = 1$.

K	M	$-f_{\eta\eta}(0)$	$-\phi_{\eta}(0)$
0.0	1.0	1.41421	0.61246
0.1		1.49071	0.60887
0.2		1.58114	0.60489
0.1	0	1.05409	0.63274
	0.5	1.17851	0.62504
	1	1.49071	0.60887
	1.5	1.90029	0.59283

Table 3.2: Steady state results for surface shear stresses $-f_{\eta\eta}(0)$, $-g_{\eta\eta}(0)$ and surface mass transfer $-\phi_{\eta}(0)$ for various values of K and M when $c = 0$ (i.e for two-dimensional flow $g = 0$)

$$Sc = \gamma = 0.5 \text{ and } \xi = 1.$$

K	M	$-f_{\eta\eta}(0)$	$-g_{\eta\eta}(0)$	$-\phi_{\eta}(0)$
0.0	1.0	1.47677	0.67981	0.66717
0.1		1.66145	0.79772	0.65588
0.2		1.96980	1.04254	0.64060
0.1	0	1.22155	0.53808	0.68627
	0.5	1.34420	0.61269	0.67685
	1.0	1.66145	0.79772	0.65588
	1.5	2.08789	1.03654	0.63389

Table 3.3: Steady state results for surface shear stresses $-f_{\eta\eta}(0)$, $-g_{\eta\eta}(0)$ and surface mass transfer $-\phi_{\eta}(0)$ for values of K and M when $c = 0.5$, $Sc = \gamma = 0.5$ and $\xi = 1$.

K	M	$-f_{\eta\eta}(0)$	$-\phi_{\eta}(0)$
0.0	1.0	1.53571	0.71629
0.1		1.86656	0.69511
0.1	0	1.408007	0.72741
	0.5	1.53459	0.71779
	1	1.86656	0.69511
	1.5	2.31942	0.66975

Table 3.4: Steady state results for surface shear stresses $-f_{\eta\eta}(0)$, $-g_{\eta\eta}(0)$ and surface mass transfer $-\phi_{\eta}(0)$ for various values of K and M when $c = 1$ (i.e for axisymmetric flow $f = g$)
 $Sc = \gamma = 0.5$ and $\xi = 1$.

γ	Sc	$-\phi_\eta(0), c = 0.0$	$-\phi_\eta(0), c = 0.5$	$-\phi_\eta(0), c = 1.0$
0.2	0.5	0.45109	0.50827	0.55472
0.5		0.60887	0.65587	0.69511
0.8		0.72883	0.77082	0.80636
1.2		0.86071	0.89855	0.93098
0.5	0.5	0.60887	0.65587	0.69511
	1.0	0.89484	0.97810	1.04905
	1.5	1.11978	1.23323	1.33078
	2.0	1.31175	1.45142	1.57211

Table 3.5: Steady state results for surface mass transfer $-\phi_\eta(0)$ for various values of γ and Sc when $K = 0.1$, $M = 1.0$ and $\xi = 1$.

Chapter 4

Thermal Radiation and Joule heating effects on MHD flow of a Maxwell fluid with thermophoresis

This chapter addresses the magnetohydrodynamic (MHD) two-dimensional flow with heat and mass transfer over a stretching sheet in the presence of Joule heating and thermophoresis. The resulting partial differential differential equations are converted into a set of coupled ordinary differential equations. Series solutions have been derived by using homotopy analysis method (HAM). The local Nusselt and Sherwood numbers are also computed. Graphical results for the dimensionless velocity, temperature and concentration fields are reported and examined for some parameters showing the interesting aspects of the obtained solutions.

4.1 Problem description

Consider the problem of heat and mass transfer characteristics in steady MHD flow of a Maxwell fluid past a vertical stretching sheet in Darcian porous medium. The surface is stretched in its

own plane with a velocity proportional to its distance from the fixed origin $x = 0$. A uniform magnetic field of strength B_0 is applied in y -direction (taken normal to flow). The magnetic Reynolds number is small and so induced magnetic field is neglected. We further assume that surface has variable temperature $T_w(x)$ and variable concentration $C_w(x)$, and fluid has uniform ambient temperature T_∞ and uniform ambient concentration C_∞ , where $T_w > T_\infty$ and $C_w > C_\infty$ respectively. In addition the effects of thermophoresis are considered in order to understand the mass deposition variation on surface. Under these assumptions and Boussineq's approximation, the governing equations for boundary layer flow are

$$\frac{\partial u}{\partial x} + \frac{\partial v}{\partial y} = 0, \quad (4.1)$$

$$u \frac{\partial u}{\partial x} + v \frac{\partial u}{\partial y} + \lambda_1 \left[u^2 \frac{\partial^2 u}{\partial x^2} + v^2 \frac{\partial^2 u}{\partial y^2} + 2uv \frac{\partial^2 u}{\partial x \partial y} \right] = \nu \frac{\partial^2 u}{\partial y^2} - \frac{\nu}{K^*} u - \frac{\sigma B_0^2}{\rho} (u + \lambda_1 v \frac{\partial u}{\partial y}) + g [\beta_T (T - T_\infty) + \beta_C (C - C_\infty)], \quad (4.2)$$

$$u \frac{\partial T}{\partial x} + v \frac{\partial T}{\partial y} = \frac{k}{\rho c_p} \frac{\partial^2 T}{\partial y^2} - \frac{1}{\rho c_p} \frac{\partial q_r}{\partial y} + \frac{\mu}{\rho c_p} \left(\frac{\partial u}{\partial y} \right)^2 + \frac{\sigma B_0^2}{\rho c_p} u^2, \quad (4.3)$$

$$u \frac{\partial C}{\partial x} + v \frac{\partial C}{\partial y} = D \frac{\partial^2 C}{\partial y^2} - \frac{\partial}{\partial y} (V_T C). \quad (4.4)$$

In above equations u and v denote the velocity components in the x - and y -directions respectively, T is the fluid temperature, C is the concentration field, g is gravitational acceleration, ν is the kinematic viscosity, K^* is permeability of porous medium, ρ is the fluid density, β_T , β_C are the thermal expansion coefficients of temperature and concentration, respectively, c_p is specific heat, q_r is the radiative heat flux, D is diffusion coefficient and V_T is the thermophetic velocity.

The radiative heat flux q_r is defined by Rosseland approximation as follows

$$q_r = \frac{-4\sigma^*}{3k^*} \frac{\partial T^4}{\partial y} \quad (4.5)$$

in which σ^* denotes the Stefan-Boltzman constant and k^* the Rosseland mean absorption coefficient. The fluid phase temperature differences within the flow are sufficiently small so that T^4 may be described as a linear function of temperature. Hence expanding T^4 in Taylors series about the free-stream temperature T_∞ and neglecting higher order terms, we have

$$T^4 \approx 4T_\infty^3 T - 3T_\infty^4 \quad (4.6)$$

Utilizing Eq. (4.3), one has

$$u \frac{\partial T}{\partial x} + v \frac{\partial T}{\partial y} = \frac{k}{\rho c_p} \frac{\partial^2 T}{\partial y^2} + \frac{16\sigma^* T_\infty^3}{3k^* \rho c_p} \frac{\partial^2 T}{\partial y^2} + \frac{\mu}{\rho c_p} \left(\frac{\partial u}{\partial y} \right)^2 + \frac{\sigma B_0^2}{\rho c_p} u^2. \quad (4.7)$$

The effect of thermophoresis is usually prescribed by means of the average velocity, which a particle will acquire when exposed to a temperature gradient. In boundary layer flow, the temperature gradient in y -direction is much larger than in the x -direction, and therefore only the thermophoretic velocity in y -direction is considered. Consequently the thermophoretic velocity V_T [137 – 142] can be expressed as

$$V_T = -k_1 \frac{\nu}{T_r} \frac{\partial T}{\partial y} \quad (4.8)$$

in which k_1 is the thermophoretic coefficient and T_r is reference temperature. A thermophoretic parameter Γ is given by the relation

$$\Gamma = -\frac{k_1(T_w - T_\infty)}{T_r}. \quad (4.9)$$

The associated boundary conditions are given by

$$\begin{aligned} u &= U_w(x) = ax, \quad v = 0, \quad T = T_w(x), \quad C = C_w(x) \quad \text{at } y = 0, \\ u &\rightarrow 0, \quad \frac{\partial u}{\partial y} \rightarrow 0, \quad T \rightarrow T_\infty, \quad C \rightarrow C_\infty \quad \text{as } y \rightarrow \infty. \end{aligned} \quad (4.10)$$

Furthermore, the wall temperature and concentration fields are taken in the following forms:

$$T_w = T_\infty + bx, \quad C_w = C_\infty + cx, \quad (4.11)$$

where a , b and c are the positive constants.

We now introduce dimensionless quantities as

$$\eta = \sqrt{\frac{a}{\nu}}y, \quad u = axf'(\eta), \quad v = -\sqrt{a\nu}f(\eta), \quad \theta(\eta) = \frac{T - T_\infty}{T_w - T_\infty}, \quad \phi(\eta) = \frac{C - C_\infty}{C_w - C_\infty}. \quad (4.12)$$

The quantities defined above automatically ensures the continuity equation (4.1) and Eqs. (4.2), (4.3) and (4.7) now are

$$f''' + ff'' - f'^2 + \beta(2ff'f'' - f^2f''') - M^2f' + M^2\beta ff'' - \gamma_1f' + \lambda(\theta + N\phi) = 0, \quad (4.13)$$

$$\left(1 + \frac{4}{3}R_d\right)\theta'' + \text{Pr}(f\theta' - \theta f') + \text{Pr}Ec f''^2 + M^2\text{Pr}Ec f'^2 = 0, \quad (4.14)$$

$$\phi'' + Sc(f\phi' - \phi f') - Sc\Gamma(\phi'\theta' - \phi\theta'') = 0, \quad (4.15)$$

$$f(0) = 0, \quad f'(0) = 1, \quad \theta(0) = 1, \quad \phi(0) = 1,$$

$$f'(\infty) \rightarrow 0, \quad f''(\infty) \rightarrow 0, \quad \theta(\infty) \rightarrow 0, \quad \phi(\infty) \rightarrow 0, \quad (4.16)$$

where $\beta = \lambda_1 a$ is the Deborah number, $M^2 = \sigma B_0^2 / \rho a$ is the Hartman number, $\gamma_1 (= \frac{\nu}{aK^*})$ is

the porosity parameter, $\lambda = \frac{Gr_x}{Re_x^2}$ is the local buoyancy parameter, $Gr_x (= \frac{g\beta(T_w - T_\infty)x^3/\nu^2}{u_w^2 x^2/\nu^2})$ is the local Grashof number, $N = (\frac{\beta_C (C_w - C_\infty)}{\beta_T (T_w - T_\infty)})$ is the constant dimensionless concentration buoyancy parameter, $Re_x = u_w x/\nu$ is the local Reynolds number, $Pr = \frac{\mu c_p}{k}$ is the Prandtl number, $R_d (= \frac{4\sigma^* T_\infty^3}{k^* k})$ is the radiation parameter, $Ec (= \frac{u_w^2}{c_p(T_w - T_\infty)})$ is the Eckert number and $Sc = (\frac{\nu}{D})$ is the Schmidt number.

The local Nusselt number Nu_x and local Sherwood number Sh can be written as

$$Nu_x = \frac{xq_w}{k(T_w - T_\infty)}, \quad Sh = \frac{xj_w}{D(C_w - C_\infty)}, \quad (4.17)$$

in which τ_w , q_w and j_w denote the wall skin friction, the wall heat flux and the mass flux from the plate which are given by

$$q_w = - \left[\left(k + \frac{16\sigma^* T_\infty^3}{3k^*} \right) \frac{\partial T}{\partial y} \right]_{y=0}, \quad j_w = - \left(\frac{\partial C}{\partial y} \right)_{y=0}, \quad (4.18)$$

which in terms of dimensionless variables become

$$Nu_x Re_x^{-1/2} \left(\frac{4}{4 + 3R_d} \right) = -\theta'(0), \quad Sh/Re_x^{1/2} = -\phi'(0), \quad (4.19)$$

4.2 Solutions by homotopy analysis method (HAM)

The velocity $f(\eta)$, temperature $\theta(\eta)$ and the concentration $\phi(\eta)$ fields for HAM solutions can be expressed by the set of base functions

$$\left\{ \eta^k \exp(-n\eta) \mid k \geq 0, n \geq 0 \right\} \quad (4.20)$$

as follows

$$f(\eta) = a_{0,0}^0 + \sum_{n=0}^{\infty} \sum_{k=0}^{\infty} a_{m,n}^k \eta^k \exp(-n\eta), \quad (4.21)$$

$$\theta(\eta) = \sum_{n=0}^{\infty} \sum_{k=0}^{\infty} b_{m,n}^k \eta^k \exp(-n\eta), \quad (4.22)$$

$$\phi(\eta) = \sum_{n=0}^{\infty} \sum_{k=0}^{\infty} c_{m,n}^k \eta^k \exp(-n\eta), \quad (4.23)$$

where $a_{m,n}^k$, $b_{m,n}^k$ and $c_{m,n}^k$ are the coefficients. The initial guesses f_0 , θ_0 and ϕ_0 of $f(\eta)$, $\theta(\eta)$ and $\phi(\eta)$ based on the rule of solution expressions and the boundary conditions are

$$f_0(\eta) = 1 - \exp(-\eta), \quad (4.24)$$

$$\theta_0(\eta) = \exp(-\eta), \quad (4.25)$$

$$\phi_0(\eta) = \exp(-\eta). \quad (4.26)$$

The auxiliary linear operators are

$$\mathcal{L}_f = \frac{d^3 f}{d\eta^3} - \frac{df}{d\eta}, \quad (4.27)$$

$$\mathcal{L}_\theta = \frac{d^2 \theta}{d\eta^2} - \theta, \quad (4.28)$$

$$\mathcal{L}_\phi = \frac{d^2 \phi}{d\eta^2} - \phi. \quad (4.29)$$

The operators given in Eqs. (4.27) – (4.29) have the following properties

$$\mathcal{L}_f [C_1 + C_2 \exp(\eta) + C_3 \exp(-\eta)] = 0, \quad (4.30)$$

$$\mathcal{L}_\theta [C_4 \exp(\eta) + C_5 \exp(-\eta)] = 0, \quad (4.31)$$

$$\mathcal{L}_\phi [C_6 \exp(\eta) + C_7 \exp(-\eta)] = 0, \quad (4.32)$$

where c_i ($i = 1 - 7$) are the arbitrary constants.

If $p \in [0, 1]$ is the embedding parameter and \hbar_f , \hbar_θ and \hbar_ϕ are the non-zero auxiliary

parameters then the zeroth-order deformation problems are expressed by the following relations

$$(1-p)\mathcal{L}_f[f(\eta,p) - f_0(\eta)] = p\hbar_f\mathcal{N}_f\left[\hat{f}(\eta,p), \hat{\theta}(\eta,p), \hat{\phi}(\eta,p)\right], \quad (4.33)$$

$$(1-p)\mathcal{L}_\theta[\hat{\theta}(\eta,p) - \theta_0(\eta)] = p\hbar_\theta\mathcal{N}_\theta\left[\hat{f}(\eta,p), \hat{\theta}(\eta,p), \hat{\phi}(\eta,p)\right], \quad (4.34)$$

$$(1-p)\mathcal{L}_\phi[\hat{\phi}(\eta,p) - \phi_0(\eta)] = p\hbar_\phi\mathcal{N}_\phi\left[\hat{f}(\eta,p), \hat{\theta}(\eta,p), \hat{\phi}(\eta,p)\right], \quad (4.35)$$

$$\hat{f}(\eta;p)\Big|_{\eta=0} = 0, \quad \frac{\partial\hat{f}(\eta;p)}{\partial\eta}\Big|_{\eta=0} = 1, \quad \frac{\partial\hat{f}(\eta;p)}{\partial\eta}\Big|_{\eta=\infty} = 0, \quad (4.36)$$

$$\hat{\theta}(\eta;p)\Big|_{\eta=0} = 1, \quad \hat{\theta}(\eta;p)\Big|_{\eta=\infty} = 0, \quad (4.37)$$

$$\hat{\phi}(\eta;p)\Big|_{\eta=0} = 1, \quad \hat{\phi}(\eta;p)\Big|_{\eta=\infty} = 0 \quad (4.38)$$

and the non-linear operators \mathcal{N}_f , \mathcal{N}_θ and \mathcal{N}_ϕ are

$$\begin{aligned} \mathcal{N}_f\left[\hat{f}(\eta;p), \hat{\theta}(\eta;p), \hat{\phi}(\eta;p)\right] &= \frac{\partial^3\hat{f}(\eta;p)}{\partial\eta^3} + (M^2\beta + 1)\hat{f}(\eta,p)\frac{\partial^2\hat{f}(\eta;p)}{\partial\eta^2} - \left(\frac{\partial\hat{f}(\eta;p)}{\partial\eta}\right)^2 \\ +\beta &\left[2\hat{f}(\eta,p)\frac{\partial\hat{f}(\eta;p)}{\partial\eta}\frac{\partial^2\hat{f}(\eta;p)}{\partial\eta^2} - \left(\hat{f}(\eta,p)\right)^2\frac{\partial^3\hat{f}(\eta;p)}{\partial\eta^3} \right] - (\gamma_1 + M^2)\frac{\partial\hat{f}(\eta;p)}{\partial\eta} + \lambda\left(\hat{\theta}(\eta,p) + N\hat{\phi}(\eta,p)\right), \end{aligned} \quad (4.39)$$

$$\begin{aligned} \mathcal{N}_\theta\left[\hat{f}(\eta;p), \hat{\theta}(\eta;p), \hat{\phi}(\eta;p)\right] &= \left(1 + \frac{4}{3}R_d\right)\frac{\partial^2\hat{\theta}(\eta;p)}{\partial\eta^2} + \text{Pr}\left(\hat{f}(\eta,p)\frac{\partial\hat{\theta}(\eta;p)}{\partial\eta} - \frac{\partial\hat{f}(\eta;p)}{\partial\eta}\hat{\theta}(\eta;p)\right) \\ &+ \text{Pr}Ec\left(\frac{\partial^2\hat{f}(\eta;p)}{\partial\eta^2}\right)^2 + M^2\text{Pr}Ec\left(\frac{\partial\hat{f}(\eta;p)}{\partial\eta}\right)^2, \end{aligned} \quad (4.40)$$

$$\begin{aligned} \mathcal{N}_\phi\left[\hat{f}(\eta;p), \hat{\theta}(\eta;p), \hat{\phi}(\eta;p)\right] &= \frac{\partial^2\hat{\phi}(\eta;p)}{\partial\eta^2} + Sc\left(\hat{f}(\eta,p)\frac{\partial\hat{\phi}(\eta;p)}{\partial\eta} - \frac{\partial\hat{f}(\eta;p)}{\partial\eta}\hat{\phi}(\eta;p)\right) \\ &- Sc\Gamma\left(\frac{\partial\hat{\theta}(\eta;p)}{\partial\eta}\frac{\partial\hat{\phi}(\eta;p)}{\partial\eta} - \hat{\phi}(\eta;p)\frac{\partial^2\hat{\theta}(\eta;p)}{\partial\eta^2}\right). \end{aligned} \quad (4.41)$$

For $p = 0$ and $p = 1$, one has

$$\hat{f}(\eta; 0) = f_0(\eta), \quad \hat{f}(\eta; 1) = f(\eta), \quad (4.42)$$

$$\hat{\theta}(\eta; 0) = \theta_0(\eta), \quad \hat{\theta}(\eta; 1) = \theta(\eta), \quad (4.43)$$

$$\hat{\phi}(\eta; 0) = \phi_0(\eta), \quad \hat{\phi}(\eta; 1) = \phi(\eta) \quad (4.44)$$

and now by Taylor's theorem one can easily write

$$\hat{f}(\eta; p) = f_0(\eta) + \sum_{m=1}^{\infty} f_m(\eta) p^m, \quad (4.45)$$

$$\hat{\theta}(\eta; p) = \theta_0(\eta) + \sum_{m=1}^{\infty} \theta_m(\eta) p^m, \quad (4.46)$$

$$\hat{\phi}(\eta; p) = \phi_0(\eta) + \sum_{m=1}^{\infty} \phi_m(\eta) p^m \quad (4.47)$$

$$f_m(\eta) = \frac{1}{m!} \left. \frac{\partial^m f(\eta; p)}{\partial \eta^m} \right|_{p=0}, \quad \theta_m(\eta) = \frac{1}{m!} \left. \frac{\partial^m \theta(\eta; p)}{\partial \eta^m} \right|_{p=0},$$

$$\phi_m(\eta) = \frac{1}{m!} \left. \frac{\partial^m \phi(\eta; p)}{\partial \eta^m} \right|_{p=0}. \quad (4.48)$$

The auxiliary parameters are so properly chosen that the series (4.33) – (4.35) converge at $p = 1$. Hence

$$f(\eta) = f_0(\eta) + \sum_{m=1}^{\infty} f_m(\eta), \quad (4.49)$$

$$\theta(\eta) = \theta_0(\eta) + \sum_{m=1}^{\infty} \theta_m(\eta), \quad (4.50)$$

$$\phi(\eta) = \phi_0(\eta) + \sum_{m=1}^{\infty} \phi_m(\eta). \quad (4.51)$$

The m th-order deformation problems satisfy the following expressions

$$\mathcal{L}_f [f_m(\eta) - \chi_m f_{m-1}(\eta)] = \hbar_f \mathcal{R}_m^f(\eta), \quad (4.52)$$

$$\mathcal{L}_\theta [\theta_m(\eta) - \chi_m \theta_{m-1}(\eta)] = \hbar_\theta \mathcal{R}_m^\theta(\eta), \quad (4.53)$$

$$\mathcal{L}_\phi [\phi_m(\eta) - \chi_m \phi_{m-1}(\eta)] = \hbar_\phi \mathcal{R}_m^\phi(\eta), \quad (4.54)$$

$$\begin{aligned} f_m(0) = 0, \quad f'_m(0) = 0, \quad f'_m(\infty) = 0, \quad \theta_m(0) = 0, \quad \theta_m(\infty) = 0, \\ \phi_m(0) = 0, \quad \phi_m(\infty) = 0, \end{aligned} \quad (4.55)$$

$$\begin{aligned} \mathcal{R}_m^f(\eta) = f_{m-1}''' - \gamma_1 f_{m-1}' + \lambda (\theta_{m-1-k} + N \phi_{m-1-k}) \\ + \sum_{k=0}^{m-1} \left[\begin{aligned} &(M^2 \beta + 1) f_{m-1-k} f_k'' - f_{m-1-k}' f_k' \\ &+ \beta \left(2 f_{m-1-k} \sum_{l=0}^k f_{k-l}' f_l'' - f_{m-1-k} \sum_{l=0}^k f_{k-l} f_l''' \right) \end{aligned} \right], \end{aligned} \quad (4.56)$$

$$\mathcal{R}_m^\theta(\eta) = \left(1 + \frac{4}{3} R_d \right) \theta_{m-1}'' + \text{Pr} \sum_{k=0}^{m-1} \left[\begin{aligned} &f_{m-1-k} \theta_k' - \theta_{m-1-k} f_k' + Ec f_{m-1-k}'' f_k'' \\ &+ M^2 Ec f_{m-1-k}' f_k' \end{aligned} \right], \quad (4.57)$$

$$\mathcal{R}_m^\phi(\eta) = \phi_{m-1}'' + Sc \sum_{k=0}^{m-1} [f_{m-1-k} \phi_k' - \phi_{m-1-k} f_k'] + Sc \Gamma (\phi' \theta' - \phi \theta_{m-1}''), \quad (4.58)$$

$$\chi_m = \begin{cases} 0, & m \leq 1, \\ 1, & m > 1. \end{cases} \quad (4.59)$$

The general solutions of Eqs. (4.52) – (4.55) are

$$f_m(\eta) = f_m^*(\eta) + C_1 + C_2 \exp(\eta) + C_3 \exp(-\eta), \quad (4.60)$$

$$\theta_m(\eta) = \theta_m^*(\eta) + C_4 \exp(\eta) + C_5 \exp(-\eta), \quad (4.61)$$

where $f_m^*(\eta)$, $\theta_m^*(\eta)$, and $\phi_m^*(\eta)$ depict the special solutions and

$$\begin{aligned} C_2 &= C_4 = C_6 = 0, \\ C_1 &= -C_3 - f_m^*(0), \quad C_3 = \left. \frac{\partial f_m^*(\eta)}{\partial \eta} \right|_{\eta=0}, \\ C_5 &= -\theta_m^*(0), \quad C_7 = -\phi_m^*(0). \end{aligned} \quad (4.62)$$

4.3 Convergence of the series solutions

It is obvious that the series solutions (4.49)–(4.51) consist of the non-zero auxiliary parameters \hbar_f , \hbar_θ , and \hbar_ϕ which can adjust and control the convergence. For range meaningful of \hbar_f , \hbar_θ , and \hbar_ϕ of the functions $f''(0)$, $\theta'(0)$ and $\phi'(0)$, the \hbar_f , \hbar_θ , and \hbar_ϕ -curves are plotted for 25th-order of approximations. Fig. 4.1 depicts that the range for the admissible values of \hbar_f , \hbar_θ , and \hbar_ϕ are $-1.1 \leq \hbar_f, \hbar_\theta, \hbar_\phi \leq -0.4$. Our analysis further shows that the series given by (4.49)–(4.51) converge in the whole region of η when $\hbar_f = \hbar_\theta = \hbar_\phi = -1.0$.

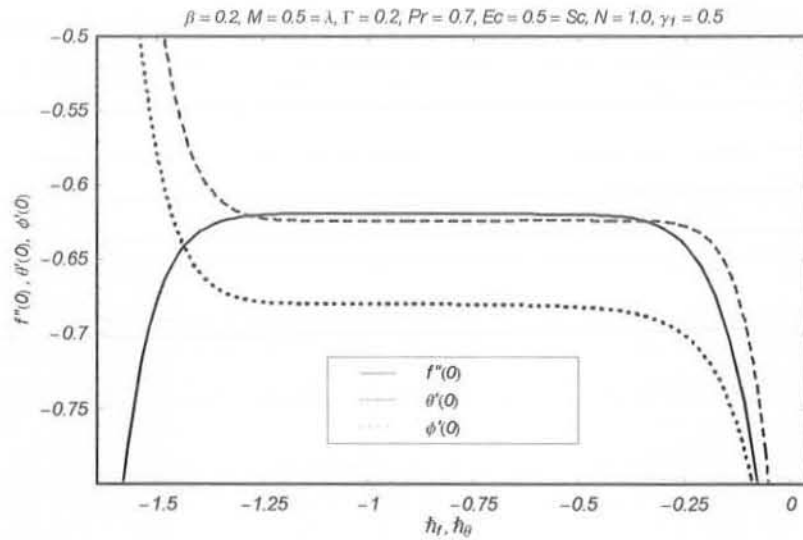


Fig. 4.1. \hbar -curves of $f''(0)$, $\theta'(0)$ and $\phi'(0)$ at 15th-order of approximation.

Table 4.1: Convergence of HAM solutions for different order of approximations when $\beta = 0.2$, $M = 0.5$, $\gamma_1 = 0.5$, $\lambda = 1.0$, $Pr = 0.7$, $\Gamma = 0.2$, $R_d = 0.3$ and $Ec = 0.5$.

Order of convergence	$-f''(0)$	$-\theta'(0)$	$-\phi'(0)$
1	0.68333	0.50416	0.68333
5	0.62111	0.62252	0.68124
10	0.61941	0.62424	0.67997
15	0.61927	0.62430	0.67978
20	0.61925	0.62428	0.67975
25	0.61925	0.62428	0.67975
30	0.61925	0.62428	0.67975

4.4 Discussion of results

This section concerns with the effects of Deborah number β , Hartman number M , porosity parameter γ_1 , local buoyancy parameter λ , the buoyancy ratio N , Prandtl number Pr , the radiation parameter R_d , Eckert number Ec and Schmidt number Sc on the velocity, temperature and concentration fields. For this purpose, Figs. 4.2 – 4.19 have been displayed. Figs. 4.2 – 4.9 show the effects of β , M , γ_1 , λ , N , Ec , R_d and Pr on the velocity field f' . The velocity profiles for different values of Deborah number β are plotted in Fig. 4.2. It is seen that the boundary layer thickness decreases with the increasing values of β . Fig. 4.3 describes the variation of M on f' . Obviously f' is a decreasing function of M . The variation of γ_1 on f' is illustrated in Fig. 4.4. This Fig. shows that γ_1 and M has similar effects on f' . Fig. 4.5 indicates the effects of λ on f' . Clearly f' is an increasing function of λ . From Fig. 4.6 one can see that the boundary layer thickness increases when N increases. The effect of radiation parameter R_d on the velocity field f' is shown in Fig. 4.7. Here the velocity profile shows a decrease with an increase in the radiation parameter. Figs. 4.8 and 4.9 describe the effects of Ec and Pr on f' ,

respectively. Both Ec and Pr decrease the velocity profile. Infact an increase in the Prandtl number leads to an increase in fluid viscosity which causes a decrease in the flow velocity.

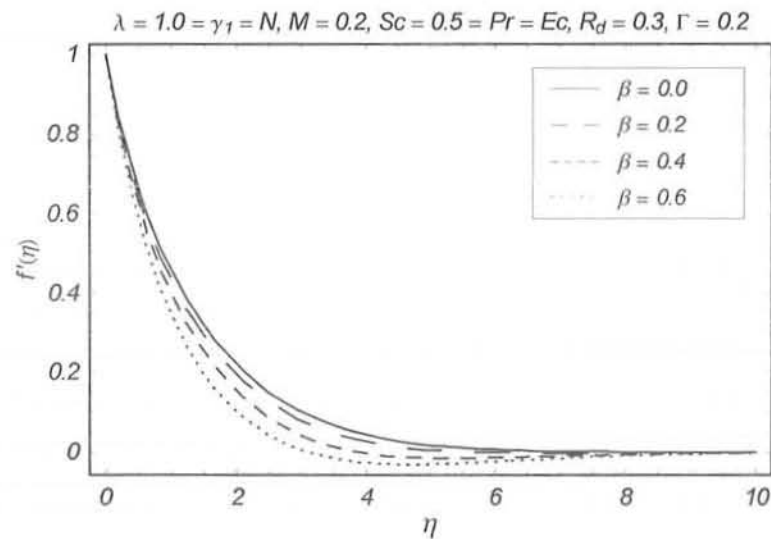
Figs. 4.10–4.16 depict the influences of β , M , γ_1 , λ , Ec , R_d and Pr on θ . From Figs. 10–12 it is observed that the temperature profile increases by increasing β , M and γ_1 . It is noticed that θ decreases when λ increases (Fig.4.13). Fig. 4.14 describes the effects of R_d on θ . Here θ increases when R_d increases. Fig. 4.15 indicates that θ is an increasing function of Ec . In Fig. 4.16 the variation of temperature θ is plotted for different values of Pr . The temperature decreases when Prandtl number is increased. The thermal boundary layer thickness decreases due to an increase in Pr .

Figs. 4.17 – 4.19 are sketched for the effects of β , Γ and Sc on concentration field ϕ . Fig. 4.17 elucidates the influence of β on the concentration field ϕ . It is obvious that the concentration field decreases by increasing β . Fig. 4.18 depicts that the concentration field ϕ increases for large Γ . Fig. 4.19 gives the effects of Sc on the concentration field. It is observed that ϕ is a decreasing function of Sc . Tables 4.2 and 4.3 are given for the numerical values of the Nusselt number and Sherwood number for the different values of involved parameters of interest. From Table 4.2 it is found that the magnitude of $-\theta'(0)$ decreases for large values of R_d . The magnitude of $-\phi'(0)$ increases when Sc is increased. Table 4.3 is prepared for the variations of N , γ_1 , β , M , and λ on $-\theta'(0)$ and $-\phi'(0)$. It is obvious from this Table that the magnitude of $-\phi'(0)$ increases for large values of λ and decreases for large values of M .

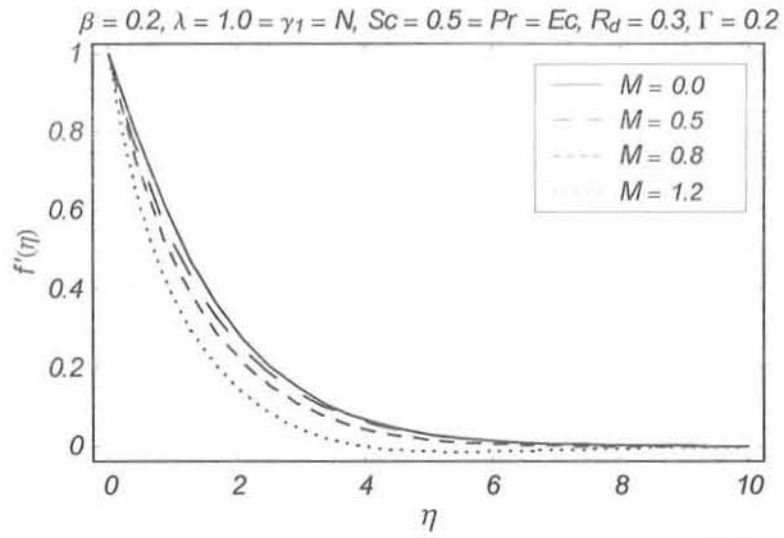
4.5 Concluding remarks

Heat and mass transfer analysis in presence of thermal radiation and thermophoresis on a steady mixed convection of an incompressible Maxwell fluid is analyzed. Series solutions for velocity, temperature and concentration fields are developed and discussed. The behaviors of embedded parameters are examined. The main results of the present analysis are mentioned as follows.

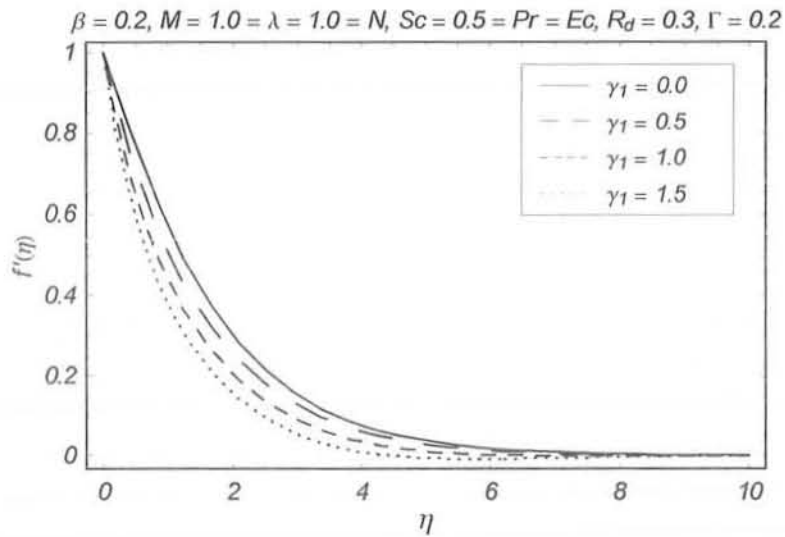
- The effects of β , M , R_d and Ec on f' are similar in a qualitative sense.
- Velocity f' is an increasing function of N .
- Behaviors of R_d and Pr on the temperature θ are opposite.
- The temperature θ decreases when Pr increases.
- Variation of Γ on temperature θ is opposite to that of Pr .
- Concentration field decreases by increasing Sc .
- The magnitude of the local Nusselt and Sherwood number increases when γ_1 is increased.
- Effects of Γ on the local Nusselt and Sherwood numbers are opposite.



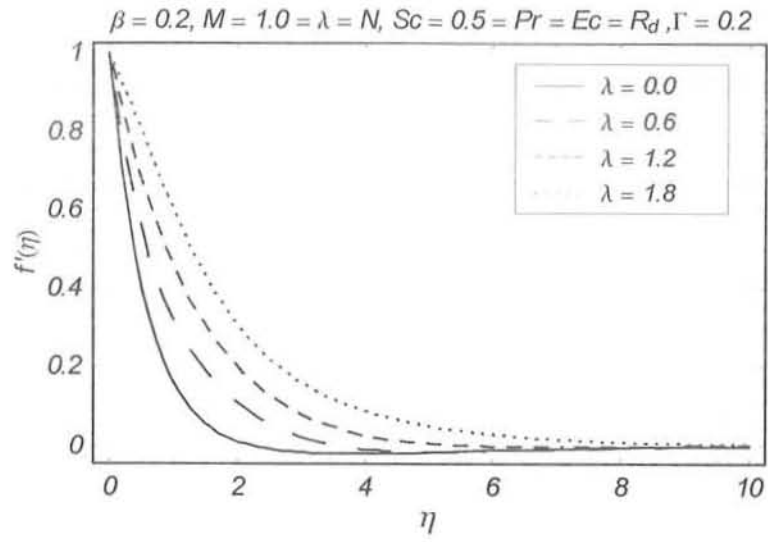
Figs 4.2: Influence of β on the velocity f' .



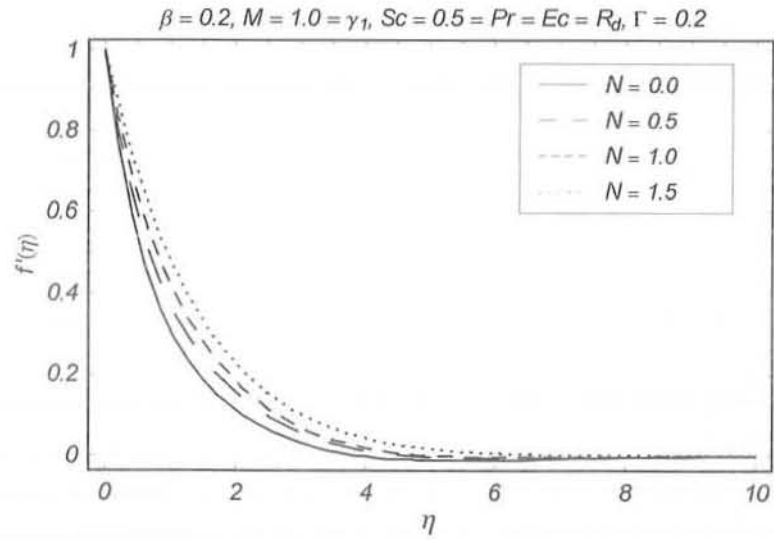
Figs 4.3: Influence of M on the velocity f' .



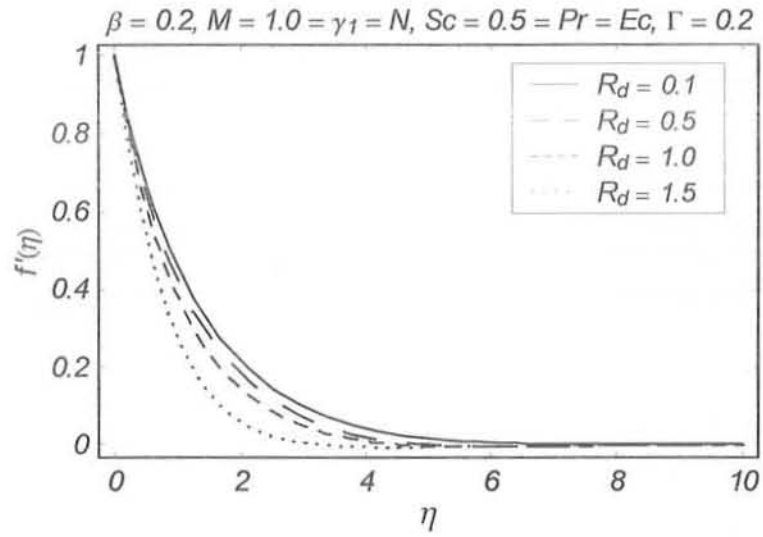
Figs 4.4: Influence of γ_1 on the velocity f' .



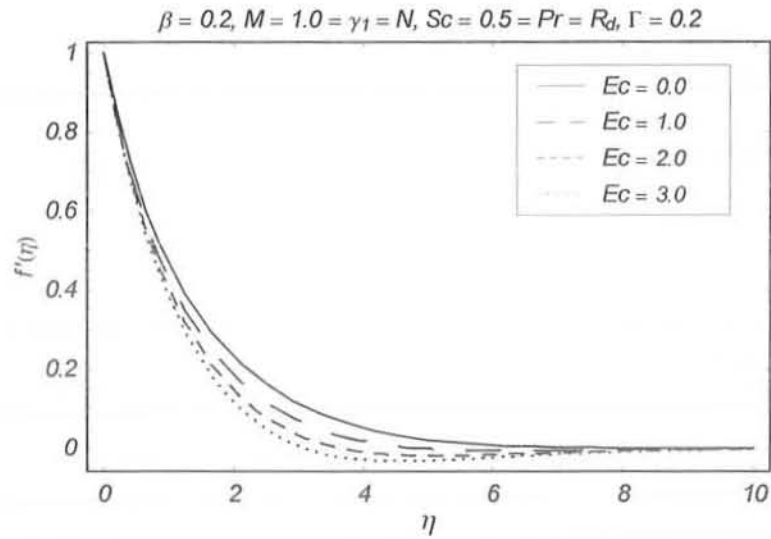
Figs 4.5: Influence of λ on the velocity f' .



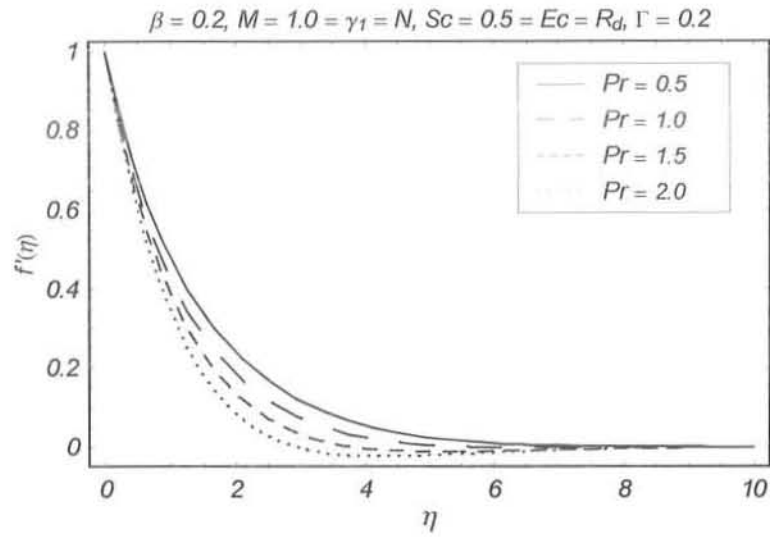
Figs 4.6: Influence of N on the velocity f' .



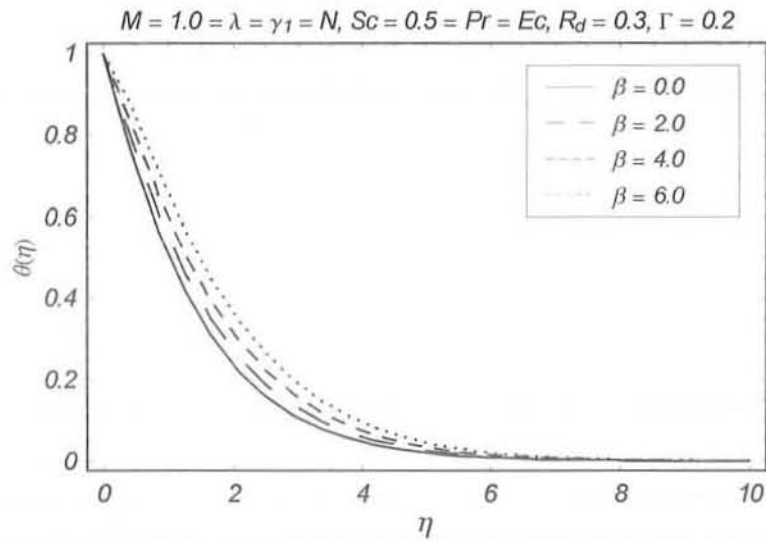
Figs 4.7: Influence of R_d on the velocity f' .



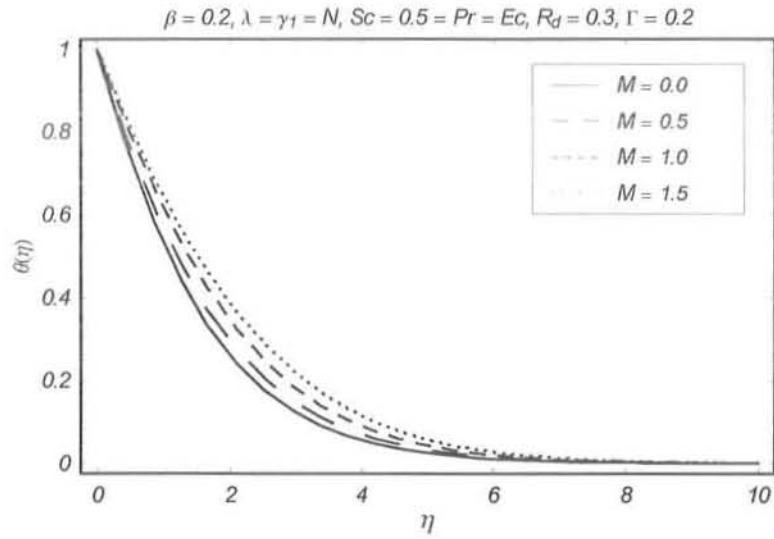
Figs 4.8: Influence of Ec on the velocity f' .



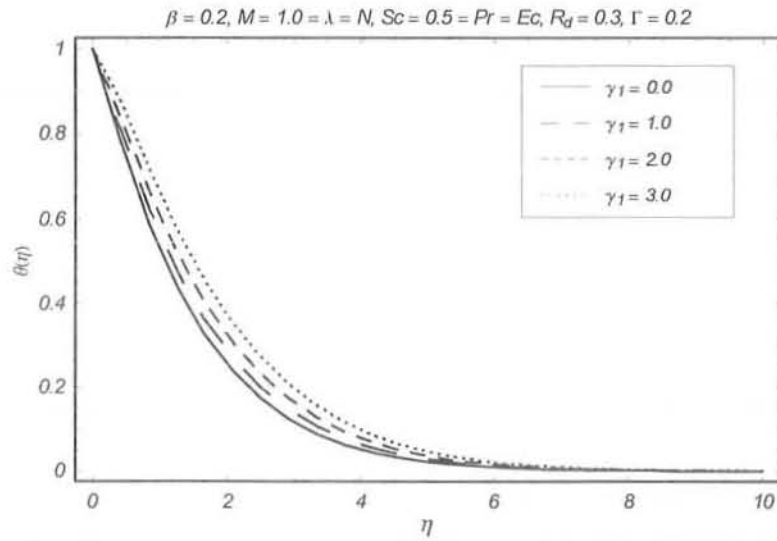
Figs 4.9: Influence of Pr on the velocity f' .



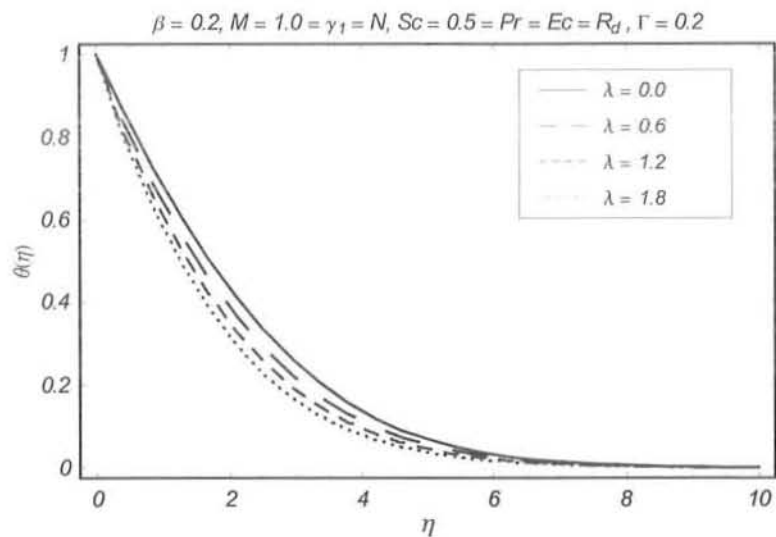
Figs. 4.10: Influence of β on the temperature θ .



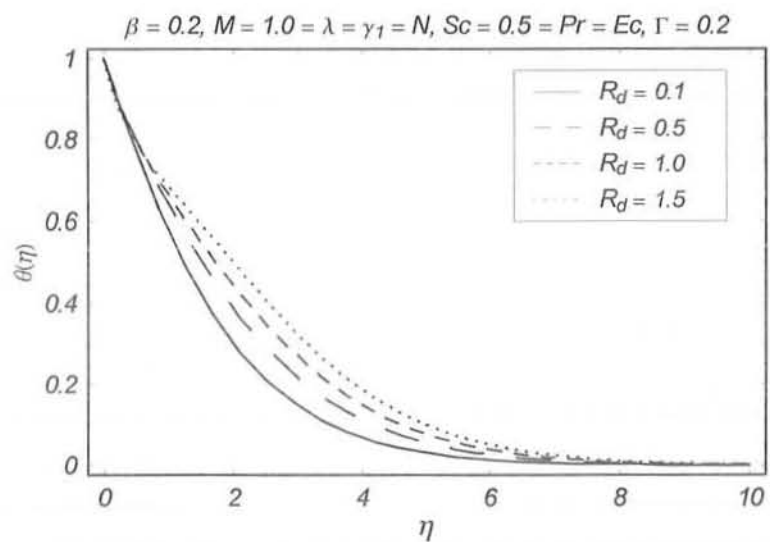
Figs. 4.11: Influence of β on the temperature θ .



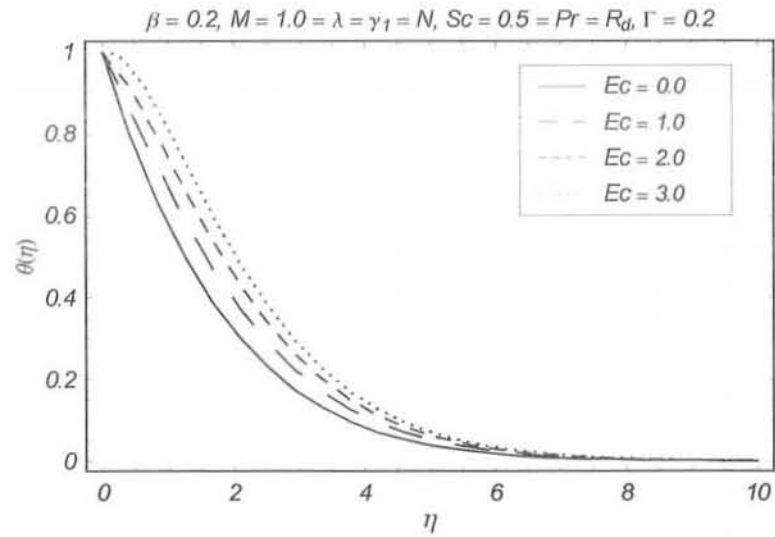
Figs. 4.12: Influence of γ_1 on the temperature θ .



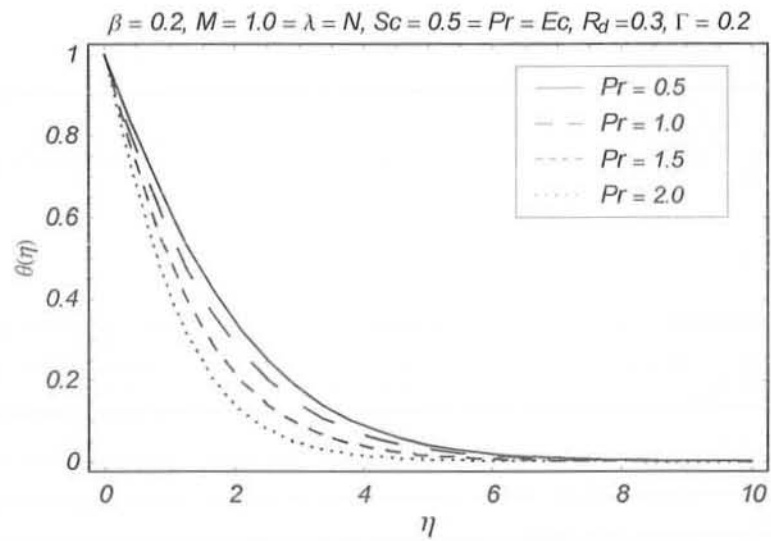
Figs. 4.13: Influence of λ on the temperature θ .



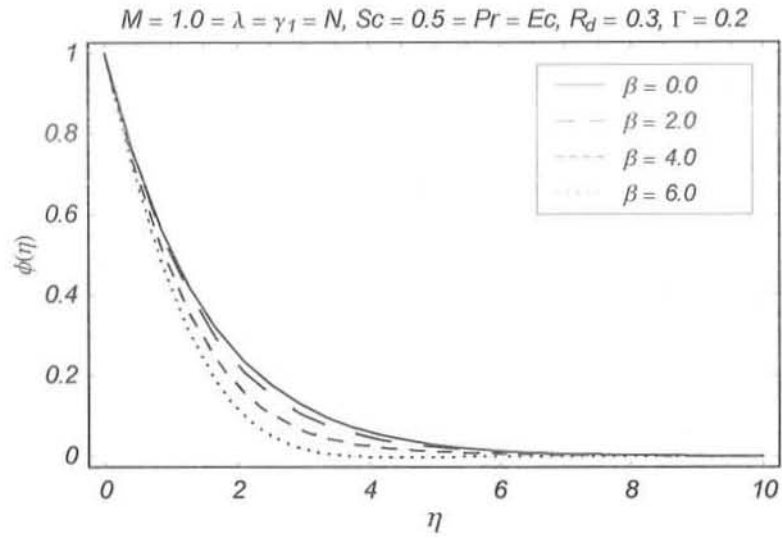
Figs. 4.14: Influence of R_d on the temperature θ .



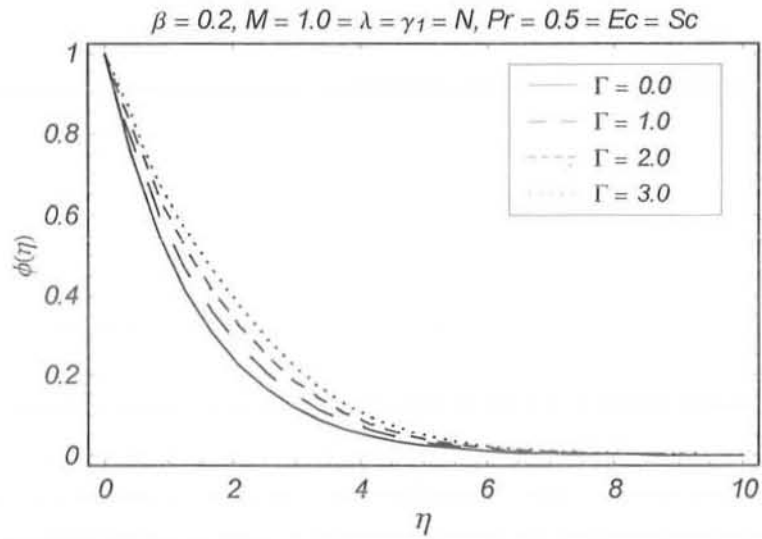
Figs. 4.15: Influence of Ec on the temperature θ .



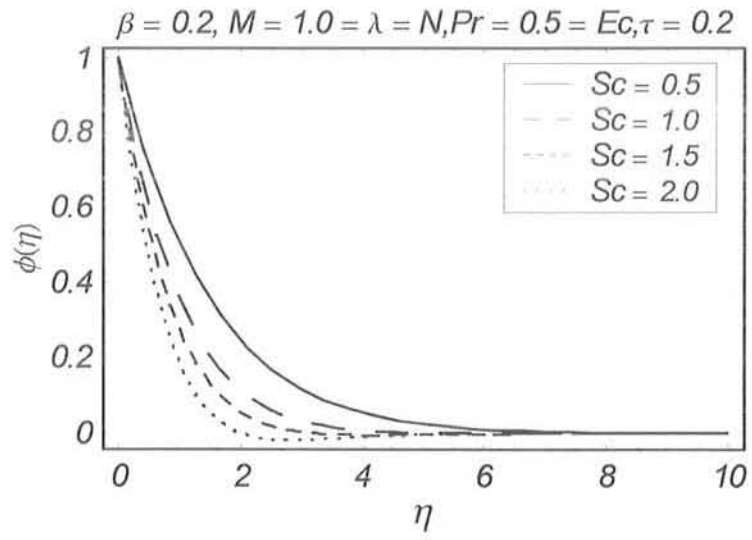
Figs. 4.16: Influence of Pr on the temperature θ .



Figs. 4.17: Influence of β on the concentration ϕ .



Figs. 4.18: Influence of Γ on the concentration ϕ .



Figs. 4.19: Influence of Sc on the concentration ϕ .

Chapter 5

Influence of thermal radiation on the steady flow of a Maxwell fluid over a moving permeable surface in a parallel free stream

The flow and heat transfer characteristics over a moving permeable surface in a Maxwell fluid in this chapter. Governing problems of flow and heat transfer are solved analytically by employing the homotopy analysis method (HAM). Effects of the involved parameters namely the Deborah number β , suction parameter S , constant velocity ratio (Here $0 < r < 1$ correspond to the sheet moving in the same direction to the free stream, while $r < 0$ and $r > 1$ are when they move in the opposite directions), the Prandtl number Pr , Eckert number Ec and the radiation parameter R_d are examined carefully. A comparative study is presented with the known numerical solution in a limiting sense and an excellent agreement is noted. It is found that f' in the Maxwell fluid is less than the viscous fluid.

5.1 Problem development

Let us investigate the steady flow of a Maxwell fluid over a moving permeable surface moving with constant velocity u_w in the same direction as that of the uniform free stream velocity u_∞ . The constant temperature of wall and free stream are denoted by T_w and T_∞ . The boundary layer flow is given by the following equations

$$\frac{\partial u}{\partial x} + \frac{\partial v}{\partial y} = 0, \quad (5.1)$$

$$u \frac{\partial u}{\partial x} + v \frac{\partial u}{\partial y} + \lambda_1 \left[u^2 \frac{\partial^2 u}{\partial x^2} + v^2 \frac{\partial^2 u}{\partial y^2} + 2uv \frac{\partial^2 u}{\partial x \partial y} \right] = \nu \frac{\partial^2 u}{\partial y^2}, \quad (5.2)$$

$$u \frac{\partial T}{\partial x} + v \frac{\partial T}{\partial y} = \frac{k}{\rho c_p} \frac{\partial^2 T}{\partial y^2} - \frac{1}{\rho c_p} \frac{\partial q_r}{\partial y} + \frac{\mu}{\rho c_p} \left(\frac{\partial u}{\partial y} \right)^2, \quad (5.3)$$

where u and v denote the velocity components in x - and y -directions respectively, T is the fluid temperature, c_p is specific heat, q_r is the radiative heat flux which is [136]

$$q_r = \frac{-4\sigma^*}{3k^*} \frac{\partial T^4}{\partial y} \quad (5.4)$$

in which σ^* represents the Stefan-Boltzman constant and k^* is Rosseland mean absorption coefficient. We assume that temperature difference with the flow are sufficiently small such that T^4 could be approached as a linear function of temperature. Hence, we expressed T^4 in Talyors series around T_∞ and neglect higher order terms. That is

$$T^4 \approx 4T_\infty^3 T - 3T_\infty^4. \quad (5.5)$$

Now Eq. (5.3) becomes

$$u \frac{\partial T}{\partial x} + v \frac{\partial T}{\partial y} = \frac{k}{\rho c_p} \frac{\partial^2 T}{\partial y^2} + \frac{16\sigma^* T_\infty^3}{3k^* \rho c_p} \frac{\partial^2 T}{\partial y^2} + \frac{\mu}{\rho c_p} \left(\frac{\partial u}{\partial y} \right)^2. \quad (5.6)$$

The boundary conditions can be written as follows

$$\begin{aligned} u &= u_w, & v &= v_w, & T &= T_w & \text{at } y &= 0, \\ u &\rightarrow u_\infty, & \frac{\partial u}{\partial y} &\rightarrow 0, & T &\rightarrow T_\infty & \text{as } y &\rightarrow \infty, \end{aligned} \quad (5.7)$$

where

$$v_w = - \left(\frac{\nu U}{2x} \right)^{1/2} f(0) \quad (5.8)$$

We define the dimensionless quantities given below

$$\begin{aligned} \psi &= \sqrt{2x\nu U} f(\eta), & \theta(\eta) &= \frac{T - T_\infty}{T_w - T_\infty}, & \eta &= \sqrt{\frac{U}{2x\nu}} y, \\ u &= U f'(\eta), & v &= -\sqrt{\frac{U\nu}{2x}} [f(\eta) - \eta f'(\eta)] \end{aligned} \quad (5.9)$$

where $U = u_w + u_\infty$ and the stream function ψ satisfies

$$u = \frac{\partial \psi}{\partial y}, \quad v = -\frac{\partial \psi}{\partial x}, \quad (5.10)$$

The above expression also satisfies the continuity equation (5.1). From Eqs. (5.2) and (5.6) we have

$$f''' + f f'' - \frac{\beta}{2} (2f f' f'' + f^2 f''' + \eta f'^2 f'') = 0, \quad (5.11)$$

$$\left(1 + \frac{4}{3} R_d \right) \theta'' + \text{Pr} f \theta' + \text{Pr} Ec f'^2 = 0, \quad (5.12)$$

and the boundary conditions (5.7) are

$$\begin{aligned} f(0) &= S, & f'(0) &= 1 - r, & \theta(0) &= 1, \\ f'(\infty) &= r, & f''(\infty) &= 0, & \theta(\infty) &= 0. \end{aligned} \quad (5.13)$$

with $f(0) = S$ with $S > 0$ corresponds to suction case and $S < 0$ implies injection. Here primes denote the differentiation with respect to η , r is the constant parameter, Pr is the Prandtl number, Ec is the Eckert number, R_d is the radiation parameter and β is the dimensionless Deborah number. These are defined by

$$r = \frac{u_\infty}{U}, \quad Pr = \frac{\mu c_p}{\alpha}, \quad \beta = \frac{\lambda_1 U}{x\nu}, \quad Ec = \frac{U^2}{c_p(T_w - T_\infty)}, \quad R_d = \frac{4\sigma^* T_\infty^3}{k^*k} \quad (5.14)$$

At this stage the local Nusselt number Nu_x and heat transfer from the plate q_w can be computed from the following expressions

$$Nu_x = \frac{xq_w}{k(T_w - T_\infty)}, \quad (5.15)$$

where q_w is the heat transfer from the plate, which is given by

$$q_w = -k \left(\frac{\partial T}{\partial y} \right)_{y=0}. \quad (5.16)$$

which in terms of variables (5.9) become

$$Re_x^{-1/2} Nu_x = -\theta'(0), \quad (5.17)$$

in which $Re_x = Ux/\nu$ is the local Reynolds number.

5.2 Homotopy analysis solutions

The initial guesses approximations of $f(\eta)$ and $\theta(\eta)$ are chosen as

$$f_0(\eta) = S + (1 - 2r) [(1 - \exp(-\eta))] + r\eta, \quad \text{for } r \neq 1/2, \quad (5.18)$$

$$\theta_0(\eta) = \exp(-\eta) + \frac{1}{2}\eta \exp(-\eta), \quad (5.19)$$

and the auxiliary linear operators \mathcal{L}_f and \mathcal{L}_θ are

$$\mathcal{L}_f(f) = \frac{d^3 f}{d\eta^3} - \frac{df}{d\eta}, \quad (5.20)$$

$$\mathcal{L}_\theta(f) = \frac{d^2 f}{d\eta^2} - f \quad (5.21)$$

with

$$\mathcal{L}_f [C_1 + C_2 \exp(\eta) + C_3 \exp(-\eta)] = 0, \quad (5.22)$$

$$\mathcal{L}_\theta [C_4 \exp(\eta) + C_5 \exp(-\eta)] = 0 \quad (5.23)$$

in which C_i , ($i = 1 - 5$) are the arbitrary constants. If $p \in [0, 1]$ is the embedding parameter and \hbar_f , and \hbar_θ are the non-zero auxiliary parameters then the zeroth-order deformation problems are given below

$$(1-p) \mathcal{L}_f [\hat{f}(\eta; p) - f_0(\eta)] = p \hbar_f \mathcal{N}_f [\hat{f}(\eta; p)], \quad (5.24)$$

$$(1-p) \mathcal{L}_\theta [\hat{\theta}(\eta; p) - \theta_0(\eta)] = p \hbar_\theta \mathcal{N}_\theta [\hat{\theta}(\eta; p), \hat{f}(\eta; p)], \quad (5.25)$$

$$\hat{f}(0; p) = 0, \quad \hat{f}'(0; p) = 1 - r, \quad \hat{f}'(\infty; p) = r, \quad \hat{f}''(\infty; p) = 0, \quad (5.26)$$

$$\hat{\theta}(0; p) = 1, \quad \hat{\theta}(\infty; p) = 0, \quad (5.27)$$

in which the non-linear operators \mathcal{N}_f and \mathcal{N}_θ are of the following forms:

$$\begin{aligned} \mathcal{N}_f [\hat{f}(\eta; p)] &= \frac{\partial^3 \hat{f}(\eta; p)}{\partial \eta^3} + \hat{f}(\eta; p) \frac{\partial^2 \hat{f}(\eta; p)}{\partial \eta^2} \\ &- \frac{\beta}{2} \left[2\hat{f}(\eta, p) \frac{\partial \hat{f}(\eta, p)}{\partial \eta} \frac{\partial^2 \hat{f}(\eta, p)}{\partial \eta^2} + (\hat{f}(\eta, p))^2 \frac{\partial^3 \hat{f}(\eta, p)}{\partial \eta^3} \right. \\ &\quad \left. + \eta \left(\frac{\partial^2 \hat{f}(\eta, p)}{\partial \eta^2} \right)^2 \frac{\partial^3 \hat{f}(\eta, p)}{\partial \eta^3} \right], \end{aligned} \quad (5.28)$$

$$\begin{aligned} \mathcal{N}_\theta \left[\widehat{\theta}(\eta; p), \widehat{f}(\eta; p) \right] &= \left(1 + \frac{4}{3} R_d\right) \frac{\partial^2 \widehat{\theta}(\eta; p)}{\partial \eta^2} + \text{Pr} \widehat{f}(\eta; p) \frac{\partial \widehat{\theta}(\eta; p)}{\partial \eta} \\ &+ \text{Pr} Ec \left(\frac{\partial^2 \widehat{f}(\eta; p)}{\partial \eta^2} \right)^2. \end{aligned} \quad (5.29)$$

For $p = 0$ and $p = 1$, the above zeroth-order deformation equations have the solutions

$$\widehat{f}(\eta; 0) = f_0(\eta), \quad \widehat{f}(\eta; 1) = f(\eta), \quad (5.30)$$

$$\widehat{\theta}(\eta; 0) = \theta_0(\eta), \quad \widehat{\theta}(\eta; 1) = \theta(\eta). \quad (5.31)$$

When p increases from 0 to 1, $\widehat{f}(\eta; p)$ and $\widehat{\theta}(\eta; p)$ vary from $f_0(\eta)$ and $\theta_0(\eta)$ to the exact solutions $f(\eta)$ and $\theta(\eta)$. In view of Taylor's theorem and Eqs. (5.25) and (5.26) one can write

$$\widehat{f}(\eta; p) = f_0(\eta) + \sum_{m=1}^{\infty} f_m(\eta) p^m, \quad (5.32)$$

$$\widehat{\theta}(\eta; p) = \theta_0(\eta) + \sum_{m=1}^{\infty} \theta_m(\eta) p^m, \quad (5.33)$$

where

$$f_m(\eta) = \frac{1}{m!} \left. \frac{\partial^m \widehat{f}(\eta; p)}{\partial p^m} \right|_{p=0}, \quad \theta_m(\eta) = \frac{1}{m!} \left. \frac{\partial^m \widehat{\theta}(\eta; p)}{\partial p^m} \right|_{p=0}, \quad (5.34)$$

The auxiliary parameters are so properly chosen that the series (5.24) and (5.25) converge at $p = 1$. Hence

$$f(\eta) = f_0(\eta) + \sum_{m=1}^{\infty} f_m(\eta), \quad (5.35)$$

$$\theta(\eta) = \theta_0(\eta) + \sum_{m=1}^{\infty} \theta_m(\eta). \quad (5.36)$$

The m th-order deformation problems are

$$\mathcal{L}_f [f_m(\eta) - \chi_m f_{m-1}(\eta)] = \hbar_f \mathcal{R}_m^f(\eta), \quad (5.37)$$

$$\mathcal{L}_\theta [\theta_m(\eta) - \chi_m \theta_{m-1}(\eta)] = \hbar_\theta \mathcal{R}_m^\theta(\eta), \quad (5.38)$$

$$f_m(0) = f'_m(0) = f'_m(\infty) = f''_m(\infty) = 0, \quad (5.39)$$

$$\theta_m(0) = \theta_m(\infty) = 0, \quad (5.40)$$

$$\mathcal{R}_m^f(\eta) = f'''_{m-1}(\eta) + \sum_{k=0}^{m-1} \left[f_{m-1-k} f''_k - \frac{\beta}{2} \left(\begin{aligned} & 2f_{m-1-k} \sum_{l=0}^k f'_{k-l} f''_l \\ & + f_{m-1-k} \sum_{l=0}^k f_{k-l} f'''_l + \eta f'_{m-1-k} \sum_{l=0}^k f'_{k-l} f''_l \end{aligned} \right) \right], \quad (5.41)$$

$$\mathcal{R}_m^\theta(\eta) = \left(1 + \frac{4}{3} R_d \right) \theta''_{m-1} + \text{Pr} \sum_{k=0}^{m-1} [\theta'_{m-1-k} f_k + Ec f''_{m-1-k} f'_k], \quad (5.42)$$

$$\chi_m = \begin{cases} 0, & m \leq 1, \\ 1, & m > 1. \end{cases} \quad (5.43)$$

5.3 Convergence of the homotopy solution

The auxiliary parameters \hbar_f and \hbar_θ in the series solutions (5.35) and (5.36) have a great role in adjusting and controlling the convergence. In order to find the admissible values of \hbar_f and \hbar_θ the \hbar_f and \hbar_θ -curves are plotted for 20th-order of approximations. Fig. 1 depicts that the range for the admissible values of \hbar_f and \hbar_θ are $-0.8 \leq \hbar_f \leq -0.2$ and $-1.0 \leq \hbar_\theta \leq -0.6$. It is found that the series given by (5.35) and (5.36) converge in the whole region of η when

$\hbar_f = -0.5$ and $\hbar_\theta = -0.7$.

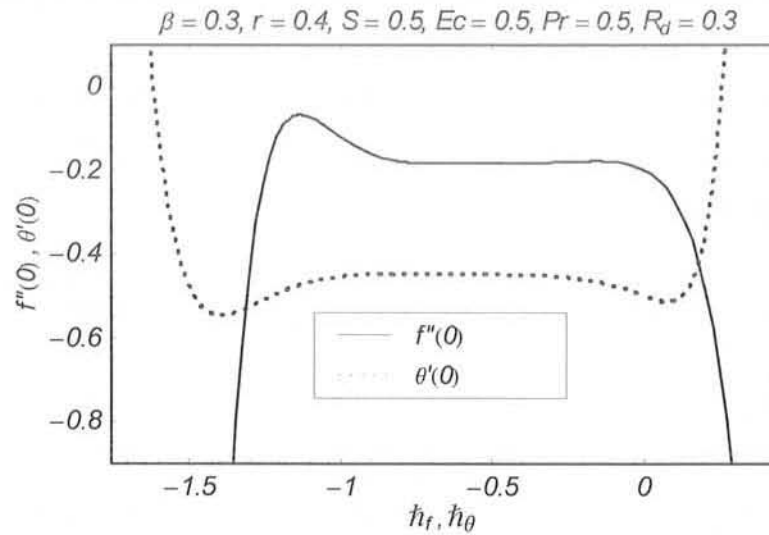


Fig. 5.1. \hbar -curves for 20th-order approximations.

5.4 Results and discussion

Our interest here is to discuss the variations of pertinent parameters such as Deborah number β , the constant velocity ratio r , suction parameter S , the Prandtl number Pr , the Eckert number Ec and the radiation parameter R_d . Therefore Figs. 5.2–5.11 have been plotted. The variation of Deborah number β , the velocity ratio r and the suction parameter S on the velocity f' can be seen through Figs. 5.2–5.6. Figs. 5.2 and 5.3 study the influence of β on f' when $r = 0.3$ and $r = 1.0$. It is revealed that the boundary layer thickness decreases with the increasing values of β . The variation of S on f' is illustrated in the Figs. 5.4 and 5.5. These Figs. show that β and S has similar effects on f' . It is noticed that decrease is larger in the case of S when compared with β . Hence a porous character of wall provides a powerful mechanism for controlling the momentum boundary layer thickness. Fig. 5.6 describes the effect of r on f' . It is found that initially f' decreases but after $\eta = 0.6$, it increases when r decreases.

Figs. 5.7–5.11 describe the effects of suction parameter S , the velocity ratio r , the Prandtl

number Pr , the Eckert number Ec and radiation parameter R_d on temperature profile θ . Fig. 5.7 elucidates the effects of S on θ . The temperature field θ decreases when S increases. Fig. 5.8 indicates the effect of r on θ . The boundary layer thickness decreases by increasing r . It is observed that θ decreases when Pr increases (Fig. 5.9). A higher Prandtl number fluid has a thinner thermal boundary layer and this increases the gradient of temperature. The influence of Eckert number Ec is shown in Fig. 5.10. It is observed that θ is an increasing function of Ec . The boundary layer thickness also increases when Ec increases. Fig. 5.11 describes the effects of R_d on θ . Here θ increases as R_d increases. Table 5.1 includes the values of the skin friction coefficient when $\beta = 0 = S$. From this Table it can be seen that the HAM solution has a good agreement with the corresponding numerical solution in a viscous fluid [131]. Table 5.2 presents the values of skin friction coefficient for some values of S when $\beta = 0$. Table 5.3 depicts the variation of heat transfer at the wall $-\theta'(0)$ for some values of Ec and r when $Pr = 0.7$, $\beta = R_d = 0 = S$. The numerical values of present result has an excellent agreement with those obtained in [131]. Table 5.4 presents the values of $-\theta'(0)$ for different values of S and R_d when $Pr = 0.7$, $r = 0.4$ and $\beta = 0$. The local Nusselt number increases when Prandtl number Pr is increased.

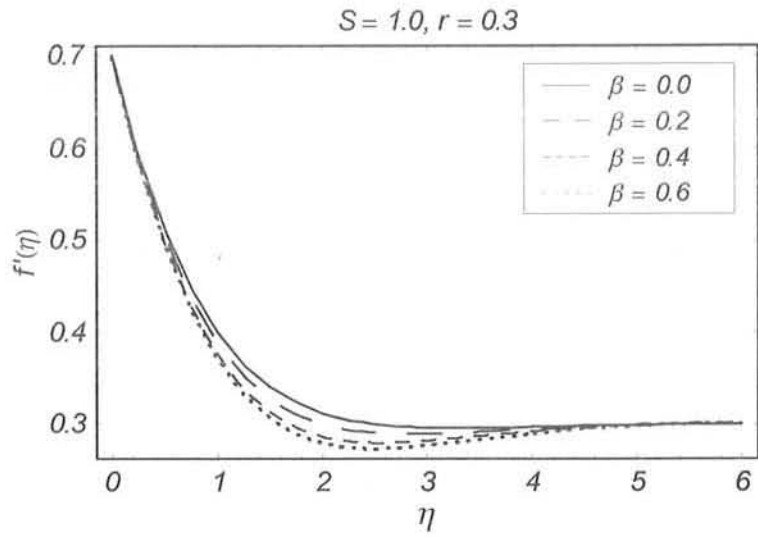


Fig. 5.2. Velocity profile $f'(\eta)$ for various values of β when $r = 0.3$.

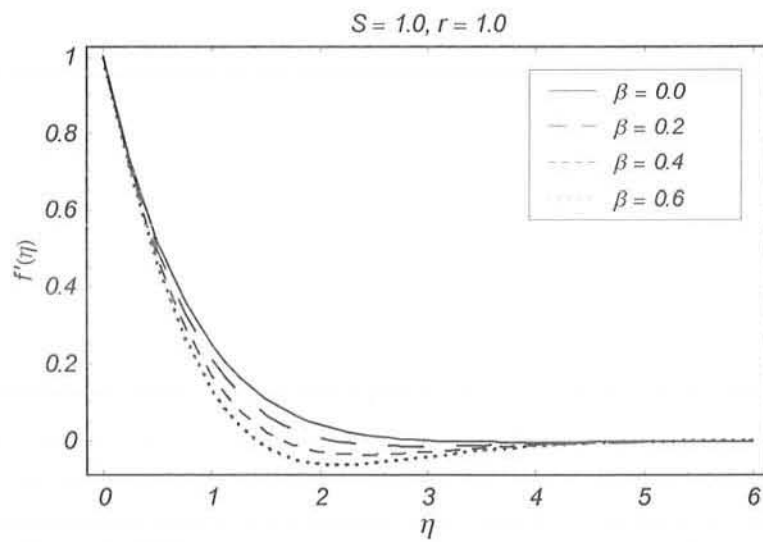


Fig. 5.3. Velocity profile $f'(\eta)$ for various values of β when $r = 1.0$.

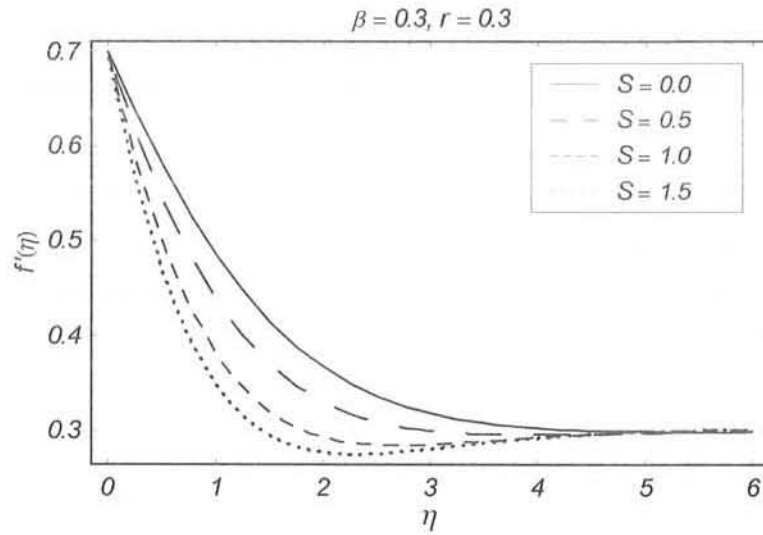


Fig. 5.4. Velocity profiles $f'(\eta)$ for various values of S when $r = 0.3$.

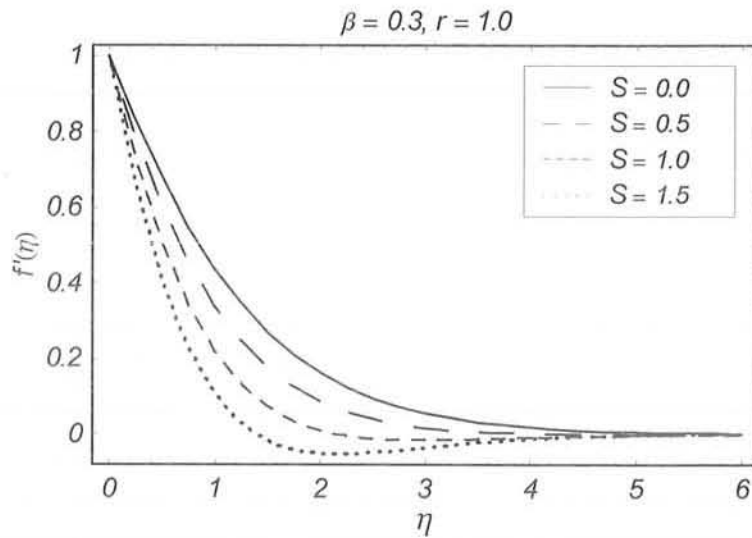


Fig. 5.5. Velocity profile $f'(\eta)$ for various values of β when $r = 1.0$.

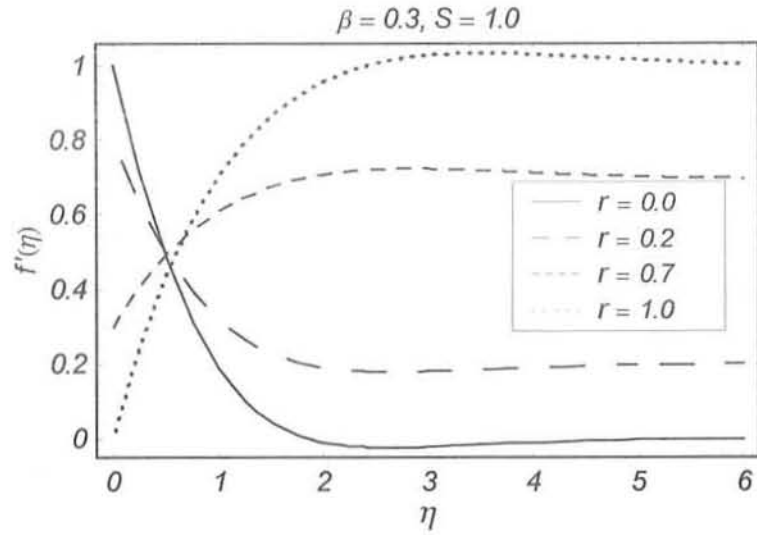


Fig. 5.6. Velocity profile $f'(\eta)$ for various values of r .

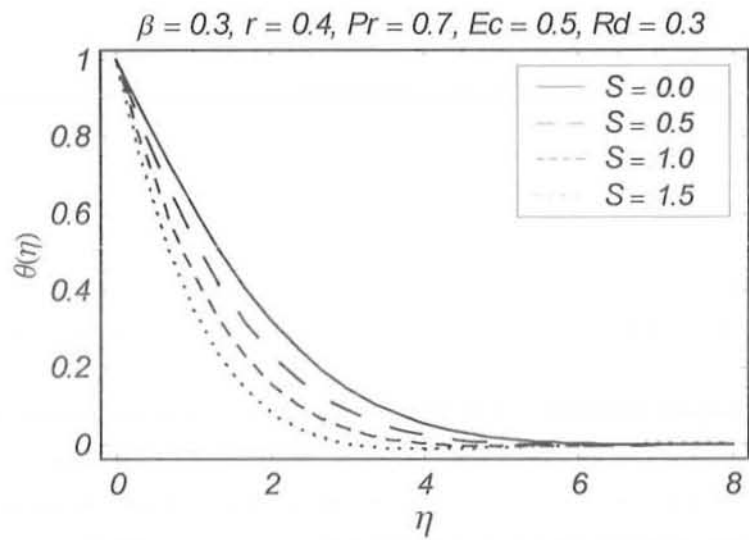


Fig. 5.7. Temperature profile $\theta(\eta)$ for various values of S .

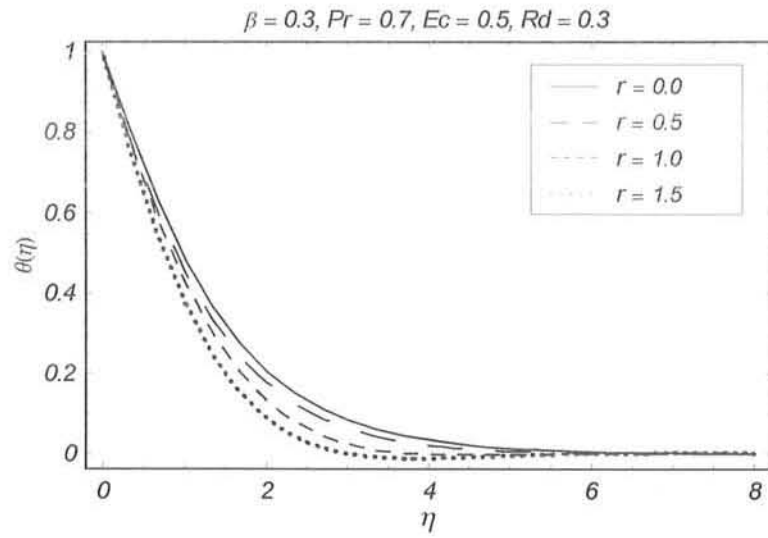


Fig. 5.8. Temperature profile $\theta(\eta)$ for various values of r .

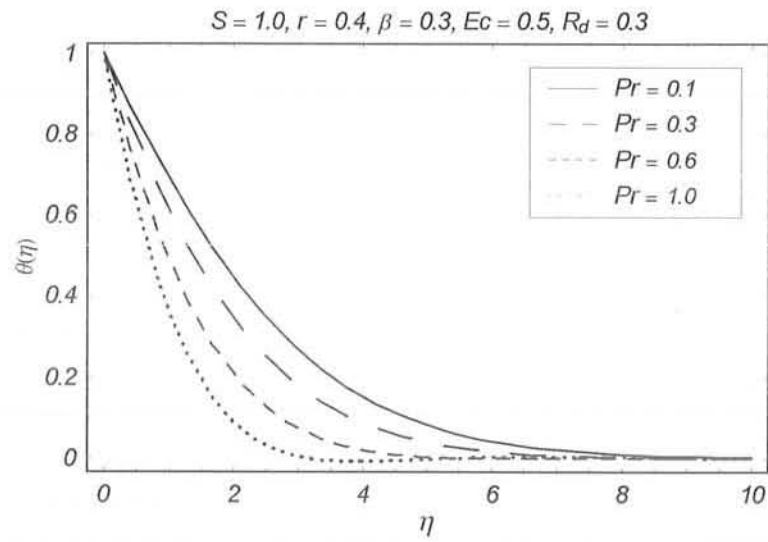


Fig. 5.9. Temperature profile $\theta(\eta)$ for various values of Pr .

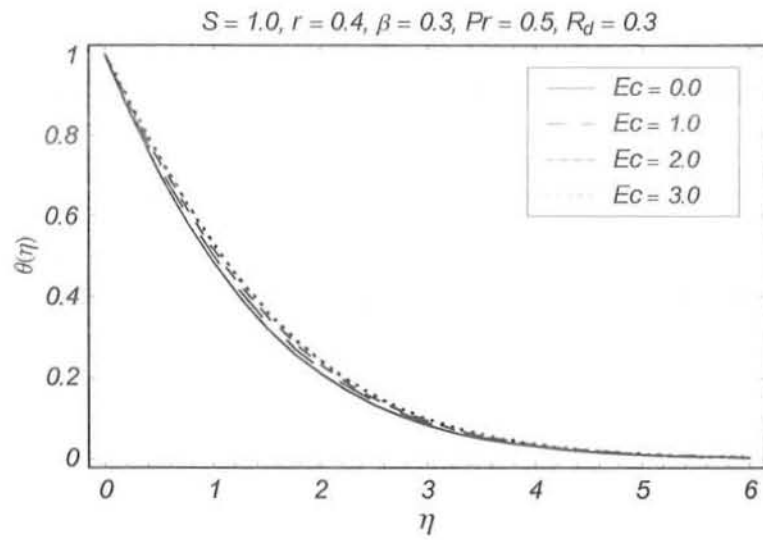


Fig. 5.10. Temperature profile $\theta(\eta)$ for various values of Ec .

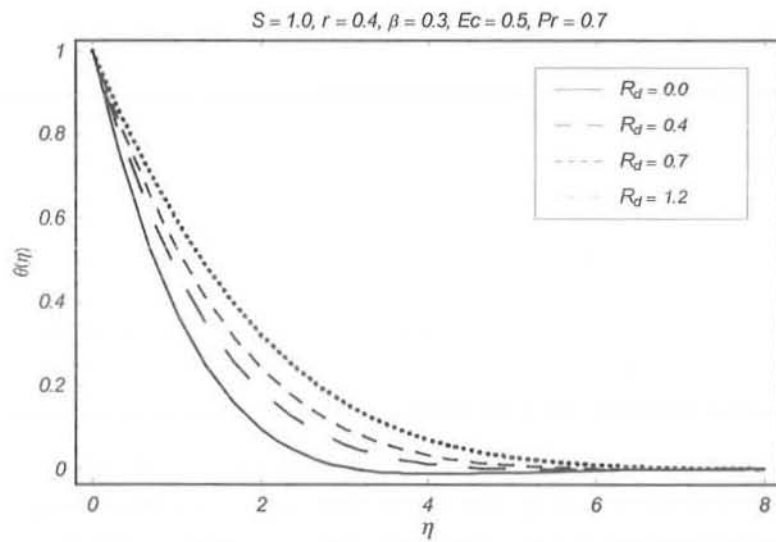


Fig. 5.11. Temperature profile $\theta(\eta)$ for various values of R_d .

r	[131]	Present results
0	-0.627562	-0.627548
0.1	-0.493760	-0.493753
0.2	-0.363346	-0.363335
0.3	-0.237133	-0.237137
0.4	-0.115810	-0.115810
0.5	0.000000	0.000000
0.6	0.109638	0.109658
0.7	0.212373	0.212392
0.8	0.307355	0.307376
0.9	0.393563	0.393528
1.0	0.469601	0.469654
1.1	0.533708	0.533813
1.2	0.583178	0.583239
1.3	0.613646	0.614732
1.4	0.616140	0.653461
1.5	0.565821	0.769748

Table 5.1: Values of $f''(0)$ for some values of r when $\beta = 0 = S$.

S	r	$f''(0)$
-0.3	0.4	-0.081214
-0.1		-0.103628
0.0		-0.115810
0.5		-0.185218
1.0		-0.265104
0.5	0.0	-0.957637
	0.3	-0.374052
	0.5	0.000000
	0.7	0.357932
	1.0	0.857625

Table 5.2: Values of $f''(0)$ for some values of S when $\beta = 0$.

Ec	r	[131]	Present Results
0.0	0.1	0.493641	0.493616
0.03		0.489305	0.489298
	0.3	0.484789	0.484812
	0.7	0.452195	0.452346
	0.9	0.425233	0.425267
	1.2	0.368048	0.368254
	1.5	0.264915	0.264998
0.1	1.2	0.346889	0.346963
	1.5	0.234991	0.235075

Table 5.3: Values of $-\theta'(0)$ for some values of Ec and r when $Pr = 0.7$, $\beta = R_d = 0 = S$.

S	R_d	Pr	$-\theta'(0)$
0.2	0.3	0.7	0.461479
0.6			0.599733
1.2			0.830794
1.5			0.954183
0.5	0.0	0.7	0.713993
	0.3		0.563952
	0.6		0.475947
	0.9		0.416898
		0.1	0.227182
		0.7	0.563846
		1.0	0.721336

Table 5.4: Values of $-\theta'(0)$ for some values of S and R_d when $\text{Pr} = 0.7$, $r = 0.4$ and $\beta = 0$.

Chapter 6

Effects of thermal radiation on unsteady MHD flow of a Micropolar fluid with heat and mass transfer

This chapter explores the combined effects of heat and mass transfer on the unsteady flow of a micropolar fluid over a stretching sheet. The thermal radiation effects are present. The arising non-linear partial differential equations are first reduced to a set of non-linear ordinary differential equations and then solved by homotopy analysis method (HAM). Plots for various interesting parameters are presented and discussed. Numerical data for surface shear stress, Nusselt number and Sherwood numbers in steady case are also tabulated. Comparison between the present and previous limiting results is given.

6.1 Mathematical formulation

We investigate the unsteady flow of a micropolar fluid over a stretching surface. The fluid is electrically conducting in the presence of a constant applied magnetic field B_0 . The induced

magnetic field is neglected under the assumption of a small magnetic Reynold number. Initially (for $t = 0$), both fluid and plate are stationary. The fluid has constant temperature T_∞ and concentration C_∞ . The plate at $y = 0$ is stretched by the velocity component $u = ax$. For $t > 0$ the surface temperature and concentration are T_w and C_w respectively. The boundary layer flow is governed by the following equations

$$\frac{\partial u}{\partial x} + \frac{\partial v}{\partial y} = 0, \quad (6.1)$$

$$\frac{\partial u}{\partial t} + u \frac{\partial u}{\partial x} + v \frac{\partial u}{\partial y} = \left(\nu + \frac{\kappa}{\rho} \right) \frac{\partial^2 u}{\partial y^2} + \frac{\kappa}{\rho} \frac{\partial N^*}{\partial y} - \frac{\sigma B_0^2}{\rho} u, \quad (6.2)$$

$$\frac{\partial N^*}{\partial t} + u \frac{\partial N^*}{\partial x} + v \frac{\partial N^*}{\partial y} = \frac{\gamma^*}{\rho j} \frac{\partial^2 N^*}{\partial y^2} - \frac{\kappa}{\rho j} \left(2N^* + \frac{\partial u}{\partial y} \right), \quad (6.3)$$

$$\rho c_p \left[\frac{\partial T}{\partial t} + u \frac{\partial T}{\partial x} + v \frac{\partial T}{\partial y} \right] = k \frac{\partial^2 T}{\partial y^2} - \frac{\partial q_r}{\partial y}, \quad (6.4)$$

$$\frac{\partial C}{\partial t} + u \frac{\partial C}{\partial x} + v \frac{\partial C}{\partial y} = D \frac{\partial^2 C}{\partial y^2} - RC \quad (6.5)$$

and the subjected conditions are

$$\begin{aligned} u &= v = N^* = 0, \quad T = T_\infty, \quad C = C_\infty, \quad t < 0, \\ u &= u_w = ax, \quad v = 0, \quad N^* = -N_0 \frac{\partial u}{\partial y}, \quad T = T_w, \quad C = C_w, \quad y = 0; \quad t \geq 0, \\ u &\rightarrow 0, \quad v \rightarrow 0, \quad N^* \rightarrow 0, \quad T \rightarrow 0, \quad C \rightarrow 0, \quad \text{as } y \rightarrow \infty. \quad t \geq 0, \end{aligned} \quad (6.6)$$

in which u and v are the velocity components along the x - and y -axes, respectively, ρ is fluid density, ν is kinematic viscosity, σ is the electrical conductivity, N^* is the microrotation or angular velocity, T the temperature, c_p the specific heat, k the thermal conductivity of the fluid, q_r the radiative heat flux, C is the concentration species of the fluid, D is the diffusion coefficient of the diffusion species in the fluid, R denotes the first-order homogeneous constant reaction rate, $j = (\nu/c)$ is microinertia per unit mass, $\gamma^* = (\mu + \kappa/2)j$ and κ are the spin

gradient viscosity and vortex viscosity, respectively. Here N_0 is a constant and $0 \leq N_0 \leq 1$. The case $N_0 = 0$, which indicates $N^* = 0$ at the wall, represents concentrated particle flows in which the microelements close to the wall surface are unable to rotate [132]. This case is also known as the strong concentration of microelements [133]. The case $N_0 = \frac{1}{2}$ indicates the vanishing of anti-symmetric part of the stress tensor and denotes weak concentration [134] of microelements. We shall consider here both cases of $N_0 = 0$ and $N_0 = \frac{1}{2}$. However, it can easily be shown that for $N_0 = \frac{1}{2}$ the governing equations can be reduced to the classical problem of steady boundary layer flow of a viscous incompressible fluid near the plane wall. However the most common boundary condition used in the literature is the vanishing of the spin on the boundary, so-called strong interaction. The opposite extreme, the weak interaction, is the vanishing of the momentum stress on the boundary [133]. A third, or compromise in the vanishing of a linear combination of spin, shearing stress and couple stress, involving some friction coefficients, a particular case of which was the condition used by Peddieson [135].

Employing Rosseland approximation we have

$$q_r = -\frac{4\sigma^*}{3k^*} \frac{\partial T^4}{\partial y}, \quad (6.7)$$

where σ^* is the Stefan–Boltzmann constant and k^* the mean absorption coefficient. Using Taylor series one can expand T^4 about T_∞ as

$$T^4 \approx 4T_\infty^3 T - 3T_\infty^4. \quad (6.8)$$

where the higher order terms have been neglected.

Now Eqs. (6.4), (6.7) and (6.8) we have

$$\rho c_p \left[\frac{\partial T}{\partial t} + u \frac{\partial T}{\partial x} + v \frac{\partial T}{\partial y} \right] = \frac{\partial}{\partial y} \left[\left(\frac{16\sigma^* T_\infty^3}{3k^*} + k \right) \frac{\partial T}{\partial y} \right]. \quad (6.9)$$

Defining

$$\begin{aligned}\psi &= (a\nu)^{1/2} \xi^{1/2} x f(\xi, \eta), \quad N^* = (a/\nu)^{1/2} \xi^{-1/2} a x g(\xi, \eta), \quad \eta = (a/\nu)^{1/2} \xi^{-1/2} y \\ \xi &= 1 - \exp(-\tau), \quad \tau = at, \quad \theta = \frac{T - T_\infty}{T_w - T_\infty}, \quad \phi = \frac{C - C_\infty}{C_w - C_\infty}.\end{aligned}\quad (6.10)$$

equation (6.1) is automatically satisfied and Eqs. (6.2), (6.3), (6.5), (6.6) and (6.9) reduce to

$$(1 + K_1) f''' + (1 - \xi) \left(\frac{\eta}{2} f'' - \xi \frac{\partial f'}{\partial \xi} \right) + \xi [f f'' - (f')^2 - M^2 f'] + K_1 g' = 0, \quad (6.11)$$

$$\left(1 + \frac{K_1}{2} \right) g'' + (1 - \xi) \left(\frac{1}{2} g + \frac{\eta}{2} g' - \xi \frac{\partial g}{\partial \xi} \right) + \xi [f g' - f' g - 2K_1 g - K_1 f''] = 0, \quad (6.12)$$

$$(1 + N_R) \theta'' + \text{Pr}(1 - \xi) \left(\frac{\eta}{2} \theta' - \xi \frac{\partial \theta}{\partial \xi} \right) + \text{Pr} \xi f \theta' = 0, \quad (6.13)$$

$$\phi'' + Sc(1 - \xi) \left(\frac{\eta}{2} \phi' - \xi \frac{\partial \phi}{\partial \xi} \right) + Sc \xi f \phi' - \gamma Sc \xi \phi = 0, \quad (6.14)$$

$$\begin{aligned}f(\xi, 0), \quad f'(\xi, 0) &= 1, \quad g(\xi, 0) = -N_0 f''(\xi, 0), \quad \theta(\xi, 0) = \phi(\xi, 0) = 1, \\ f'(\xi, \infty) &= g(\xi, \infty) = \theta(\xi, \infty) = \phi(\xi, \infty) = 0,\end{aligned}\quad (6.15)$$

where prime denotes the derivative with respect to η . Here material parameter K_1 , Hartman number M , Prandtl number Pr , radiation parameter N_R , Schmidt number Sc and chemical reaction parameter γ are given by

$$K_1 = \frac{\kappa}{\mu}, \quad M^2 = \frac{\sigma B_0^2}{\rho a}, \quad \text{Pr} = \frac{\nu}{a}, \quad N_R = \frac{16\sigma^* T_\infty^3}{3kk^*}, \quad Sc = \frac{\nu}{D}, \quad \gamma = \frac{R}{a}. \quad (6.16)$$

The skin friction coefficient C_{fx} , local Nusselt number Nu and local Sherwood number Sh are defined by the following expressions

$$\begin{aligned}
C_{fx} &= \frac{\left[(\mu + \kappa) \frac{\partial u}{\partial y} + \kappa N \right]_{y=0}}{\rho u_w^2}, \\
Nu &= \frac{-x(\partial T / \partial y)_{y=0}}{(T_w - T_\infty)}, \quad Sh = \frac{-x(\partial C / \partial y)_{y=0}}{(C_w - C_\infty)}.
\end{aligned} \tag{6.17}$$

Utilizing Eq. (6.10) we obtain

$$\begin{aligned}
Re_x^{1/2} \xi^{1/2} C_{fx} &= [1 + (1 - N_0) K_1] f''(\xi, 0), \\
Nu Re_x^{-1/2} \xi^{1/2} &= -\theta'(\xi, 0), \quad Sh Re_x^{-1/2} \xi^{1/2} = -\phi'(\xi, 0).
\end{aligned} \tag{6.18}$$

where $Re_x = ax^2/\nu$ is the local Reynolds number.

For $\xi = 0$ (initial unsteady-state flow), Eqs. (6.11) – (6.14) can be written as

$$(1 + K_1) f''' + \frac{\eta}{2} f'' + K_1 g' = 0, \tag{6.19}$$

$$\left(1 + \frac{K_1}{2}\right) g'' + \frac{\eta}{2} g' + \frac{1}{2} g = 0, \tag{6.20}$$

$$(1 + N_R) \theta'' + Pr \frac{\eta}{2} \theta' = 0, \tag{6.21}$$

$$\phi'' + Sc \frac{\eta}{2} \phi' = 0. \tag{6.22}$$

When $\xi = 1$ (final steady state flow) then Eqs. (6.11) – (6.14) become

$$(1 + K_1) f''' + f f'' - (f')^2 - M^2 f' + K_1 g' = 0, \tag{6.23}$$

$$\left(1 + \frac{K_1}{2}\right) g'' + f g' - f' g - 2K_1 g - K_1 f'' = 0, \tag{6.24}$$

$$(1 + N_R) \theta'' + Pr f \theta' = 0, \tag{6.25}$$

$$\phi'' + Scf\phi' - \gamma Sc\phi = 0. \quad (6.26)$$

6.2 Homotopy analysis solutions

For homotopy analysis solutions, we write $f(\xi, \eta)$, $g(\xi, \eta)$, $\theta(\xi, \eta)$ and $\phi(\xi, \eta)$ by a set of base functions

$$\left\{ \xi^k \eta^j \exp(-n\eta) \mid k \geq 0, n \geq 0, j \geq 0 \right\}$$

in the forms

$$f(\eta, \xi) = a_{0,0}^0 + \sum_{k=0}^{\infty} \sum_{j=0}^{\infty} \sum_{n=1}^{\infty} a_{j,n}^k \xi^k \eta^j \exp(-n\eta), \quad (6.27)$$

$$g(\eta, \xi) = \sum_{k=0}^{\infty} \sum_{j=0}^{\infty} \sum_{n=1}^{\infty} b_{j,n}^k \xi^k \eta^j \exp(-n\eta), \quad (6.28)$$

$$\theta(\eta, \xi) = \sum_{k=0}^{\infty} \sum_{j=0}^{\infty} \sum_{n=1}^{\infty} c_{j,n}^k \xi^k \eta^j \exp(-n\eta), \quad (6.29)$$

$$\phi(\eta, \xi) = \sum_{k=0}^{\infty} \sum_{j=0}^{\infty} \sum_{n=1}^{\infty} d_{j,n}^k \xi^k \eta^j \exp(-n\eta), \quad (6.30)$$

in which $a_{j,n}^k$, $b_{j,n}^k$, $c_{j,n}^k$ and $d_{j,n}^k$ are the coefficients. By rule of solution expressions and the boundary conditions (6.15), we can choose the initial guesses f_0 , g_0 , θ_0 and ϕ_0 of $f(\xi, \eta)$, $g(\xi, \eta)$, $\theta(\xi, \eta)$ and $\phi(\xi, \eta)$ as follows:

$$f_0(\xi, \eta) = 1 - \exp(-\eta), \quad (6.31)$$

$$g_0(\xi, \eta) = N_0 \exp(-\eta), \quad (6.32)$$

$$\theta_0(\xi, \eta) = \exp(-\eta), \quad (6.33)$$

$$\phi_0(\xi, \eta) = \exp(-\eta). \quad (6.34)$$

The auxiliary linear operators are defined by the following equations

$$\mathcal{L}_f = \frac{d^3 f}{d\eta^3} - \frac{df}{d\eta}, \quad (6.35)$$

$$\mathcal{L}_g = \frac{d^2 g}{d\eta^2} - g, \quad (6.36)$$

$$\mathcal{L}_\theta = \frac{d^2 \theta}{d\eta^2} - \theta, \quad (6.37)$$

$$\mathcal{L}_\phi = \frac{d^2 \phi}{d\eta^2} - \phi, \quad (6.38)$$

which satisfy

$$\mathcal{L}_f [C_1 + C_2 \exp(\eta) + C_3 \exp(-\eta)] = 0, \quad (6.39)$$

$$\mathcal{L}_g [C_4 \exp(\eta) + C_5 \exp(-\eta)] = 0, \quad (6.40)$$

$$\mathcal{L}_\theta [C_6 \exp(\eta) + C_7 \exp(-\eta)] = 0, \quad (6.41)$$

$$\mathcal{L}_\phi [C_8 \exp(\eta) + C_9 \exp(-\eta)] = 0, \quad (6.42)$$

where $C_i (i = 1 - 9)$ are the arbitrary constants.

If $p \in [0, 1]$ denotes the embedding parameter and \hbar_f , \hbar_g , \hbar_θ and \hbar_ϕ the non-zero auxiliary parameters then we construct the zeroth order deformation equations

$$(1 - p)\mathcal{L}_f[\hat{f}(\xi, \eta; p) - f_0(\xi, \eta)] = p\hbar_f \mathcal{N}_f [\hat{f}(\xi, \eta; p)], \quad (6.43)$$

$$(1 - p)\mathcal{L}_g[\hat{g}(\xi, \eta; p) - g_0(\xi, \eta)] = p\hbar_g \mathcal{N}_g [\hat{f}(\xi, \eta; p), \hat{g}(\xi, \eta; p)], \quad (6.44)$$

$$(1 - p)\mathcal{L}_\theta [\hat{\theta}(\xi, \eta; p) - \theta_0(\xi, \eta)] = p\hbar_\theta \mathcal{N}_\theta [\hat{f}(\xi, \eta; p), \hat{\theta}(\xi, \eta; p)], \quad (6.45)$$

$$(1 - p)\mathcal{L}_\phi [\hat{\phi}(\xi, \eta; p) - \phi_0(\xi, \eta)] = p\hbar_\phi \mathcal{N}_\phi [\hat{f}(\xi, \eta; p), \hat{\phi}(\xi, \eta; p)] \quad (6.46)$$

subjected to the following boundary conditions

$$\begin{aligned}
\hat{f}(\eta; \xi) \Big|_{\eta=0} &= 0, \quad \hat{g}(\eta; \xi) \Big|_{\eta=0} = -N_0 \frac{\partial^2 \hat{f}(\eta; \xi)}{\partial \eta^2} \Big|_{\eta=0}, \\
\hat{\theta}(\eta; \xi) \Big|_{\eta=0} &= \hat{\phi}(\eta; \xi) \Big|_{\eta=0} = \frac{\partial \hat{f}(\eta; \xi)}{\partial \eta} \Big|_{\eta=0} = 1, \\
\hat{g}(\eta; \xi) \Big|_{\eta=\infty} &= 0, \quad \frac{\partial \hat{f}(\eta; \xi)}{\partial \eta} \Big|_{\eta=\infty} = \hat{\theta}(\eta; \xi) \Big|_{\eta=\infty} = \hat{\phi}(\eta; \xi) \Big|_{\eta=\infty} = 0,
\end{aligned} \tag{6.47}$$

in which we define the non-linear operators \mathcal{N}_f , \mathcal{N}_g , \mathcal{N}_θ and \mathcal{N}_ϕ as

$$\begin{aligned}
\mathcal{N}_f [\hat{f}(\xi, \eta; p), \hat{g}(\xi, \eta; p)] &= (1 + K_1) \frac{\partial^3 \hat{f}(\xi, \eta; p)}{\partial \eta^3} + (1 - \xi) \left(\frac{\eta}{2} \frac{\partial^2 \hat{f}(\xi, \eta; p)}{\partial \eta^2} - \xi \frac{\partial^2 \hat{f}(\xi, \eta; p)}{\partial \eta \partial \xi} \right) \\
&+ \xi \left[\hat{f}(\xi, \eta; p) \frac{\partial^2 \hat{f}(\xi, \eta; p)}{\partial \eta^2} - \left(\frac{\partial \hat{f}(\xi, \eta; p)}{\partial \eta} \right)^2 \right. \\
&\quad \left. - M^2 \frac{\partial \hat{f}(\xi, \eta; p)}{\partial \eta} \right] + K_1 g',
\end{aligned} \tag{6.48}$$

$$\begin{aligned}
\mathcal{N}_g [\hat{f}(\xi, \eta; p), \hat{g}(\xi, \eta; p)] &= (1 + \frac{K_1}{2}) \frac{\partial^2 \hat{g}(\xi, \eta; p)}{\partial \eta^2} + (1 - \xi) \left(\frac{\eta}{2} \frac{\partial \hat{g}(\xi, \eta; p)}{\partial \eta} - \xi \frac{\partial \hat{g}(\xi, \eta; p)}{\partial \xi} + \frac{1}{2} \hat{g}(\xi, \eta; p) \right) \\
&+ \xi \left[\hat{f}(\xi, \eta; p) \frac{\partial \hat{g}(\xi, \eta; p)}{\partial \eta} - \hat{f}(\xi, \eta; p) \frac{\partial \hat{g}(\xi, \eta; p)}{\partial \eta} \right. \\
&\quad \left. - 2K \hat{g}(\xi, \eta; p) - K_1 \frac{\partial^2 \hat{f}(\xi, \eta; p)}{\partial \eta^2} \right],
\end{aligned} \tag{6.49}$$

$$\begin{aligned}
\mathcal{N}_\theta [\hat{\theta}(\xi, \eta; p), \hat{f}(\xi, \eta; p)] &= (1 + N_R) \frac{\partial^2 \hat{\theta}(\xi, \eta; p)}{\partial \eta^2} + \text{Pr}(1 - \xi) \left(\frac{\eta}{2} \frac{\partial \hat{\theta}(\xi, \eta; p)}{\partial \eta} - \xi \frac{\partial \hat{\theta}(\xi, \eta; p)}{\partial \xi} \right) \\
&+ \text{Pr} \xi \hat{f}(\xi, \eta; p) \frac{\partial \hat{\theta}(\xi, \eta; p)}{\partial \eta},
\end{aligned} \tag{6.50}$$

$$\begin{aligned}
\mathcal{N}_\phi [\hat{\phi}(\xi, \eta; p), \hat{f}(\xi, \eta; p)] &= \frac{\partial^2 \hat{\phi}(\xi, \eta; p)}{\partial \eta^2} + Sc(1 - \xi) \left(\frac{\eta}{2} \frac{\partial \hat{\phi}(\xi, \eta; p)}{\partial \eta} - \xi \frac{\partial \hat{\phi}(\xi, \eta; p)}{\partial \xi} \right) \\
&+ Sc \xi \hat{f}(\xi, \eta; p) \frac{\partial \hat{\phi}(\xi, \eta; p)}{\partial \eta} - \gamma Sc \xi \hat{\phi}(\xi, \eta; p).
\end{aligned} \tag{6.51}$$

Obviously when $p = 0$ and $p = 1$ then

$$\hat{f}(\xi, \eta; 0) = f_0(\xi, \eta), \quad \hat{f}(\xi, \eta; 1) = f(\xi, \eta), \quad (6.52)$$

$$\hat{g}(\xi, \eta; 0) = g_0(\xi, \eta), \quad \hat{g}(\xi, \eta; 1) = g(\xi, \eta), \quad (6.53)$$

$$\hat{\theta}(\xi, \eta; 0) = \theta_0(\xi, \eta), \quad \hat{\theta}(\xi, \eta; 1) = \theta(\xi, \eta), \quad (6.54)$$

$$\hat{\phi}(\xi, \eta; 0) = \phi_0(\xi, \eta), \quad \hat{\phi}(\xi, \eta; 1) = \phi(\xi, \eta), \quad (6.55)$$

In view of Taylor series with respect to p we have

$$\hat{f}(\xi, \eta; p) = f_0(\xi, \eta) + \sum_{m=1}^{\infty} f_m(\xi, \eta) p^m, \quad (6.56)$$

$$\hat{g}(\xi, \eta; p) = g_0(\xi, \eta) + \sum_{m=1}^{\infty} g_m(\xi, \eta) p^m, \quad (6.57)$$

$$\hat{\theta}(\xi, \eta; p) = \theta_0(\xi, \eta) + \sum_{m=1}^{\infty} \theta_m(\xi, \eta) p^m, \quad (6.58)$$

$$\hat{\phi}(\xi, \eta; p) = \phi_0(\xi, \eta) + \sum_{m=1}^{\infty} \phi_m(\xi, \eta) p^m \quad (6.59)$$

$$\begin{aligned} f_m(\eta) &= \left. \frac{1}{m!} \frac{\partial^m f(\xi, \eta; p)}{\partial \eta^m} \right|_{p=0}, & g_m(\eta) &= \left. \frac{1}{m!} \frac{\partial^m g(\xi, \eta; p)}{\partial \eta^m} \right|_{p=0}, \\ \theta_m(\eta) &= \left. \frac{1}{m!} \frac{\partial^m \theta(\xi, \eta; p)}{\partial \eta^m} \right|_{p=0}, & \phi_m(\eta) &= \left. \frac{1}{m!} \frac{\partial^m \phi(\xi, \eta; p)}{\partial \eta^m} \right|_{p=0}. \end{aligned} \quad (6.60)$$

The auxiliary parameters are so properly chosen that the series (6.56) – (6.59) converge at $p = 1$, then we have

$$f(\xi, \eta) = f_0(\xi, \eta) + \sum_{m=1}^{\infty} f_m(\xi, \eta), \quad (6.61)$$

$$\mathcal{R}_m^\phi(\eta) = \phi_{m-1}'' - Sc(1-\xi)\left(\frac{\eta}{2}\phi_{m-1}' - \xi\frac{\partial\phi_{m-1}}{\partial\xi}\right) + \xi Sc \sum_{k=0}^{m-1} f_k \phi_{m-1-k}' - \gamma Sc \xi \phi_{m-1}, \quad (6.73)$$

$$\chi_m = \begin{cases} 0, & m \leq 1, \\ 1, & m > 1. \end{cases} \quad (6.74)$$

The general solutions of Eqs (6.65) – (6.68) are

$$f_m(\xi, \eta) = f_m^*(\xi, \eta) + C_1 + C_2 \exp(\eta) + C_3 \exp(-\eta), \quad (6.75)$$

$$g_m(\xi, \eta) = g_m^*(\xi, \eta) + C_4 + C_5 \exp(\eta) + C_6 \exp(-\eta), \quad (6.76)$$

$$\theta_m(\xi, \eta) = \theta_m^*(\xi, \eta) + C_7 \exp(\eta) + C_8 \exp(-\eta), \quad (6.77)$$

$$\phi_m(\xi, \eta) = \phi_m^*(\xi, \eta) + C_9 \exp(\eta) + C_{10} \exp(-\eta) \quad (6.78)$$

in which $f_m^*(\xi, \eta)$, $g_m^*(\xi, \eta)$, $\theta_m^*(\xi, \eta)$, $\phi_m^*(\xi, \eta)$ are the particular solutions of the Eqs. (6.65) – (6.68). Note that Eqs. (6.65) – (6.68) can be solved by Mathematica one after the other in the order $m = 1, 2, 3, \dots$

6.3 Convergence of the homotopy solutions

Obviously the series solutions (6.61) – (6.64) depend upon the non-zero auxiliary parameters \hbar_f , \hbar_g , \hbar_θ and \hbar_ϕ which can adjust and control the convergence of the HAM solutions. For suitable values of \hbar_f , \hbar_g , \hbar_θ and \hbar_ϕ , the \hbar -curves of the functions $f''(\xi, 0)$, $g'(\xi, 0)$, $\theta'(\xi, 0)$, and $\phi'(\xi, 0)$ are plotted for 10th-order of approximations. It is noticed from Fig. 6.1 that the range for the admissible values of \hbar_f , \hbar_g , \hbar_θ and \hbar_ϕ are $-0.8 \leq \hbar_f \leq -0.3$, $-0.9 \leq \hbar_\theta \leq -0.2$, and $-0.8 \leq \hbar_g$, $\hbar_\phi \leq -0.3$. Furthermore, it is noticed that the series given by (6.61) – (6.64) converge in the

whole region of η for $h_f = h_g = -0.7 = h_\theta = h_\phi$.

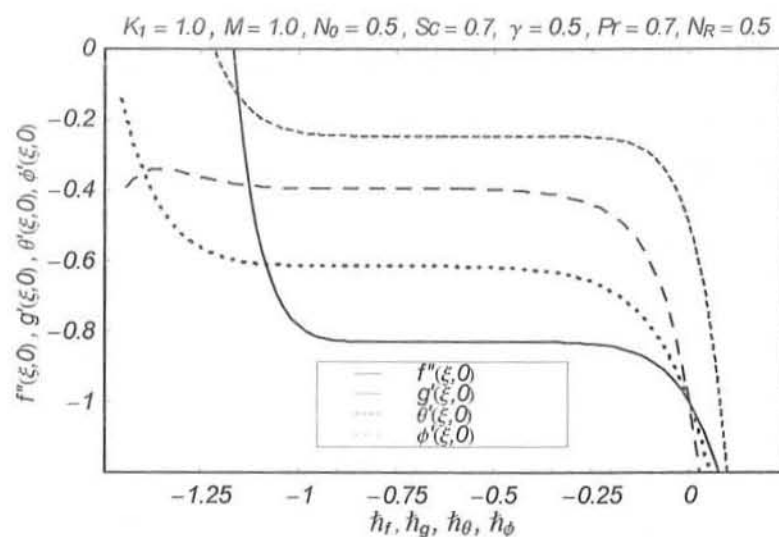


Fig. 6. 1. shows h -curves for velocity and concentration when $\xi = 0.5$.

6.4 Results and discussion

Here we analyze the variations of material parameter K_1 , Hartman number M , Prandtl number Pr , radiation parameter N_R , Schmidt number Sc and chemical reaction parameter γ on the velocity components, concentration field and skin friction coefficient. Figs. 6.2–6.16 have been sketched for this purpose. Figs. 6.2–6.7 display the effects of dimensionless time τ , material parameter K_1 and Hartman number M on the velocity component $f'(\eta, \xi)$ and skin-friction coefficient $\xi^{1/2} Re_x^{1/2} C_{fx}$. The variation of dimensionless time τ on the velocity component $f'(\eta, \xi)$ is shown in Fig. 6.2. Clearly, the velocity component $f'(\eta, \xi)$ increases by increasing τ . Fig. 6.3 gives the variations of M on the velocity component $f'(\eta, \xi)$. The velocity component $f'(\eta, \xi)$ is a decreasing function of M . Figs. 6.4 and 6.5 represent the velocity profiles for various values of K_1 when $N_0 = 0.5$ and $N_0 = 0.0$ respectively. It is seen that results here are similar in both cases but change in Fig. 6.4 is slightly smaller when compared with Fig. 6.5. The effects of K_1 and M on the skin-friction coefficient $\xi^{1/2} Re_x^{1/2} C_{fx}$ are shown in the Figs. 6.6 and 6.7.

It is observed that the magnitude of skin friction coefficient $\xi^{1/2} \text{Re}_x^{1/2} C_{fx}$ increases when K_1 and M are increased. Figs. 6.8 – 6.11 are plotted for the microrotation profile $g(\eta, \xi)$. From Figs. 6.10 and 6.11, one can observed that the microrotation profile for $N_0 = 0$ is different than $N_0 = 0.5$.

Figs. 6.12 – 6.14. are prepared for the effects of Prandtl number Pr , radiation parameter N_R and dimensionless time τ on the temperature field $\theta(\eta, \xi)$. The variation of Pr on temperature field is sketched in Fig. 6.12. It is found that θ is a decreasing function of Pr . Fig. 13 gives the effects of radiation parameter N_R on the temperature field. It has opposite results when compared with Fig. 6.12. Fig. 6.14 elucidates the influence of τ on $\theta(\eta, \xi)$. It is noticed that temperature field $\theta(\eta, \xi)$ is an increasing function of τ and the concentration boundary layer thickness also increases for large values of τ . Figs. 6.15 – 6.18 are prepared for the effects of dimensionless time τ , the Schmidt number Sc and the chemical reaction parameter γ on the concentration field $\phi(\eta, \xi)$ and the surface mass transfer $\xi^{1/2} \text{Re}_x^{-1/2} C_{fx} Sh$. Fig. 6.15 shows the influence of τ on the concentration field $\phi(\eta, \xi)$ in the case of destructive chemical reaction $\gamma > 0$. It is noted that concentration field $\phi(\eta, \xi)$ is an increasing function of τ and the concentration boundary layer thickness also increases for large values of τ . The variation of Sc on the concentration field is sketched in Fig. 6.16. It is observed that ϕ is a decreasing function of Sc . Fig. 6.17 gives the effects of destructive chemical reaction ($\gamma > 0$) on the concentration field. It is seen that results here are similar to $\gamma < 0$ but change in Fig. 6.17 is slightly smaller when compared with Fig. 6.16. Fig. 6.18 illustrates the variation of generative chemical reaction ($\gamma < 0$). It has opposite results when compared with Fig. 6.17.

Tables 6.1 – 6.4 give the steady-state results ($\xi = 1$) for the surface shear stress, surface heat transfer and surface mass transfer for different values of the emerging parameters. Table 6.1 includes the values of skin friction coefficient $C_{fx} \text{Re}_x^{1/2}$. This table indicates that HAM solution has a good agreement with the numerical solution [66]. From Table 6.2 it is noticed that the magnitude of skin friction coefficient increases for large values of M and K . It is also

observed from the comparison of these tables that the magnitude of skin friction coefficient $C_{fx} \text{Re}_x^{1/2}$ is larger in case of magnetohydrodynamic flow. Table 6.3 depicts the variation of heat transfer characteristic at the wall $-\theta'(0)$ for different values of N_R , Pr , K_1 and M . The magnitude of $-\theta'(0)$ increases for larger values of K_1 . Table 4 is prepared for the variation of K_1 , M , Sc and γ on surface mass transfer. It is apparent from this table that the magnitude of $-\phi'(0)$ increases for large values of K_1 and decreases for large values of M . The magnitude of $-\phi'(0)$ increases when Sc and γ are increased.

6.5 Closing remarks

A mathematical model for the unsteady flow of a micropolar fluid with heat and mass transfer is presented. Computations for the nonlinear problems are made. The main results can be summarized as follows:

- The increasing values of M leads to a decrease in the boundary layer thickness.
- The fluid velocity increases as the microgyration parameter N_0 increases.
- Microrotation profile has a parabolic distribution for $N_0 = 0$.
- The temperature θ decreases when Pr increases.
- The variation of Pr on temperature is opposite to that of N_R .
- The influence of destructive chemical reaction parameter is to decrease the concentration field.
- The concentration field ϕ has opposite results for destructive ($\gamma > 0$) and generative ($\gamma < 0$) chemical reactions.
- The effects of Sc and destructive chemical reaction parameter ($\gamma > 0$) on the concentration field are opposite.

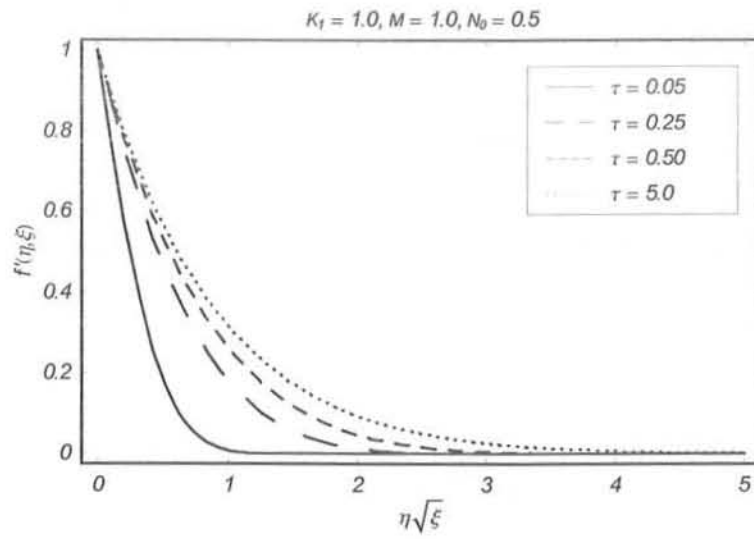


Fig. 6.2. Influence of τ on velocity profile f' .

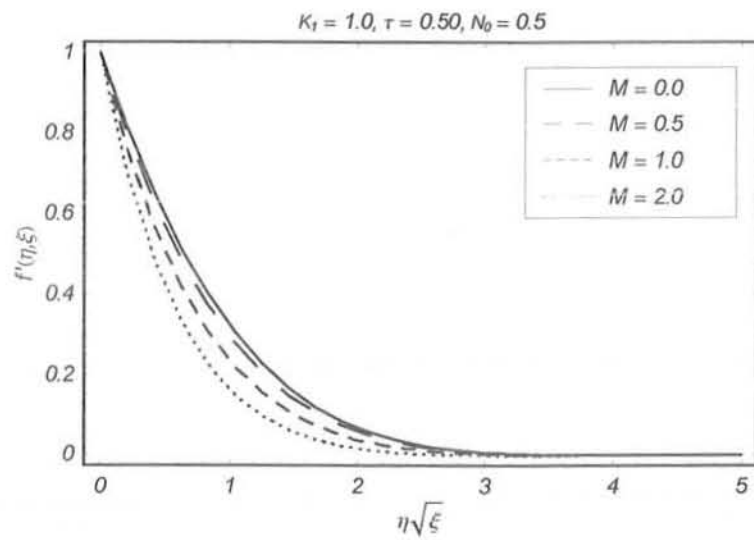


Fig. 6.3. Influence of M on velocity profile f' .

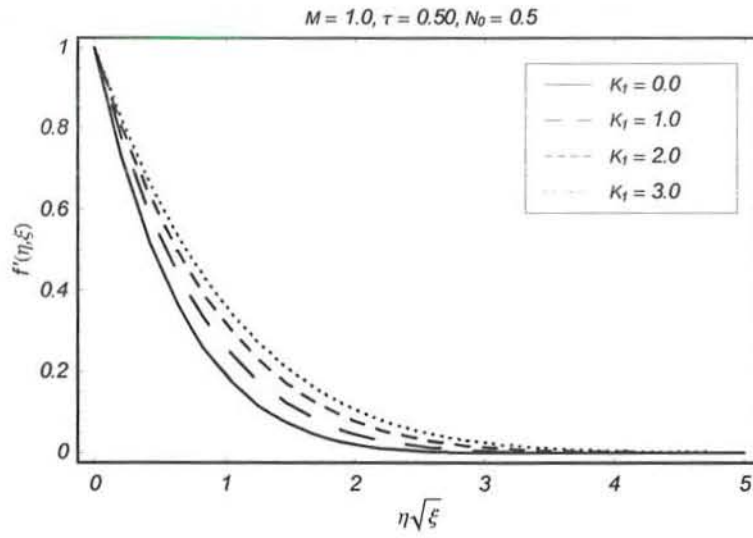


Fig. 6.4. Influence of K_1 on velocity profile f' when $N_0 = 0.5$

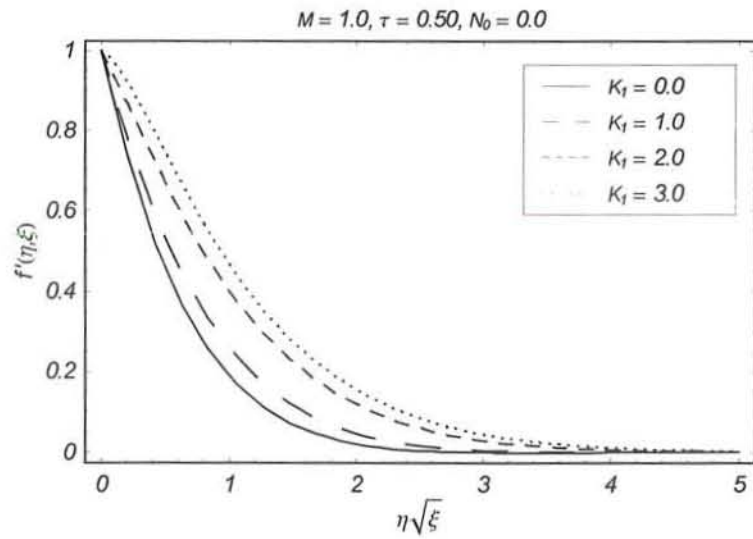


Fig. 6.5. Influence of K_1 on velocity profile f' when $N_0 = 0.0$

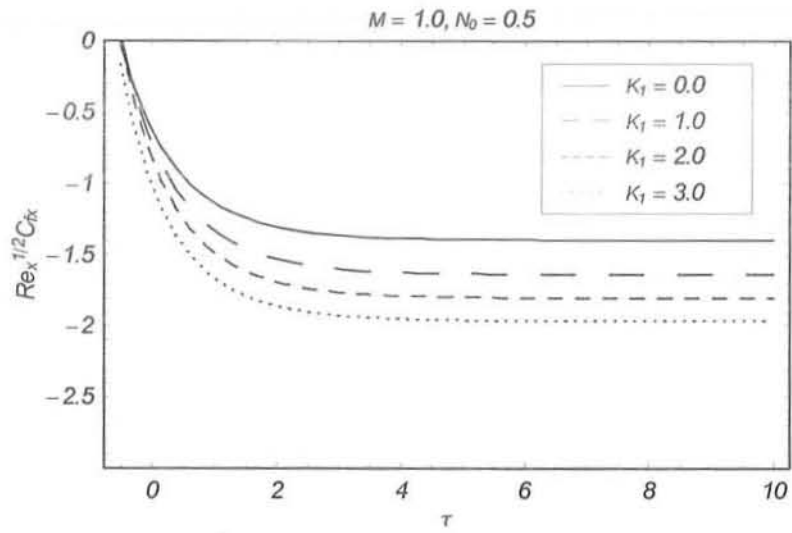


Fig. 6.7. Influence of K_1 on $\xi^{1/2} \text{Re}_x^{1/2} Cf$.

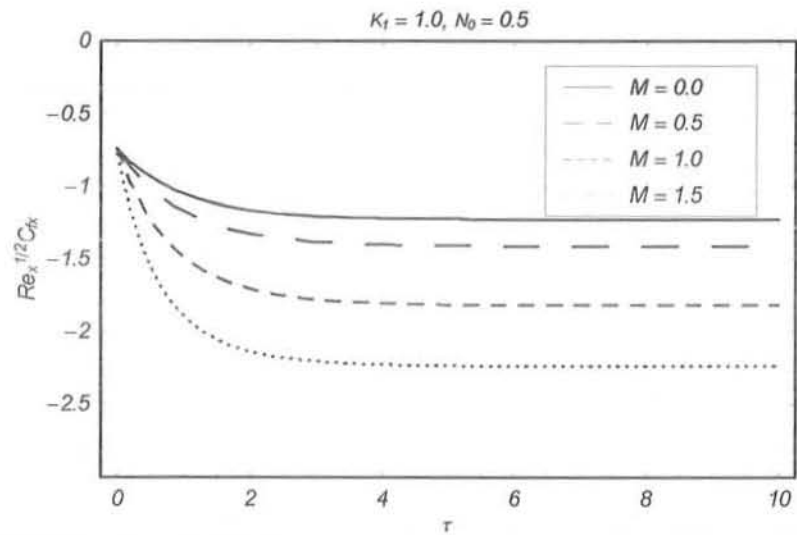


Fig. 6.8. Influence of M on $\xi^{1/2} \text{Re}_x^{1/2} Cf$.

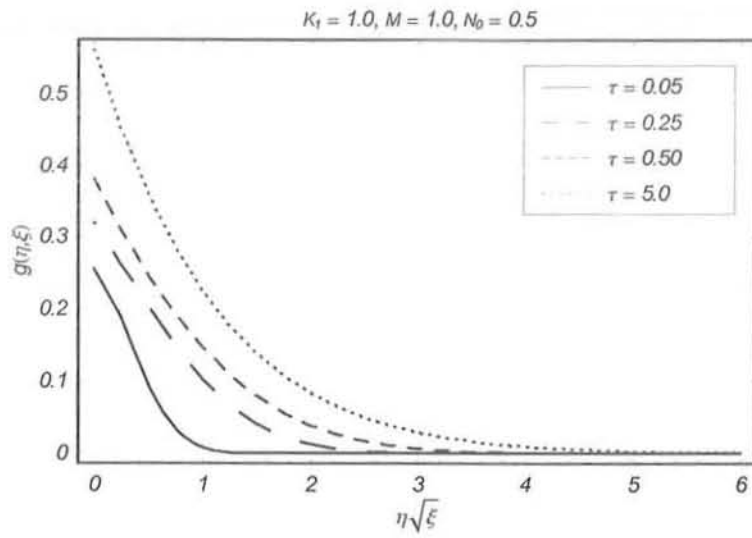


Fig. 6.8. Influence of τ on microrotation profile g when $N_0 = 0.5$.

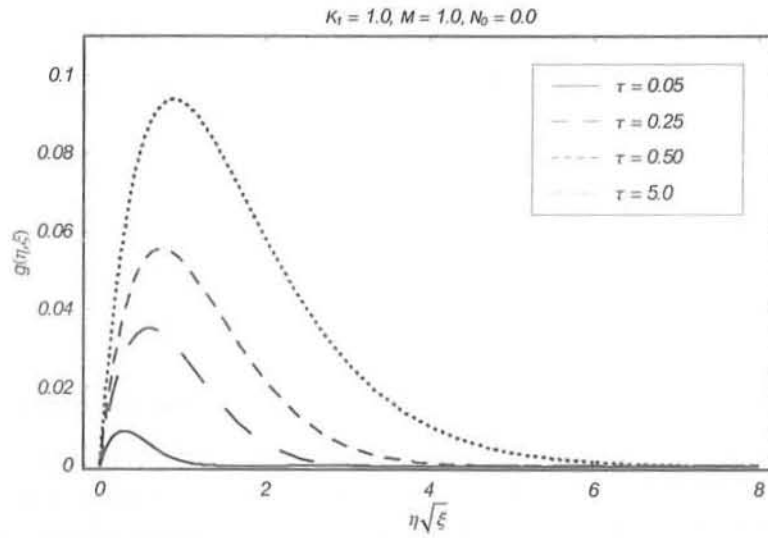


Fig. 6.9. Influence of τ on microrotation profile g when $N_0 = 0.0$.

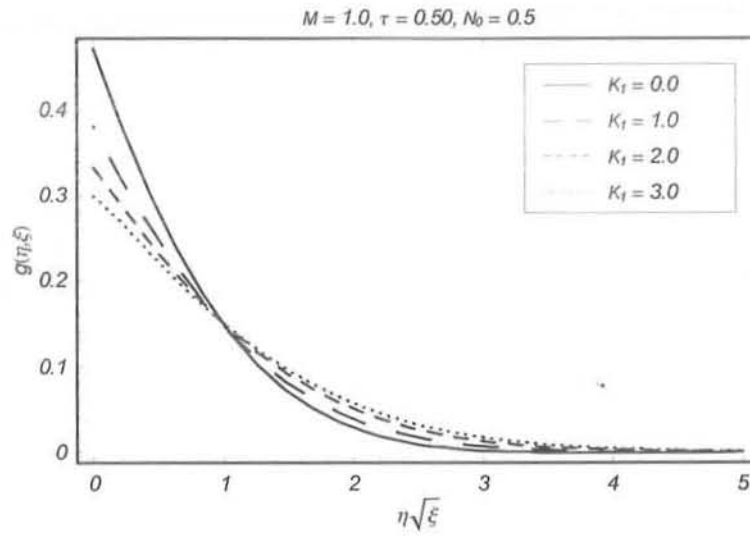


Fig. 6.10. Influence of K_1 on microrotation profile g when $N_0 = 0.5$.

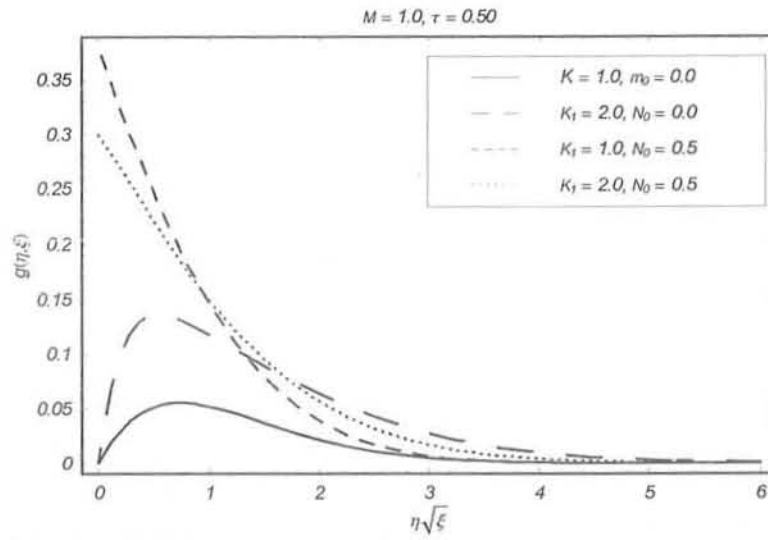


Fig. 6.11. Influence of K_1 and N_0 on microrotation profile g .

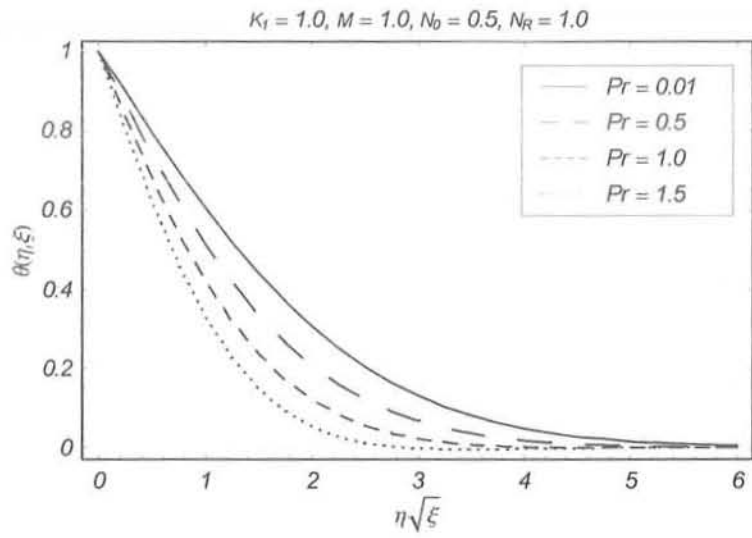


Fig. 6.12. Influence of Pr on temperature profile θ .

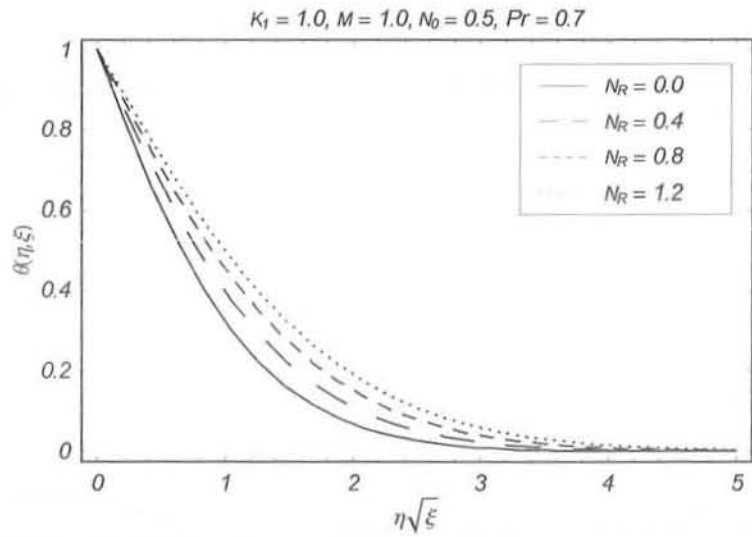


Fig. 6.13. Influence of N_R on temperature profile θ .

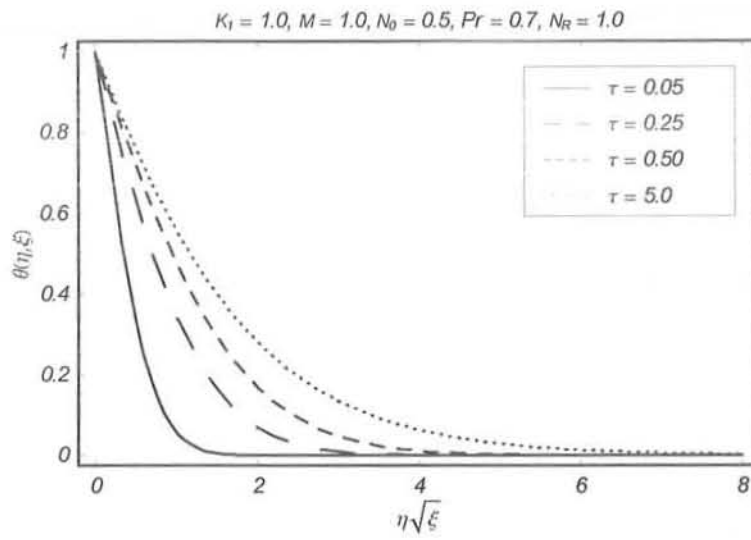


Fig. 6.14. Influence of τ on temperature profile θ .

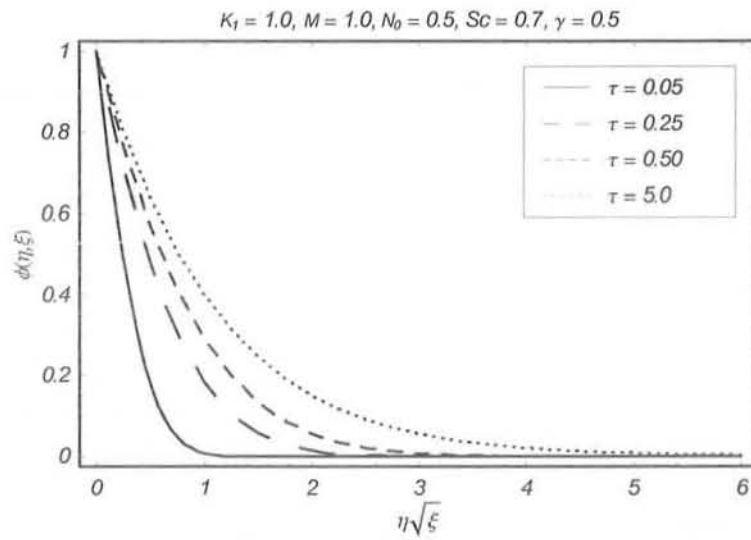


Fig. 6.15. Influence of τ on concentration profile ϕ .

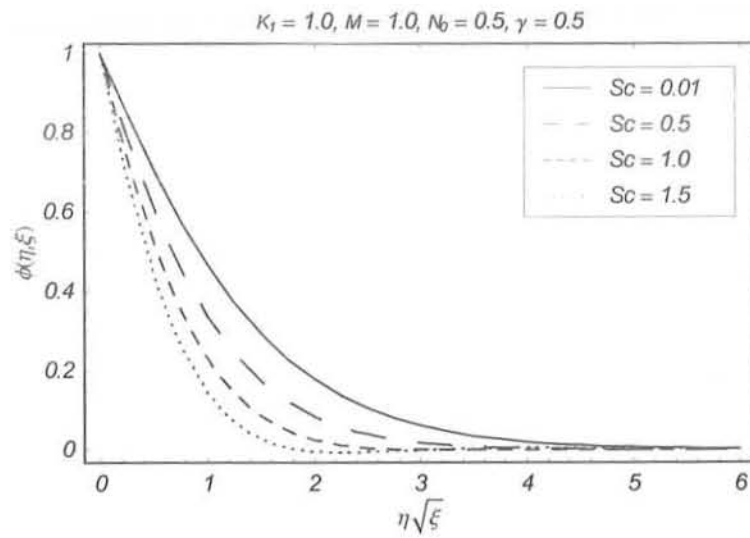


Fig. 6.16. Influence of Sc on concentration profile ϕ .

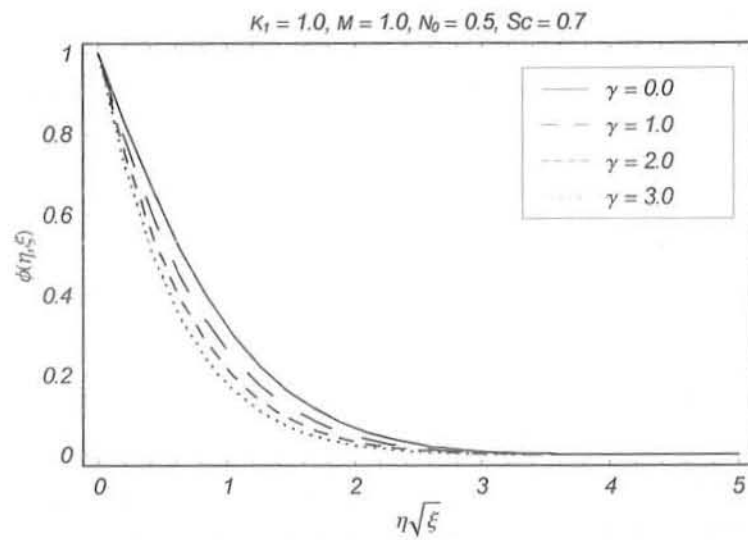


Fig. 6.17. Influence of $\gamma > 0$ on concentration profile ϕ .

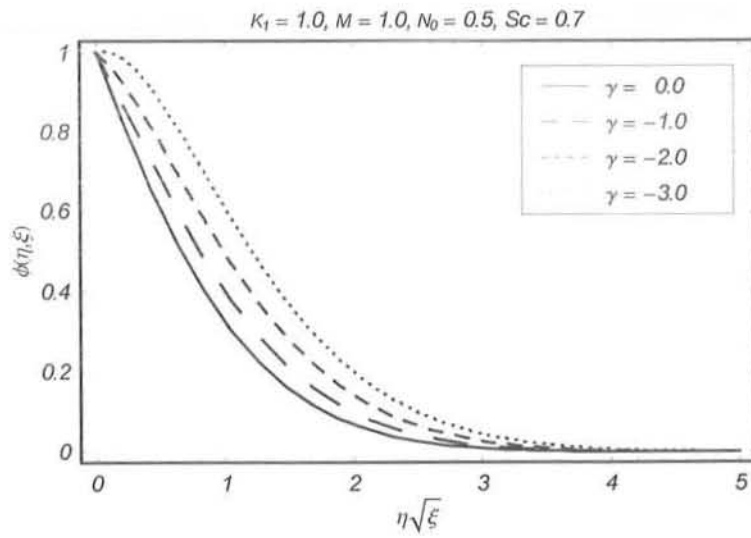


Fig. 6.18. Influence of $\gamma < 0$ on concentration profile ϕ .

$K_1 \setminus N_0$		0.0	0.5
0.0	[66]	-1.0000	-1.0000
	HAM	-1.000000	-1.000000
1.0	[66]	-1.3679	-1.2247
	HAM	-1.367872	-1.224741
2.0	[66]	-1.6213	-1.4142
	HAM	-1.621225	-1.414218
4.0	[66]	-2.0042	-1.7321
	HAM	-2.004133	-1.732052

Table 6.1: Comparison of the values of skin friction coefficient $C_{fx} Re_x^{1/2}$ for values of K_1 and N_0 when $M = 0$ and $\xi = 1$.

M	K_1	$C_{fx} Re_x^{1/2}$	$C_{fx} Re_x^{1/2}$
		$N_0 = 0.0$	$N_0 = 0.5$
0.0	1.0	-1.367872	-1.224754
0.5		-1.530501	-1.363638
1.0		-1.942227	-1.706493
1.5		-2.487393	-2.147621
0.5	0.0	-1.118038	-1.118032
	1.0	-1.530501	-1.363638
	2.0	-1.815277	-1.574471
	4.0	-2.245602	-1.929364

Table 6.2. Values of skin friction coefficient $C_{fx} Re_x^{1/2}$ for various values of K_1 and M when $\xi = 1$.

N_R	K	Pr	M	[53]	Present
1.0	1.0	1.0	0.0	0.3893	0.389321
	2.0			0.4115	0.411524
2.0	0.0			0.2588	0.259632
	1.0			0.2895	0.289547
	2.0			0.3099	0.309981
0.5	1.0	0.7	0.0	—	0.371412
			0.5	—	0.353991
			1.0	—	0.321648

Table 6.3. Values of $-\theta'(0)$ for some values of N_R , K_1 and Pr when $N_0 = 0.5$ and $\xi = 1$.

Sc	γ	K_1	M	$-\phi'(0)$
0.5	1.0	1.0	0.5	0.820814
0.7				0.979971
1.2				1.299943
2.0				1.696172
0.5	1.0	1.0	0.5	0.820813
		2.0		1.088922
		3.0		1.301085
0.7	1.0	1.0	0.5	0.979971
		2.0		0.784003
		4.0		0.797627
0.7	1.0	1.0	0.0	0.781761
			0.5	0.773298
			1.0	0.754651
			1.5	0.734822

Table 6.4. Values of $-\phi'(0)$ for some values of K_1 , M , Sc and γ when $N_0 = 0.5$ and $\xi = 1$.

Chapter 7

Mixed convection flow of a micropolar fluid in the presence of radiation and chemical reaction

This chapter discloses the effects of heat and mass transfer on the mixed convection flow of a magnetohydrodynamic (MHD) micropolar fluid bounded by a stretching surface. Homotopy analysis procedure is adopted for computations of a set of coupled nonlinear ordinary differential equations. Numerical values of skin friction coefficient and Nusselt and Sherwood numbers are worked out. A comparative study is provided with the limiting available numerical solution.

7.1 Mathematical formulation

We consider the steady mixed convection boundary layer flow of a micropolar fluid over a stretching surface. The fluid is electrically conducting in the presence of a constant applied magnetic field B_0 . The induced magnetic field is neglected under small magnetic Reynolds number assumption. The effects of electric field are absent. We further assume that the surface

has temperature T_w , the concentration C_w , and fluid has uniform ambient temperature T_∞ and uniform ambient concentration C_∞ (Here $T_w > T_\infty$ and $C_w > C_\infty$). The governing equations can be expressed in the forms:

$$\frac{\partial u}{\partial x} + \frac{\partial v}{\partial y} = 0, \quad (7.1)$$

$$u \frac{\partial u}{\partial x} + v \frac{\partial u}{\partial y} = \left(\nu + \frac{\kappa}{\rho} \right) \frac{\partial^2 u}{\partial y^2} + \frac{\kappa}{\rho} \frac{\partial N^*}{\partial y} + g\beta_T(T - T_\infty) + g\beta_C(C - C_\infty) - \frac{\sigma B_0^2}{\rho} u, \quad (7.2)$$

$$u \frac{\partial N^*}{\partial x} + v \frac{\partial N^*}{\partial y} = \frac{\gamma^*}{\rho j} \frac{\partial^2 N^*}{\partial y^2} - \frac{\kappa}{\rho j} \left(2N^* + \frac{\partial u}{\partial y} \right), \quad (7.3)$$

$$\rho c_p \left[u \frac{\partial T}{\partial x} + v \frac{\partial T}{\partial y} \right] = k \frac{\partial^2 T}{\partial y^2} - \frac{\partial q_r}{\partial y}, \quad (7.4)$$

$$u \frac{\partial C}{\partial x} + v \frac{\partial C}{\partial y} = D \frac{\partial^2 C}{\partial y^2} - RC \quad (7.5)$$

with the following conditions

$$\begin{aligned} u &= u_w = ax, \quad v = 0, \quad N^* = -N_0 \frac{\partial u}{\partial y}, \quad T = T_w, \quad C = C_w, \quad y = 0, \\ u &\rightarrow 0, \quad v \rightarrow 0, \quad N^* \rightarrow 0, \quad T \rightarrow 0, \quad C \rightarrow 0, \quad \text{as } y \rightarrow \infty. \end{aligned} \quad (7.6)$$

In above expressions u and v are the velocity components parallel to the x - and y -axes, respectively, μ the dynamic viscosity, ρ the fluid density, ν the kinematic viscosity, σ the electrical conductivity, N^* the microrotation or angular velocity, T the temperature, c_p the specific heat, k the thermal conductivity of the fluid, q_r the radiative heat flux, C the concentration species of the fluid, D is the diffusion coefficient of the diffusion species in the fluid, R denotes the first-order homogeneous constant reaction rate, $j = (\nu/c)$ is microinertia, $\gamma^* = (\mu + \kappa/2)j$ and κ are the spin gradient viscosity and vortex viscosity, respectively. Here for $\kappa = 0$ we have the case of viscous fluid. Further the boundary parameter N_0 has range $0 \leq N_0 \leq 1$. It should be noted that when $N_0 = 0$ (called strong concentration) then $N^* = 0$ near the wall. This represents the concentrated particle flows in which the microelements close to the wall surface

are unable to rotate. The case $N_0 = 1/2$ corresponds to the vanishing of anti-symmetric part of the stress tensor and it shows weak concentration of microelements (see [53] for detail).

Employing Rosseland approximation, one can write

$$q_r = -\frac{4\sigma^*}{3k^*} \frac{\partial T^4}{\partial y}, \quad (7.7)$$

in which σ^* is the Stefan–Boltzmann constant and k^* the mean absorption coefficient.

Using Taylor series and neglecting higher order terms one obtains

$$T^4 \approx 4T_\infty^3 T - 3T_\infty^4. \quad (7.8)$$

In view of Eqs. (7.4), (7.7) and (7.8) we have

$$\rho c_p \left(u \frac{\partial T}{\partial x} + v \frac{\partial T}{\partial y} \right) = \frac{\partial}{\partial y} \left[\left(\frac{16\sigma^* T_\infty^3}{3k^*} + k \right) \frac{\partial T}{\partial y} \right]. \quad (7.9)$$

Introducing the following quantities

$$\begin{aligned} \eta &= (a/\nu)^{1/2} y, \quad u = cx f'(\eta), \quad v = -(c\nu)^{1/2} f(\eta), \quad N^* = (a/\nu)^{1/2} axg(\eta), \\ \theta &= \frac{T - T_\infty}{T_w - T_\infty}, \quad \phi = \frac{C - C_\infty}{C_w - C_\infty} \end{aligned} \quad (7.10)$$

equation (7.1) is automatically satisfied and Eqs. (7.2), (7.3), (7.4), (7.6) and (7.9) become

$$(1 + K_1) f'''' + f f'' - (f')^2 - M^2 f' + K_1 g' + \lambda(\theta + N\phi) = 0, \quad (7.11)$$

$$\left(1 + \frac{K_1}{2} \right) g'' + f g' - f' g - 2K_1 g - K_1 f'' = 0, \quad (7.12)$$

$$(1 + N_R) \theta'' + \text{Pr} f \theta' = 0, \quad (7.13)$$

$$\phi'' + \text{Sc} f \phi' - \gamma \text{Sc} \phi = 0, \quad (7.14)$$

$$\begin{aligned}
f(0) &= 0, \quad f'(0) = 1, \quad g(0) = -N_0 f''(0), \quad \theta(0) = \phi(0) = 1, \\
f'(\infty) &= g(\infty) = \theta(\infty) = \phi(\infty) = 0,
\end{aligned} \tag{7.15}$$

where prime denotes the derivative with respect to η . Here micropolar parameter K_1 , Hartman number M , Prandtl number Pr , radiation parameter N_R , Schmidt number Sc , chemical reaction parameter γ , local buoyancy parameter λ and local Grashof number Gr_x are given by

$$\begin{aligned}
K_1 &= \frac{\kappa}{\mu}, \quad M^2 = \frac{\sigma B_0^2}{\rho a}, \quad Pr = \frac{\nu}{a}, \quad N_R = \frac{16\sigma^* T_\infty^3}{3kk^*}, \quad Sc = \frac{\nu}{D}, \\
\gamma &= \frac{R}{a}, \quad \lambda = \frac{Gr_x}{Re_x^2}, \quad Gr_x = \frac{g\beta(T_w - T_\infty)x^3/\nu^2}{u_w^2 x^2/\nu^2}, \quad N = \frac{\beta_C (C_w - C_\infty)}{\beta_T (T_w - T_\infty)}.
\end{aligned} \tag{7.16}$$

The skin friction coefficients C_{fx} , local Nusselt number Nu and local Sherwood number Sh can be expressed as

$$\begin{aligned}
C_{fx} &= \frac{\left[(\mu + \kappa) \frac{\partial u}{\partial y} + \kappa N^* \right]_{y=0}}{\rho u_w^2}, \\
Nu &= \frac{-x(\partial T/\partial y)_{y=0}}{(T_w - T_\infty)}, \quad Sh = \frac{-x(\partial C/\partial y)_{y=0}}{(C_w - C_\infty)}.
\end{aligned} \tag{7.17}$$

which after invoking Eq. (7.10) take the following forms:

$$\begin{aligned}
Re_x^{1/2} C_{fx} &= [1 + (1 - N_0) K] f''(0), \\
Nu Re_x^{-1/2} &= -\theta'(0), \quad Sh Re_x^{-1/2} = -\phi'(0),
\end{aligned} \tag{7.18}$$

where $Re_x = ax^2/\nu$ is the local Reynolds number.

7.2 Homotopy analysis solutions

Keeping (7.15) in mind we express $f(\eta)$, $g(\eta)$, $\theta(\eta)$ and $\phi(\eta)$ by a set of base functions

$$\left\{ \eta^k \exp(-n\eta) \mid k \geq 0, n \geq 0 \right\} \quad (7.19)$$

in the forms

$$f(\eta) = a_{0,0}^0 + \sum_{n=0}^{\infty} \sum_{k=0}^{\infty} a_{m,n}^k \eta^k \exp(-n\eta), \quad (7.20)$$

$$g(\eta) = \sum_{n=0}^{\infty} \sum_{k=0}^{\infty} b_{m,n}^k \eta^k \exp(-n\eta), \quad (7.21)$$

$$\theta(\eta) = \sum_{n=0}^{\infty} \sum_{k=0}^{\infty} c_{m,n}^k \eta^k \exp(-n\eta), \quad (7.22)$$

$$\phi(\eta) = \sum_{n=0}^{\infty} \sum_{k=0}^{\infty} d_{m,n}^k \eta^k \exp(-n\eta) \quad (7.23)$$

in which $a_{m,n}^k$, $b_{m,n}^k$, $c_{m,n}^k$ and $d_{m,n}^k$ are the coefficients. By rule of solution expressions and the boundary conditions (7.15), the initial guesses f_0 , g_0 , θ_0 and ϕ_0 of $f(\eta)$, $g(\eta)$, $\theta(\eta)$ and $\phi(\eta)$ are selected as follows

$$f_0(\eta) = 1 - \exp(-\eta), \quad (7.24)$$

$$g_0(\eta) = N_0 \exp(-\eta), \quad (7.25)$$

$$\theta_0(\eta) = \exp(-\eta), \quad (7.26)$$

$$\phi_0(\eta) = \exp(-\eta). \quad (7.27)$$

We select the auxiliary linear operators as

$$\mathcal{L}_f = \frac{d^3 f}{d\eta^3} - \frac{df}{d\eta}, \quad (7.28)$$

$$\mathcal{L}_g = \frac{d^2 g}{d\eta^2} - g, \quad (7.29)$$

$$\mathcal{L}_\theta = \frac{d^2 \theta}{d\eta^2} - \theta, \quad (7.30)$$

$$\mathcal{L}_\phi = \frac{d^2 \phi}{d\eta^2} - \phi. \quad (7.31)$$

The linear operators in Eqs. (7.29) – (7.32) have the following properties

$$\mathcal{L}_f [C_1 + C_2 \exp(\eta) + C_3 \exp(-\eta)] = 0, \quad (7.32)$$

$$\mathcal{L}_g [C_4 \exp(\eta) + C_5 \exp(-\eta)] = 0, \quad (7.33)$$

$$\mathcal{L}_\theta [C_6 \exp(\eta) + C_7 \exp(-\eta)] = 0, \quad (7.34)$$

$$\mathcal{L}_\phi [C_8 \exp(\eta) + C_9 \exp(-\eta)] = 0, \quad (7.35)$$

where $C_i (i = 1 - 9)$ are the arbitrary constants.

The zeroth order deformation problems can be written as

$$(1 - p)\mathcal{L}_f[\hat{f}(\eta; p) - f_0(\eta)] = p\hbar_f \mathcal{N}_f [\hat{f}(\eta; p)], \quad (7.36)$$

$$(1 - p)\mathcal{L}_g[\hat{g}(\eta; p) - g_0(\eta)] = p\hbar_g \mathcal{N}_g [\hat{f}(\eta; p), \hat{g}(\eta; p)], \quad (7.37)$$

$$(1 - p)\mathcal{L}_\theta [\hat{\theta}(\eta; p) - \theta_0(\eta)] = p\hbar_\theta \mathcal{N}_\theta [\hat{f}(\eta; p), \hat{\theta}(\eta; p)], \quad (7.38)$$

$$(1 - p)\mathcal{L}_\phi [\hat{\phi}(\eta; p) - \phi_0(\eta)] = p\hbar_\phi \mathcal{N}_\phi [\hat{f}(\eta; p), \hat{\phi}(\eta; p)], \quad (7.39)$$

$$\begin{aligned} \hat{f}(\eta)|_{\eta=0} &= 0, \quad \hat{g}(\eta)|_{\eta=0} = -N_0 \frac{\partial^2 \hat{f}(\eta)}{\partial \eta^2} \Big|_{\eta=0}, \quad \hat{\theta}(\eta)|_{\eta=0} = \hat{\phi}(\eta)|_{\eta=0} = \frac{\partial \hat{f}(\eta)}{\partial \eta} \Big|_{\eta=0} = 1, \\ \hat{g}(\eta)|_{\eta=\infty} &= 0, \quad \frac{\partial \hat{f}(\eta)}{\partial \eta} \Big|_{\eta=\infty} = \hat{\theta}(\eta)|_{\eta=\infty} = \hat{\phi}(\eta)|_{\eta=\infty} = 0, \end{aligned} \quad (7.40)$$

where $p \in [0, 1]$ indicates the embedding parameter and h_f, h_g, h_θ and h_ϕ the nonzero auxiliary parameters. Moreover the nonlinear operators $\mathcal{N}_f, \mathcal{N}_g, \mathcal{N}_\theta$ and \mathcal{N}_ϕ are prescribed below as

$$\begin{aligned} \mathcal{N}_f \left[\hat{f}(\eta; p), \hat{g}(\eta; p), \hat{\theta}(\eta; p), \hat{\phi}(\eta; p) \right] &= (1 + K_1) \frac{\partial^3 \hat{f}(\eta; p)}{\partial \eta^3} + K_1 \frac{\partial \hat{g}(\eta; p)}{\partial \eta} + \lambda \left(\hat{\theta}(\eta; p) + N \hat{\phi}(\eta; p) \right) \\ &+ \left[\hat{f}(\eta; p) \frac{\partial^2 \hat{f}(\eta; p)}{\partial \eta^2} - \left(\frac{\partial \hat{f}(\eta; p)}{\partial \eta} \right)^2 - M^2 \frac{\partial \hat{f}(\eta; p)}{\partial \eta} \right] \end{aligned} \quad (7.42)$$

$$\begin{aligned} \mathcal{N}_g \left[\hat{f}(\eta; p), \hat{g}(\eta; p), \hat{\theta}(\eta; p), \hat{\phi}(\eta; p) \right] &= (1 + \frac{K_1}{2}) \frac{\partial^2 \hat{g}(\eta; p)}{\partial \eta^2} \\ &+ \left[\hat{f}(\eta; p) \frac{\partial \hat{g}(\eta; p)}{\partial \eta} - \hat{f}(\xi, \eta; p) \frac{\partial \hat{g}(\eta; p)}{\partial \eta} \right. \\ &\quad \left. - 2K_1 \hat{g}(\eta; p) - K_1 \frac{\partial^2 \hat{f}(\eta; p)}{\partial \eta^2} \right], \end{aligned} \quad (7.43)$$

$$\mathcal{N}_\theta \left[\hat{f}(\eta; p), \hat{g}(\eta; p), \hat{\theta}(\eta; p), \hat{\phi}(\eta; p) \right] = (1 + N_R) \frac{\partial^2 \hat{\theta}(\eta; p)}{\partial \eta^2} + P_r \hat{f}(\eta; p) \frac{\partial \hat{\theta}(\eta; p)}{\partial \eta}, \quad (7.44)$$

$$\mathcal{N}_\phi \left[\hat{f}(\eta; p), \hat{g}(\eta; p), \hat{\theta}(\eta; p), \hat{\phi}(\eta; p) \right] = \frac{\partial^2 \hat{\phi}(\eta; p)}{\partial \eta^2} + S_c \hat{f}(\eta; p) \frac{\partial \hat{\phi}(\eta; p)}{\partial \eta} - \gamma S_c \hat{\phi}(\eta; p). \quad (7.45)$$

For $p = 0$ and $p = 1$ we have

$$\hat{f}(\eta; 0) = f_0(\eta), \quad \hat{f}(\eta; 1) = f(\eta), \quad (7.46)$$

$$\hat{g}(\eta; 0) = g_0(\eta), \quad \hat{g}(\eta; 1) = g(\eta), \quad (7.47)$$

$$\hat{\theta}(\eta; 0) = \theta_0(\eta), \quad \hat{\theta}(\eta; 1) = \theta(\eta), \quad (7.48)$$

$$\hat{\phi}(\eta; 0) = \phi_0(\eta), \quad \hat{\phi}(\eta; 1) = \phi(\eta). \quad (7.49)$$

By means of Taylors series

$$\hat{f}(\eta; p) = f_0(\eta) + \sum_{m=1}^{\infty} f_m(\eta) p^m, \quad (7.50)$$

$$\hat{g}(\eta; p) = g_0(\eta) + \sum_{m=1}^{\infty} g_m(\eta) p^m, \quad (7.51)$$

$$\hat{\theta}(\eta; p) = \theta_0(\eta) + \sum_{m=1}^{\infty} \theta_m(\eta) p^m, \quad (7.52)$$

$$\hat{\phi}(\eta; p) = \phi_0(\eta) + \sum_{m=1}^{\infty} \phi_m(\eta) p^m, \quad (7.53)$$

$$\begin{aligned} f_m(\eta) &= \left. \frac{1}{m!} \frac{\partial^m f(\eta; p)}{\partial \eta^m} \right|_{p=0}, & g_m(\eta) &= \left. \frac{1}{m!} \frac{\partial^m g(\eta; p)}{\partial \eta^m} \right|_{p=0}, \\ \theta_m(\eta) &= \left. \frac{1}{m!} \frac{\partial^m \theta(\eta; p)}{\partial \eta^m} \right|_{p=0}, & \phi_m(\eta) &= \left. \frac{1}{m!} \frac{\partial^m \phi(\eta; p)}{\partial \eta^m} \right|_{p=0}. \end{aligned} \quad (7.54)$$

The auxiliary parameters are so properly chosen that series (7.51) – (7.54) converge when $p = 1$ and thus

$$f(\eta) = f_0(\eta) + \sum_{m=1}^{\infty} f_m(\eta), \quad (7.55)$$

$$g(\eta) = g_0(\eta) + \sum_{m=1}^{\infty} g_m(\eta), \quad (7.56)$$

$$\theta(\eta) = \theta_0(\eta) + \sum_{m=1}^{\infty} \theta_m(\eta). \quad (7.57)$$

$$\phi(\eta) = \phi_0(\eta) + \sum_{m=1}^{\infty} \phi_m(\eta). \quad (7.58)$$

The resulting problems at the m th– order deformation are

$$\mathcal{L}_f [f_m(\eta) - \chi_m f_{m-1}(\eta)] = \hbar_f \mathcal{R}_m^f(\eta), \quad (7.59)$$

$$\mathcal{L}_g [g_m(\eta) - \chi_m g_{m-1}(\eta)] = \hbar_g \mathcal{R}_m^g(\eta), \quad (7.60)$$

$$\mathcal{L}_\theta [\theta_m(\eta) - \chi_m \theta_{m-1}(\eta)] = \hbar_\theta \mathcal{R}_m^\theta(\eta), \quad (7.61)$$

$$\mathcal{L}_\phi [\phi_m(\eta) - \chi_m \phi_{m-1}(\eta)] = \hbar_\phi \mathcal{R}_m^\phi(\eta), \quad (7.62)$$

$$\begin{aligned} f_m(0) &= 0, f'_m(0) = 0, f'_m(\infty) = 0, g_m(0) = 0, g_m(\infty) = 0, g'_m(\infty) = 0, \\ \theta_m(0) &= 0, \theta_m(\infty) = 0, \phi_m(0) = 0, \phi_m(\infty) = 0 \end{aligned} \quad (7.63)$$

with the following definitions

$$\mathcal{R}_m^f(\eta) = (1 + K_1) f'''_{m-1} + \left[\sum_{k=0}^{m-1} [f_k f''_{m-1-k} - f'_k f'_{m-1-k}] - M^2 f'_{m-1} \right] + K_1 g'_{m-1} + \lambda (\theta_{m-1} + N \phi_{m-1}), \quad (7.64)$$

$$\mathcal{R}_m^g(\eta) = \left(1 + \frac{K_1}{2} \right) g''_{m-1} + \left[\sum_{k=0}^{m-1} [f_k g'_{m-1-k} - g_k f'_{m-1-k}] \right], \quad (7.65)$$

$$\mathcal{R}_m^\theta(\eta) = (1 + N_R) \theta''_{m-1} + \text{Pr} \sum_{k=0}^{m-1} [f_k \theta'_{m-1-k} + g_k \theta'_{m-1-k}], \quad (7.66)$$

$$\mathcal{R}_m^\phi(\eta) = \phi''_{m-1} + \text{Sc} \sum_{k=0}^{m-1} f_k \phi'_{m-1-k} - \gamma \text{Sc} \phi_{m-1}, \quad (7.67)$$

$$\chi_m = \begin{cases} 0, & m \leq 1, \\ 1, & m > 1. \end{cases} \quad (7.68)$$

The general solutions of Eqs (7.60) – (7.63) are given by

$$f_m(\eta) = f_m^*(\eta) + C_1 + C_2 \exp(\eta) + C_3 \exp(-\eta), \quad (7.69)$$

$$g_m(\eta) = g_m^*(\eta) + C_4 + C_5 \exp(\eta) + C_6 \exp(-\eta), \quad (7.70)$$

$$\theta_m(\eta) = \theta_m^*(\eta) + C_7 \exp(\eta) + C_8 \exp(-\eta), \quad (7.71)$$

$$\phi_m(\eta) = \phi_m^*(\eta) + C_9 \exp(\eta) + C_{10} \exp(-\eta). \quad (7.72)$$

Here $f_m^*(\eta)$, $g_m^*(\eta)$, $\theta_m^*(\eta)$, $\phi_m^*(\eta)$ are the particular solutions of the Eqs. (7.60) – (7.63). Note

that Eqs. (7.60) – (7.63) can be solved by Mathematica one after the other in the order $m = 1, 2, 3, \dots$

7.3 Convergence of the homotopy solutions

We note that the series solutions (7.56) – (7.59) contain the non-zero auxiliary parameters \hbar_f , \hbar_g , \hbar_θ and \hbar_ϕ . We can adjust and control the convergence of the HAM solutions with the help of these auxiliary parameters. Hence to compute the range of admissible values of \hbar_f , \hbar_g , \hbar_θ and \hbar_ϕ , we display the \hbar -curves of the functions $f''(0)$, $g'(0)$, $\theta'(0)$ and $\phi'(0)$ for 20th-order of approximations. Fig. 1 depicts that the range for the reliable values of \hbar_f , \hbar_g , \hbar_θ and \hbar_ϕ are $-0.8 \leq \hbar_f \leq -0.3$, $-0.9 \leq \hbar_\theta \leq -0.2$ and $-0.8 \leq \hbar_g, \hbar_\phi \leq -0.3$. The series given by (7.56) – (7.59) converge in the whole region of η when $\hbar_f = \hbar_g = -0.7 = \hbar_\theta = \hbar_\phi$. Fig. 7.1. shows the \hbar -curves for velocity, microrotation, temperature and concentration. Table 1 indicates the convergence of the homotopy solutions for different order of approximations.

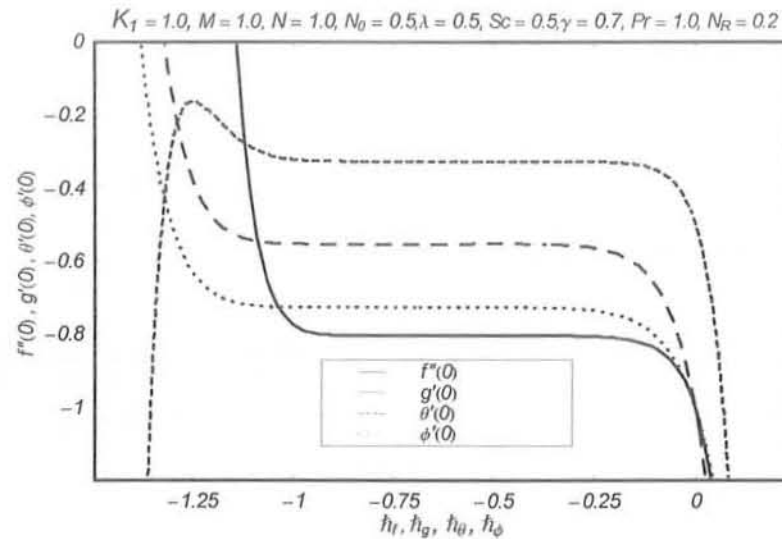


Fig. 7.1. The \hbar -curves of $f''(0)$, $g'(0)$, $\theta'(0)$ and $\phi'(0)$ at 20th-order of approximations.

Order of convergence	$-f''(0)$	$-g'(0)$	$-\theta'(0)$	$-\phi'(0)$
1	0.82500	0.32500	0.69666	0.83083
5	0.80405	0.32671	0.55507	0.72949
10	0.80344	0.32639	0.55285	0.72666
15	0.80357	0.32642	0.55342	0.72662
20	0.80357	0.32642	0.55343	0.72662
25	0.80357	0.32642	0.55342	0.72662
30	0.80357	0.32642	0.55342	0.72662
35	0.80357	0.32642	0.55342	0.72662

Table 7.1: Numerical values for the convergence of $f''(0)$, $g'(0)$, $\theta'(0)$ and $\phi'(0)$.

7.4 Results and discussion

The purpose of this section is to analyze the graphical results for the effects of Hartman number M , material parameter K_1 , local buoyancy parameter λ , the buoyancy ratio N , Prandtl number Pr , radiation parameter N_R , Schmidt number Sc and chemical reaction parameter γ on the velocity, temperature and concentration fields. Hence the Figs. 7.2 – 7.22 have been displayed. Figs. 7.2 – 7.7 are presented to show the effects of λ , N , K_1 , M , Pr and Sc on f' . Fig. 7.2 shows the effect of λ on the velocity f' . It is observed from this Fig. that the boundary layer thickness increases by increasing λ . It is found that f' also increases when N increases (Fig. 7.3). Fig. 7.4 represent the velocity profiles for various values of K_1 when $N_0 = 0.5$. Here the qualitative effects of K are found similar to that of λ and N of f' . Fig. 7.5 gives the variations of M on velocity component f' . The velocity component f' is a decreasing function of M . This is in view of the fact that an increase of M signifies the increase of Lorentz force, therefore decreasing the magnitude of the velocity. Figs. 7.6 and 7.7 describe the effects of Pr and Sc on f' , respectively. Both Pr and Sc decrease the velocity profile. Infact an increase in the Prandtl

number leads to an increase in fluid viscosity which causes the decrease in the flow velocity.

Figs. 7.8 – 7.11 are prepared for the effects of M and K_1 on the microrotation profile $g(\eta)$. Fig. 7.8 is drawn when $N_0 = 0.0$. From Fig. 7.8, we have seen that it increases initially but at $\eta = 2$ it starts decreasing. Fig. 7.9 is drawn for $N_0 = 0.5$. We see that g increases by increasing the Hartman number. From Figs. 7.10 – 7.11, it is clear that the microrotation profile for $N_0 = 0.0$ and that $N_0 = 0.5$ are different. Figs. 7.12 – 7.16 are plotted for the effects of buoyancy ratio N , local buoyancy parameter λ , Prandtl number Pr , radiation parameter N_R and Hartman number M on the temperature profile $\theta(\eta)$. The qualitative effects of N and λ on the temperature is similar (Figs. 7.12 and 7.13). The variation of Pr on the temperature field is sketched in Fig. 7.14. As expected, it is found that θ is decreasing when Pr is increased. Fig. 7.15 gives the effects of radiation parameter N_R on the temperature field. It has opposite result when compared with Fig. 7.14. The temperature profile increases by increasing the Hartman number M (Fig. 16). The increasing frictional drag due to the Lorentz force is responsible for an increment in the thermal boundary layer thickness. Figs. 7.17–7.22 display the effects of M , N , λ , γ and Sc on the concentration profiles. Fig. 7.17 displays the effect of Hartman number M on the concentration profile ϕ . It is observed that concentration boundary layer increases by increasing M . The behaviors of N and λ on concentration profile are seen in the Figs. 7.18 and 7.19. Both N and λ decrease the concentration profile. Fig. 7.20 illustrates the effects of destructive chemical reaction parameter ($\gamma > 0$). It is obvious that the fluid concentration decreases with an increase in the destructive chemical reaction parameter. Fig. 7.21 shows the influence of generative chemical reaction parameter ($\gamma < 0$) on the concentration profile ϕ . This Fig. illustrates that concentration field has opposite behavior for ($\gamma < 0$) when compared with the case of chemical reaction parameter ($\gamma > 0$).

Tables 7.2 – 7.5 are given for the numerical values of the skin friction coefficients, Nusselt number and Sherwood number for the different values of involved parameters of interest. From Table 7.2 it is noticed that the magnitude of skin friction coefficient decreases for large value

of N and λ . From Table 7.3 it is found that the magnitude of $-\theta'(0)$ increases for large values of K_1 . This Table indicates that HAM solution has a good agreement with limiting numerical solution [53]. Table 7.4 is prepared for the variations of N , λ , K_1 , M , Sc and γ on the surface mass transfer. It is obvious from this Table that the magnitude of $-\phi'(0)$ increases for large values of K_1 and decreases for large values of M . The magnitude of $-\phi'(0)$ increases when Sc and γ are increased.

7.5 Conclusions

Heat and mass transfer analysis in the presence of thermal radiation is analyzed for the steady mixed convection flow of an incompressible micropolar fluid. The behavior of the embedded parameters in the derived series solutions are examined. The main observations are

- Velocity f' is an increasing function of N and λ .
- Microrotation profile for $N_0 = 0$ has a parabolic distribution.
- The temperature θ is a decreasing function of Pr .
- Behaviors of N_R and Pr on the temperature are opposite.
- Concentration field decreases when Sc increases.
- There are opposite results for destructive ($\gamma > 0$) and generative ($\gamma < 0$) chemical reactions on the concentration field ϕ .

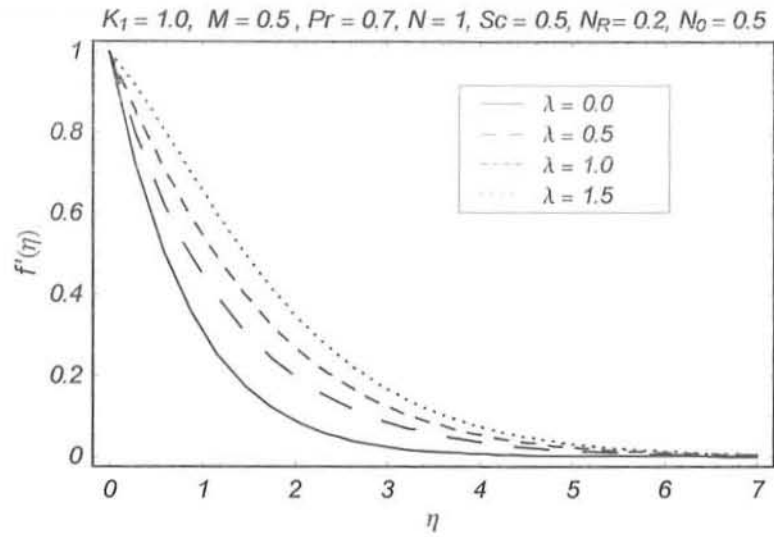


Fig. 7.2. Influence of λ on velocity profile f' .

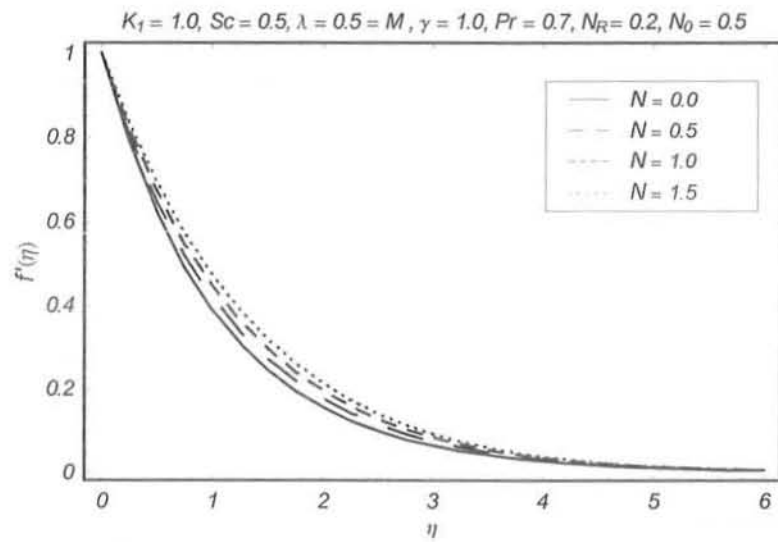


Fig. 7.3. Influence of N on velocity profile f' .

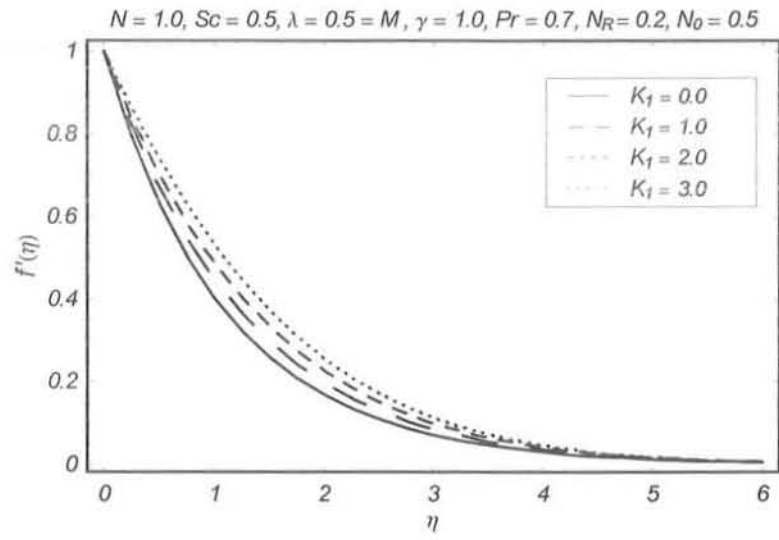


Fig. 7.4. Influence of K on velocity profile f' .

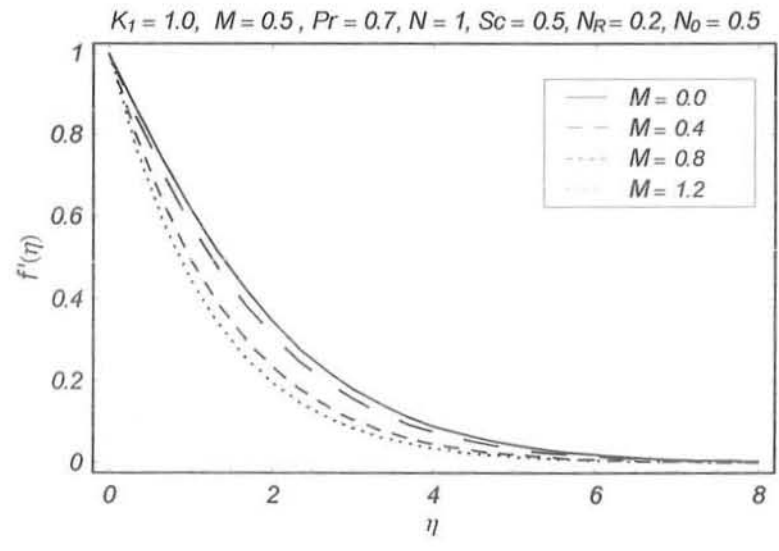


Fig. 7.5. Influence of M on velocity profile f' .

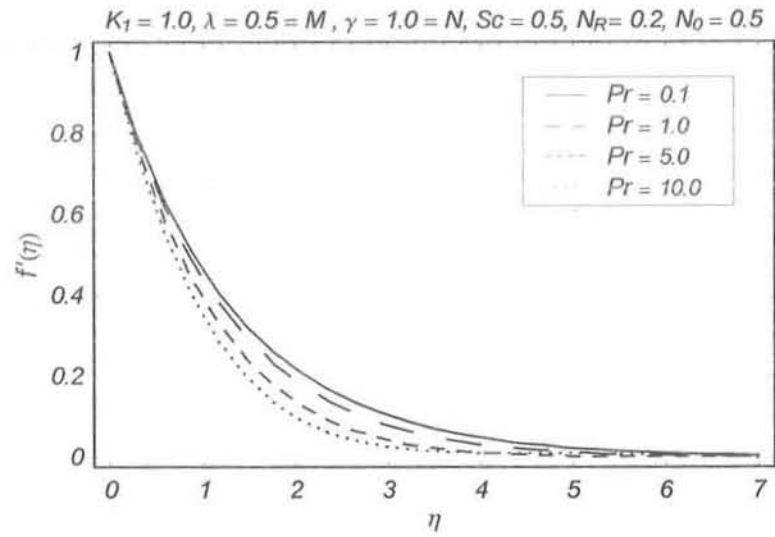


Fig. 7.6. Influence of Pr on velocity profile f' .

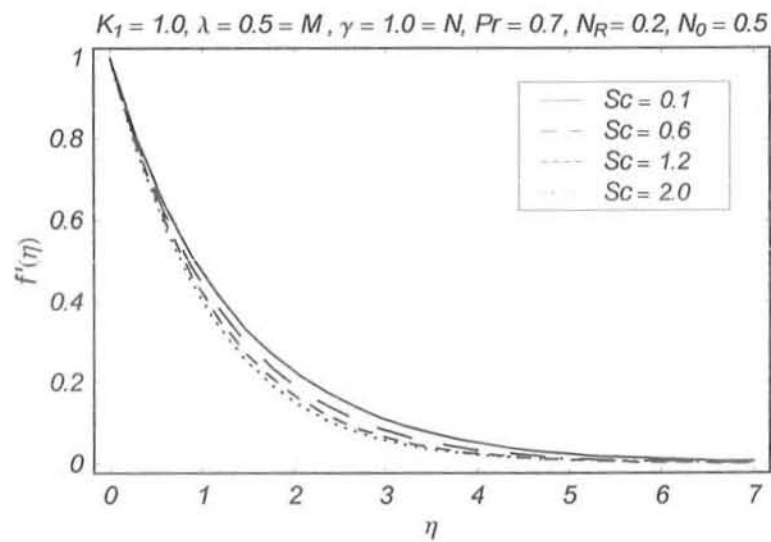


Fig. 7.7. Influence of Sc on velocity profile f' .

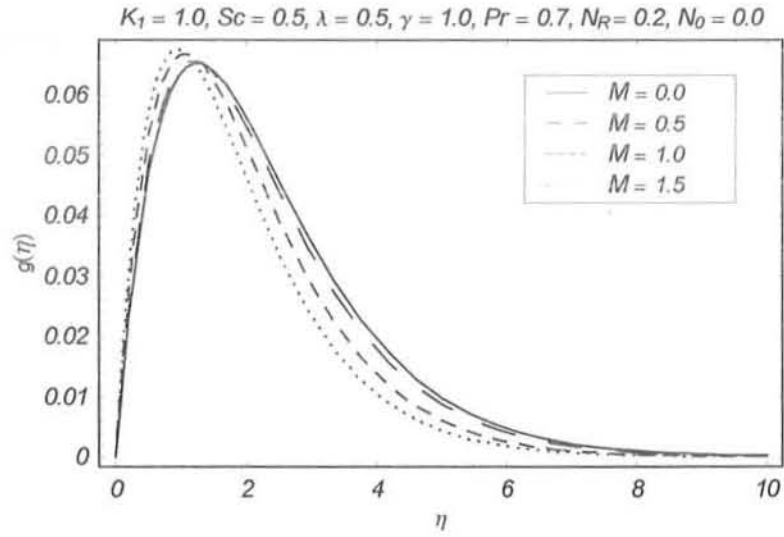


Fig. 7.8. Influence of M on microrotation profile g when $N_0 = 0.0$.

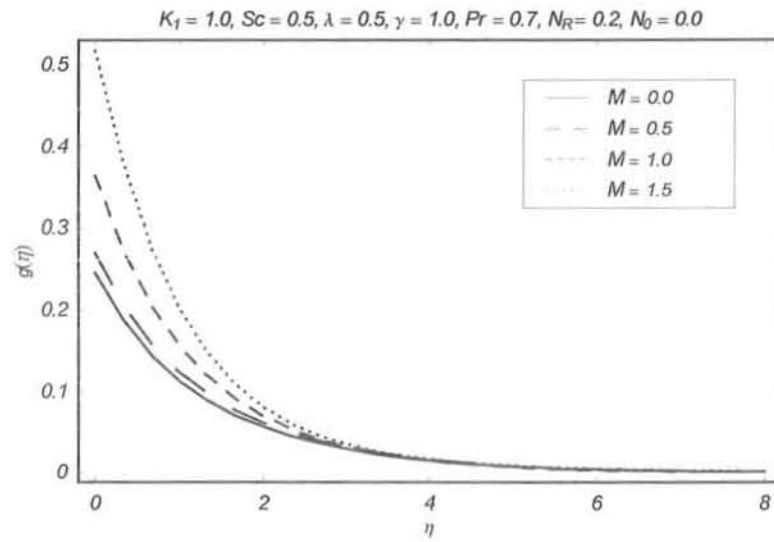


Fig. 7.9. Influence of M on microrotation profile g when $N_0 = 0.5$.

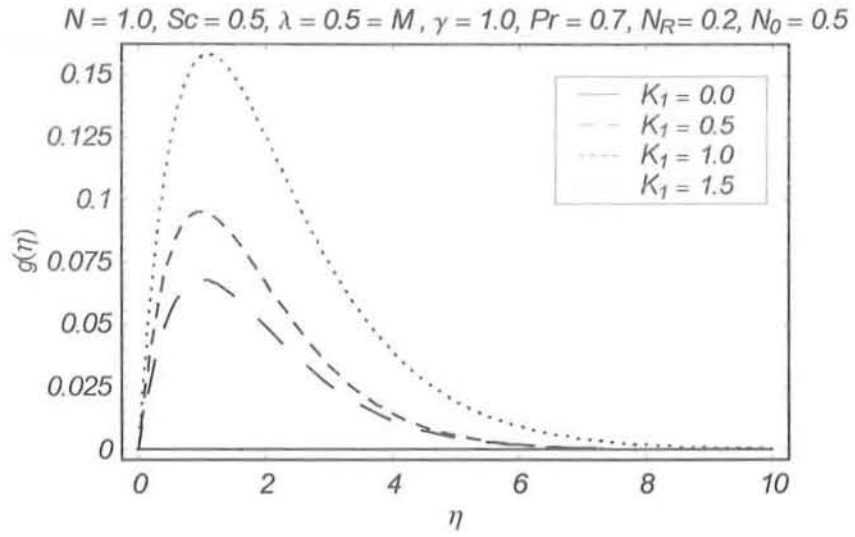


Fig. 7.10. Influence of K on microrotation profile g when $N_0 = 0.0$.

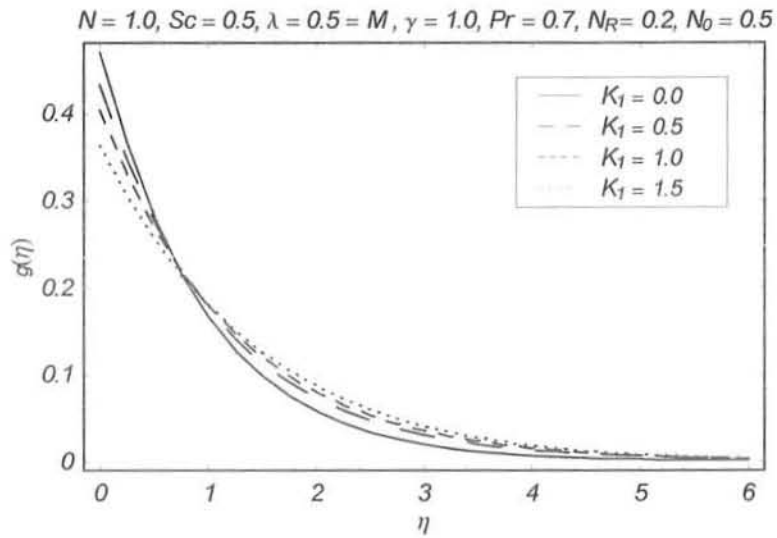


Fig. 7.11. Influence of K on microrotation profile g when $N_0 = 0.5$.

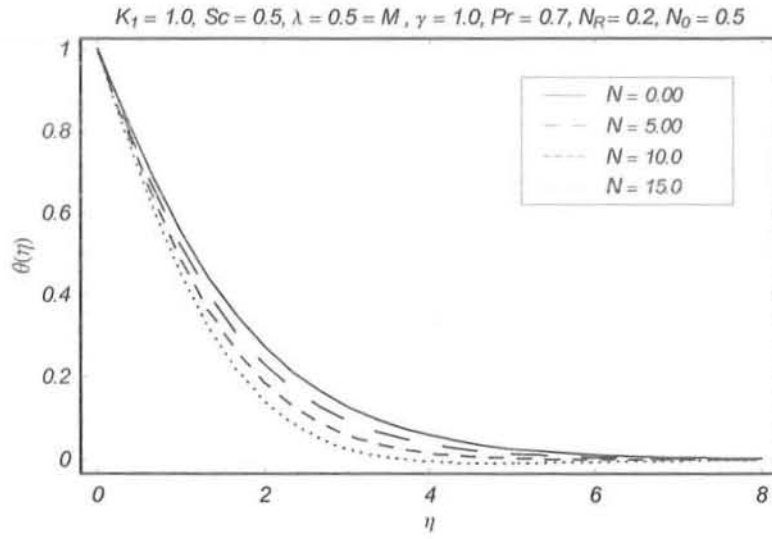


Fig. 7.12. Influence of N on temperature profile θ .

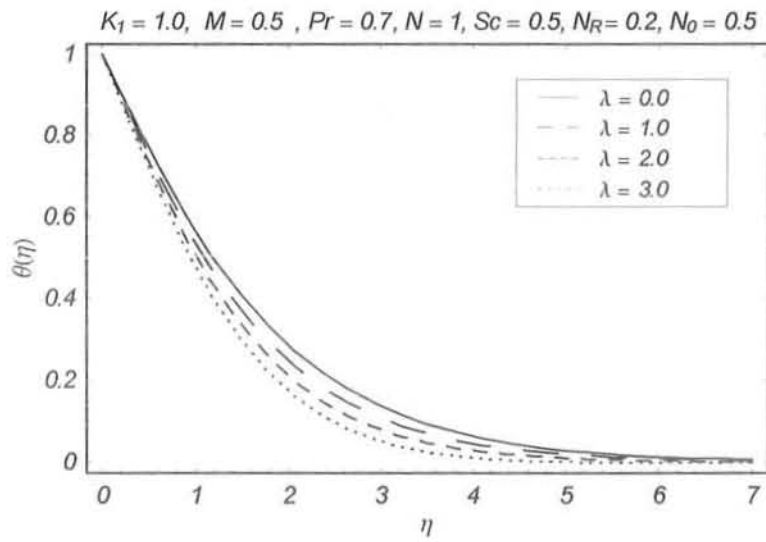


Fig. 7.13. Influence of λ on temperature profile θ .

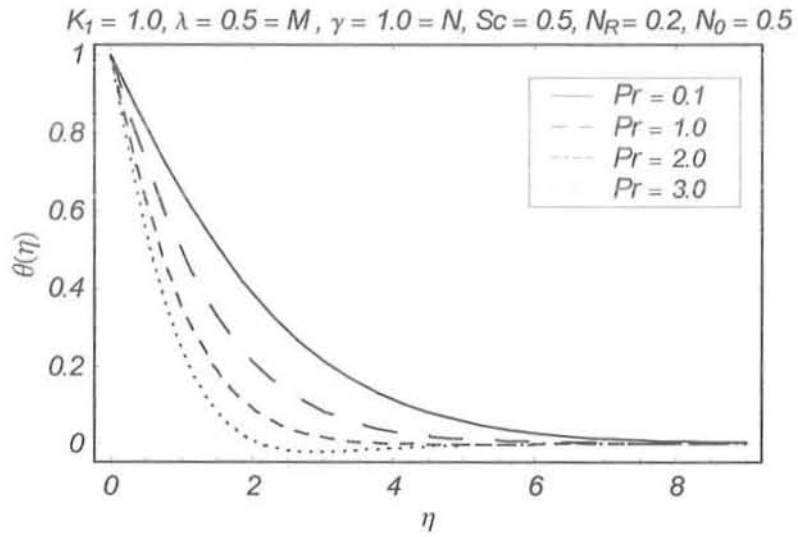


Fig. 7.14. Influence of Pr on temperature profile θ .

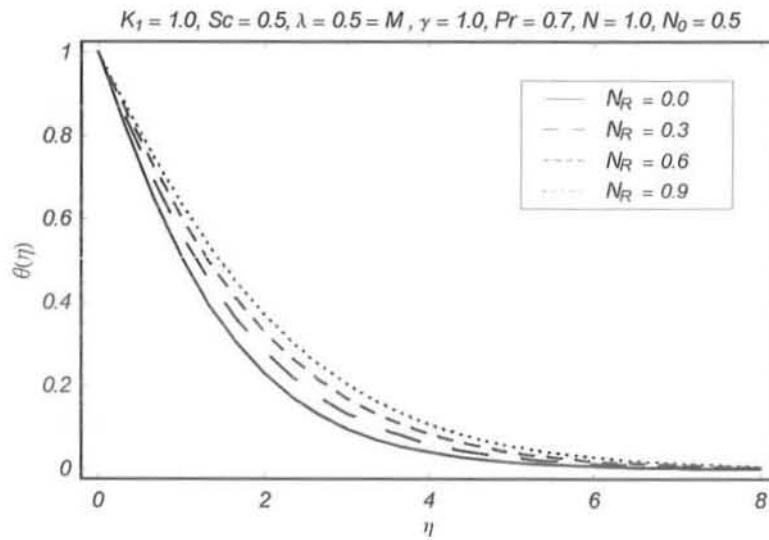


Fig. 7.15. Influence of N_R on temperature profile θ .

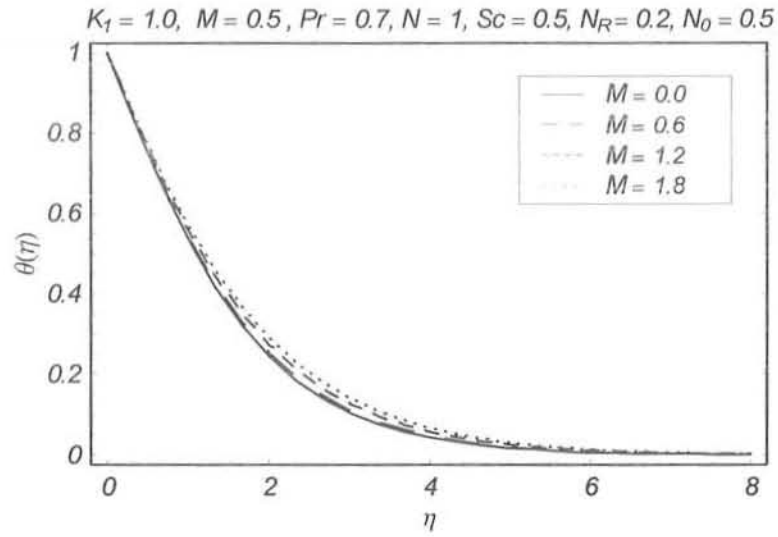


Fig. 7.16. Influence of M on temperature profile θ .

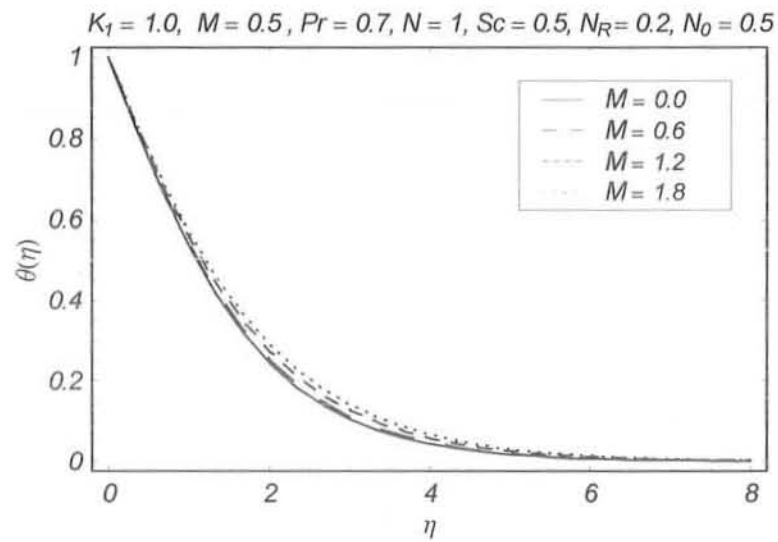


Fig. 7.17. Influence of M on temperature profile ϕ

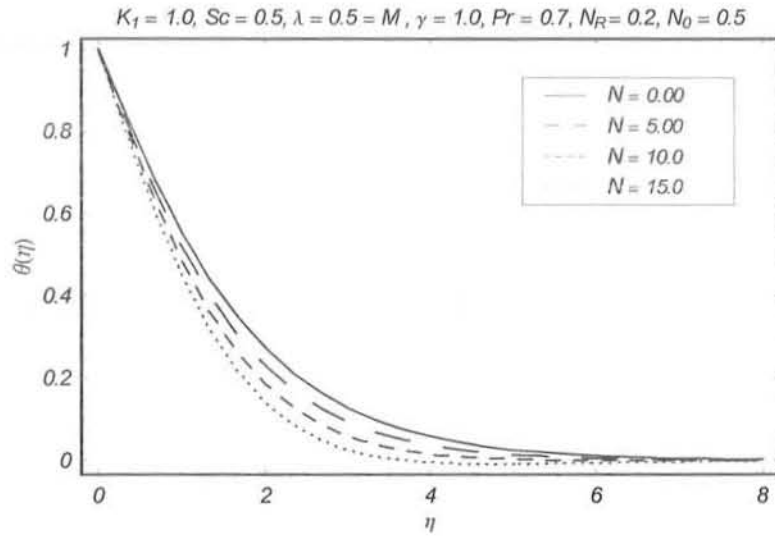


Fig. 7.18. Influence of N on concentration profile ϕ .

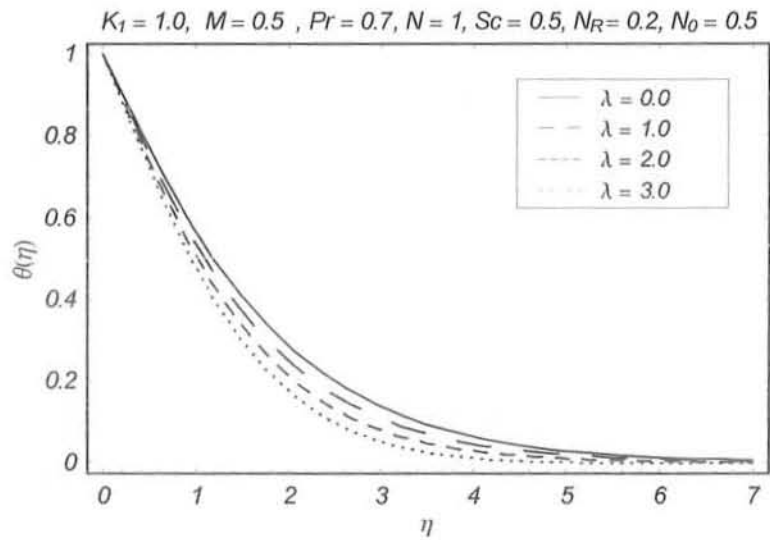


Fig. 7.19. Influence of λ on concentration profile ϕ .

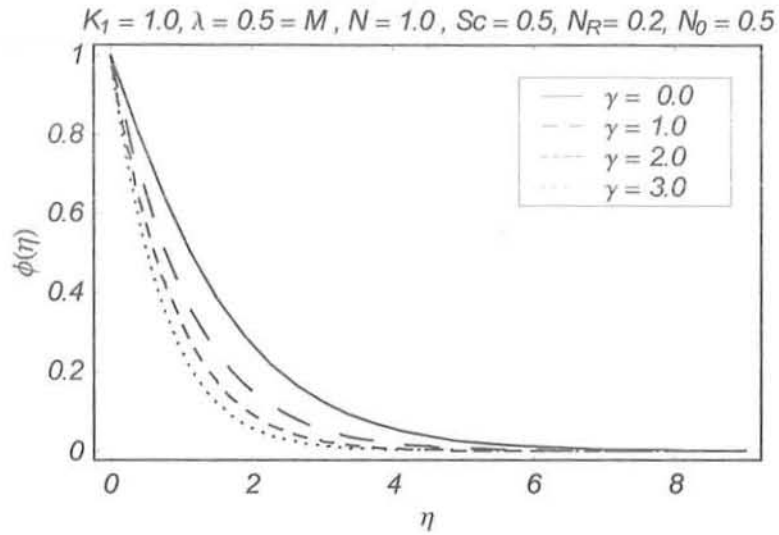


Fig. 7.20. Influence of $\gamma > 0$ on concentration profile ϕ .

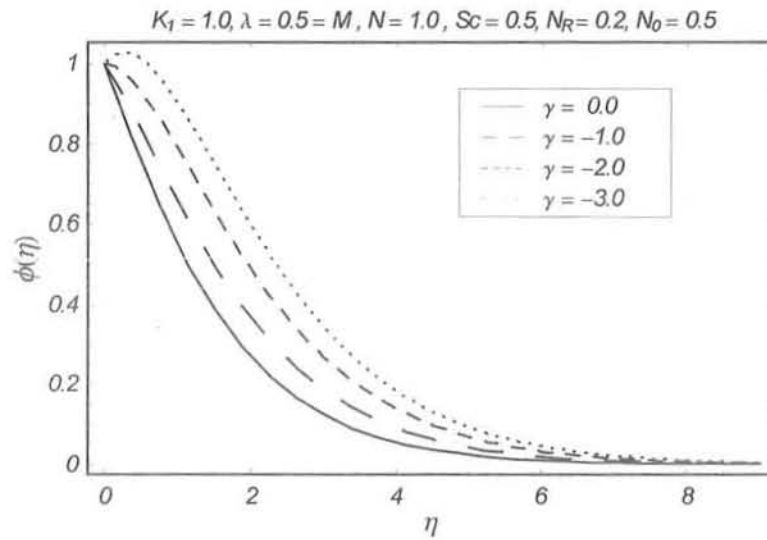


Fig. 7.21. Influence of $\gamma < 0$ on concentration profile ϕ .

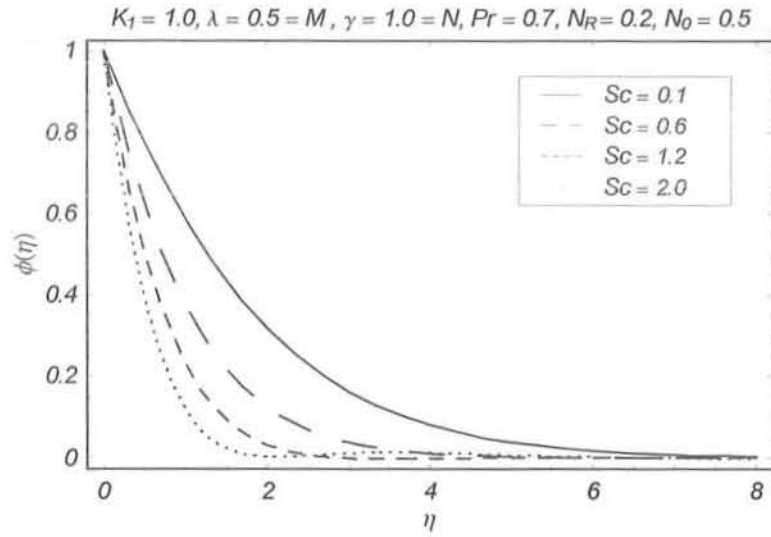


Fig. 7.22. Influence of Sc on concentration profile ϕ .

N	λ	K_1	$C_{fx} Re_x^{1/2}$	$C_{fx} Re_x^{1/2}$
			$N_0 = 0.0$	$N_0 = 0.5$
0.0	0.5	0.7	-1.61091	-1.40874
1.0			-1.36232	-1.19014
2.0			-1.11835	-0.97610
3.0			-0.87861	-0.97611
1.0	0.0	1.0	-1.94222	-1.70649
	0.2		-1.70191	-1.49091
	0.5		-1.36232	-1.19015
	1.0		-0.83192	-0.72411
1.0	0.5	0.0	-0.92897	-0.92897
		0.5	-1.16966	-1.06471
		1.0	-1.36231	-1.19019
		1.5	-1.52876	-1.30789

Table 7.2: Values of skin friction coefficient $C_{fx} \text{Re}_x^{1/2}$ for various values of N , λ , K_1 and M when $\text{Pr} = 0.7$, $\text{Sc} = 0.5$ and $\gamma = 1 = M$.

N_R	K_1	Pr	M	[53]	Present
1.0	1.0	1.0	0.0	0.3893	0.389321
	2.0			0.4115	0.411524
2.0	0.0			0.2588	0.259632
	1.0			0.2895	0.289547
	2.0			0.3099	0.309981
0.5	1.0	0.7	0.0	–	0.371412
			0.5	–	0.353991
			1.0	–	0.321648

Table 7.3: Comparison of values of $-\theta'(0)$ for some values of N_R , K_1 and Pr when $N_0 = 0.5$

Sc	γ	K_1	M	N	λ	$-\phi'(0)$
0.5	1.0	1.0	0.5	0.0	0.0	0.820814
1.2						1.299943
2.0						1.696172
0.5	1.0	1.0	0.5			0.820813
	2.0					1.088922
	3.0					1.301085
0.7	1.0	1.0	0.5			0.979971
		2.0				0.784003
		4.0				0.797627
0.7	1.0	1.0	0.0			0.781761
			0.5			0.773298
			1.5			0.734822
0.5	1.0	1.0	1.0	1.0	0.5	0.827542
				2.0		0.833643
				3.0		0.839325
				1.0	0.0	0.809882
					1.0	0.841481
					2.0	0.864091

Table 7.4: Values of $-\phi'(0)$ for some values of K_1 , M , Sc and γ when $N_0 = 0.5$.

Chapter 8

MHD steady flow and mass transfer of Jeffrey fluid over a non-linear stretching surface with mass transfer

The aim of this chapter is to investigate the MHD boundary layer flow of a Jeffrey fluid induced by a non-linearly stretching sheet with mass transfer. The relevant system of partial differential equations has been reduced into ordinary differential equations by employing the similarity transformation. Series solutions of velocity and concentration fields are developed by using homotopy analysis method (HAM). Effects of the various parameters such as Hartman number, Schmidt number and chemical reaction parameter on velocity and concentration fields are discussed by displaying graphs. Numerical values of the mass transfer coefficient are also tabulated and analyzed.

8.1 Mathematical formulation

We consider the steady, incompressible and MHD flow of a two-dimensional Jeffrey fluid over a non-linear stretching sheet. We choose x -axis parallel and y -axis normal to the stretching surface. A uniform magnetic field exerted in the y -direction. For small magnetic Reynolds number the induced magnetic field is neglected. We also considered the presence of first-order chemical reaction. For the present problem, the equations governing the flow are given below

$$\frac{\partial u}{\partial x} + \frac{\partial v}{\partial y} = 0, \quad (8.1)$$

$$\begin{aligned} & u \frac{\partial u}{\partial x} + v \frac{\partial u}{\partial y} + \lambda_1 \left[u^2 \frac{\partial^2 u}{\partial x^2} + v^2 \frac{\partial^2 u}{\partial y^2} + 2uv \frac{\partial^2 u}{\partial x \partial y} \right] \\ = & \nu \left[\frac{\partial^2 u}{\partial y^2} + \lambda_2 \left\{ u \frac{\partial^3 u}{\partial x \partial y^2} + v \frac{\partial^3 u}{\partial y^3} - \frac{\partial u}{\partial x} \frac{\partial^2 u}{\partial y^2} - \frac{\partial u}{\partial y} \frac{\partial^2 v}{\partial y^2} \right\} \right] - \frac{\sigma B_0^2}{\rho} u, \end{aligned} \quad (8.2)$$

$$u \frac{\partial C}{\partial x} + v \frac{\partial C}{\partial y} = D \frac{\partial^2 C}{\partial y^2} - RC. \quad (8.3)$$

In the above equations, u and v are components of the velocity along x and y directions respectively, ν is kinematic viscosity, ρ is the fluid density, σ is the electrical conductivity, λ_1 is relaxation time, λ_2 is retardation time. C is the species concentration in the fluid, D is the mass diffusion coefficient and R is the first order chemical reaction parameter.

The appropriate boundary conditions are

$$\begin{aligned} u(x, y) &= ax + bx^2, \quad v(x, y) = 0, \quad C(x, y) = C_w \quad \text{at } y = 0, \\ u &\rightarrow 0, \quad C \rightarrow 0 \quad \text{as } y \rightarrow \infty, \end{aligned} \quad (8.4)$$

where a and b are the dimensional constants.

In order to make the problem simpler, we introduce the following quantities

$$\begin{aligned}\eta &= \sqrt{\frac{a}{\nu}}y, \quad u = axf'(\eta) + bx^2g'(\eta), \\ v &= -\sqrt{a\nu}f(\eta) - 2bx\sqrt{\frac{\nu}{a}}g(\eta), \\ C &= C_w \left\{ C_0(\eta) + \frac{2bx}{a}C_1(\eta) \right\},\end{aligned}\tag{8.5}$$

where prime denotes the derivative with respect to η . We note that Eq. (8.1) is satisfied identically and Eqs. (8.2) – (8.4) are transformed as follows:

$$f''' - M^2f' - f'^2 + ff'' + \beta_1(2ff'f'' - f^2f''') + \beta_2(f''^2 - ff'''') = 0,\tag{8.6}$$

$$\begin{aligned}g''' - M^2g' - 3f'g' + 2f''g + g''f + \beta_1 \left(\begin{array}{l} 4ff'g'' + 2fg'f'' - f^2g''' \\ -4fgf''' + 4f'f''g - 2f'^2g' \end{array} \right) \\ + \beta_2 \left(\begin{array}{l} f'g''' - g'f''' - fg'''' \\ -2gf'''' + 3f''g'' \end{array} \right) = 0,\end{aligned}\tag{8.7}$$

$$C_0'' + ScfC_0' - Sc\gamma C_0 = 0,\tag{8.8}$$

$$C_1'' + ScfC_1' - Scf'C_1 - Sc\gamma C_1 + ScgC_0' = 0,\tag{8.9}$$

$$f(0) = 0, \quad f'(0) = 1, \quad f'(\infty) = 0,$$

$$g(0) = 0, \quad g'(0) = 1, \quad g'(\infty) = 0,$$

$$C_0(0) = 1, \quad C_0(\infty) = 0,$$

$$C_1(0) = 0, \quad C_1(\infty) = 0,\tag{8.10}$$

in which the chemical reaction parameter γ , the Schmidt number Sc , the Hartman number M

and the Deborah numbers β_1, β_2 are

$$\gamma = \frac{R}{a}, S = \frac{\nu}{D}, M^2 = \frac{\sigma B_0^2}{a\rho}, \beta_1 = \lambda_1 a, \beta_2 = \lambda_2 a. \quad (8.11)$$

Here $\gamma > 0$ indicates the destructive chemical reaction and $\gamma < 0$ for generative chemical reaction. For $\gamma = 0$ we have the case for a non - reactive species. The expressions of the mass transfer C'_0 and C'_1 at the wall are

$$C'_0(0) = \left(\frac{\partial C_0}{\partial \eta} \right)_{\eta=0} \leq 0, C'_1(0) = \left(\frac{\partial C_1}{\partial \eta} \right)_{\eta=0} \leq 0. \quad (8.12)$$

8.2 Homotopy analysis solutions

For the series solutions, we express $f(\eta)$, $g(\eta)$ and concentration fields $C_0(\eta)$ and $C_1(\eta)$ by the set of base functions

$$\left\{ \eta^k \exp(-n\eta) / k \geq 0, n \geq 0 \right\} \quad (8.13)$$

in the patterns

$$f(\eta) = a_{0,0}^0 + \sum_{n=0}^{\infty} \sum_{k=0}^{\infty} a_{m,n}^k \eta^k \exp(-n\eta), \quad (8.14)$$

$$g(\eta) = b_{0,0}^0 + \sum_{n=0}^{\infty} \sum_{k=0}^{\infty} b_{m,n}^k \eta^k \exp(-n\eta), \quad (8.15)$$

$$C_0(\eta) = \sum_{n=0}^{\infty} \sum_{k=0}^{\infty} d_{m,n}^k \eta^k \exp(-n\eta), \quad (8.16)$$

$$C_1(\eta) = \sum_{n=0}^{\infty} \sum_{k=0}^{\infty} e_{m,n}^k \eta^k \exp(-n\eta), \quad (8.17)$$

in which $a_{m,n}^k, b_{m,n}^k, d_{m,n}^k$ and $e_{m,n}^k$ are the coefficients. The initial guesses $f_0(\eta), g_0(\eta), C_{0,0}(\eta)$ and $C_{1,0}(\eta)$ of $f(\eta), g(\eta), C_0(\eta)$ and $C_1(\eta)$ are

$$f_0(\eta) = 1 - \exp(-\eta) , \quad (8.18)$$

$$g_0(\eta) = 1 - \exp(-\eta) , \quad (8.19)$$

$$C_{0,0}(\eta) = \exp(-\eta) , \quad (8.20)$$

$$C_{1,0}(\eta) = \eta \exp(-\eta) \quad (8.21)$$

with the following auxiliary linear operators

$$\mathcal{L}_1(f) = \frac{d^3 f}{d\eta^3} - \frac{df}{d\eta} , \quad (8.22)$$

$$\mathcal{L}_2(g) = \frac{d^3 g}{d\eta^3} - \frac{dg}{d\eta} , \quad (8.23)$$

$$\mathcal{L}_3(C_0) = \frac{d^2 C_0}{d\eta^2} - C_0 , \quad (8.24)$$

$$\mathcal{L}_4(C_1) = \frac{d^2 C_1}{d\eta^2} - C_1 \quad (8.25)$$

and

$$\mathcal{L}_1[c_1 + c_2 \exp(\eta) + c_3 \exp(-\eta)] = 0, \quad (8.26)$$

$$\mathcal{L}_2[c_4 + c_5 \exp(\eta) + c_6 \exp(-\eta)] = 0, \quad (8.27)$$

$$\mathcal{L}_3[c_7 \exp(\eta) + c_8 \exp(-\eta)] = 0, \quad (8.28)$$

$$\mathcal{L}_4[c_9 \exp(\eta) + c_{10} \exp(-\eta)] = 0, \quad (8.29)$$

where $c_i (i = 1 - 10)$ are the arbitrary constants. If $p \in [0,1]$ is an embedding parameter and $\hbar_f, \hbar_g, \hbar_{C_0}$ and \hbar_{C_1} indicate the non-zero auxiliary parameters respectively then the zeroth order deformation problems are constructed as follows.

$$(1-p)\mathcal{L}_1[\hat{f}(\eta, p) - f_0(\eta)] = p\hbar_f\mathcal{N}_f[\hat{f}(\eta, p)], \quad (8.30)$$

$$(1-p)\mathcal{L}_1[\hat{g}(\eta, p) - g_0(\eta)] = p\hbar_g\mathcal{N}_g[\hat{f}(\eta, p), \hat{g}(\eta, p)], \quad (8.31)$$

$$(1-p)\mathcal{L}_2[\hat{C}_0(\eta, p) - C_{0,0}(\eta)] = p\hbar_{C_0}\mathcal{N}_{C_0}[\hat{C}_0(\eta, p), \hat{f}(\eta, p)], \quad (8.32)$$

$$(1-p)\mathcal{L}_2[\hat{C}_1(\eta, p) - C_{1,0}(\eta)] = p\hbar_{C_1}\mathcal{N}_{C_1}[\hat{C}_0(\eta, p), \hat{C}_1(\eta, p), \hat{f}(\eta, p), \hat{g}(\eta, p)], \quad (8.33)$$

$$\hat{f}(\eta; p)\Big|_{\eta=0} = 0, \quad \frac{\partial \hat{f}(\eta; p)}{\partial \eta}\Big|_{\eta=0} = 1, \quad \frac{\partial \hat{f}(\eta; p)}{\partial \eta}\Big|_{\eta=\infty} = 0. \quad (8.34)$$

$$\hat{g}(\eta; p)\Big|_{\eta=0} = 0, \quad \frac{\partial \hat{g}(\eta; p)}{\partial \eta}\Big|_{\eta=0} = 1, \quad \frac{\partial \hat{g}(\eta; p)}{\partial \eta}\Big|_{\eta=\infty} = 0. \quad (8.35)$$

$$\frac{\partial \hat{C}_0(\eta; p)}{\partial \eta}\Big|_{\eta=0} = 1, \quad \frac{\partial \hat{C}_0(\eta; p)}{\partial \eta}\Big|_{\eta=\infty} = 0. \quad (8.36)$$

$$\frac{\partial \hat{C}_1(\eta; p)}{\partial \eta}\Big|_{\eta=0} = 0, \quad \frac{\partial \hat{C}_1(\eta; p)}{\partial \eta}\Big|_{\eta=\infty} = 0. \quad (8.37)$$

in which the non-linear differential operators $\mathcal{N}_f, \mathcal{N}_g, \mathcal{N}_{C_0}$ and \mathcal{N}_{C_1} are

$$\begin{aligned} \mathcal{N}_f[\hat{f}(\eta; p)] &= \frac{\partial^3 \hat{f}(\eta; p)}{\partial \eta^3} - M^2 \frac{\partial \hat{f}(\eta; p)}{\partial \eta} + \hat{f}(\eta; p) \frac{\partial^2 \hat{f}(\eta; p)}{\partial \eta^2} - \left(\frac{\partial \hat{f}(\eta; p)}{\partial \eta} \right)^2 \\ &+ \beta_1 \left(2\hat{f}(\eta; p) \frac{\partial \hat{f}(\eta; p)}{\partial \eta} \frac{\partial^2 \hat{f}(\eta; p)}{\partial \eta^2} - \hat{f}^2(\eta; p) \frac{\partial^3 \hat{f}(\eta; p)}{\partial \eta^3} \right) \\ &+ \beta_2 \left[\left(\frac{\partial^2 \hat{f}(\eta; p)}{\partial \eta^2} \right)^2 - \hat{f}(\eta; p) \frac{\partial^4 \hat{f}(\eta; p)}{\partial \eta^4} \right] \end{aligned} \quad (8.38)$$

$$\begin{aligned}
\mathcal{N}_g[\hat{f}(\eta; p), \hat{g}(\eta; p)] &= \frac{\partial^3 \hat{g}(\eta; p)}{\partial \eta^3} - M^2 \frac{\partial \hat{g}(\eta; p)}{\partial \eta} - 3 \frac{\partial \hat{g}(\eta; p)}{\partial \eta} \frac{\partial \hat{f}(\eta; p)}{\partial \eta} \\
&\quad + 2 \hat{g}(\eta; p) \frac{\partial^2 \hat{f}(\eta; p)}{\partial \eta^2} + \hat{f}(\eta; p) \frac{\partial^2 \hat{g}(\eta; p)}{\partial \eta^2} \\
&\quad + \beta_1 \left(\begin{aligned} &4 \hat{f}(\eta; p) \frac{\partial \hat{f}(\eta; p)}{\partial \eta} \frac{\partial^2 \hat{g}(\eta; p)}{\partial \eta^2} + 2 \hat{f}(\eta; p) \frac{\partial \hat{g}(\eta; p)}{\partial \eta} \frac{\partial^2 \hat{f}(\eta; p)}{\partial \eta^2} \\ &- \hat{f}^2(\eta; p) \frac{\partial^3 \hat{g}(\eta; p)}{\partial \eta^3} - 4 \hat{f}(\eta; p) \hat{g}(\eta; p) \frac{\partial^3 \hat{f}(\eta; p)}{\partial \eta^3} \\ &+ 4 \frac{\partial \hat{f}(\eta; p)}{\partial \eta} \frac{\partial^2 \hat{f}(\eta; p)}{\partial \eta^2} \hat{g}(\eta; p) - 2 \left(\frac{\partial \hat{f}(\eta; p)}{\partial \eta} \right)^2 \frac{\partial \hat{g}(\eta; p)}{\partial \eta} \end{aligned} \right) \\
&\quad + \beta_2 \left(\begin{aligned} &\frac{\partial \hat{f}(\eta; p)}{\partial \eta} \frac{\partial^3 \hat{g}(\eta; p)}{\partial \eta^3} - \frac{\partial \hat{g}(\eta; p)}{\partial \eta} \frac{\partial^3 \hat{f}(\eta; p)}{\partial \eta^3} - \hat{f}(\eta; p) \frac{\partial^4 \hat{g}(\eta; p)}{\partial \eta^4} \\ &- 2 \hat{g}(\eta; p) \frac{\partial^4 \hat{f}(\eta; p)}{\partial \eta^4} + 3 \frac{\partial^2 \hat{f}(\eta; p)}{\partial \eta^2} \frac{\partial^2 \hat{g}(\eta; p)}{\partial \eta^2} \end{aligned} \right) \tag{8.39}
\end{aligned}$$

$$\mathcal{N}_{C_0} [\hat{C}_0(\eta; p), \hat{f}(\eta; p)] = \frac{\partial^2 \hat{C}_0(\eta; p)}{\partial \eta^2} + Sc \hat{f}(\eta; p) \frac{\partial \hat{C}_0(\eta; p)}{\partial \eta} - Sc \gamma C_0, \tag{8.40}$$

$$\begin{aligned}
\mathcal{N}_{C_1} [\hat{C}_0(\eta; p), \hat{C}_1(\eta; p), \hat{f}(\eta; p), \hat{g}(\eta; p)] &= \frac{\partial^2 \hat{C}_1(\eta; p)}{\partial \eta^2} - Sc \gamma C_1 \\
&\quad + Sc \left(\begin{aligned} &-\frac{\partial \hat{f}(\eta; p)}{\partial \eta} \hat{C}_1(\eta; p) \\ &+ \hat{g}(\eta; p) \frac{\partial \hat{C}_0(\eta; p)}{\partial \eta} \\ &+ \hat{f}(\eta; p) \frac{\partial \hat{C}_1(\eta; p)}{\partial \eta} \end{aligned} \right). \tag{8.41}
\end{aligned}$$

Obviously for $p = 0$ and $p = 1$, we have

$$\hat{f}(\eta; 0) = f_0(\eta), \quad \hat{f}(\eta; 1) = f(\eta), \tag{8.42}$$

$$\hat{g}(\eta; 0) = g_0(\eta), \quad \hat{g}(\eta; 1) = g(\eta), \tag{8.43}$$

$$\hat{C}_0(\eta; 0) = C_{0,0}(\eta), \quad \hat{C}_0(\eta; 1) = C_0(\eta), \tag{8.44}$$

$$\widehat{C}_1(\eta, 0) = C_{1,0}(\eta), \quad \widehat{C}_1(\eta, 1) = C_1(\eta) \quad (8.45)$$

Expanding $\widehat{f}(\eta; p)$, $\widehat{g}(\eta, p)$, $\widehat{C}_0(\eta, p)$ and $\widehat{C}_1(\eta, p)$ in Taylor series with respect to embedding parameter p , we obtain

$$\widehat{f}(\eta; p) = f_0(\eta) + \sum_{m=1}^{\infty} f_m(\eta) p^m, \quad (8.46)$$

$$\widehat{g}(\eta, p) = g_0(\eta) + \sum_{m=1}^{\infty} g_m(\eta) p^m, \quad (8.47)$$

$$\widehat{C}_0(\eta, p) = C_{0,0}(\eta) + \sum_{m=1}^{\infty} C_{0,m}(\eta) p^m, \quad (8.48)$$

$$\widehat{C}_1(\eta, p) = C_{1,0}(\eta) + \sum_{m=1}^{\infty} C_{1,m}(\eta) p^m, \quad (8.49)$$

$$f_m(\eta) = \frac{1}{m!} \left. \frac{\partial^m f(\eta; p)}{\partial \eta^m} \right|_{p=0}, \quad g_m(\eta) = \frac{1}{m!} \left. \frac{\partial^m g(\eta; p)}{\partial \eta^m} \right|_{p=0}, \quad (8.50)$$

$$C_{0,m}(\eta) = \frac{1}{m!} \left. \frac{\partial^m \widehat{C}_0(\eta, p)}{\partial p^m} \right|_{p=0}, \quad C_{1,m}(\eta) = \frac{1}{m!} \left. \frac{\partial^m \widehat{C}_1(\eta, p)}{\partial p^m} \right|_{p=0}, \quad (8.51)$$

in which the series convergence in Eqs. (8.47) – (8.50) is dependent upon \hbar_f , \hbar_g , \hbar_{C_0} and \hbar_{C_1} . The values of \hbar_f , \hbar_g , \hbar_{C_0} and \hbar_{C_1} are chosen in such a way that the series (8.47) – (8.50) are convergent at $p = 1$ and hence

$$f(\eta) = f_0(\eta) + \sum_{m=0}^{\infty} f_m(\eta), \quad (8.52)$$

$$g(\eta) = g_0(\eta) + \sum_{m=0}^{\infty} g_m(\eta), \quad (8.53)$$

$$C_0(\eta) = C_{0,0}(\eta) + \sum_{m=1}^{\infty} C_{0,m}(\eta), \quad (8.54)$$

$$C_1(\eta) = C_{1,0}(\eta) + \sum_{m=1}^{\infty} C_{1,m}(\eta). \quad (8.55)$$

The problems corresponding to the m^{th} - order deformation are

$$\mathcal{L}_1 [f_m(\eta) - \chi_m f_{m-1}(\eta)] = \hbar_f \mathcal{R}_{f,m}(\eta), \quad (8.56)$$

$$\mathcal{L}_2 [g_m(\eta) - \chi_m g_{m-1}(\eta)] = \hbar_g \mathcal{R}_{g,m}(\eta), \quad (8.57)$$

$$\mathcal{L}_3 [C_{0,m}(\eta) - \chi_m C_{0,m-1}(\eta)] = \hbar_{C_0} \mathcal{R}_{C_{0,m}}(\eta), \quad (8.58)$$

$$\mathcal{L}_4 [C_{1,m}(\eta) - \chi_m C_{1,m-1}(\eta)] = \hbar_{C_1} \mathcal{R}_{C_{1,m}}(\eta), \quad (8.59)$$

$$f_m(0) = 0, f'_m(0) = 0, f'_m(\infty) = 0, \quad (8.60)$$

$$g_m(0) = 0, g'_m(0) = 0, g'_m(\infty) = 0, \quad (8.61)$$

$$C_{0,m}(0) = C_{0,m}(\infty) = 0, \quad (8.62)$$

$$C_{1,m}(0) = C_{1,m}(\infty) = 0, \quad (8.63)$$

$$\begin{aligned} \mathcal{R}_{f,m}(\eta) = & f'''_{m-1} - M^2 f'_{m-1} + \sum_{k=0}^{m-1} [f_{m-1-k} f''_k - f'_{m-1-k} f'_k] + \beta_1 \sum_{k=0}^{m-1} f_{m-1-k} \sum_{l=0}^k [2f'_{k-l} f''_l - f_{k-l} f'''_l] \\ & + \beta_2 \sum_{k=0}^{m-1} f''_{m-1-k} f''_k - f_{m-1-k} f''''_k \end{aligned} \quad (8.64)$$

$$\begin{aligned} \mathcal{R}_{g,m}(\eta) = & g'''_{m-1} - M^2 g'_{m-1} + \sum_{k=0}^{m-1} [-3f'_{m-1-k} g'_k + 2g_{m-1-k} f''_k + f_{m-1-k} g''_k] \\ & + \beta_1 \left[\sum_{k=0}^{m-1} f_{m-1-k} \sum_{l=0}^k [4f'_{k-l} g''_l + 2f''_{k-l} g'_l - f_{k-l} g'''_l - 4f'''_{k-l} g_l] \right. \\ & \left. + \sum_{k=0}^{m-1} f'_{m-1-k} \sum_{l=0}^k [4f''_{k-l} g_l - 2f'_{k-l} g'_l] \right] \\ & + \beta_2 \sum_{k=0}^{m-1} \left[\begin{array}{l} f'_{m-1-k} g'''_k - g'_{m-1-k} f'''_k - \\ f_{m-1-k} g''''_k - 2g_{m-1-k} f''''_k + 3f''_{m-1-k} g''_k \end{array} \right] \end{aligned} \quad (8.65)$$

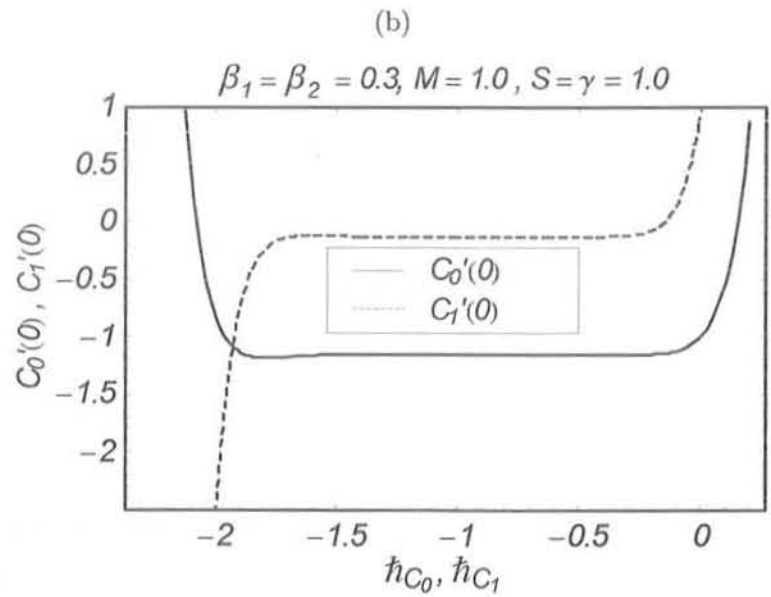
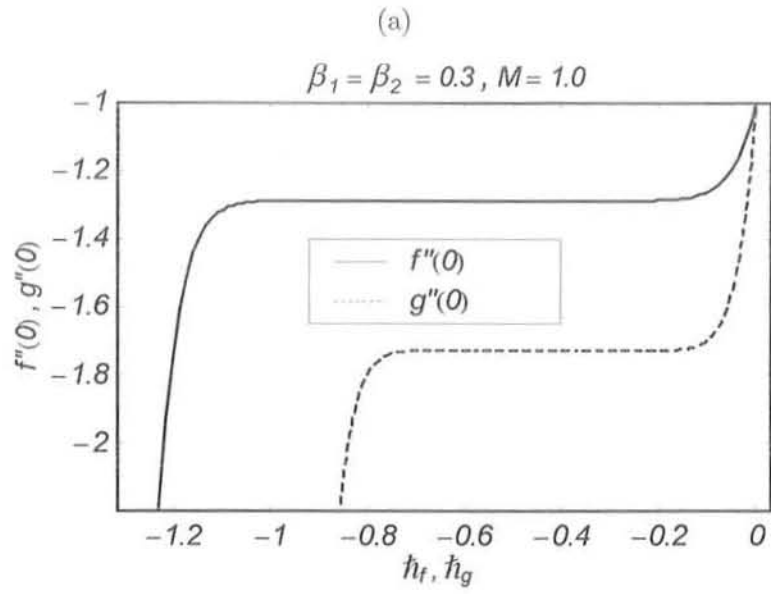
$$\mathcal{R}_{C_0,m}(\eta) = C''_{0,m-1} - Sc\gamma C_{0,m-1} + Sc \sum_{k=0}^{m-1} C'_{0,m-1-k} f_k, \quad (8.66)$$

$$\mathcal{R}_{C_1,m}(\eta) = C''_{1,m-1} - Sc\gamma C_{1,m-1} + Sc \sum_{k=0}^{m-1} (-C_{1,m-1-k} f'_k + C'_{1,m-1-k} f_k + C'_{0,m-1-k} g_k), \quad (8.67)$$

$$\chi_m = \begin{cases} 0, & m \leq 1, \\ 1, & m > 1. \end{cases} \quad (8.68)$$

8.3 Convergence of homotopy solutions

The convergence of series solutions are dependent upon the values of auxiliary parameters \hbar_f , \hbar_g , \hbar_{C_0} and \hbar_{C_1} . In order to determine the range of the admissible values of \hbar_f , \hbar_g , \hbar_{C_0} and \hbar_{C_1} for the functions $f''(0)$, $g''(0)$, $C'_0(0)$ and $C'_1(0)$, the \hbar -curves are plotted for 15th-order of approximation in Figs.8.1(a, b). It is clear that admissible values of \hbar_f , \hbar_g , \hbar_{C_0} and \hbar_{C_1} are $-1 \leq \hbar_f \leq -0.3$, $-0.7 \leq \hbar_g \leq -0.2$, $-1.5 \leq \hbar_{C_0} \leq -0.5$, and $-1.8 \leq \hbar_{C_1} \leq -0.5$. Furthermore the series solutions (8.53) – (8.56) converge in the whole region of η when $\hbar_f = \hbar_g = -0.5$ and $\hbar_{C_0} = \hbar_{C_1} = -1$. Table 8.1 shows the convergence of HAM solutions at different order of approximations.



Figs. 8.1(a, b): The h -curves of the functions $f''(0)$, $g''(0)$, $C_0'(0)$ and $C_1'(0)$ at 15th order of approximation.

order of approximation	$-f''(0)$	$-g''(0)$	$-C_0'(0)$	$-C_1'(0)$
1	1.212500	1.787500	1.166667	0.250000
5	1.286329	1.729082	1.1602806	0.128032
10	1.286998	1.728359	1.1600012	0.128054
15	1.287000	1.728356	1.160005	0.128064
20	1.287000	1.728356	1.160005	0.128063
25	1.287000	1.728356	1.160005	0.128063

Table 8.1: Convergence of HAM solution for different order of approximations when $M = 1.0$, $\beta = 0.2$, $S = 1.0$ and $\gamma = 0.2$.

8.4 Results and discussion

In this section, the graphical results are presented for the effects of Deborah numbers β_1, β_2 , Hartman number M , Schmidt number Sc and the chemical reaction parameter γ on the velocity and concentration fields. Such effects are discussed by Figs. 8.2 – 8.10. Figs. 8.2 – 8.4 show the effects of β_1, β_2 and M on f' and g' . For different values of Deborah number β_1 , the velocity profiles are plotted in Fig. 8.2. It is obvious that velocity distribution across the boundary layer decreases by increasing values of β . Fig. 8.2 shows the variation of Deborah number β_1 on f' and g' . It is found that the velocity components f' and g' decrease as β_1 increases. However such increase is small in f' when compared with g' . The boundary layer thickness decreases when Deborah number β_1 is increased. The effects of Deborah number β_2 on the velocity components f' and g' are opposite to β_1 (Figs. 8.3a and 8.3b). It can be seen from Figs. 8.4(a, b) that the effect of Hartman number M is similar to β_1 on the velocity components f' and g' . The variations of the emerging parameters on the concentration fields C_0 and C_1 are plotted in the Figs. 8.5 – 8.10. Figs. 8.5(a, b). are the graphical representations showing the

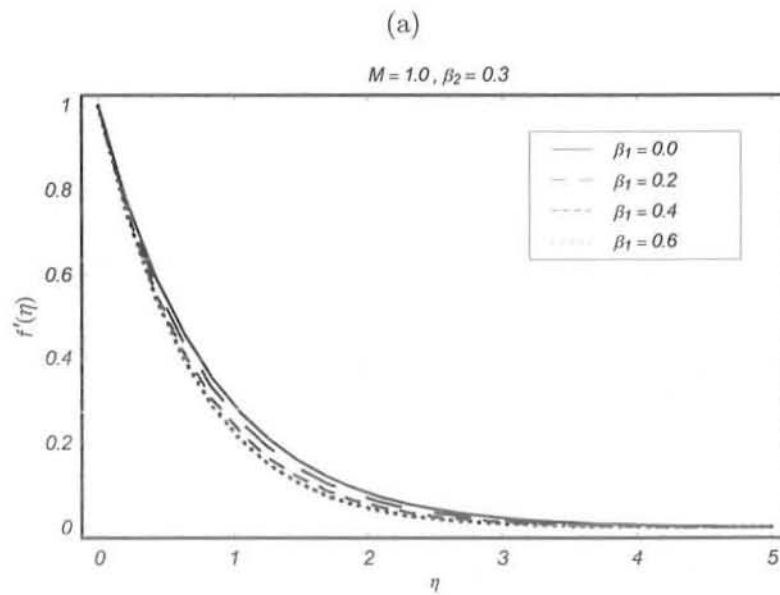
effects of the Deborah number β_1 on C_0 and C_1 in the case of destructive chemical reaction ($\gamma > 0$). The concentration field C_0 increases for large values of β_1 while the magnitude of C_1 decreases when β_1 increases. It should be pointed out that the variation in C_1 is larger in comparison to C_0 for large values of β_1 . Figs. 8.6(a, b) are displayed for the variations of β_2 on the concentration fields C_0 and C_1 in case of destructive chemical reaction ($\gamma > 0$). It can be seen that Figs. 8.6(a, b) have the opposite qualitative effects when compared with Figs 8.5(a, b). Fig. 8.7a shows the effects of M on C_0 . It is observed that the concentration field C_0 is increased when M increases. The variation of M on C_1 is sketched in Fig. 8.7b. Figs. 8.8 gives the variations of Schmidt number Sc on the concentration fields C_0 and C_1 for $\gamma = 0.2$. Both C_0 and C_1 decrease when Sc increases. The effects of destructive chemical reaction parameter ($\gamma > 0$) on the concentration fields C_0 and C_1 are displayed in Figs. 8.9. It is found from Figs 8.9a that the concentration field C_0 is a decreasing function of γ . It is also clear from Fig. 8.9b that the magnitude of C_1 decreases when γ increases. Figs. 8.10 depict the variation of generative chemical reaction ($\gamma < 0$) on the concentration fields C_0 and C_1 . It is found from Fig 8.10a that C_0 increases for large generative chemical reaction parameter. Fig. 8.10b depicts that the magnitude of C_1 also increases as γ ($\gamma < 0$) increases.

8.5 Closing remarks

The present study investigates the mass transfer in the MHD flow of a Jeffrey fluid bounded by a non-linearly stretching surface. The velocity and the concentration fields are derived. Homotopy analysis method is utilized for the series solutions. The behaviors of various embedded parameters in the considered problem are analyzed. The gradient of mass transfer are also computed in the tabulated forms. The main observations are pointed out below.

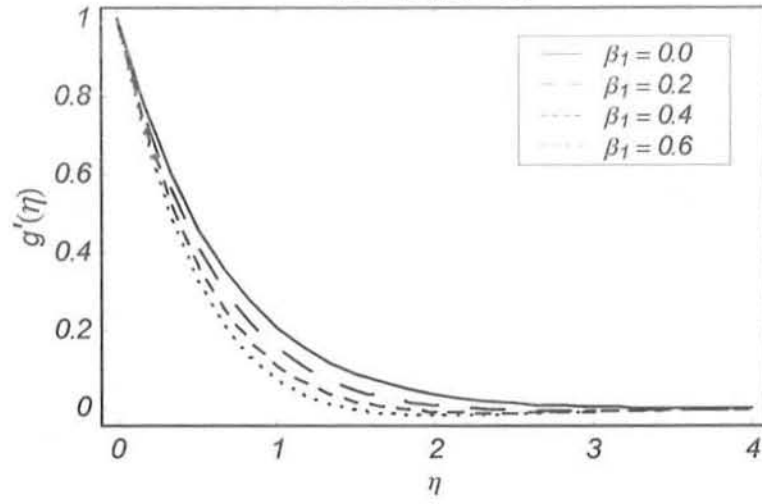
- The behavior of β_1 and M on $f'(\eta)$ and $g'(\eta)$ are same.
- The effects of increasing the values of M is to decrease the boundary layer thickness.

- The concentrations fields C_0 and C_1 decreases as Sc increases.
- The influence of the destructive ($\gamma > 0$) is to decrease the concentration fields.
- The concentration fields C_0 and C_1 has opposite results for destructive ($\gamma > 0$) and generative ($\gamma < 0$) chemical reactions.
- The surface mass transfer decreases by increasing M .

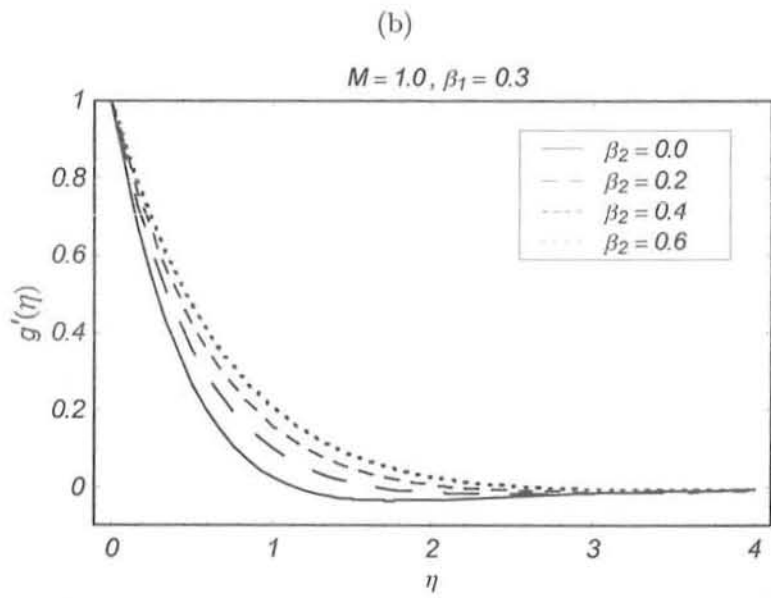
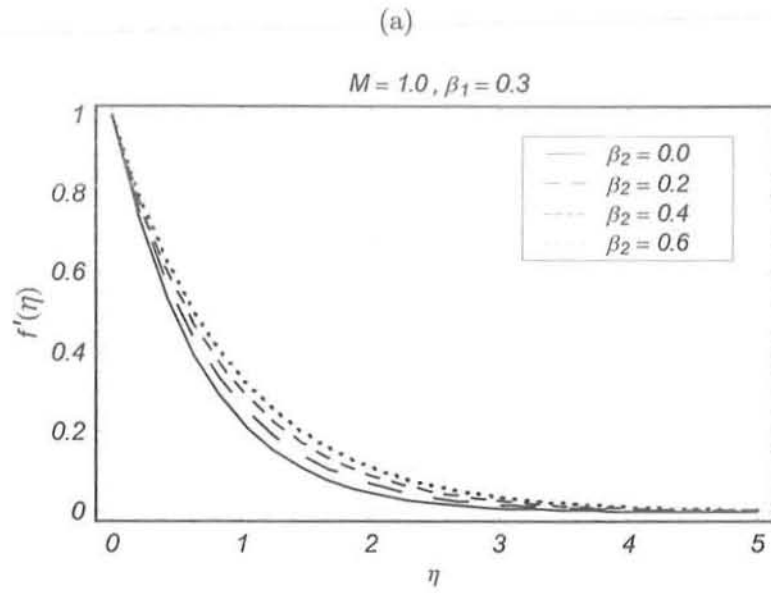


(b)

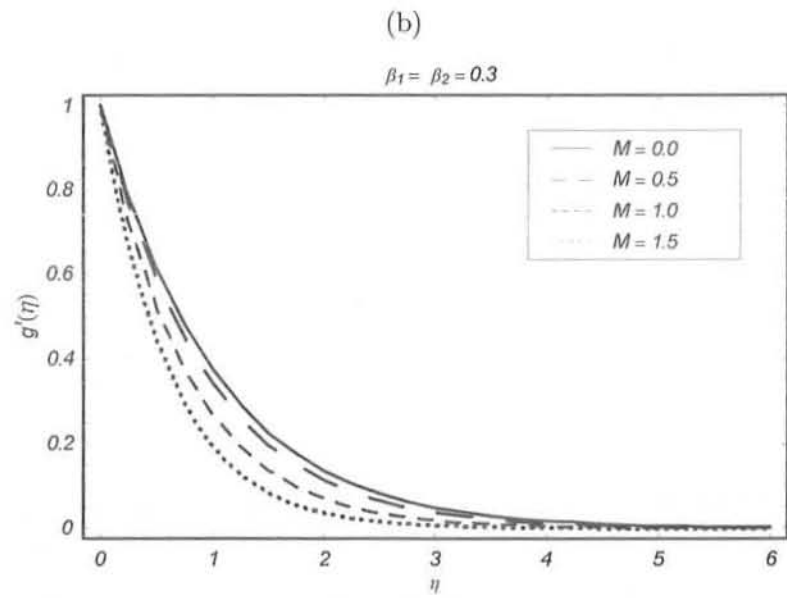
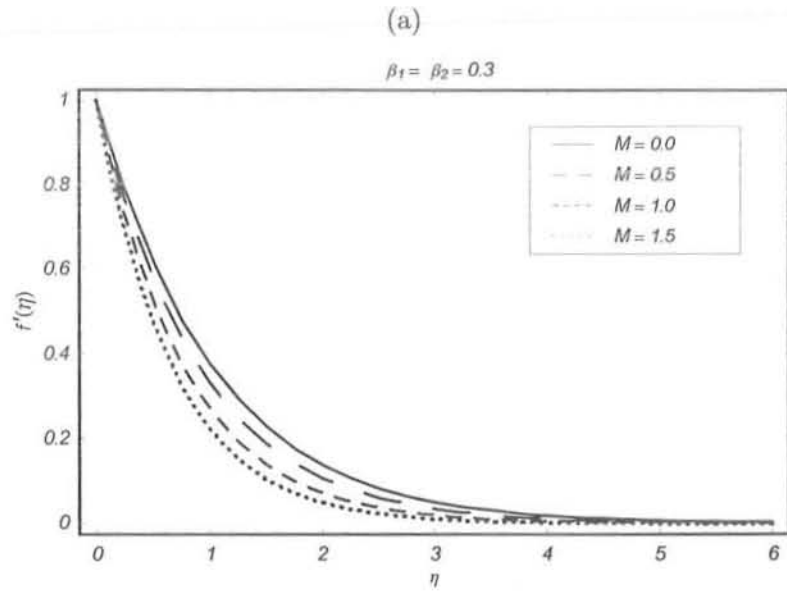
$M = 1.0, \beta_2 = 0.3$



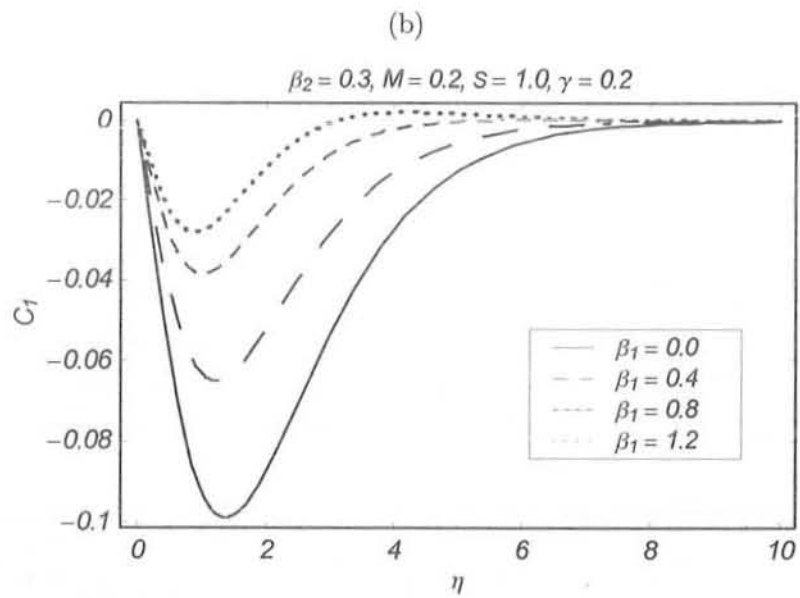
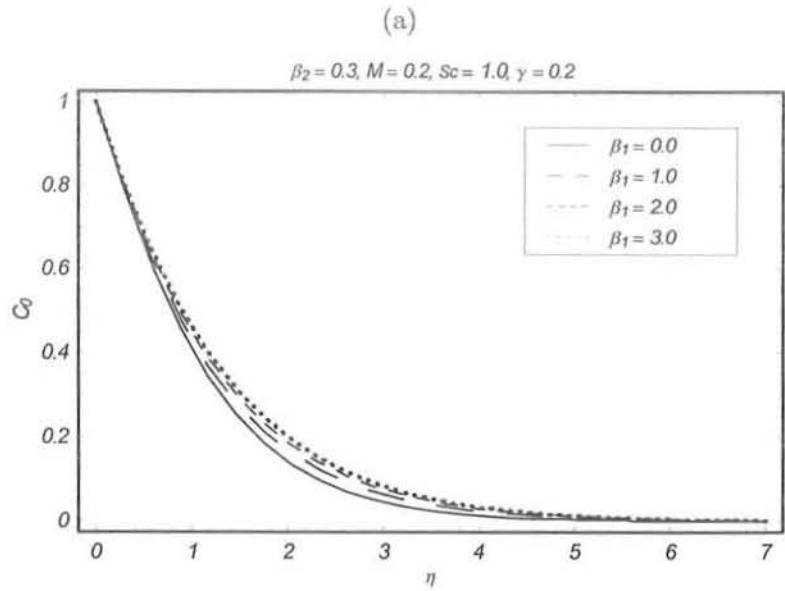
Figs. 8.2 (a, b). The variation of Deborah number β_1 on f' and g' .



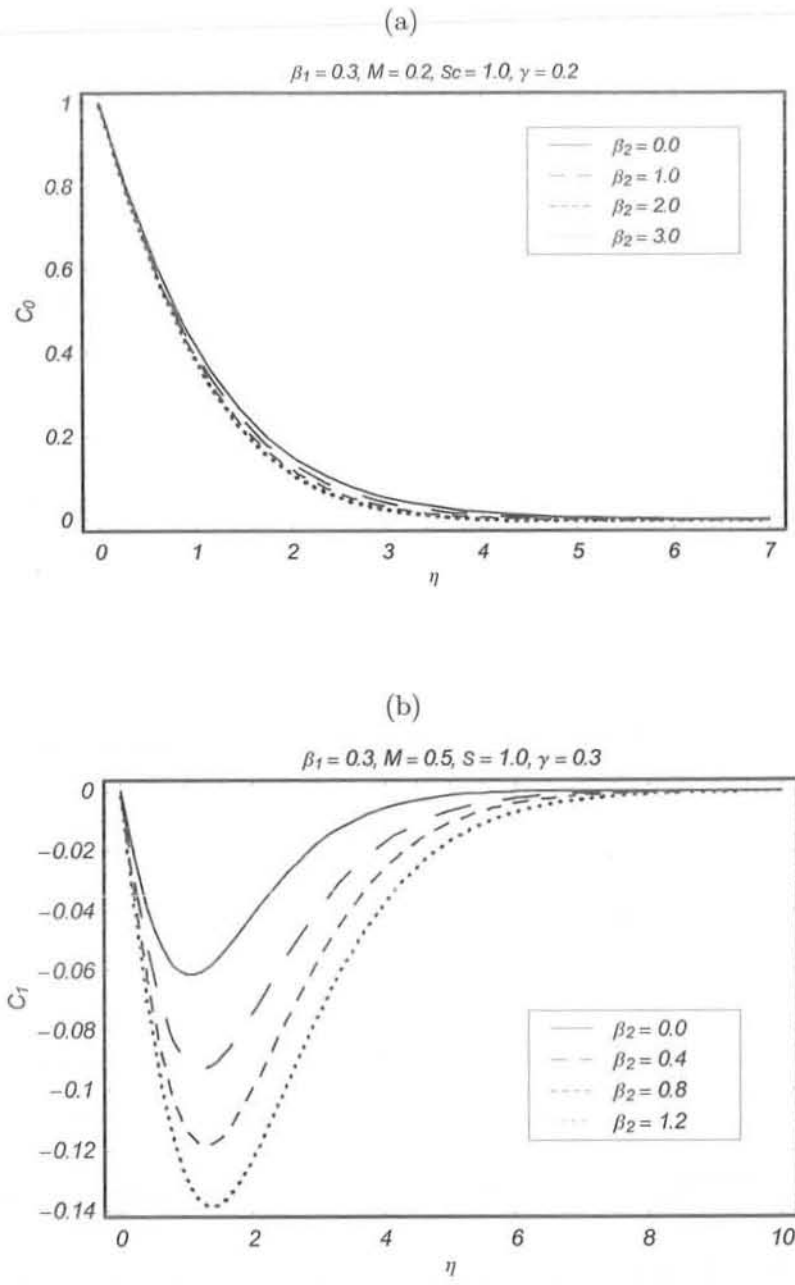
Figs. 8.3 (a, b). The variation of Deborah number β_2 on f' and g' .



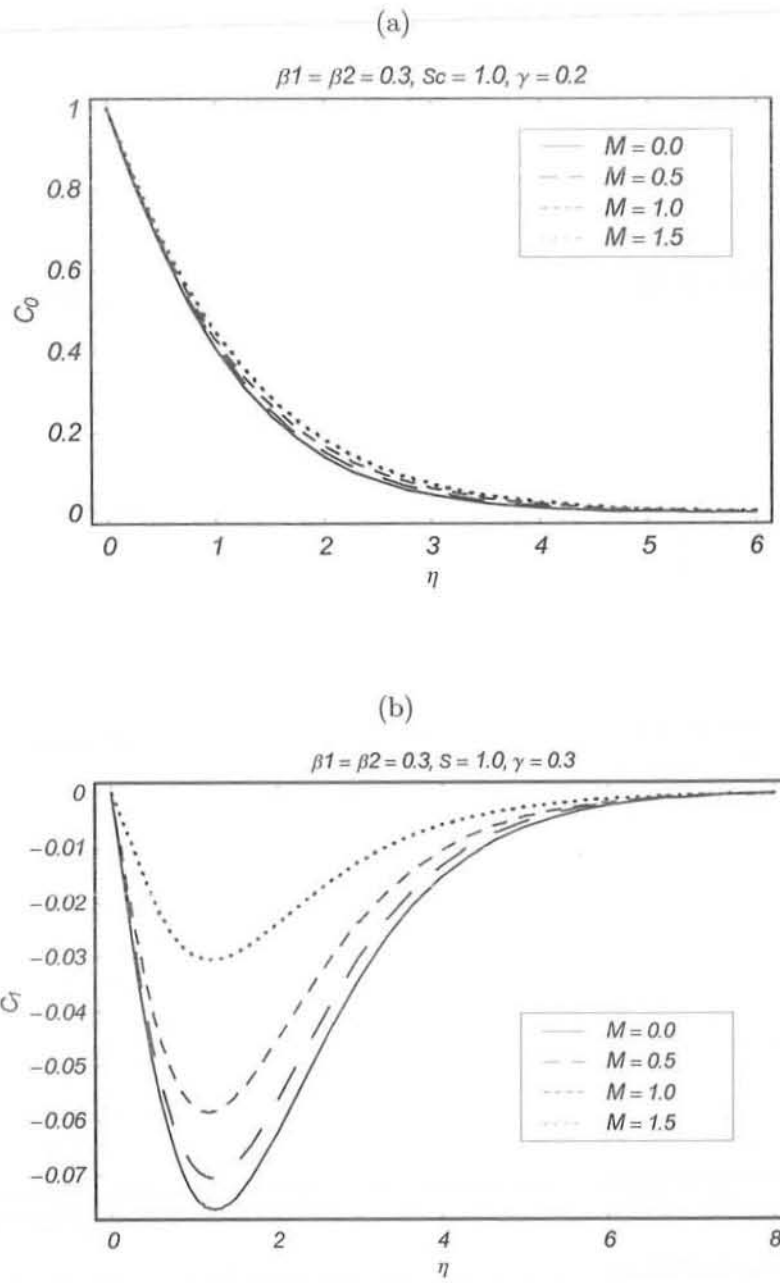
Figs. 8.4 (a, b). The variation of Hartman number M on f' and g' .



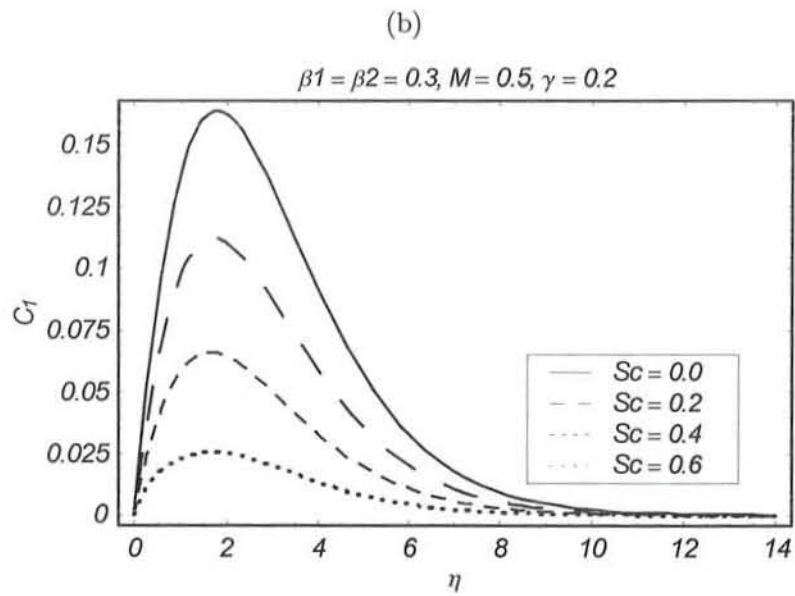
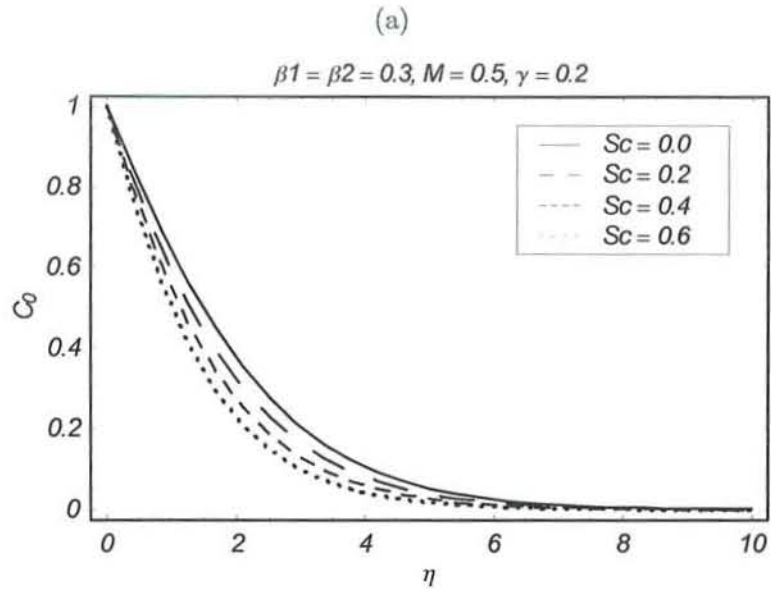
Figs. 8.5(a, b). The variation of Deborah number β_1 on C_0 and C_1 .



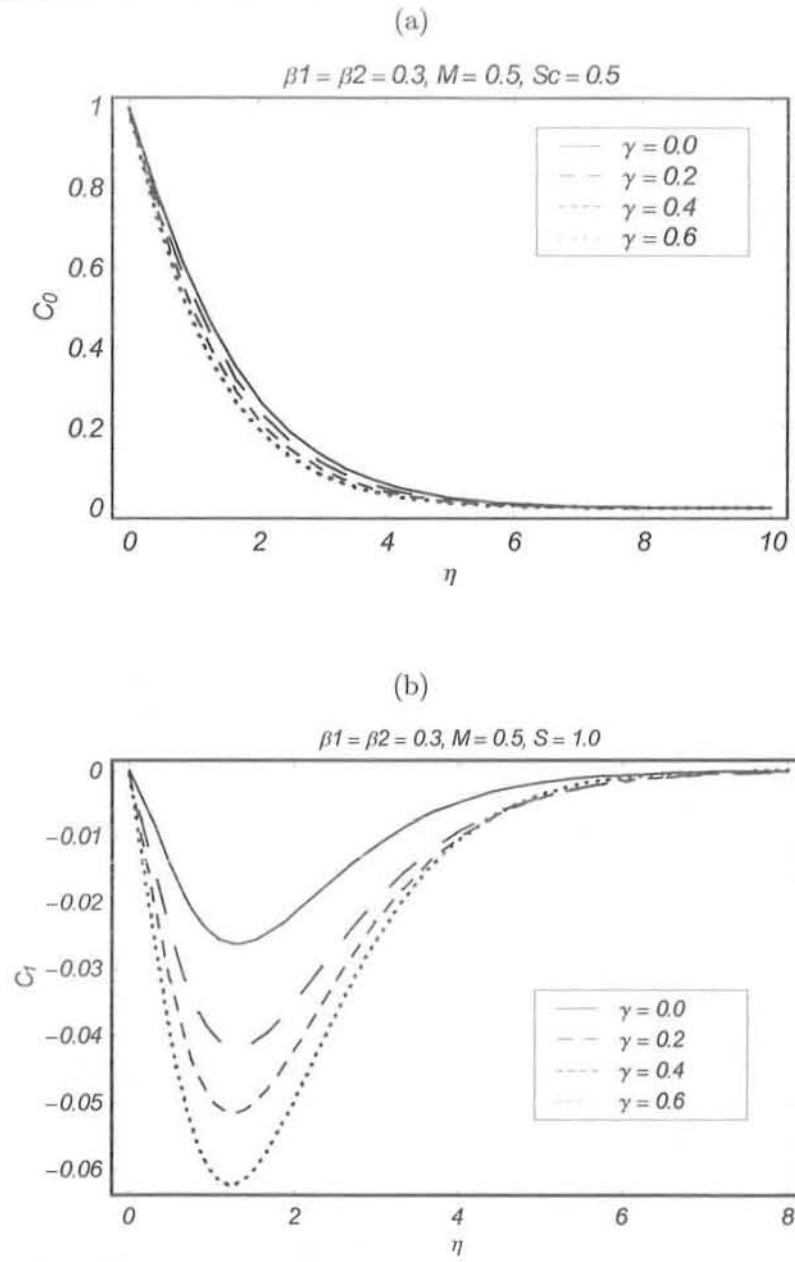
Figs. 8.6(a, b). The variation of Deborah number β_2 on C_0 and C_1 .



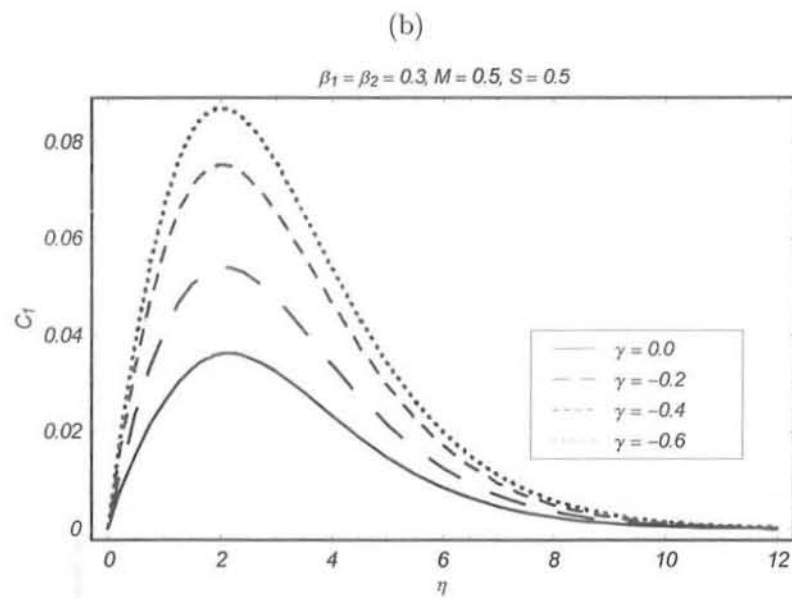
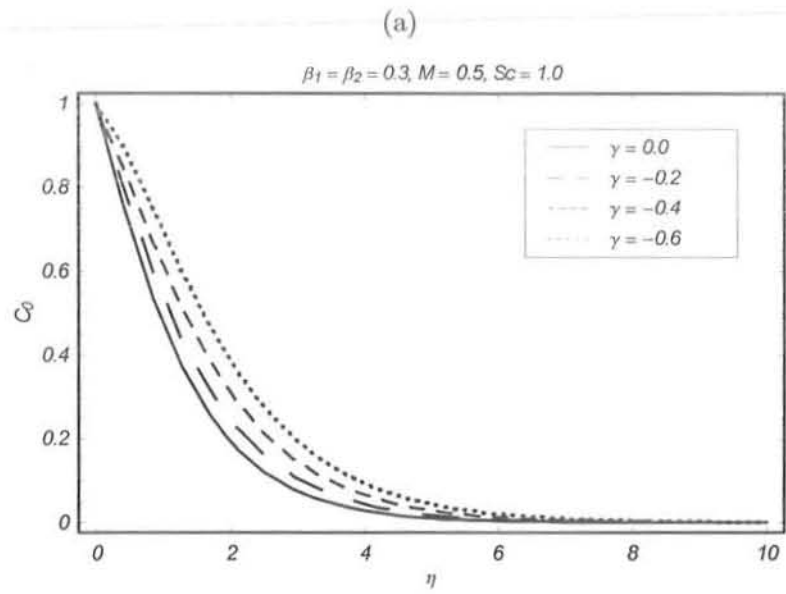
Figs. 8.7(a, b). The variation of Hartman number M on C_0 and C_1 .



Figs. 8.8(a, b). The variation of Schmidt number Sc on C_0 and C_1 .



Figs. 8.9(a, b). The variation of chemical reaction parameter γ on C_0 and C_1 in the case of destructive chemical reaction.



Figs. 8.10(a, b). The variation of chemical reaction parameter γ on C_0 and C_1 in case of generative chemical reaction.

Sc	γ	M	$\beta_1 = \beta_2$	$-C'_0(0)$	$-C'_1(0)$
1	0.4	1.2	0.2	0.83412	0.15646
	0.8			1.05823	0.13321
	1.0			1.15258	0.12582
	2.0			1.53473	0.10372
0.5	1.0			0.79841	0.07527
1.0				0.87943	0.08653
1.5				1.42758	0.16663
2.0				1.66074	0.20171
1.0	1.0	0		1.17773	0.12365
		0.3		1.17554	0.12416
		0.6		1.16966	0.12526
		0.9		1.16153	0.12605
		1.2		1.15258	0.12583
		1.2	0	1.14848	0.11841
			0.2	1.15258	0.12582
			0.4	1.55658	0.12992
			0.8	1.16029	0.13383
			1.0	1.16204	0.13469

Table 10.2: Values of the surface mass transfer $C'_0(0)$ and $C'_1(0)$ for some values of M , β_1 , β_2 , Sc and γ .

Chapter 9

Stagnation point flow of a Jeffrey fluid with mass transfer

This chapter reports the stagnation-point flow of an incompressible Jeffrey fluid bounded by a linear stretching surface. The analysis of mass transfer is also analyzed. The resulting partial differential equations are reduced into ordinary differential equations. Computations for dimensionless velocity and concentration fields are performed by an efficient approach namely the homotopy analysis method (HAM). Plots are prepared to illustrate the details of flow and mass transfer characteristics and their dependence upon the physical parameters. The values of surface mass transfer and gradient of mass transfer are evaluated and analyzed.

9.1 Problem formulation

We consider the two-dimensional flow near a stagnation point in the half space $y > 0$. The sheet in XOZ plane is stretched in the x -direction such that the velocity component in x -direction varies linearly along it. The ambient fluid moves with a velocity ax . In addition the mass transfer effects are considered. The velocity $U_w(x)$ and the concentration $C_w(x)$ of the stretching sheet is proportional to the distance x from the stagnation-point, where $C_w(x) > C_\infty$.

The boundary layer flow is governed by the following equations

$$\frac{\partial u}{\partial x} + \frac{\partial v}{\partial y} = 0, \quad (9.1)$$

$$u \frac{\partial u}{\partial x} + v \frac{\partial u}{\partial y} = U_{\infty} \frac{\partial U_{\infty}}{\partial x} + \frac{\nu}{1 + \lambda_1} \left[\frac{\partial^2 u}{\partial y^2} + \lambda_2 \left(u \frac{\partial^3 u}{\partial x \partial y^2} + v \frac{\partial^3 u}{\partial y^3} - \frac{\partial u}{\partial x} \frac{\partial^2 u}{\partial y^2} + \frac{\partial u}{\partial y} \frac{\partial^2 u}{\partial x \partial y} \right) \right], \quad (9.2)$$

$$u \frac{\partial C}{\partial x} + v \frac{\partial C}{\partial y} = D \frac{\partial^2 C}{\partial y^2} - RC, \quad (9.3)$$

In above equations u , v are the velocity components along the x - and y -axes, ρ the fluid density, ν the kinematic viscosity, D is the mass diffusion, C the concentration field and R the reaction rate. Here λ_1 indicates the ratio of relaxation and retardation times and λ_2 is the relaxation time.

The subjected boundary conditions are

$$u = U_w(x) = cx, \quad v = 0, \quad C = C_w(x) = C_{\infty} + bx \quad \text{at } y = 0, \quad (9.4)$$

$$u = U_{\infty}(x) = ax, \quad C = C_{\infty} \quad \text{as } y \rightarrow \infty, \quad (9.5)$$

where c is a stretching rate and the subscripts w and ∞ are written for the wall and free stream conditions.

Defining the following relations

$$\eta = \sqrt{\frac{c}{\nu}} y, \quad u = cx f'(\eta), \quad v = -\sqrt{c\nu} f(\eta), \quad \phi = \frac{C - C_{\infty}}{C_w - C_{\infty}}. \quad (9.6)$$

equation (9.1) is satisfied and the non-dimensional form of Eqs. (9.2) – (9.5) can be presented as

$$f''' + (1 + \lambda_1) (f f'' - f'^2) + \beta (f'^2 - f f''''') + (1 + \lambda_1) \frac{a^2}{c^2} = 0, \quad (9.7)$$

$$\phi'' + Sc(f\phi' - \phi f' - \gamma\phi) = 0, \quad (9.8)$$

$$\begin{aligned}
 f &= 0, f' = 1, \phi = 1 \quad \text{at } \eta = 0 \\
 f' &= \frac{a}{c}, \phi = 0 \quad \text{at } \eta \rightarrow \infty.
 \end{aligned}
 \tag{9.9}$$

$$\beta = \lambda_2 c, Sc = \frac{\nu}{D}, \gamma = \frac{k_1}{c}.
 \tag{9.10}$$

Here prime denotes a differentiation with respect to η . Furthermore, Sc , β and γ are the Schmidt, Deborah and chemical reaction parameters respectively. The surface mass transfer is expressed in the form

$$\phi'(0) = \left(\frac{\partial \phi}{\partial \eta} \right)_{\eta=0} \leq 0.
 \tag{9.11}$$

The Eqs. (9.7) and (9.9) for $\lambda_1 = \beta = a/c = 0$, has an exact solution of the form

$$f(\eta) = 1 - \exp(-\eta)
 \tag{9.12}$$

9.2 Homotopy solutions

In deriving the HAM solutions we have the base functions of the form

$$\left\{ \eta^k \exp(-n\eta), k \geq 0, n \geq 0 \right\}$$

and

$$f(\eta) = a_{0,0}^0 + \sum_{n=0}^{\infty} \sum_{k=0}^{\infty} a_{m,n}^k \eta^k \exp(-n\eta),
 \tag{9.13}$$

$$\phi(\eta) = \sum_{n=0}^{\infty} \sum_{k=0}^{\infty} b_{m,n}^k \eta^k \exp(-n\eta),
 \tag{9.14}$$

where $a_{m,n}^k$ and $b_{m,n}^k$ are the coefficients. The initial approximations are f_0 and ϕ_0 and auxiliary linear operators are

$$\begin{aligned} f_0(\eta) &= \frac{a}{c}\eta + (1 - \frac{a}{c}) [(1 - \exp(-\eta))], \\ \phi_0(\eta) &= \exp(-\eta). \end{aligned} \quad (9.15)$$

$$\mathcal{L}_f(f) = \frac{d^3 f}{d\eta^3} - \frac{df}{d\eta}, \quad (9.16)$$

$$\mathcal{L}_\phi(f) = \frac{d^2 f}{d\eta^2} - f, \quad (9.17)$$

whence

$$\mathcal{L}_f[C_1 + C_2 \exp(\eta) + C_3 \exp(-\eta)] = 0, \quad (9.18)$$

$$\mathcal{L}_\phi[C_4 \exp(\eta) + C_5 \exp(-\eta)] = 0 \quad (9.19)$$

and C_i ($i = 1 - 5$) are the arbitrary constants. The embedding parameter is $p \in [0, 1]$ and non-zero auxiliary parameters are h_f and h_ϕ . The problems at the zeroth order are written in the forms

$$(1 - p)\mathcal{L}_f[f(\eta; p) - f_0(\eta)] = ph_f N_f[f(\eta; p)], \quad (9.20)$$

$$(1 - p)\mathcal{L}_\phi[\phi(\eta; p) - \phi_0(\eta)] = ph_\phi N_\phi[\phi(\eta; p), f(\eta; p)], \quad (9.21)$$

$$f(\eta; p)|_{\eta=0} = 0, \quad \left. \frac{\partial f(\eta; p)}{\partial \eta} \right|_{\eta=0} = 1, \quad \left. \frac{\partial f(\eta; p)}{\partial \eta} \right|_{\eta=\infty} = \frac{a}{c}, \quad (9.22)$$

$$\phi(\eta; p)|_{\eta=0} = 1, \quad \phi(\eta; p)|_{\eta=\infty} = 0, \quad (9.23)$$

$$\begin{aligned}
N_f[f(\eta; p)] &= \frac{\partial^3 f(\eta, p)}{\partial \eta^3} + (1 + \lambda_1) \left[f(\eta, p) \frac{\partial^2 f(\eta, p)}{\partial \eta^2} - \left(\frac{\partial f(\eta, p)}{\partial \eta} \right)^2 \right] \\
&\quad + \beta \left[\left(\frac{\partial^2 \hat{f}(\eta, p)}{\partial \eta^2} \right)^2 - \hat{f}(\eta, p) \frac{\partial^4 \hat{f}(\eta, p)}{\partial \eta^4} \right] \\
&\quad + (1 + \lambda_1) \frac{a^2}{c^2},
\end{aligned} \tag{9.24}$$

$$N_\phi[\phi(\eta; p), f(\eta; p)] = \frac{\partial^2 \phi(\eta; p)}{\partial \eta^2} + Sc \left[f(\eta; p) \frac{\partial \phi(\eta; p)}{\partial \eta} - \phi(\eta; p) \frac{\partial f(\eta; p)}{\partial \eta} - \gamma \phi(\eta; p) \right]. \tag{9.25}$$

The above zeroth-order deformation equations (9.20) and (9.21) for $p = 0$ and $p = 1$ have the following solutions

$$f(\eta; 0) = f_0(\eta), \quad f(\eta; 1) = f(\eta), \tag{9.26}$$

$$\phi(\eta; 0) = \phi_0(\eta), \quad \phi(\eta; 1) = \phi(\eta). \tag{9.27}$$

Obviously when p increases from 0 to 1, $f(\eta, p)$ varies from initial guess $f_0(\eta)$ to the exact solution $f(\eta)$. Therefore, by Taylor's theorem and Eqs. (9.26) and (9.27) we get

$$f(\eta; p) = f_0(\eta) + \sum_{m=0}^{\infty} f_m(\eta) p^m, \tag{9.28}$$

$$\phi(\eta; p) = \phi_0(\eta) + \sum_{m=0}^{\infty} \phi_m(\eta) p^m, \tag{9.29}$$

$$f_m(\eta) = \frac{1}{m!} \left. \frac{\partial^m f(\eta; p)}{\partial \eta^m} \right|_{p=0}, \quad \phi_m(\eta) = \frac{1}{m!} \left. \frac{\partial^m \phi(\eta; p)}{\partial \eta^m} \right|_{p=0}. \tag{9.30}$$

Clearly Eqs. (9.20) and (9.21) involve non-zero auxiliary parameters h_f and h_ϕ . The convergence of the series (9.28) and (9.29) depends upon h_f and h_ϕ . The values of h_f and h_ϕ are selected such that the Eqs. (9.28) and (9.29) are convergent at $p = 1$. Hence we write

$$f(\eta) = f_0(\eta) + \sum_{m=0}^{\infty} f_m(\eta), \tag{9.31}$$

$$\phi(\eta) = \phi_0(\eta) + \sum_{m=0}^{\infty} \phi_m(\eta). \quad (9.32)$$

The m th-order deformation problems are

$$\mathcal{L}_f[f_m(\eta) - \chi_m f_{m-1}(\eta)] = h_f R_m^f(\eta), \quad (9.33)$$

$$\mathcal{L}_f[\phi_m(\eta) - \chi_m \phi_{m-1}(\eta)] = h_\phi R_m^\phi(\eta), \quad (9.34)$$

$$f_m(0) = f'_m(0) = f'_m(\infty) = 0, \quad \phi_m(0) = \phi_m(\infty) = 0, \quad (9.35)$$

$$R_m^f(\eta) = f_{m-1}'''(\eta) + (1 - \chi_m) \left[(1 + \lambda_1) \frac{a^2}{c^2} \right] + \sum_{k=0}^{m-1} \left[(1 + \lambda_1) (f_{m-1-k} f_k'' - f'_{m-1-k} f_k') + \beta (f_{m-1-k}'' f_k'' - f_{m-1-k} f_k^{iv}) \right], \quad (9.36)$$

$$R_m^\phi(\eta) = \phi_{m-1}''(\eta) - Sc\gamma\phi_{m-1} + Sc \sum_{k=0}^{m-1} [\phi_{m-1-k}' f_k - \phi_k f_{m-1-k}'], \quad (9.37)$$

$$\chi_m = \begin{cases} 0, & m \leq 1, \\ 1, & m > 1. \end{cases} \quad (9.38)$$

The general solutions are

$$f_m(\eta) = f_m^*(\eta) + C_1 + C_2 \exp(\eta) + C_3 \exp(-\eta), \quad (9.39)$$

$$\phi_m(\eta) = \phi_m^*(\eta) + C_4 \exp(\eta) + C_5 \exp(-\eta), \quad (9.40)$$

where f_m^* and ϕ_m^* are the particular solutions and after invoking Eqs. (9.35) the constants are given by

$$\begin{aligned} C_2 &= C_4 = 0, & C_3 &= \left. \frac{\partial f_m^*(\eta)}{\partial \eta} \right|_{\eta=0}, \\ C_1 &= -C_3 - f_m^*(0), & C_5 &= -\phi_m^*(0). \end{aligned} \quad (9.41)$$

By symbolic software Mathematica, the system of Eqs. (9.33) – (9.35) can be solved when $m = 1, 2, 3, \dots$

9.3 Convergence of homotopy solutions

The auxiliary parameters \hbar_f and \hbar_ϕ in the series solutions (9.31) and (9.32) play a vital role in adjusting and controlling the convergence. In order to find the admissible values of \hbar_f and \hbar_ϕ the \hbar_f and \hbar_ϕ -curves are plotted for 20th-order of approximations. Fig. 9.1 shows that the range for the admissible values of \hbar_f and \hbar_ϕ are $-1.2 \leq \hbar_f \leq -0.5$ and $-1.5 \leq \hbar_\phi \leq -0.8$. Our computations also indicates that the series given by (9.31) and (9.32) converge in the whole region of η when $\hbar_f = -0.5$ and $\hbar_\phi = -1$. Table 9.1 shows the convergence of the homotopy

solutions for different order of approximations for $\lambda_1 = 0.2$, $\beta = 0.3$, $a/c = 0.1$, $Sc = 0.5 = \gamma$.

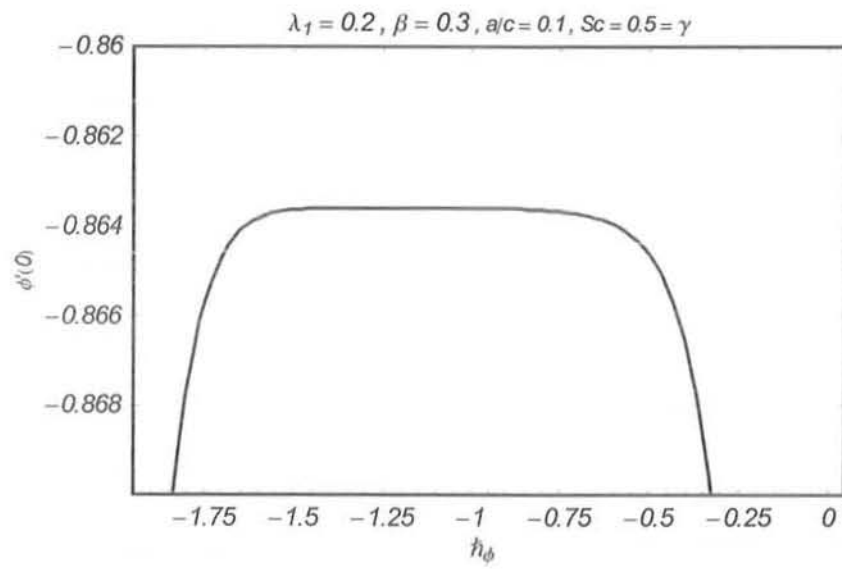
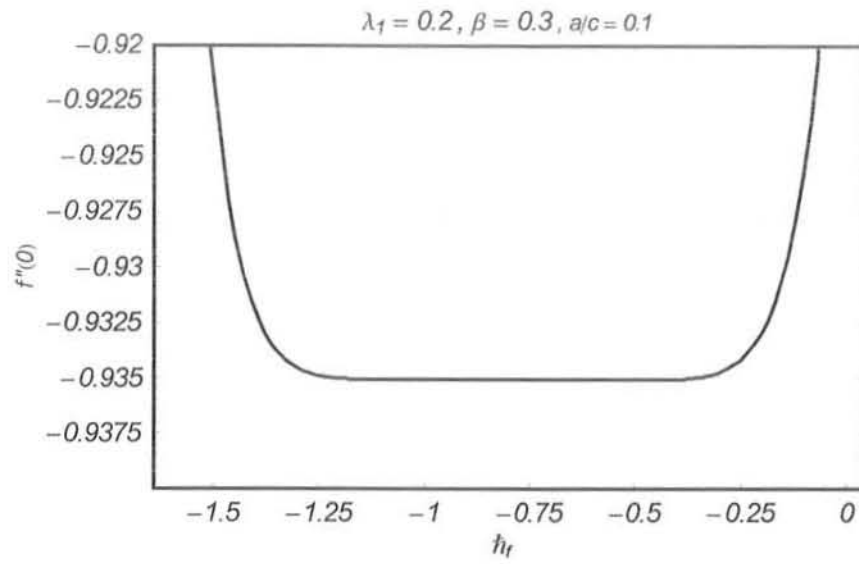


Fig. 9.1. The h -curves $f''(0)$ and $\phi'(0)$ at 20th-order of approximations.

Order of approximation	$-f''(0)$	$-\phi'(0)$
1	0.921376	0.887509
5	0.934758	0.864394
10	0.935072	0.863623
15	0.935068	0.863615
20	0.935068	0.863615
25	0.935068	0.863615
30	0.935068	0.863615

Table 9.1: Convergence of the HAM solutions for different order of approximation when

$$\lambda_1 = 0.2, \beta = 0.3, a/c = 0.1, Sc = 0.5 = \gamma,$$

9.4 Results and discussion

In this section, the influence of emerging parameters on the velocity and concentration fields is studied. Figs. 9.2 and 9.3 are plotted to show the comparison between exact and the homotopy solution for the velocity $f(\eta)$ and the concentration field $\phi(\eta)$ in the case of $\beta = \lambda_1 = a/c = 0$. It is noted from these Figs. that the exact solution has an excellent agreement with HAM solution at 15th-order of approximations. Figs. 9.4 – 9.12. represent the variations of β , λ_1 , a/c , Sc and γ . Figs. 9.4 – 9.6. describe the effects of β , λ_1 and a/c on the velocity profile f' . From Fig. 9.4 it can be seen that the velocity field and boundary layer thickness are increasing functions of β . It is observed from Fig. 9.5 that the effect of λ_1 is opposite to the effect of the Deborah number β . Fig. 9.6. elucidates that f' is increasing function a/c .

The effects of β , λ_1 , a/c , Sc and γ on the concentration profile $\phi(\eta)$ are examined in the

Figs. 9.7 – 9.12. Fig 9.7. gives the variation of β on ϕ for the destructive ($\gamma > 0$) chemical reaction. Increasing the value of β decreases ϕ . The variation of λ_1 on ϕ is given in Fig. 9.8. As λ_1 increases, the concentration field increases. The effects of a/c is opposite to of λ_1 on ϕ (Fig. 9.9). The variation of Schmidt number Sc on ϕ is shown in Fig. 9.10. The concentration field ϕ decreases when Sc increases. As expected the fluid concentration increases with an increase in generative chemical reaction parameter ($\gamma < 0$) (Fig. 9.11.) . The fluid concentration ϕ has the opposite behavior for destructive chemical reaction parameter ($\gamma > 0$) in comparison to the case of generative chemical reaction (Fig. 9.12).

The values of the surface mass transfer $-\phi'(0)$ and the gradient of mass transfer $-\phi'(\eta)$ are presented in the Tables 9.2 and 9.3. Table 9.2 depicts that the surface mass transfer $-\phi'(0)$ increases by increasing β and a/c while decreases for large values of λ_1 . Table 9.3 shows that the surface mass transfer $-\phi'(0)$ increases by increasing both Sc and γ . The gradient of mass transfer $-\phi'(\eta)$ increases as both Sc and γ are increased when $\eta = 0.2$ and $\eta = 0.5$. The magnitude of $-\phi'(\eta)$ is larger for $\eta = 0.2$.

9.5 Closing remarks

The present study describes the stagnation point flow of a Jeffrey fluid with mass transfer effect. Analytical solution to the governing nonlinear problem is derived. Analysis of Table 9.1 shows that solution upto 15th order of approximations is enough. It is also observed by fixing Sc and γ that the influence of increasing β on the surface mass transfer is larger than λ_1 . The surface mass transfer is larger for increasing values of γ when compared with Sc .

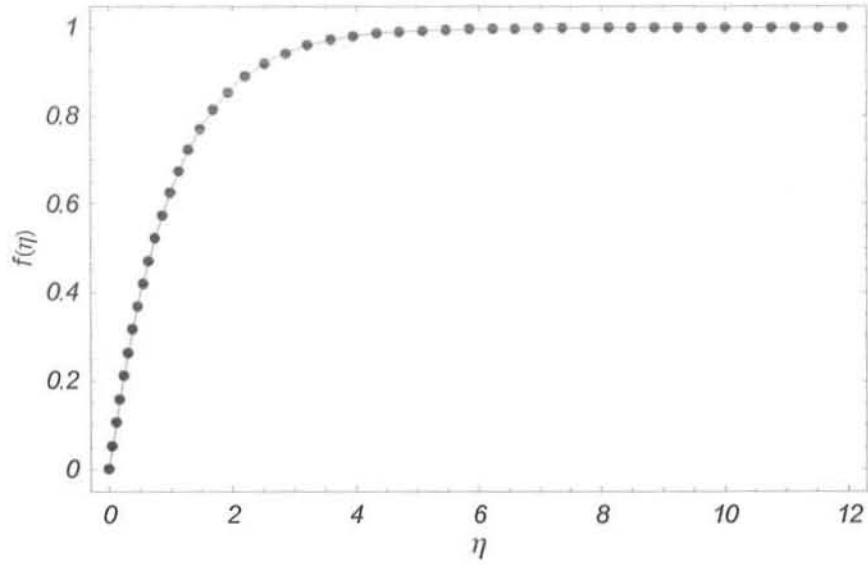


Fig. 9.2. The comparison of $f(\eta)$ for the analytical approximation with an exact solution when $\lambda_1 = \beta = a/c = 0$. Filled circle: exact solution; Solid line: 15th-order HAM solution.

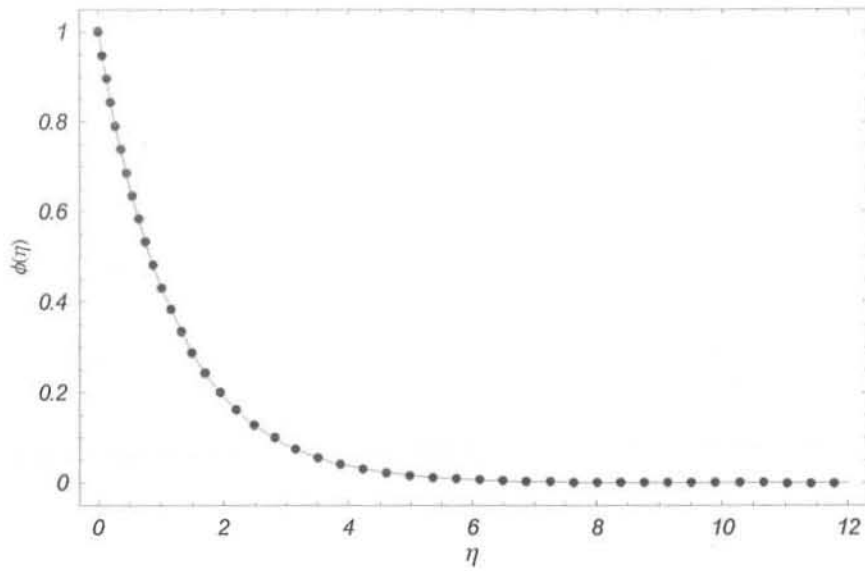


Fig. 10.3. The comparison of $\phi(\eta)$ for the analytical approximation with the numerical solutions when $\lambda_1 = \beta = a/c = 0$. Filled circle: numerical solution; Solid line: 15th-order HAM solution.

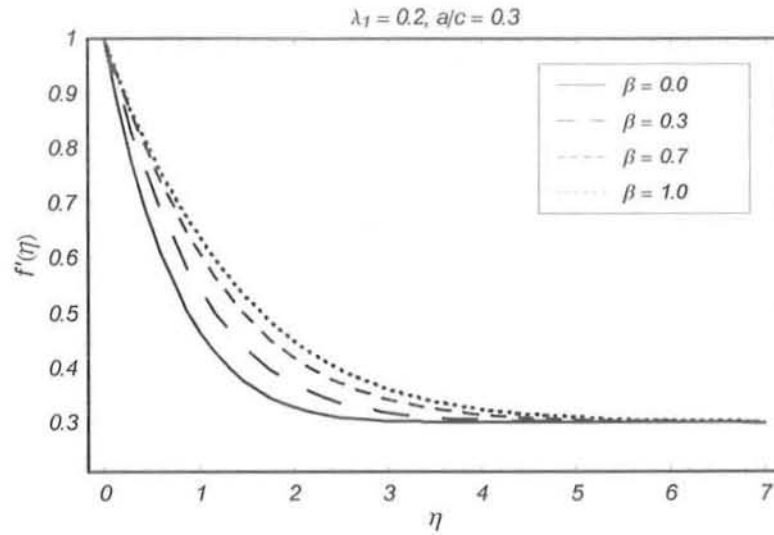


Fig. 9.4. Influence of β on f' .

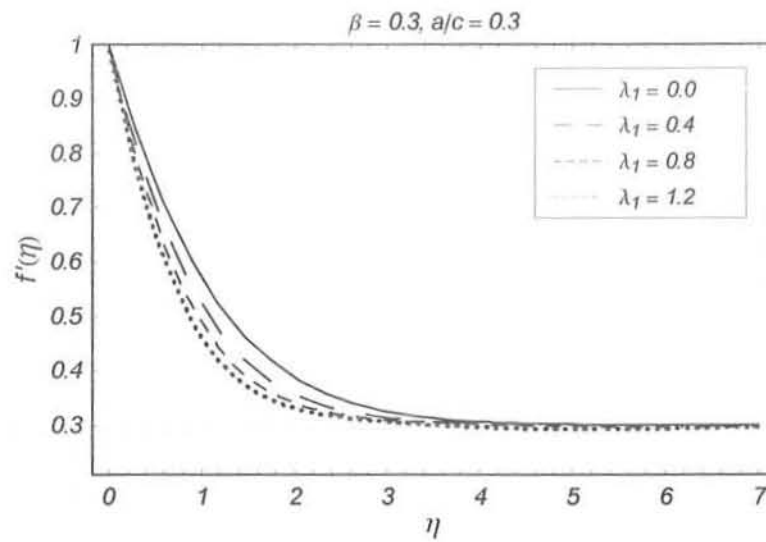


Fig. 9.5. Influence of λ_1 on f' .

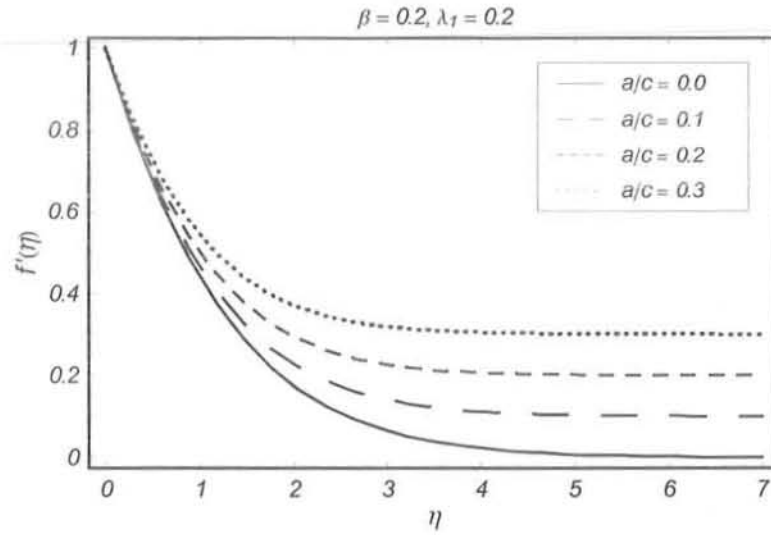


Fig. 9.6. Influence of a/c on the velocity f' .

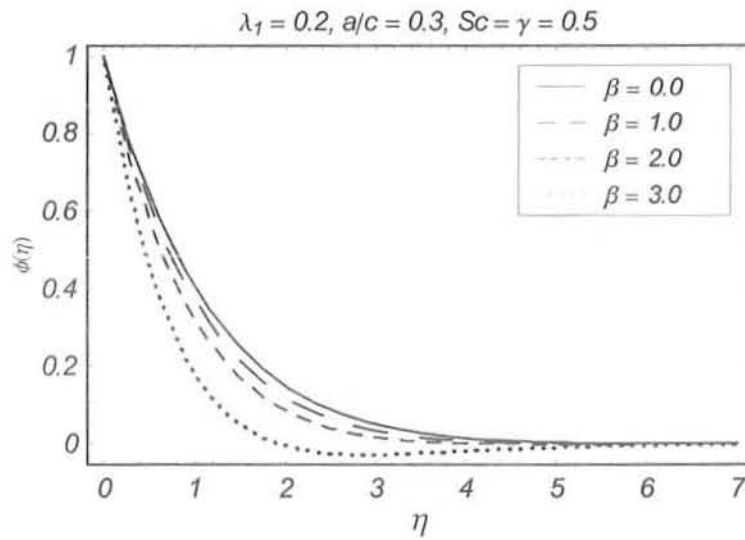


Fig. 9.7. Influence of β on ϕ .

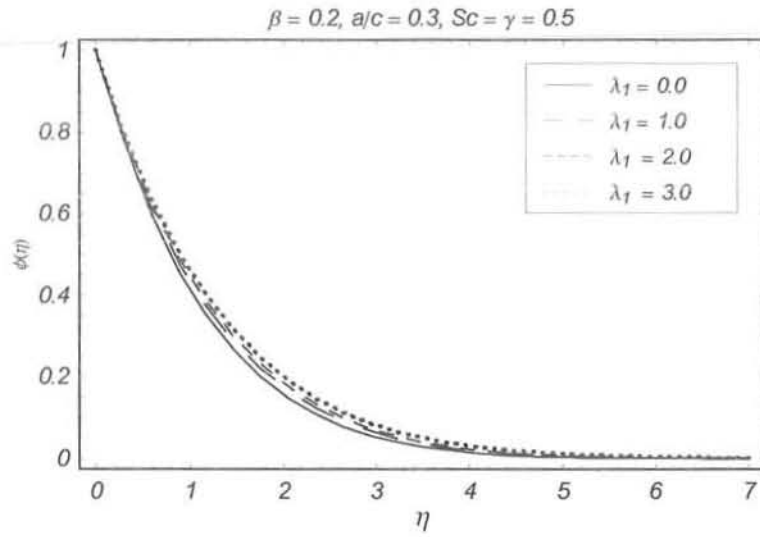


Fig. 9.8. Influence of λ_1 on ϕ .

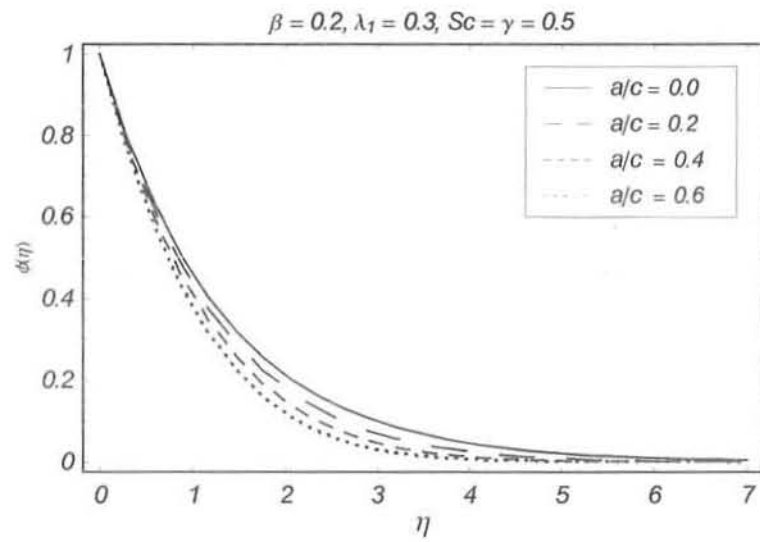


Fig. 9.9. Influence of a/c on ϕ .

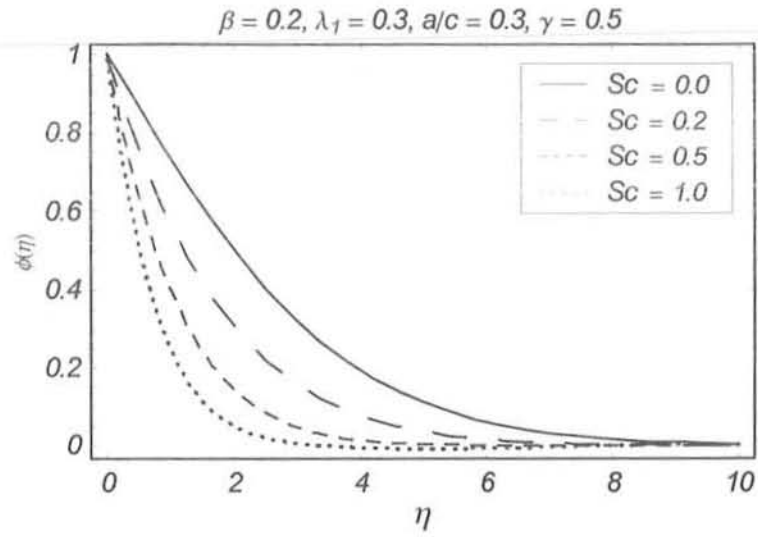


Fig. 9.10. Influence of Sc on ϕ .

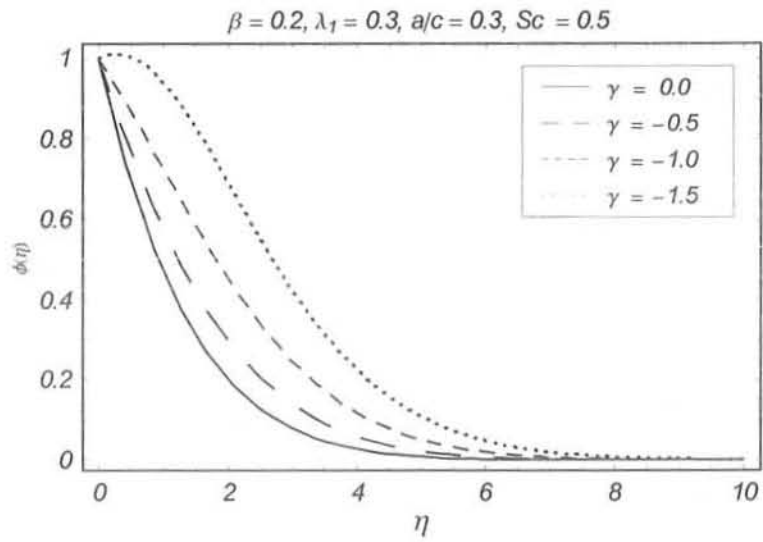


Fig. 9.11. Influence of $\gamma(< 0)$ on ϕ .

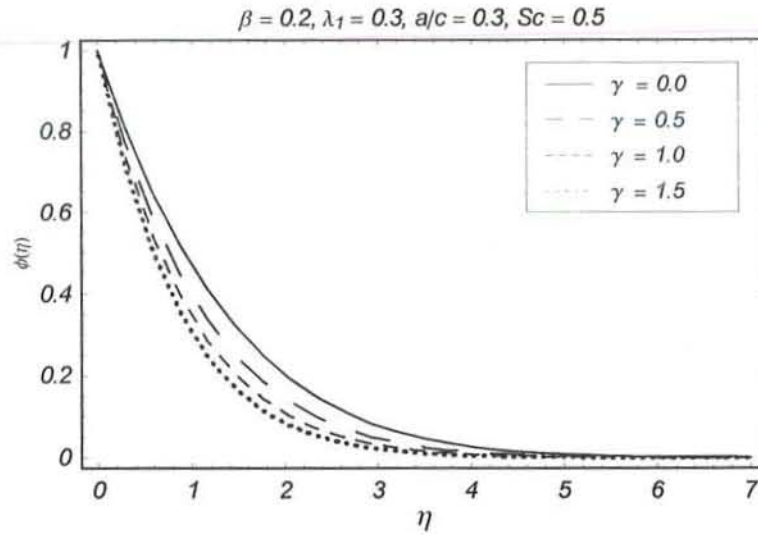


Fig. 12. Influence of $\gamma(> 0)$ on ϕ .

a/c	β	λ_1	$-\phi'(0)$
0	0.2	0.2	0.86269
0.05			0.86748
0.12			0.87561
0.2			0.88621
0.35			0.90833
0.1	0		0.84477
	0.2		0.87316
	0.6		0.90221
	0.8		0.91159
0.1	0.2	0	0.88354
		0.2	0.87315
		0.4	0.86403
		0.8	0.84858
		1.0	0.84193

Table 9.2: Values of the surface mass transfer $-\phi'(0)$ when $Sc = \gamma = 0.5$.

γ	Sc	$-\phi'(0)$	η	γ	Sc	$-\phi'(\eta)$
0	1.0	1.04752	0.2	0	1.0	0.86319
0.2		1.15128		0.6		1.03916
0.5		1.28689		1.5		1.10435
0.8		1.40642	0.5	0	1.0	0.64004
1.5		1.64828		0.6		0.70779
1.8		1.74036		1.5		0.74569
1.0	0.2	0.61615	0.2	1.0	0.4	0.75509
	0.4	0.90205			0.8	1.02579
	0.8	1.31358			1.0	1.12394
	1.0	1.48045	0.5	1.0	0.4	0.57759
	1.2	1.63168			0.8	0.69941
					1.0	0.73015

Table 9.3: Values of the surface mass transfer $-\phi'(0)$ and the gradient of mass transfer when $\beta = 0.2$, $\lambda_1 = 0.2$ and $a/c = 0.1$.

Chapter 10

Unsteady stagnation point flow of a second grade fluid with heat transfer

The stagnation-point flow of an incompressible second grade fluid over an unsteady stretching surface in the presence of variable free stream is examined. Flow analysis has been carried out when heat transfer is present. The resulting partial differential equations have been reduced into the ordinary differential equations by the suitable transformations. Computations of dimensionless velocity and temperature fields have been performed by using homotopy analysis method (HAM). Graphical plots are prepared in order to illustrate the details of flow and heat transfer characteristics and their dependence upon the embedded parameters. Numerical values of skin-friction coefficient and Nusselt number are given and examined very carefully.

10.1 Definition of the problem

Consider the unsteady stagnation point flow of an incompressible second grade fluid over a porous stretching surface with variable free stream. We select x -axis along the surface and y -axis normal to it. In addition, the heat transfer is considered. The boundary layer equations which can govern the present flow are

$$\frac{\partial u}{\partial x} + \frac{\partial v}{\partial y} = 0, \quad (10.1)$$

$$\frac{\partial u}{\partial t} + u \frac{\partial u}{\partial x} + v \frac{\partial u}{\partial y} = \frac{\partial U}{\partial t} + U \frac{\partial U}{\partial x} + \nu \frac{\partial^2 u}{\partial y^2} + \frac{\alpha_1}{\rho} \left[\frac{\partial^3 u}{\partial t \partial y^2} + u \frac{\partial^3 u}{\partial x \partial y^2} + \frac{\partial u}{\partial x} \frac{\partial^2 u}{\partial y^2} + \frac{\partial u}{\partial y} \frac{\partial^2 v}{\partial y^2} + v \frac{\partial^3 u}{\partial y^3} \right] \quad (10.2)$$

$$\rho c_p \left[\frac{\partial T}{\partial t} + u \frac{\partial T}{\partial x} + v \frac{\partial T}{\partial y} \right] = k \frac{\partial^2 T}{\partial y^2}, \quad (10.3)$$

where u, v being the velocity components along the x - and y -axes, ρ the fluid density, ν the kinematic viscosity, T the fluid temperature, ρ the fluid density and c_p the specific heat.

The associated boundary conditions of the problem are

$$\begin{aligned} u &= U_w(x, t), \quad v = V_w(x, t), \quad T = T_w(x, t) \quad \text{at } y = 0, \\ u &\rightarrow U(x, t), \quad T \rightarrow T_\infty \quad \text{as } y \rightarrow \infty. \end{aligned} \quad (10.4)$$

with V_w defined by

$$V_w = -\frac{v_0}{(1 - \varepsilon t)^{1/2}} \quad (10.5)$$

represents the mass transfer at surface with $V_w > 0$ for injection and $V_w < 0$ for suction. Further the stretching velocity $U_w(x, t)$ and surface temperature $T_w(x, t)$ are taken of the forms

$$U_w(x, t) = \frac{cx}{1 - \varepsilon t}, \quad T_w(x, t) = T_\infty + \frac{bx}{1 - \varepsilon t}, \quad U(x, t) = \frac{ax}{1 - \varepsilon t} \quad (10.6)$$

in which a, c and ε are the constants with $a > 0$ and $\varepsilon \geq 0$ (with $\varepsilon t < 1$), and both a and ε have dimension time^{-1} .

We introduce the following transformations

$$\eta = \sqrt{\frac{U_w}{\nu x}} y, \quad \psi = \sqrt{\nu x U_w} f(\eta), \quad \theta(\eta) = \frac{T - T_\infty}{T_w - T_\infty}, \quad (10.7)$$

and the velocity components

$$u = \frac{\partial \psi}{\partial y} \quad v = -\frac{\partial \psi}{\partial x}, \quad (10.8)$$

where ψ is a stream function, the continuity equation is identically satisfied and the resulting problems for f and θ become

$$f''' - f'^2 + ff'' - A \left(f' + \frac{1}{2}\eta f'' \right) + \alpha \left[2f' f''' - f''^2 - ff'''' + A \left(2f''' + \frac{1}{2}\eta f'''' \right) \right] + \frac{a^2}{c^2} + A \frac{a}{c} = 0, \quad (10.9)$$

$$\theta'' + \text{Pr} (f\theta' - f'\theta) - \text{Pr} A \left(\theta + \frac{1}{2}\eta\theta' \right), \quad (10.10)$$

$$f(0) = S, \quad f'(0) = 1, \quad f'(\infty) \rightarrow a/c, \quad \theta(0) = 1, \quad \theta(\infty) \rightarrow 0. \quad (10.11)$$

Here $A = \varepsilon/c$ is the unsteadiness parameter, $\alpha = c\alpha_1/\mu(1 - \varepsilon t)$ the dimensionless second grade parameter, $\text{Pr} = \frac{\mu c_p}{k}$ the Prandtl number and primes indicate the differentiation with respect to η .

The skin friction coefficient C_f and local Nusselt number Nu_x are

$$C_f = \frac{\tau_w}{\rho u_w^2}, \quad (10.12)$$

$$Nu = \frac{xq_w}{k(T_w - T_\infty)} \quad (10.13)$$

where the skin-friction τ_w and wall heat flux q_w are defined as

$$\tau_w = \left[\mu \frac{\partial u}{\partial y} + \alpha_1 \left(\frac{\partial^2 u}{\partial y \partial t} + 2 \frac{\partial u}{\partial x} \frac{\partial u}{\partial y} + u \frac{\partial^2 u}{\partial x \partial y} + v \frac{\partial^2 u}{\partial y^2} \right) \right]_{y=0}, \quad (10.14)$$

$$q_w = -k \left(\frac{\partial T}{\partial y} \right)_{y=0}. \quad (10.15)$$

Due to Eqs. (10.7) we obtain

$$R_{e_x}^{1/2} C_f = \left[f''(\eta) + \alpha \left(3f'(\eta)f''(\eta) - f(\eta)f'''(\eta) + \frac{A}{2} (3f''(\eta) + \eta f'''(\eta)) \right) \right]_{\eta=0}, \quad (10.16)$$

$$R_{e_x}^{-1/2} Nu_x = -\theta'(0). \quad (10.17)$$

10.2 Solution expressions

For the HAM solutions we consider $f(\eta)$ and $\theta(\eta)$ in the set of base functions

$$\left\{ \eta^k \exp(-n\eta) \mid k \geq 0, n \geq 0 \right\}$$

and write

$$f(\eta) = a_{0,0}^0 + \sum_{n=0}^{\infty} \sum_{k=0}^{\infty} a_{m,n}^k \eta^k \exp(-n\eta), \quad (10.18)$$

$$\theta(\eta) = \sum_{n=0}^{\infty} \sum_{k=0}^{\infty} b_{m,n}^k \eta^k \exp(-n\eta), \quad (10.19)$$

in which $a_{m,n}$ and $b_{m,n}$ are the coefficients. The initial guesses f_0 and θ_0 are taken in the following expressions

$$f_0(\eta) = \frac{a}{c}\eta + \left(1 - \frac{a}{c}\right) [1 - \exp(-\eta)], \quad (10.20)$$

$$\theta_0(\eta) = \exp(-\eta). \quad (10.21)$$

and the operators

$$\mathcal{L}_f = \frac{d^3 f}{d\eta^3} - \frac{df}{d\eta}, \quad (10.22)$$

$$\mathcal{L}_\theta = \frac{d^2 \theta}{d\eta^2} - \theta. \quad (10.23)$$

with the following properties

$$\mathcal{L}_f [C_1 + C_2 \exp(\eta) + C_3 \exp(-\eta)] = 0, \quad (10.24)$$

$$\mathcal{L}_\theta [C_4 \exp(\eta) + C_5 \exp(-\eta)] = 0, \quad (10.25)$$

in which C_i ($i = 1 - 5$) are the arbitrary constants.

If $p \in [0, 1]$ is an embedding parameter, \hbar_f and \hbar_θ the non-zero auxiliary parameters then the zeroth-order deformation problems can be written as

$$(1 - p)\mathcal{L}_f[\hat{f}(\eta, p) - f_0(\eta)] = p\hbar_f \mathcal{N}_f [\hat{f}(\eta, p), \hat{\theta}(\eta, p)], \quad (10.26)$$

$$(1 - p)\mathcal{L}_\theta[\hat{\theta}(\eta, p) - \theta_0(\eta)] = p\hbar_\theta \mathcal{N}_\theta [\hat{f}(\eta, p), \hat{\theta}(\eta, p)], \quad (10.27)$$

$$\hat{f}(\eta; p)\Big|_{\eta=0} = S, \quad \frac{\partial \hat{f}(\eta; p)}{\partial \eta}\Big|_{\eta=0} = 1, \quad \frac{\partial \hat{f}(\eta; p)}{\partial \eta}\Big|_{\eta=\infty} = a/c, \quad (10.28)$$

$$\hat{\theta}(\eta; p)\Big|_{\eta=0} = 1, \quad \hat{\theta}(\eta; p)\Big|_{\eta=\infty} = 0, \quad (10.29)$$

$$\begin{aligned} \mathcal{N}_f [\hat{f}(\eta; p)] &= \frac{\partial^3 \hat{f}(\eta; p)}{\partial \eta^3} - \left(\frac{\partial \hat{f}(\eta; p)}{\partial \eta}\right)^2 + \hat{f}(\eta; p) \frac{\partial^2 \hat{f}(\eta; p)}{\partial \eta^2} - A \left(\frac{\eta}{2} \frac{\partial^2 \hat{f}(\eta; p)}{\partial \eta^2} + \frac{\partial \hat{f}(\eta; p)}{\partial \eta}\right) + \frac{a^2}{c^2} + A \frac{a}{c} \\ &+ \alpha \left[- \left(\frac{\partial^2 \hat{f}(\eta; p)}{\partial \eta^2}\right)^2 - A \left(2 \frac{\partial^3 \hat{f}(\eta; p)}{\partial \eta^3} + \frac{1}{2} \eta \frac{\partial^4 \hat{f}(\eta; p)}{\partial \eta^4}\right) + 2 \frac{\partial \hat{f}(\eta; p)}{\partial \eta} \frac{\partial^3 \hat{f}(\eta; p)}{\partial \eta^3} - \frac{\partial \hat{f}(\eta; p)}{\partial \eta} \frac{\partial^4 \hat{f}(\eta; p)}{\partial \eta^4} \right] \end{aligned} \quad (10.30)$$

$$\begin{aligned} \mathcal{N}_\theta [\hat{f}(\eta; p), \hat{\theta}(\eta; p)] &= \frac{\partial^2 \hat{\theta}(\eta; p)}{\partial \eta^2} + \text{Pr} \left(\hat{f}(\eta; p) \frac{\partial \hat{\theta}(\eta; p)}{\partial \eta} - \hat{\theta}(\eta; p) \frac{\partial \hat{f}(\eta; p)}{\partial \eta} \right) \\ &- \text{Pr} A \left(\hat{\theta}(\eta; p) + \frac{1}{2} \eta \frac{\partial \hat{\theta}(\eta; p)}{\partial \eta} \right). \end{aligned} \quad (10.31)$$

For $p = 0$ and $p = 1$, we have

$$\widehat{f}(\eta; 0) = f_0(\eta), \quad \widehat{f}(\eta; 1) = f(\eta), \quad (10.32)$$

$$\widehat{\theta}(\eta; 0) = \theta_0(\eta), \quad \widehat{\theta}(\eta; 1) = \theta(\eta) \quad (10.33)$$

and when p increases from 0 to 1, $\widehat{f}(\eta; p)$ and $\widehat{\theta}(\eta; p)$ deforms from $f_0(\eta)$ and $\theta_0(\eta)$ to $f(\eta)$ and $\theta(\eta)$ respectively. Expanding $\widehat{f}(\eta; p)$ and $\widehat{\theta}(\eta; p)$ one can write

$$\widehat{f}(\eta; p) = f_0(\eta) + \sum_{m=1}^{\infty} f_m(\eta) p^m, \quad (10.34)$$

$$\widehat{\theta}(\eta; p) = \theta_0(\eta) + \sum_{m=1}^{\infty} \theta_m(\eta) p^m, \quad (10.35)$$

$$f_m(\eta) = \left. \frac{1}{m!} \frac{\partial^m \widehat{f}(\eta; p)}{\partial p^m} \right|_{p=0}, \quad \theta_m(\eta) = \left. \frac{1}{m!} \frac{\partial^m \widehat{\theta}(\eta; p)}{\partial p^m} \right|_{p=0} \quad (10.36)$$

and the auxiliary parameters \hbar_f and \hbar_θ have been chosen in such a way that the series (10.39) and (10.40) converge at $p = 1$. Hence

$$f(\eta) = f_0(\eta) + \sum_{m=1}^{\infty} f_m(\eta), \quad (10.37)$$

$$\theta(\eta) = \theta_0(\eta) + \sum_{m=1}^{\infty} \theta_m(\eta). \quad (10.38)$$

The problems corresponding to the m th order deformation are

$$\mathcal{L}_f [f_m(\eta) - \chi_m f_{m-1}(\eta)] = \hbar_f \mathcal{R}_m^f(\eta), \quad (10.39)$$

$$\mathcal{L}_\theta [\theta_m(\eta) - \chi_m \theta_{m-1}(\eta)] = \hbar_\theta \mathcal{R}_m^\theta(\eta), \quad (10.40)$$

$$f_m(0) = 0, f'_m(0) = 0, f''_m(\infty) = 0, \quad \theta_m(0) = 0, \theta_m(\infty) = 0,$$

$$\phi_m(0) = 0, \phi_m(\infty) = 0, \quad (10.41)$$

$$\begin{aligned} \mathcal{R}_m^f(\eta) = & f'''_{m-1} - A \left(f'_{m-1} + \frac{1}{2}\eta f''_{m-1} \right) + \alpha A \left(2f'''_{m-1} + \frac{1}{2}\eta f''''_{m-1} \right) \\ & \left(\frac{a^2}{c^2} + A \frac{a}{c} \right) (1 - \chi_m) + \sum_{k=0}^{m-1} \left[\begin{array}{l} f_{m-1-k} f''_k - f'_{m-1-k} f'_k \\ + \alpha (2f'_{m-1-k} f'''_k - f''_{m-1-k} f''_k - f_{m-1-k} f''''_k) \end{array} \right] \end{aligned} \quad (10.42)$$

$$\mathcal{R}_m^\theta(\eta) = \theta''_{m-1} - A \text{Pr} \left[\theta_{m-1} + \frac{1}{2}\eta \theta'_{m-1} \right] + \text{Pr} \sum_{k=0}^{m-1} (f_{m-1-k} \theta'_k - f'_{m-1-k} \theta_k) \quad (10.43)$$

$$\chi_m = \begin{cases} 0, & m \leq 1 \\ 1, & m > 1 \end{cases}. \quad (10.44)$$

The general solutions of Eqs. (10.39) – (10.41) are

$$f_m(\eta) = f_m^*(\eta) + C_1 + C_2 \exp(\eta) + C_3 \exp(-\eta), \quad (10.45)$$

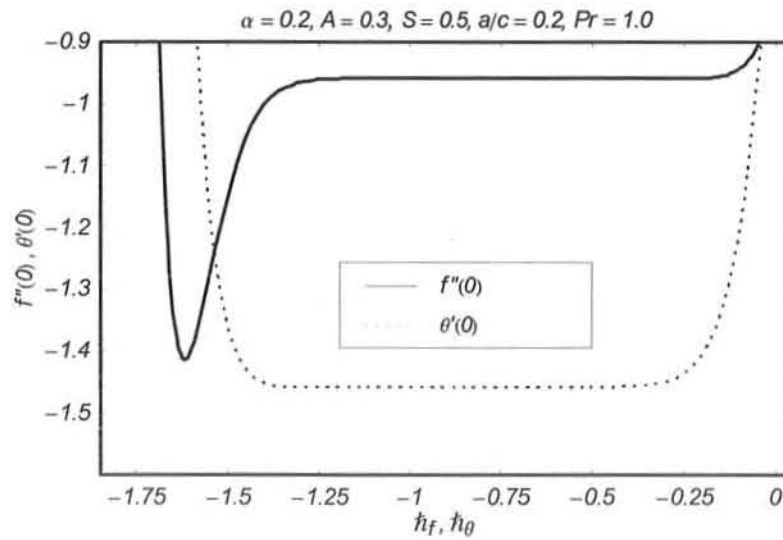
$$\theta_m(\eta) = \theta_m^*(\eta) + C_4 \exp(\eta) + C_5 \exp(-\eta), \quad (10.46)$$

in which $f_m^*(\eta)$ and $\theta_m^*(\eta)$ are the special solutions and

$$\begin{aligned} C_2 &= C_4 = 0, \\ C_1 &= -C_3 - f_m^*(0), \quad C_3 = \left. \frac{\partial f_m^*(\eta)}{\partial \eta} \right|_{\eta=0}, \\ C_5 &= -\theta_m^*(0). \end{aligned} \quad (10.47)$$

10.3 Convergence of the derived solution expressions

It can be clearly seen that the series solutions (10.37) and (10.38) contain the non-zero auxiliary parameters \hbar_f and \hbar_θ . These parameters are useful in adjusting and controlling the convergence. For the appropriate values of \hbar_f and \hbar_θ of the functions $f''(0)$ and $\theta'(0)$ the \hbar_f and \hbar_θ -curves are plotted for 20th-order of approximations. Fig. 10.1 clearly indicates that the range for the admissible values of \hbar_f and \hbar_θ are $-1. \leq \hbar_f, \hbar_\theta \leq -0.3$. The series given by (10.37) and (10.38) converge in the whole region of η when $\hbar_f = \hbar_\theta = -0.7$.



Figs. 10.1: The \hbar -curves of the functions $f''(0)$ and $\theta'(0)$ at 15th order of approximation.

Order of convergence	$-f''(0)$	$-\theta'(0)$
1	0.979200	1.156667
5	0.959231	1.459734
10	0.959203	1.458497
15	0.959204	1.458505
20	0.959204	1.458503
25	0.959204	1.458503
30	0.959204	1.458503

Table 10.1: Convergence of HAM solutions for different order of approximations when $\alpha = 0.2$, $A = 0.3$, $S = 0.5$, $Pr = 1.0$ and $a/c = 0.2$.

10.4 Results and discussion

In this section, our main interest is to discuss the variation of the emerging parameters such as a/c , α , A , S and Pr on the velocity components, temperature fields, skin friction coefficient and Nusselt number. The analysis of such variation is made by Figs. 10.2 – 10.13. Fig. 10.2 shows the effects of a/c on the velocity component f' . When $a/c = 0$ then there is no stagnation point flow. Velocity f' increases when the parameter a/c increases. It is noticed that flow has a boundary layer structure for values of $a/c > 1$ and thickness of boundary layer decreases with an increase in a/c . Further Fig. 10.2 clearly depicts that when the stretching velocity of the surface is greater than the stagnation velocity of the external stream (i.e. $a/c < 1$) the flow has inverted boundary layer structure. Fig. 10.3. is drawn for the several values α and a/c when $S = 1.0$ and $A = 0.3$. It is seen that velocity f' is greater for second grade fluid when compared to a Newtonian fluid. Figs. 10.4 and 10.5 depict the effects of α on f' in suction and injection respectively. In both cases, α increases the velocity profile. The boundary layer thickness also increases. However, in injection case such increase is larger than suction case.

The behaviors of A and S on velocity profile are seen in the Figs. 10.6 and 10.7. Both A and S decrease the velocity profile. Sucking fluid particles through porous wall reduce the growth of the fluid boundary layer. This is in accordance with the fact that suction causes reduction in the boundary layer thickness. Fig. 10.8 is plotted for the variation of vertical component of velocity f . We see that f increases by increasing a/c . Fig. 10.9. presents the effect of S on f . It is also found that f increases when S increases. The qualitative effects of a/c and S on the temperature are similar (Figs. 10.10. and 10.11). The variation of Pr on temperature field is sketched in the Figs. 10.12 and 10.13 for suction and injection respectively. As expected θ is decreasing when Pr increases. However such decrease is larger for suction when compared with injection case (Figs. 10.13). From Table 10.2 it is noticed that the magnitude of skin friction coefficient increases for large values of α , A , a/c and S . The skin friction coefficient parameter increases by increasing A . We found that for a fixed values of other parameters, the local Nusselt number increases when there is an increase in α .

10.5 Concluding remarks

We studied the stagnation point flow of a second fluid with heat transfer effect in the presence of variable free stream. The governing nonlinear problem has been computed and the main points can be summarized as follows:

- Velocity component f' is a decreasing function of $a/c < 1$.
- The effects of A and S on the velocity profile f' are similar in a qualitative sense.
- The velocity f' increases when α increases.
- The influence of A is to increase the boundary layer thickness.
- Both f' and θ are decreasing functions of S .

- The temperature θ yields a decrease when Pr increases.
- Local Nusselt number is an increasing function of α , S and a/c .

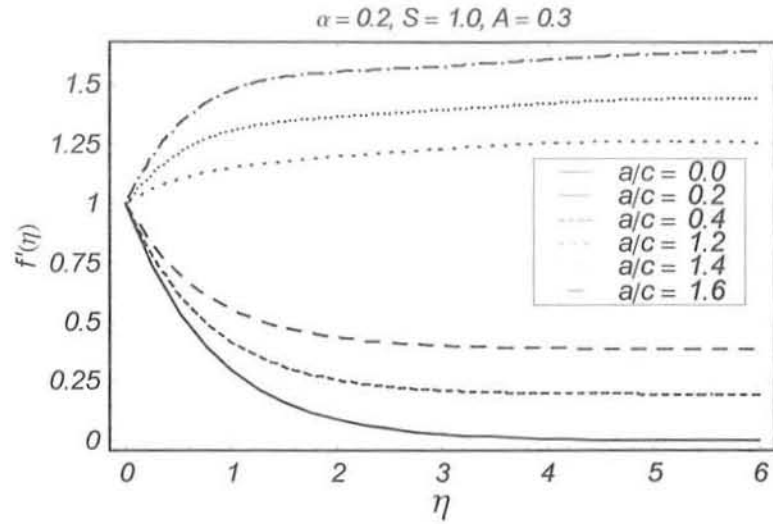


Fig. 10.2. Influence of a/c on f' .

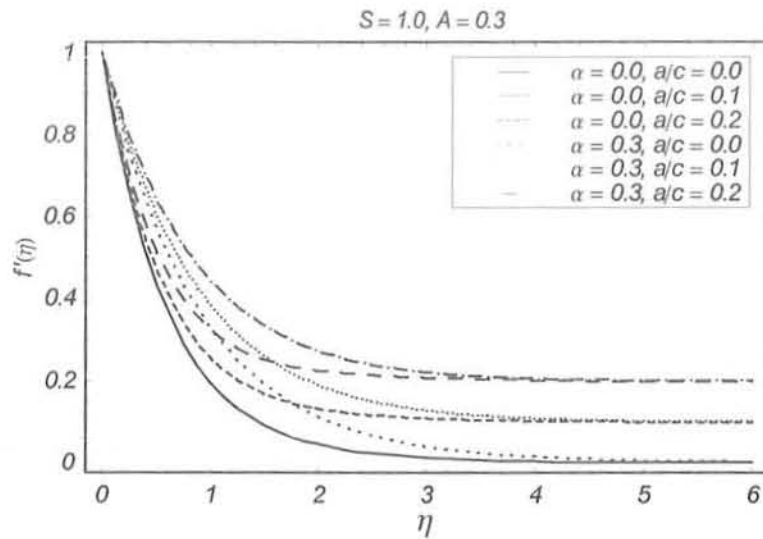


Fig. 10.3. Influence of α and a/c on f' .

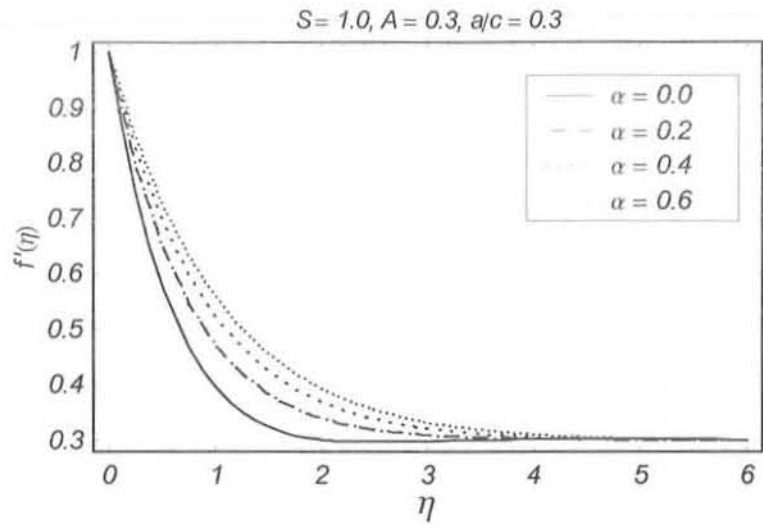


Fig. 10.4. Influence of α on f' for suction.

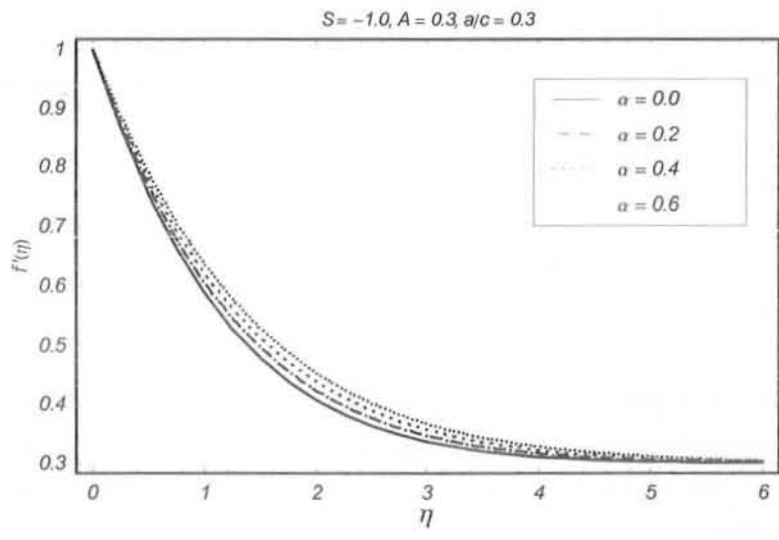


Fig. 10.5. Influence of α on f' for injection.

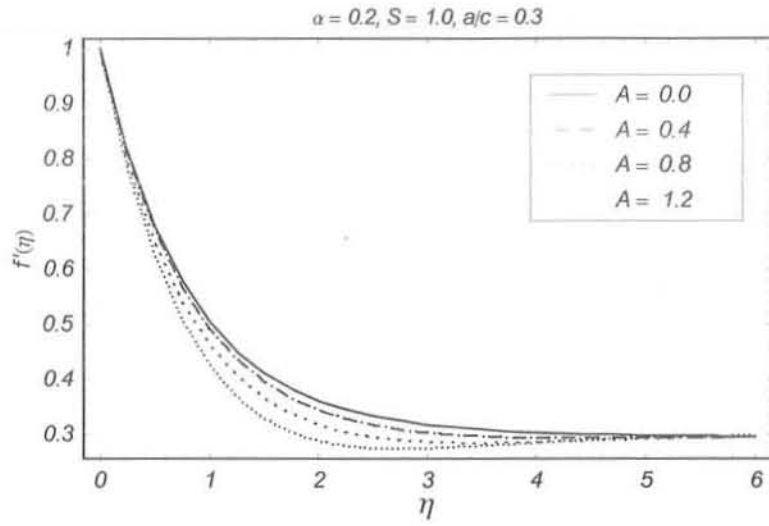


Fig. 10.6. Influence of A on f' .

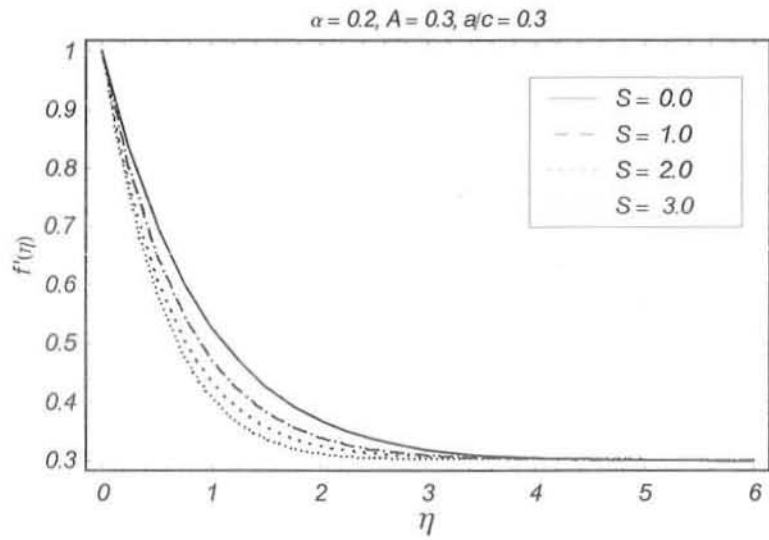


Fig. 10.7. Influence of S on f' .

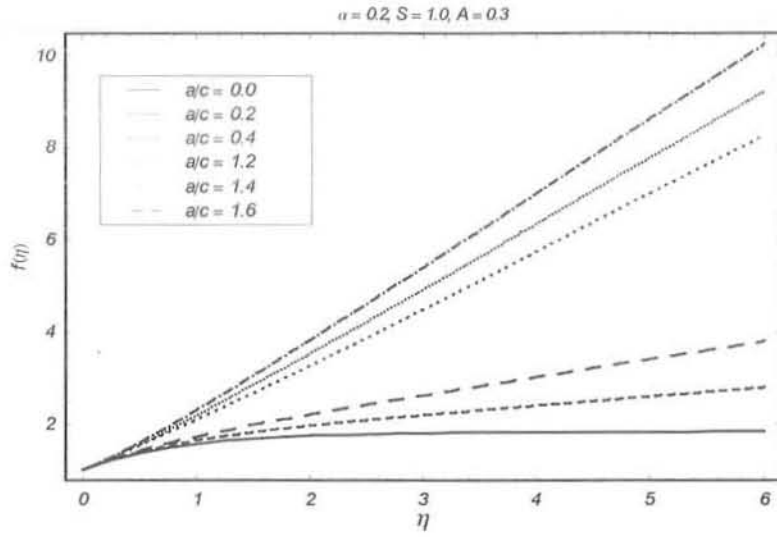


Fig. 10.8. Influence of a/c on f .

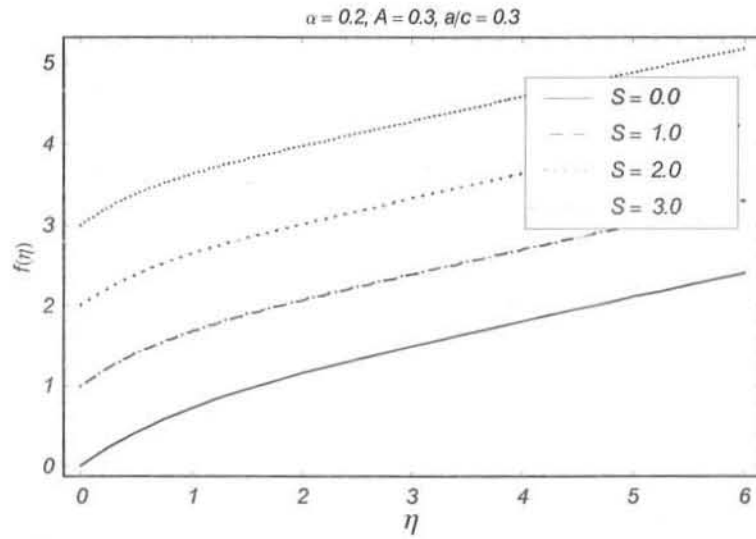


Fig. 10.9. Influence of S on f .

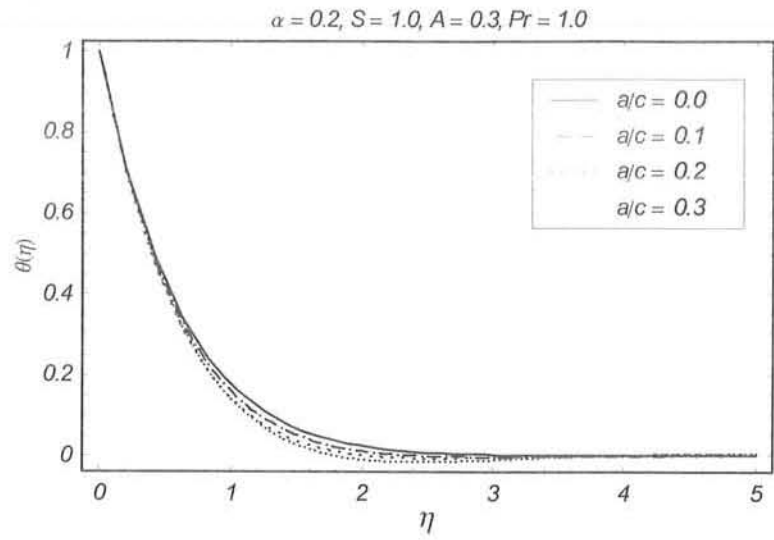


Fig. 10.10. Influence of a/c on θ .

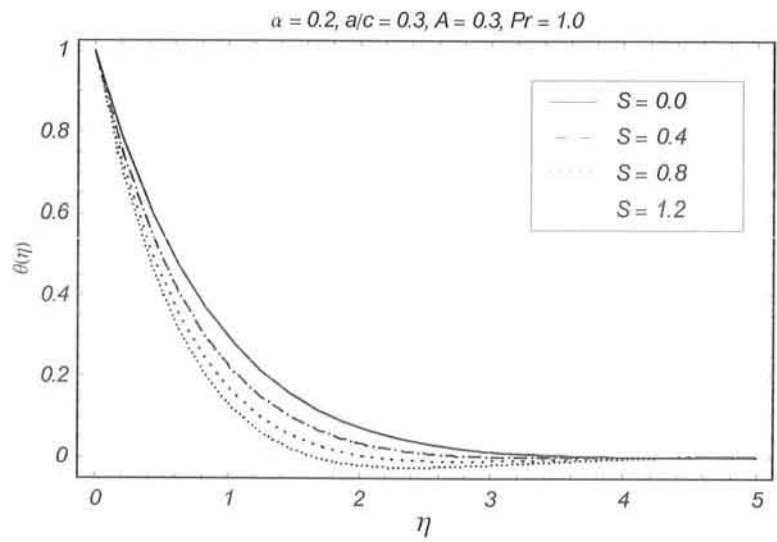


Fig. 10.11. Influence of S on θ .

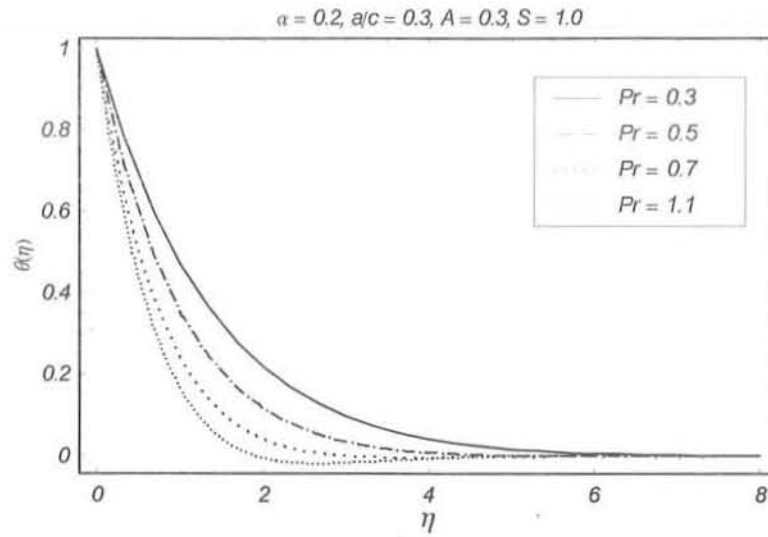


Fig. 10.12. Influence of Pr on θ for suction.

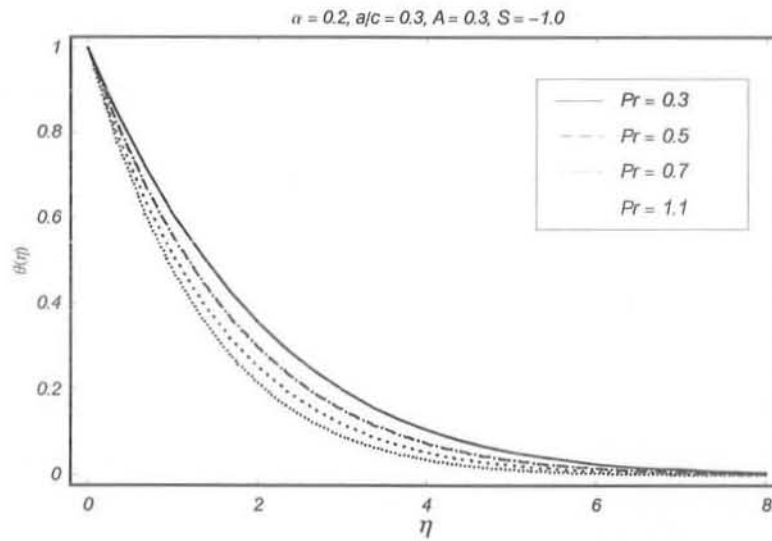


Fig. 10.13. Influence of Pr on θ for injection.

α	A	S	a/c	$-Re_x^{-1/2} C_f$	$-Re_x^{-1/2} Nu_x$
0.0	0.3	1.0	0.2	1.469456	1.753764
0.1				1.627582	1.782792
0.2				1.792047	1.801183
0.1	0.2	1.0	0.2	1.602816	1.757819
	0.4			1.652567	1.807621
	0.7			1.728709	1.881074
	1.0			1.806307	1.952925
0.1	0.5	0.0	0.3	1.172283	1.237817
		0.5		1.341659	1.522888
		1.0		1.506370	1.855564
0.1	0.5	1.0	0.0	1.968956	1.785723
			0.1	1.833141	1.808871
			0.2	1.677760	1.832274
			0.3	1.506372	1.855564

Table 10.2: Values of skin friction coefficient $Re_x^{-1/2} C_f$ and local Nusselt number $Re_x^{-1/2} Nu_x$ for some values of α , A , S and a/c when $Pr = 1.0$.

Chapter 11

Mixed convection stagnation point flow of a micropolar fluid towards a stretching surface with thermal radiation

This chapter describes the mixed convection stagnation point flow with heat and mass transfer in a micropolar fluid towards a stretching surface. Mathematical . The governing partial differential equations are first reduced into the ordinary differential equations and then solved by using homotopy analysis method (HAM). Numerical values of skin friction coefficients, local Nusselt number and Sherwood number are computed. The present results are also compared with the existing numerical solution in a limiting sense.

11.1 Mathematical formulation

Let us consider the steady mixed convection stagnation point flow of a micropolar fluid over a stretching surface. We consider that the surface has temperature T_w , the concentration C_w , and fluid has uniform ambient temperature T_∞ and uniform ambient concentration C_∞ (Here $T_w > T_\infty$ and $C_w > C_\infty$). The associated equations and boundary conditions are

$$\frac{\partial u}{\partial x} + \frac{\partial v}{\partial y} = 0, \quad (11.1)$$

$$u \frac{\partial u}{\partial x} + v \frac{\partial u}{\partial y} = u_e \frac{du_e}{dx} + \left(\nu + \frac{\kappa}{\rho} \right) \frac{\partial^2 u}{\partial y^2} + \frac{\kappa}{\rho} \frac{\partial N^*}{\partial y} + g\beta_T(T - T_\infty) + g\beta_C(C - C_\infty), \quad (11.2)$$

$$u \frac{\partial N^*}{\partial x} + v \frac{\partial N^*}{\partial y} = \frac{\gamma^*}{\rho j} \frac{\partial^2 N^*}{\partial y^2} - \frac{\kappa}{\rho j} \left(2N^* + \frac{\partial u}{\partial y} \right), \quad (11.3)$$

$$\rho c_p \left[u \frac{\partial T}{\partial x} + v \frac{\partial T}{\partial y} \right] = k \frac{\partial^2 T}{\partial y^2} - \frac{\partial q_r}{\partial y}, \quad (11.4)$$

$$u \frac{\partial C}{\partial x} + v \frac{\partial C}{\partial y} = D \frac{\partial^2 C}{\partial y^2} \quad (11.5)$$

$$\begin{aligned} u &= u_w(x) = cx, \quad v = 0, \quad N^* = -N_0 \frac{\partial u}{\partial y}, \quad T = T_w(x), \quad C = C_w(x) \quad \text{at } y = 0, \\ u &\rightarrow u_c(x) = ax, \quad N^* \rightarrow 0, \quad T \rightarrow 0, \quad C \rightarrow 0 \quad \text{as } y \rightarrow \infty, \end{aligned} \quad (11.6)$$

where u and v are the velocity components parallel to the x - and y -axes, respectively, ρ the fluid density, ν the kinematic viscosity, σ the electrical conductivity, N^* the microrotation or angular velocity, T the temperature, c_p the specific heat, k the thermal conductivity of the fluid, q_r the radiative heat flux, C the concentration species of the fluid, D is the diffusion coefficient of the diffusion species in the fluid, $j = (\nu/c)$ is microinertia, $\gamma^* = (\mu + \kappa/2)j$ and κ are the spin gradient viscosity and vortex viscosity, respectively. Here for $\kappa = 0$ we have the case of viscous fluid. Further the boundary parameter N_0 has range $0 \leq N_0 \leq 1$. It should be noted

that when $N_0 = 0$ (called strong concentration) then $N^* = 0$ near the wall. This represents the concentrated particle flows in which the microelements close to the wall surface are unable to rotate. The case $N_0 = 1/2$ corresponds to the vanishing of anti-symmetric part of the stress tensor and it shows weak concentration of microelements.

Rosseland approximation gives

$$q_r = -\frac{4\sigma^*}{3k^*} \frac{\partial T^4}{\partial y}, \quad (11.7)$$

where σ^* is the Stefan-Boltzmann constant and k^* the mean absorption coefficient.

Through the use of Taylor's series

$$T^4 \cong 4T_\infty^3 T - 3T_\infty^4. \quad (11.8)$$

Invoking Eqs. (11.4), (11.7) and (11.8) we have

$$\rho c_p \left(u \frac{\partial T}{\partial x} + v \frac{\partial T}{\partial y} \right) = \frac{\partial}{\partial y} \left[\left(\frac{16\sigma^* T_\infty^3}{3k^*} + k \right) \frac{\partial T}{\partial y} \right]. \quad (11.9)$$

Selecting

$$\begin{aligned} \eta = (c/\nu)^{1/2} y, \quad u = cx f'(\eta), \quad v = -(c\nu)^{1/2} f(\eta), \quad N^* = (c/\nu)^{1/2} cx g(\eta), \\ \theta = \frac{T-T_\infty}{T_w-T_\infty}, \quad \phi = \frac{C-C_\infty}{C_w-C_\infty}. \end{aligned} \quad (11.10)$$

equation (11.1) is automatically satisfied and Eqs. (11.2), (11.3), (11.5), (11.6) and (11.9) finally yield

$$(1 + K_1) f'''' + f f'' - (f')^2 + K_1 g' + \frac{a^2}{c^2} + \lambda(\theta + N\phi) = 0, \quad (11.11)$$

$$\left(1 + \frac{K_1}{2} \right) g'' + f g' - f' g - 2K_1 g - K_1 f'' = 0, \quad (11.12)$$

$$(1 + N_R) \theta'' + \text{Pr} (f\theta' - f'\theta) = 0, \quad (11.13)$$

$$\phi'' + Sc(f\phi' - f'\phi) = 0, \quad (11.14)$$

$$\begin{aligned} f(0) &= 0, \quad f'(0) = 1, \quad g(0) = -N_0 f''(0), \quad \theta(0) = \phi(0) = 1, \\ f'(\infty) &= a/c, \quad g(\infty) = \theta(\infty) = \phi(\infty) = 0, \end{aligned} \quad (11.15)$$

where prime denotes the derivative with respect to η . Here micropolar parameter K , Prandtl number Pr , radiation parameter N_R , Schmidt number Sc , chemical reaction parameter γ , local buoyancy parameter λ and local Grashof number Gr_x are prescribed as follows.

$$\begin{aligned} K_1 &= \frac{\kappa}{\mu}, \quad Pr = \frac{\nu}{a}, \quad N_R = \frac{16\sigma^* T_\infty^3}{3kk^*}, \quad Sc = \frac{\nu}{D}, \\ \lambda &= \frac{Gr_x}{Re_x^2}, \quad Gr_x = \frac{g\beta(T_w - T_\infty)x^3/\nu^2}{u_w^2 x^2/\nu^2}, \quad N = \frac{\beta_C(C_w - C_\infty)}{\beta_T(T_w - T_\infty)}. \end{aligned} \quad (11.16)$$

The definitions of skin friction coefficients C_{fx} , local Nusselt number Nu and local Sherwood number Sh are

$$\begin{aligned} C_{fx} &= \frac{\left[(\mu + \kappa) \frac{\partial u}{\partial y} + \kappa N \right]_{y=0}}{\rho u_w^2}, \\ Nu &= \frac{-x(\partial T/\partial y)_{y=0}}{(T_w - T_\infty)}, \quad Sh = \frac{-x(\partial C/\partial y)_{y=0}}{(C_w - C_\infty)}. \end{aligned} \quad (11.17)$$

which after invoking Eq. (11.10) become

$$\begin{aligned} Re_x^{1/2} C_{fx} &= [1 + (1 - N_0) K_1] f''(0), \\ Nu Re_x^{-1/2} &= -\theta'(0), \quad Sh Re_x^{-1/2} = -\phi'(0), \end{aligned} \quad (11.18)$$

in which $Re_x = ax^2/\nu$ denotes the local Reynolds number.

11.2 Homotopy analysis solutions

Considering a set of base functions

$$\{\eta^k \exp(-n\eta) | k \geq 0, n \geq 0\} \quad (11.19)$$

we express

$$f(\eta) = a_{0,0}^0 + \sum_{n=0}^{\infty} \sum_{k=0}^{\infty} a_{m,n}^k \eta^k \exp(-n\eta), \quad (11.20)$$

$$g(\eta) = \sum_{n=0}^{\infty} \sum_{k=0}^{\infty} b_{m,n}^k \eta^k \exp(-n\eta), \quad (11.21)$$

$$\theta(\eta) = \sum_{n=0}^{\infty} \sum_{k=0}^{\infty} c_{m,n}^k \eta^k \exp(-n\eta), \quad (11.22)$$

$$\phi(\eta) = \sum_{n=0}^{\infty} \sum_{k=0}^{\infty} d_{m,n}^k \eta^k \exp(-n\eta) \quad (11.23)$$

in which $a_{m,n}^k$, $b_{m,n}^k$, $c_{m,n}^k$ and $d_{m,n}^k$ are the coefficients. The rule of solution expressions and the boundary conditions (11.15), the initial guesses f_0 , g_0 , θ_0 and ϕ_0 of $f(\eta)$, $g(\eta)$, $\theta(\eta)$ and $\phi(\eta)$ are given by

$$f_0(\eta) = \frac{a}{c}\eta + (1 - \frac{a}{c}) [(1 - \exp(-\eta))], \quad (11.24)$$

$$g_0(\eta) = N_0 \exp(-\eta), \quad (11.25)$$

$$\theta_0(\eta) = \exp(-\eta), \quad (11.26)$$

$$\phi_0(\eta) = \exp(-\eta), \quad (11.27)$$

with the auxiliary linear operators of the forms

$$\mathcal{L}_f = \frac{d^3 f}{d\eta^3} - \frac{df}{d\eta}, \quad (11.28)$$

$$\mathcal{L}_g = \frac{d^2 g}{d\eta^2} - g, \quad (11.29)$$

$$\mathcal{L}_\theta = \frac{d^2 \theta}{d\eta^2} - \theta, \quad (11.30)$$

$$\mathcal{L}_\phi = \frac{d^2 \phi}{d\eta^2} - \phi, \quad (11.31)$$

having properties

$$\mathcal{L}_f [C_1 + C_2 \exp(\eta) + C_3 \exp(-\eta)] = 0, \quad (11.32)$$

$$\mathcal{L}_g [C_4 \exp(\eta) + C_5 \exp(-\eta)] = 0, \quad (11.33)$$

$$\mathcal{L}_\theta [C_6 \exp(\eta) + C_7 \exp(-\eta)] = 0, \quad (11.34)$$

$$\mathcal{L}_\phi [C_8 \exp(\eta) + C_9 \exp(-\eta)] = 0, \quad (11.35)$$

where $C_i (i = 1 - 9)$ are the arbitrary constants.

The associated zeroth order deformation problems are

$$(1 - p)\mathcal{L}_f[\hat{f}(\eta; p) - f_0(\eta)] = p\hbar_f \mathcal{N}_f [\hat{f}(\eta; p)], \quad (11.36)$$

$$(1 - p)\mathcal{L}_g[\hat{g}(\eta; p) - g_0(\eta)] = p\hbar_g \mathcal{N}_g [\hat{f}(\eta; p), \hat{g}(\eta; p)], \quad (11.37)$$

$$(1 - p)\mathcal{L}_\theta [\hat{\theta}(\eta; p) - \theta_0(\eta)] = p\hbar_\theta \mathcal{N}_\theta [\hat{f}(\eta; p), \hat{\theta}(\eta; p)], \quad (11.38)$$

$$(1 - p)\mathcal{L}_\phi [\hat{\phi}(\eta; p) - \phi_0(\eta)] = p\hbar_\phi \mathcal{N}_\phi [\hat{f}(\eta; p), \hat{\phi}(\eta; p)], \quad (11.39)$$

$$\begin{aligned} \hat{f}(\eta)|_{\eta=0} &= 0, \quad \hat{g}(\eta)|_{\eta=0} = -N_0 \frac{\partial^2 \hat{f}(\eta)}{\partial \eta^2} \Big|_{\eta=0}, \quad \hat{\theta}(\eta)|_{\eta=0} = \hat{\phi}(\eta)|_{\eta=0} = \frac{\partial \hat{f}(\eta)}{\partial \eta} \Big|_{\eta=0} = 1, \\ \hat{g}(\eta)|_{\eta=\infty} &= 0, \quad \frac{\partial \hat{f}(\eta)}{\partial \eta} \Big|_{\eta=\infty} = a/c, \quad \hat{\theta}(\eta)|_{\eta=\infty} = \hat{\phi}(\eta)|_{\eta=\infty} = 0, \end{aligned} \quad (11.40)$$

in which $p \in [0, 1]$ depicts the embedding parameter and $\hbar_f, \hbar_g, \hbar_\theta$ and \hbar_ϕ the nonzero auxiliary parameters. Further the nonlinear operators $\mathcal{N}_f, \mathcal{N}_g, \mathcal{N}_\theta$ and \mathcal{N}_ϕ

$$\begin{aligned} \mathcal{N}_f \left[\hat{f}(\eta; p), \hat{g}(\eta; p), \hat{\theta}(\eta; p), \hat{\phi}(\eta; p) \right] &= (1 + K) \frac{\partial^3 \hat{f}(\eta; p)}{\partial \eta^3} + \left[\hat{f}(\eta; p) \frac{\partial^2 \hat{f}(\eta; p)}{\partial \eta^2} - \left(\frac{\partial \hat{f}(\eta; p)}{\partial \eta} \right)^2 \right] \\ &+ K \frac{\partial \hat{g}(\eta; p)}{\partial \eta} + \frac{a^2}{c^2} + \lambda \left(\hat{\theta}(\eta; p) + N \hat{\phi}(\eta; p) \right), \end{aligned} \quad (11.41)$$

$$\mathcal{N}_g \left[\hat{f}(\eta; p), \hat{g}(\eta; p), \hat{\theta}(\eta; p), \hat{\phi}(\eta; p) \right] = \left(1 + \frac{K}{2} \right) \frac{\partial^2 \hat{g}(\eta; p)}{\partial \eta^2} \quad (11.42)$$

$$+ \left[\begin{array}{l} \hat{f}(\eta; p) \frac{\partial \hat{g}(\eta; p)}{\partial \eta} - \hat{f}(\xi, \eta; p) \frac{\partial \hat{g}(\eta; p)}{\partial \eta} \\ -2K \hat{g}(\eta; p) - K \frac{\partial^2 \hat{f}(\eta; p)}{\partial \eta^2} \end{array} \right], \quad (11.43)$$

$$\mathcal{N}_\theta \left[\hat{f}(\eta; p), \hat{g}(\eta; p), \hat{\theta}(\eta; p), \hat{\phi}(\eta; p) \right] = (1 + N_R) \frac{\partial^2 \hat{\theta}(\eta; p)}{\partial \eta^2} + Pr \left(\begin{array}{l} \hat{f}(\eta; p) \frac{\partial \hat{\theta}(\eta; p)}{\partial \eta} \\ -\hat{\theta}(\eta; p) \frac{\partial \hat{f}(\eta; p)}{\partial \eta} \end{array} \right), \quad (11.44)$$

$$\mathcal{N}_\phi \left[\hat{f}(\eta; p), \hat{g}(\eta; p), \hat{\theta}(\eta; p), \hat{\phi}(\eta; p) \right] = \frac{\partial^2 \hat{\phi}(\eta; p)}{\partial \eta^2} + Sc \left(\begin{array}{l} \hat{f}(\eta; p) \frac{\partial \hat{\phi}(\eta; p)}{\partial \eta} \\ -\hat{\phi}(\eta; p) \frac{\partial \hat{f}(\eta; p)}{\partial \eta} \end{array} \right). \quad (11.45)$$

For $p = 0$ and $p = 1$ then

$$\hat{f}(\eta; 0) = f_0(\eta), \quad \hat{f}(\eta; 1) = f(\eta), \quad (11.46)$$

$$\hat{g}(\eta; 0) = g_0(\eta), \quad \hat{g}(\eta; 1) = g(\eta), \quad (11.47)$$

$$\hat{\theta}(\eta; 0) = \theta_0(\eta), \quad \hat{\theta}(\eta; 1) = \theta(\eta), \quad (11.48)$$

$$\hat{\phi}(\eta; 0) = \phi_0(\eta), \quad \hat{\phi}(\eta; 1) = \phi(\eta). \quad (11.49)$$

and so through Taylors series one can write

$$\hat{f}(\eta; p) = f_0(\eta) + \sum_{m=1}^{\infty} f_m(\eta)p^m, \quad (11.50)$$

$$\hat{g}(\eta; p) = g_0(\eta) + \sum_{m=1}^{\infty} g_m(\eta)p^m, \quad (11.51)$$

$$\hat{\theta}(\eta; p) = \theta_0(\eta) + \sum_{m=1}^{\infty} \theta_m(\eta)p^m, \quad (11.52)$$

$$\hat{\phi}(\eta; p) = \phi_0(\eta) + \sum_{m=1}^{\infty} \phi_m(\eta)p^m, \quad (11.53)$$

$$\begin{aligned} f_m(\eta) &= \frac{1}{m!} \left. \frac{\partial^m f(\eta; p)}{\partial \eta^m} \right|_{p=0}, & g_m(\eta) &= \frac{1}{m!} \left. \frac{\partial^m g(\eta; p)}{\partial \eta^m} \right|_{p=0}, \\ \theta_m(\eta) &= \frac{1}{m!} \left. \frac{\partial^m \theta(\eta; p)}{\partial \eta^m} \right|_{p=0}, & \phi_m(\eta) &= \frac{1}{m!} \left. \frac{\partial^m \phi(\eta; p)}{\partial \eta^m} \right|_{p=0}. \end{aligned} \quad (11.54)$$

The auxiliary parameters are so properly chosen that series (11.51) – (11.54) converge when $p = 1$ and hence

$$f(\eta) = f_0(\eta) + \sum_{m=1}^{\infty} f_m(\eta), \quad (11.55)$$

$$g(\eta) = g_0(\eta) + \sum_{m=1}^{\infty} g_m(\eta), \quad (11.56)$$

$$\theta(\eta) = \theta_0(\eta) + \sum_{m=1}^{\infty} \theta_m(\eta). \quad (11.57)$$

$$\phi(\eta) = \phi_0(\eta) + \sum_{m=1}^{\infty} \phi_m(\eta). \quad (11.58)$$

The related problems at the m th– order deformation are given below

$$\mathcal{L}_f [f_m(\eta) - \chi_m f_{m-1}(\eta)] = \hbar_f \mathcal{R}_m^f(\eta), \quad (11.59)$$

$$\mathcal{L}_g [g_m(\eta) - \chi_m g_{m-1}(\eta)] = \hbar_g \mathcal{R}_m^g(\eta), \quad (11.60)$$

$$\mathcal{L}_\theta [\theta_m(\eta) - \chi_m \theta_{m-1}(\eta)] = \hbar_\theta \mathcal{R}_m^\theta(\eta), \quad (11.61)$$

$$\mathcal{L}_\phi [\phi_m(\eta) - \chi_m \phi_{m-1}(\eta)] = \hbar_\phi \mathcal{R}_m^\phi(\eta), \quad (11.62)$$

$$\begin{aligned} f_m(0) &= 0, f'_m(0) = 0, f''_m(\infty) = 0, & g_m(0) &= 0, g_m(\infty) = 0, g'_m(\infty) = 0, \\ \theta_m(0) &= 0, \theta_m(\infty) = 0, \phi_m(0) = 0, & \phi_m(\infty) &= 0, \end{aligned} \quad (11.63)$$

with the following definitions

$$\mathcal{R}_m^f(\eta) = (1 + K) f'''_{m-1} + \left[\sum_{k=0}^{m-1} [f_k f''_{m-1-k} - f'_k f'_{m-1-k}] \right] + K g'_{m-1} + \frac{a^2}{c^2} + \lambda (\theta_{m-1} + N \phi_{m-1}), \quad (11.64)$$

$$\mathcal{R}_m^g(\eta) = \left(1 + \frac{K}{2} \right) g''_{m-1} + \left[\sum_{k=0}^{m-1} [f_k g'_{m-1-k} - g_k f'_{m-1-k}] \right], \quad (11.65)$$

$$\mathcal{R}_m^\theta(\eta) = (1 + N_R) \theta''_{m-1} + Pr \sum_{k=0}^{m-1} [f_k \theta'_{m-1-k} + g_k \theta'_{m-1-k}], \quad (11.66)$$

$$\mathcal{R}_m^\phi(\eta) = \phi''_{m-1} + Sc \sum_{k=0}^{m-1} [f_k \phi'_{m-1-k} - \phi_k f'_{m-1-k}], \quad (11.67)$$

$$\chi_m = \begin{cases} 0, & m \leq 1, \\ 1, & m > 1. \end{cases} \quad (11.68)$$

The general solutions of Eqs (11.60) – (11.63) are

$$f_m(\eta) = f_m^*(\eta) + C_1 + C_2 \exp(\eta) + C_3 \exp(-\eta), \quad (11.69)$$

$$g_m(\eta) = g_m^*(\eta) + C_4 + C_5 \exp(\eta) + C_6 \exp(-\eta), \quad (11.70)$$

$$\theta_m(\eta) = \theta_m^*(\eta) + C_7 \exp(\eta) + C_8 \exp(-\eta), \quad (11.71)$$

$$\phi_m(\eta) = \phi_m^*(\eta) + C_9 \exp(\eta) + C_{10} \exp(-\eta), \quad (11.72)$$

where $f_m^*(\eta)$, $g_m^*(\eta)$, $\theta_m^*(\eta)$, $\phi_m^*(\eta)$ are the particular solutions of the Eqs. (11.60) – (11.63). Note that Eqs. (11.60) – (11.63) can be solved by Mathematica one after the other in the order $m = 1, 2, 3, \dots$

11.3 Convergence of the series solutions

Obviously the series solutions (11.56) – (11.59) involves the non-zero auxiliary parameters \hbar_f , \hbar_g , \hbar_θ and \hbar_ϕ . Such parameters help in the adjustment and control the radius of convergence of the series solutions. In the present case, the range of reliable values of \hbar_f , \hbar_g , \hbar_θ and \hbar_ϕ can be computed by showing the \hbar -curves of the functions $f''(0)$, $g'(0)$, $\theta'(0)$ and $\phi'(0)$ for 15th-order of approximations. Fig. 1 depicts that the range for the values of \hbar_f , \hbar_g , \hbar_θ and \hbar_ϕ are $-0.8 \leq \hbar_f \leq -0.3$, $-0.9 \leq \hbar_\theta \leq -0.2$ and $-0.8 \leq \hbar_g, \hbar_\phi \leq -0.3$. The series given by (11.56) – (11.59) converge in the whole region of η when $\hbar_f = \hbar_g = -0.7 = \hbar_\theta = \hbar_\phi$. Fig. 11.1 depicts the \hbar -curves of velocity, microrotation, temperature and concentration. Table 11.1

indicates the convergence of the homotopy solutions for different order of approximations.

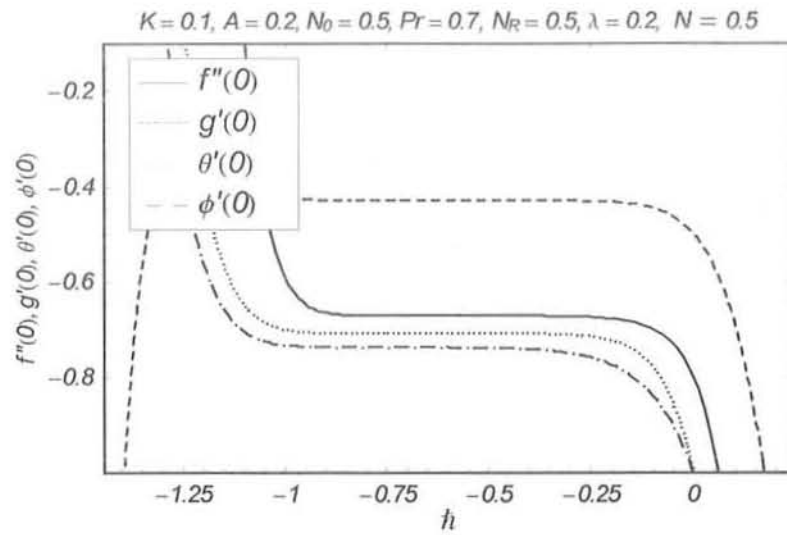


Fig. 11. 1. The h -curves of $f''(0)$, $g'(0)$, $\theta'(0)$ and $\phi'(0)$ at 15th-order of approximations.

Order of convergence	$-f''(0)$	$-g'(0)$	$-\theta'(0)$	$-\phi'(0)$
5	0.67194	0.42945	0.70923	0.74751
10	0.67115	0.42918	0.70818	0.73809
15	0.67116	0.42917	0.70826	0.73757
20	0.67116	0.42917	0.70827	0.73756
25	0.67116	0.42917	0.70827	0.73756
30	0.67116	0.42917	0.70827	0.73756
35	0.67116	0.42917	0.70827	0.73756

Table 11.1: Numerical values for the convergence of $f''(0)$, $g'(0)$, $\theta'(0)$ and $\phi'(0)$.

11.4 Results and discussion

In this section, we look for the variations of the material parameter K_1 , local buoyancy parameter λ , the buoyancy ratio N , constant velocity ratio a/c , Prandtl number Pr , radiation parameter N_R , Schmidt number Sc on the velocity, temperature and concentration fields. This can be achieved by plotting the Figs. 11.2 – 11.16. Figs. 11.2 – 11.5 are presented in order to show the effects of λ , N , K_1 and a/c on f' . Fig. 11.2 presents the effect of λ on the velocity f' . It is observed from this Fig. that the boundary layer thickness increases by increasing λ . It is also found that f' increases when N increases (Fig. 11.3). Fig. 11.4 displays the velocity profiles for various values of K_1 when $N_0 = 0.5$. The qualitative effects of K_1 are found similar to that of λ and N of f' . Fig. 11.5 gives the variations of a/c on velocity component f' . The velocity component f' is a decreasing function of $a/c < 1$ while for $a/c > 1$ it decreases.

The effects of a/c and K on the microrotation profile $g(\eta)$ are plotted in the Figs. 11.6–11.9. Fig. 11.6 is drawn when $N_0 = 0.5$. From Fig. 11.6, we have seen that g increases initially but at $\eta = 2$ it starts decreasing. Fig. 11.7 is drawn for $N_0 = 0.5$. We see that g increases by increasing a/c . From Figs. 11.8 and 11.9, it is clear that the microrotation profile for $N_0 = 0.0$ and that $N_0 = 0.5$ are quite different. Figs. 11.10 – 11.13 depict the effects of ratio a/c , local buoyancy parameter λ , Prandtl number Pr and radiation parameter N_R on the temperature profile $\theta(\eta)$. The qualitative effects of a/c and λ on the temperature are similar (Figs. 11.10 and 11.11). The variation of Pr on the temperature field is sketched in Fig. 11.12. As expected, it is found that θ is decreasing when Pr is increased. Fig. 11.13 gives the effects of radiation parameter N_R on the temperature field. It has opposite result when compared with Fig. 11.12. Figs. 11.14 – 11.16 plot the effects of a/c , λ and Sc on the concentration profiles. Fig. 11.14 shows the effect of a/c on the concentration profile ϕ . It is observed that concentration boundary layer decreases by increasing a/c . The behaviors of λ and Sc on concentration profile are seen in the Figs. 11.15 and 11.16. Both λ and Sc decrease the concentration profile.

Tables 11.2 – 11.5 are given for the numerical values of the skin friction coefficients, Nusselt number and Sherwood number for the different values of involved parameters of interest. From Table 11.2 it is noticed that the magnitude of skin friction coefficient decreases for large values of N and λ . From Table 11.3 it is found that the magnitude of $-\theta'(0)$ increases for large values of K_1 . These Tables indicates that HAM solution has a good agreement with the numerical solution [94]. Table 11.4 is prepared for the variations of N , λ , K_1 , Sc and a/c on the surface mass transfer. It is obvious from this Table that the magnitude of $-\phi'(0)$ increases for large values of K_1 and Sc .

11.5 Conclusions

The series solution of steady two-dimensional mixed convection stagnation point flow of a micropolar fluid with heat and mass transfer is investigated. The behavior of the embedded parameters are examined and the following points are noted.

- Velocity component f' is a decreasing function of $a/c < 1$ whereas for $a/c > 1$ it increases.
- Velocity f' is an increasing function of K_1 , N and λ .
- Microrotation profile is parabolic distribution when $N_0 = 0$.
- The temperature θ decreases when Pr is increased
- The role of N_R and Pr on the temperature is opposite.

- There is a decrease in concentration field when Sc increases.

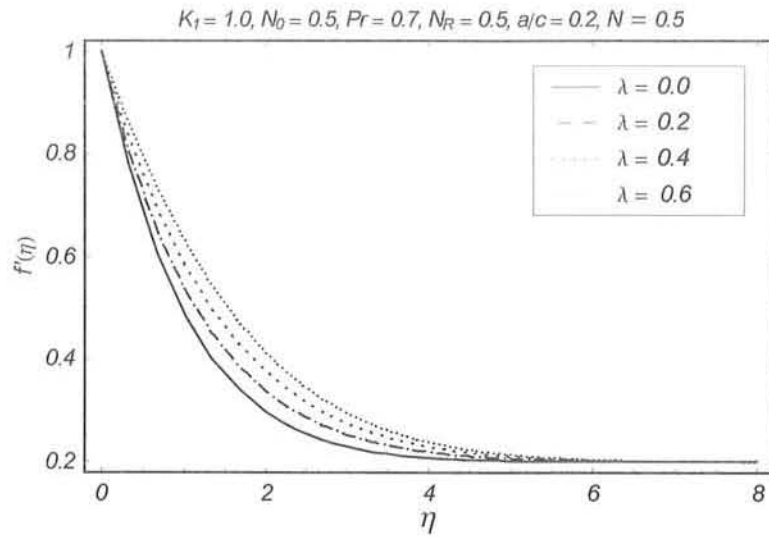


Fig. 11.2. Influence of λ on velocity profile f' .

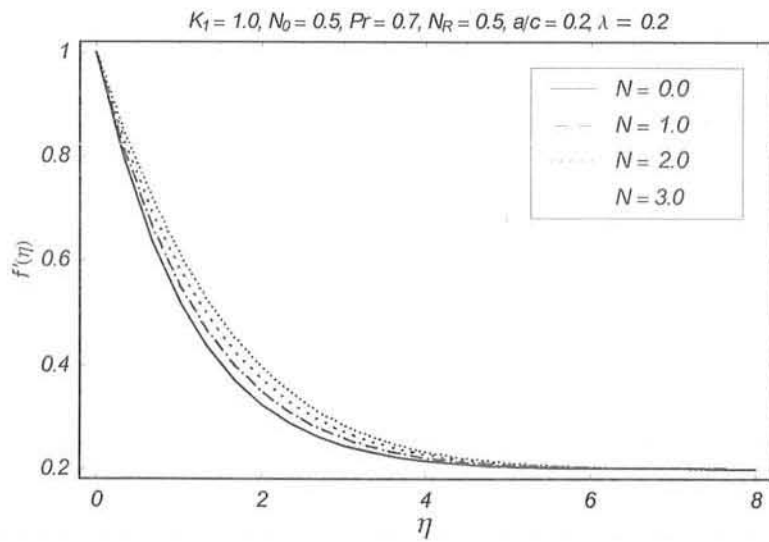


Fig. 11.3. Influence of N on velocity profile f' .

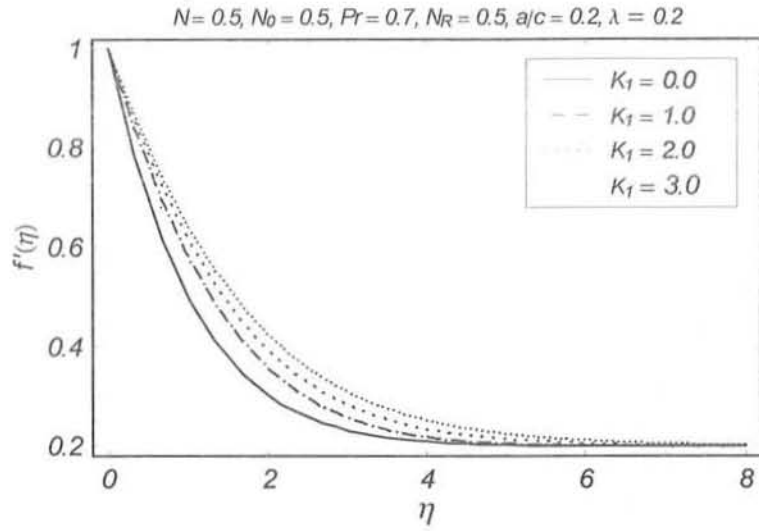


Fig. 11.4. Influence of K_1 on velocity profile f' .

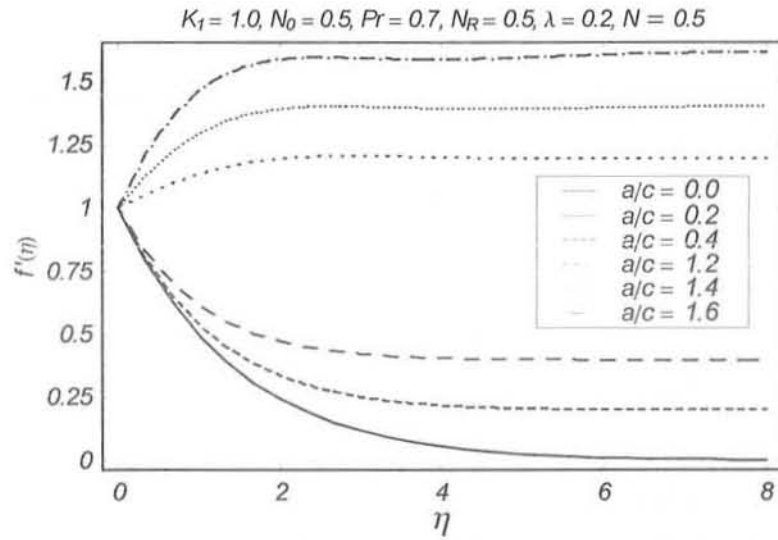


Fig. 11.5. Influence of a/c on velocity profile f' .

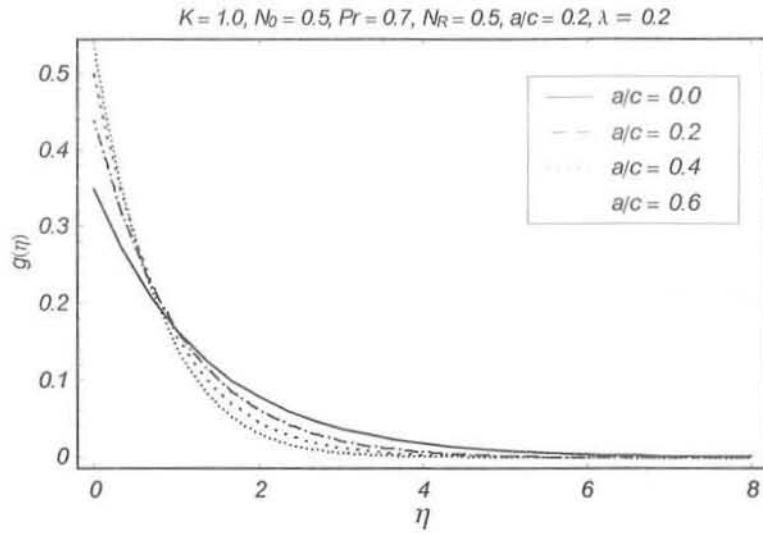


Fig. 11.6. Influence of a/c on microrotation profile g when $N_0 = 0.5$.

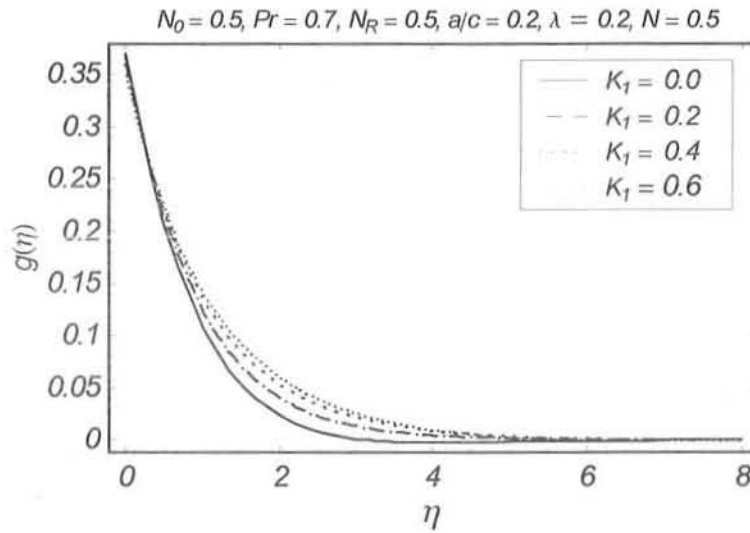


Fig. 11.7. Influence of K on microrotation profile g when $N_0 = 0.5$

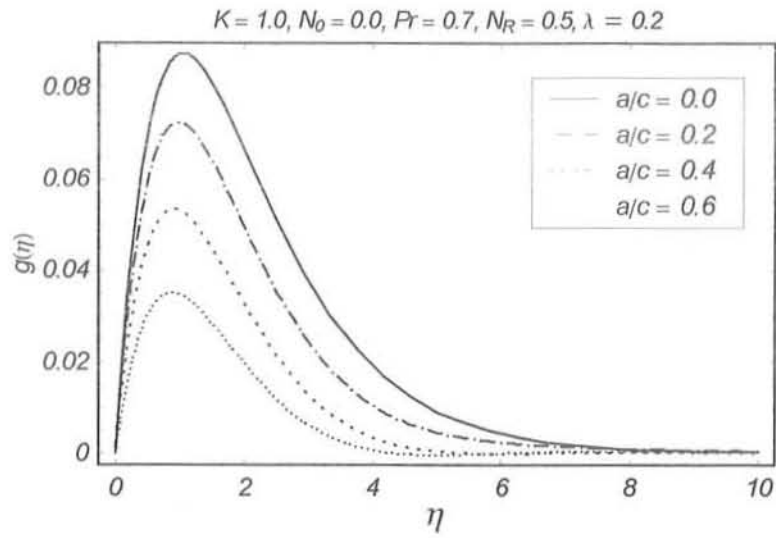


Fig. 11.8. Influence of a/c on microrotation profile g when $N_0 = 0.0$.

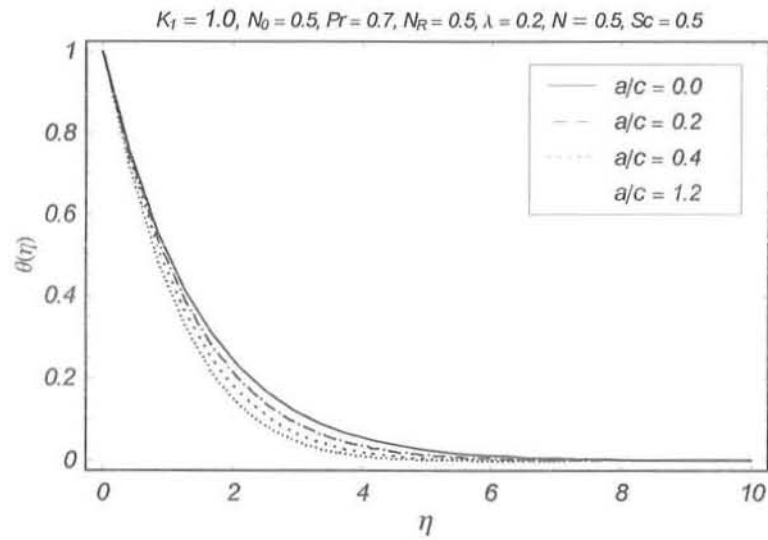


Fig. 11.10. Influence of a/c on temperature profile θ .

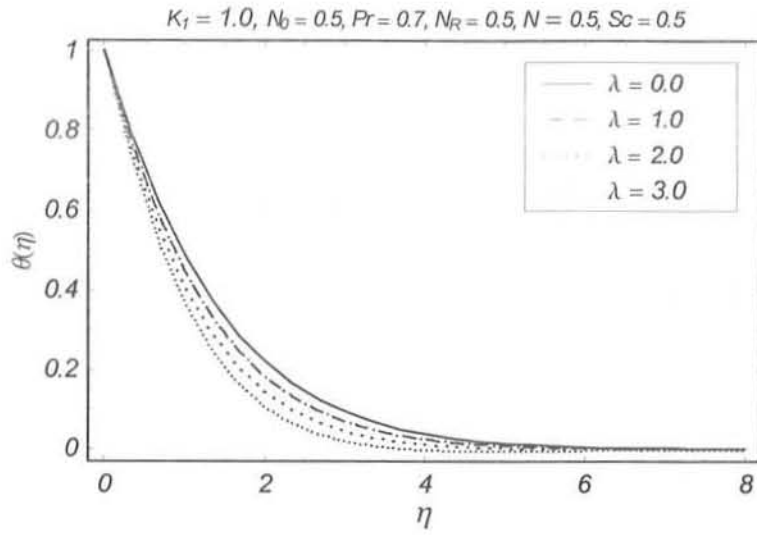


Fig. 11.11. Influence of λ on temperature profile θ .

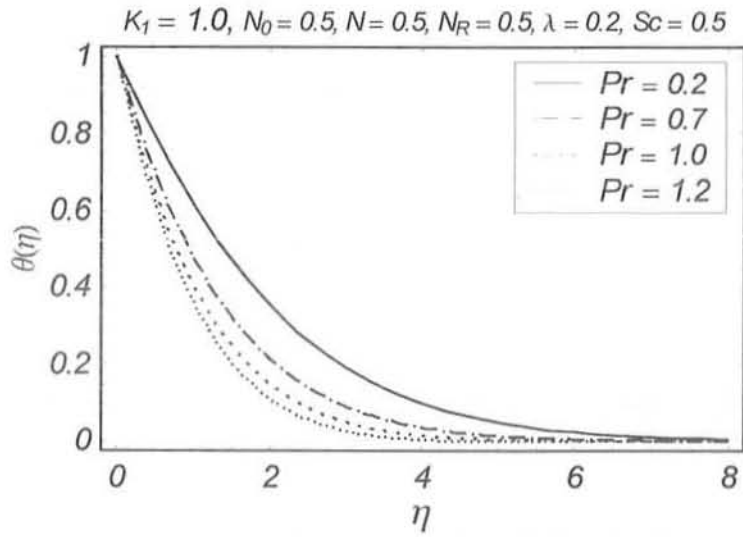


Fig. 11.12. Influence of Pr on temperature profile θ .

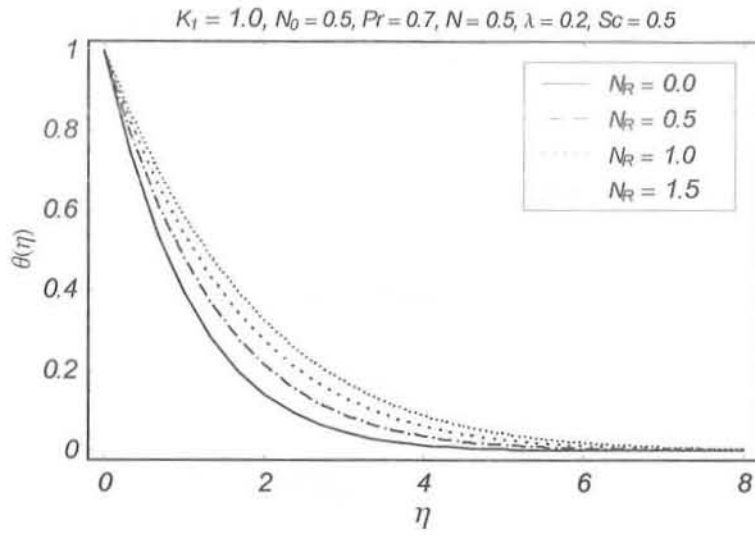


Fig. 11.13. Influence of N_R on temperature profile θ .

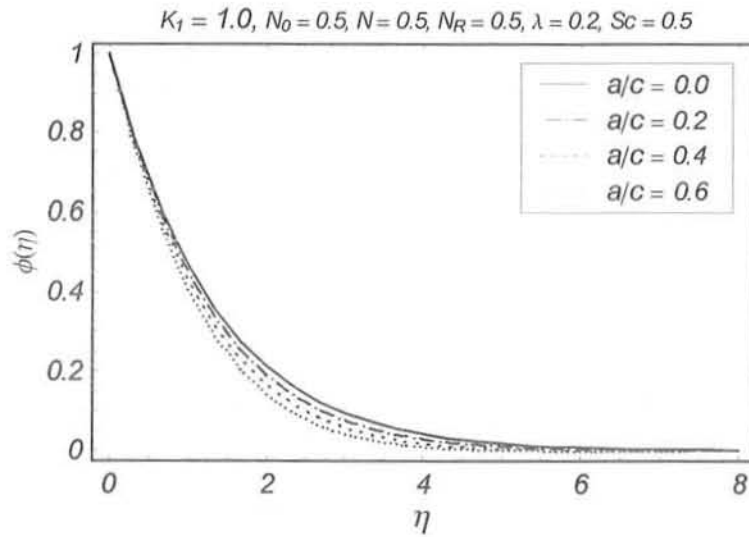


Fig. 11.14. Influence of a/c on concentration profile ϕ .

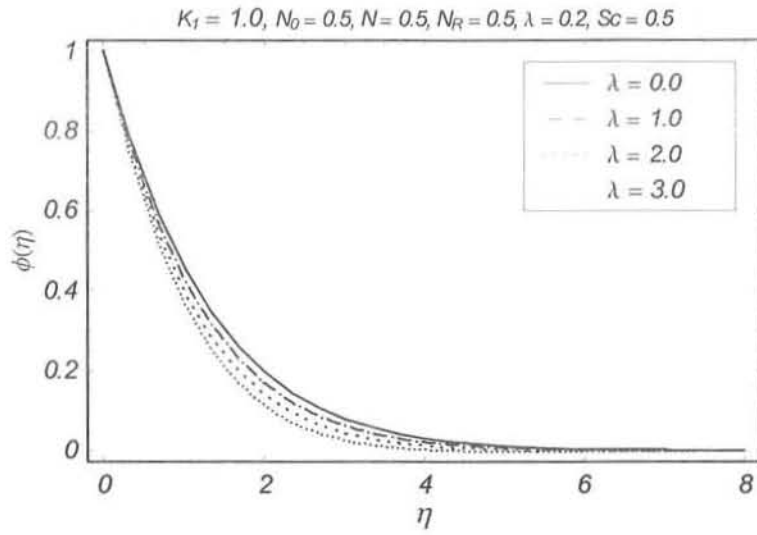


Fig. 11.15. Influence of λ on concentration profile ϕ .

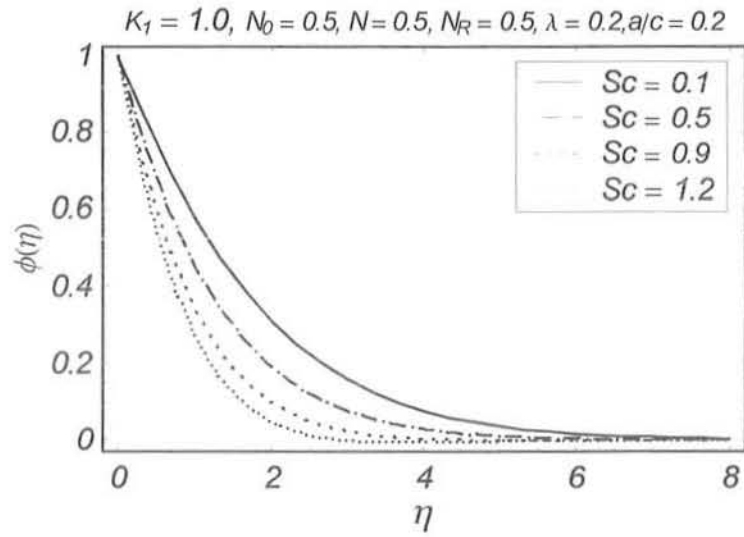


Fig. 11.16. Influence of Sc on concentration profile ϕ .

	$K_1 = 0$			
a/c	$N_0 = 0.0$		$N_0 = 0.5$	
	[89]	HAM	[89]	HAM
0.01	-0.9980	-0.99891	-0.9980	-0.99891
0.02	-0.9958	-0.99575	-0.9958	-0.99575
0.05	-0.9876	-0.98745	-0.9876	-0.98745
0.10	-0.9694	-0.96934	-0.9694	-0.96934
0.20	-0.9181	-0.91823	-0.9181	-0.91823
0.50	-0.6673	-0.66745	-0.6673	-0.66745
1.00	0.0000	0.00000	0.0000	0.00000
2.00	2.0175	2.01844	2.0175	2.01844

Table 11.2: Comparison of values of skin friction coefficient for some values of a/c when $\lambda = 0$.

	$K_1 = 1$			
a/c	$N_0 = 0.0$		$N_0 = 0.5$	
	[89]	HAM	[89]	HAM
0.01	-1.3653	-1.3653	-1.2224	-1.2224
0.02	-1.3622	-1.3622	-1.2196	-1.2196
0.05	-1.3512	-1.3512	-1.2095	-1.2095
0.10	-1.3268	-1.3268	-1.1872	-1.1872
0.20	-1.2579	-1.2579	-1.1244	-1.1244
0.50	-0.9175	-0.9175	-0.8172	-0.8172
1.00	0.00000	0.00000	0.0000	0.0000
2.00	2.8062	2.8062	2.4710	2.4710

Table 11.3: Comparison of values of skin friction coefficient for some values of a/c when

$\lambda = 0.$

a/c	$K_1 = 2$			
	$N_0 = 0.0$		$N_0 = 0.5$	
	[94]	HAM	[89]	HAM
0.01	-1.6183	-1.61834	-1.4116	-1.41162
0.02	-1.6147	-1.61472	-1.4084	-1.40847
0.05	-1.6015	-1.60153	-1.3967	-1.39676
0.10	-1.5726	-1.57263	-1.3709	-1.37098
0.20	-1.4914	-1.49144	-1.2984	-1.29846
0.50	-1.0893	-1.08933	-0.9437	-0.94376
1.00	0.0000	0.00000	0.0000	0.00000
2.00	3.3595	3.35952	2.8532	2.85322

Table 11.4: Comparison of values of skin friction coefficient for some values of a/c when

$\lambda = 0.$

Sc	K_1	a/c	N	λ	$-\phi'(0)$
0.5	1.0	0.2	0.5	0.2	0.73754
1.0					1.09641
1.5					1.37524
0.5	0.0				0.72196
	0.5				0.73042
	1.0				0.73754
0.7	1.0	0.0	0.5	0.2	0.71356
		0.2			0.73748
		0.4			0.77075
0.7	1.0	0.2	0.0	0.2	0.73068
			0.5		0.71356
			1.0		0.74398
0.7	1.0	0.2	0.5	0.0	0.71437
				0.3	0.74732
				0.6	0.77262

Table 11.5: Values of $-\phi'(0)$ for some values of K_1 , M , Sc and λ when $Pr = 0.7$, $N_R = 0.5$ and $N_0 = 0.5$.

Bibliography

- [1] K. R. Rajagopal, Boundedness and uniqueness of fluids of the differential type, *Acta Cienca Indica* 18 (1982) 1.
- [2] K. R. Rajagopal and P. N. Kaloni, Some remarks on boundary conditions for fluids of differential type, in: G.A.C. Graham, S.K. Malik (Eds.) *Continuum mechanics and applications*, Hemisphere, New York (1989) 935.
- [3] J. E. Dunn and K. R. Rajagopal, Fluids of differential type: Critical review and thermodynamic analysis, *Int. J. Eng. Sci.* 33 (1995) 689.
- [4] R. L. Fosdick and K. R. Rajagopal, Anomalous features in the model of second grade fluids, *Arch. Ration. Mech. Anal.* 70 (1979) 145.
- [5] K. R. Rajagopal, On creeping flow of a second grade fluid, *J. Non-Newtonian Fluid Mech.* 48 (1994) 239.
- [6] P. N. Kaloni and A. M. Siddiqui, The flow of second grade fluid, *Int. J. Eng. Sci.* 21 (1983) 1157.
- [7] A. M. Siddiqui and A. M. Benharbit, Hodograph transformation methods in incompressible second grade fluid, *Mechanics research comm.* 24 (1997) 463.
- [8] C. Fetecau and C. Fetecau, Starting solutions for some unsteady unidirectional flows of a second grade fluid, *Int. J. Eng. Sci.* 43 (2005) 781.

- [9] C. Fetecau and J. Zierep, On a class of exact solutions of equations of motion of a second grade fluid, *Acta Mech.* 15 (2005) 135.
- [10] S. Asghar, T. Hayat and P.D. Ariel, Unsteady Couette flows in a second grade fluid with variable material properties, *Comm. Non-linear Sci. Num. Simul.* 14 (2009) 154.
- [11] M. E. Erdogan and C. E. Imark, On the steady unidirectional flows of a second grade fluid, *Int. J. Non-linear Mech.* 40 (2005) 1238.
- [12] W. C. Tan and T. Masuoka, Stokes problem for a second grade fluid in a porous half space with heated boundary, *Int. J. Non-Linear Mech.* 40 (2005) 515.
- [13] W. C. Tan and M. Y. Xu, The impulsive motion of a flat plate in a generalized second grade fluid, *Mech. Res. Comm.* 29 (2002) 3.
- [14] T. Hayat, S. Nadeem, S. Asghar and A. M. Siddiqui, Effects of Hall current on unsteady flow of a second grade fluid in a rotating system, *Chem. Eng. Comm.* 192 (2005) 1272.
- [15] T. Hayat, I. Naeem, M. Ayub, A.M. Siddiqui, S. Asghar and C.M. Khalique, Exact solutions of second grade aligned MHD fluid with prescribed vorticity, *Nonlinear Analysis: Real World Appl* 10 (2009) 2117.
- [16] M. Khan, S. Nadeem, T. Hayat and A. M. Siddiqui, Unsteady motions of a generalized second-grade fluid, *Mathematical and Computer Modelling* 41 (2005) 629.
- [17] R. K. Bhatnagar, G. Gupta, K. R. Rajagopal, Flow of an Oldroyd-B model due to a stretching sheet in the presence of free stream velocity, *Int. J. Non-Linear Mech.* 30 (1995) 391.
- [18] J. J. Choi, Z. Rusak and J. A. Tichy, Maxwell fluid suction flow in a channel, *J. Non-Newtonian Fluid Mech.* 85 (1999) 165.

- [19] T. Hayat, C. Fetecau, Z. Abbas and N. Ali, Flow of a Maxwell fluid between two side walls due to suddenly moved plate, *Nonlinear Analysis: Series B* 9 (2008) 2288.
- [20] J. Zierep, R.Bohning and C.Fetecau, Numerical results for the conservation of energy of Maxwell media for the Rayleigh–Stokes problem, *Int. J. Nonlinear Mech.* 44 (2009) 862.
- [21] H. T. Qi and M. Y. Xu, Unsteady flow of a viscoelastic fluid with fractional Maxwell model in a Channel, *Mech. Res. Commun.* 34 (2007) 210.
- [22] C. Fetecau, M.Jamil, C. Fetecau and I.Siddique, A note on the second problem of Stokes for Maxwell fluids, *Int. J. Non-Linear Mech.* 44 (2009)1085.
- [23] C. Fetecau, M. Athar and C. Fetecau, Unsteady flow of a generalized Maxwell fluid with fractional derivative due to a constantly accelerating plate, *Comp. Math. App.* 57 (2009) 596.
- [24] T. Hayat, C. Fetecau and M. Sajid, On MHD transient flow of a Maxwell fluid in a porous medium and rotating frame, *Phys. Lett. A* 372 (2008) 1639.
- [25] W. C. Tan and T. Masuoka, Stability analysis of a Maxwell fluid in a porous medium heated from below, *Phys. Lett. A* 360 (2007) 454.
- [26] A. C. Eringen, Simple micropolarfluids, *Int. J. Eng. Sci.* 2 (1964) 205.
- [27] A. C. Eringen, Theory of micropolar fluids, *J. Math. Mech.* 16 (1966) 1.
- [28] A. C. Eringen, *Microcontinuum field theories II: Fluent Media*, Springer, Newyork, 2001.
- [29] G. Lukaszewicz, *Micropolar fluids: Theory and applications*, Brikhauser Basel, 1999.
- [30] H. Schlichting, *Boundary Layer Theory*, McGraw-Hill, New York, 1964.
- [31] B. C. Sakiadis, Boundary layer behavior on continuous solid surfaces: I. Boundary layer equations for two-dimensional and axisymmetric flow. *AIChE J.* 7 (1961) 26.

- [32] L. J. Crane, Flow past a stretching plate, *Z. Angew Math. Mech.* 21 (1970) 645.
- [33] J. Vleegar, Laminar boundary layer behavior on continuous, accelerating surfaces, *Chem. Eng. Sci.* 32 (1977) 1517.
- [34] P. S. Gupta and A. S. Gupta, Heat and mass transfer on a stretching sheet with suction and blowing, *Canad. J. Chem. Eng.* 55 (1977) 744.
- [35] V. M. Soundalgekar and T. V. R. Murty, Heat transfer in flow past a continuous moving plate with variable temperature, *Warme und st.* 14 (1980) 91.
- [36] C. K. Chen and M. I. Char, Heat transfer of a continuous stretching surface with suction or blowing, *Can. J. Chem. Eng.* 55 (1977) 744.
- [37] B. Siddappa and B. S. Khapate, Rivlin- Ericksen fluid flow past a stretching sheet, *Rev. Roum. Sci. Tech. Mech.* 21 (1976) 497.
- [38] K. R. Rajagopal, T. Y. Na and A. S. Gupta, Flow of a viscoelastic fluid over a stretching sheet, *Rheol. Acta* 23 (1984) 213.
- [39] P. S. Lawrence and B. N. Rao, The nonuniqueness of the MHD flow of a viscoelastic fluid past a stretching sheet, *Acta Mech.* 112 (1995) 223.
- [40] W. C. Troy, E. A. Overman, G. B. Ermentrout and J. P. Keener, Uniqueness of flow of a second-order fluid past a stretching surface, *Q. Appl. Math.* 44 (1987) 753.
- [41] H. I. Anderson and B. S. Dandapat, Flow of a power law fluid over a stretching sheet, *Stability Appl. Anal. Continuous Media* 1 (1991) 24.
- [42] R. Cortell, Toward an Understanding of the Motion and Mass Transfer with Chemically Reactive Species for Two Classes of Viscoelastic Fluid over a Porous Stretching Sheet, *Chem. Eng & Process* 46 (2007) 982.

- [43] R. Cortell, A Note on Flow and Heat Transfer of a Viscoelastic Fluid over a Stretching Sheet, *Int. J. Nonlinear Mech.* 41 (2006) 78.
- [44] T. Hayat , Z. Abbas , I. Pop. Mixed convection in the stagnation point flow adjacent to a vertical surface in a viscoelastic fluid, *Int. J. Heat Mass Transfer.* 51 (2008) 3200.
- [45] T. Hayat, Z. Abbas and M. Sajid, Series solution for the upper-convected Maxwell fluid over a porous stretching plate, *Phys. Lett. A* 358 (2006) 396.
- [46] M. Sajid, T. Hayat and S. Asghar, Non-similar analytic solution for MHD flow and heat transfer in a third-order fluid over stretching sheet, *Int. Heat Mass Transfer* 50 (2007) 1723.
- [47] T. Hayat, Z. Abbas and N. Ali, MHD flow and mass transfer of a upper-convected Maxwell fluid past a porous shrinking sheet with chemical reaction species, *Phys. Lett. A* 372 (2008) 4698.
- [48] T. Hayat, T. Javed and Z. Abbas, MHD flow of a micropolar fluid near a stagnation-point towards a non-linear stretching surface. *Nonlinear Analysis:Real World Applications* 10 (2009) 1514.
- [49] T. Hayat, M. Mustafa and I. Pop, Heat and mass transfer for Soret and Dufour effect on mixed convection boundary layer flow over a stretching vertical surface in a porous medium filled with a viscoelastic fluid, 15 (2010) 1183.
- [50] P. D. Ariel, T. Hayat and S. Asghar, The flow of an elastico-viscous fluid past a stretching sheet with partial slip, *Acta Mech.* 187 (2006) 29.
- [51] P. D. Ariel, Axisymmetric flow of a second grade past a stretching sheet, *Int. J. Eng. Sci.* 39 (2001) 529.

- [52] M. Mushtaq, S. Asghar and M. A. Hossain. Mixed convection flow of second grade fluid along a vertical stretching surface with variable surface temperature. *Heat Mass Transfer*, 43 (2007) 1049.
- [53] A. Ishak, Thermal boundary layer flow over a stretching sheet in a micropolar fluid with radiation effect, *Meccanica* DOI 10.1007/s11012 – 009 – 9257 – 4.
- [54] K. Vajravelu, Viscous flow over a nonlinearly stretching sheet, *App. Math. Comput.* 124 (2001) 281.
- [55] K. Vajravelu and J.R.Cannon, Fluid flow over a nonlinearly stretching sheet, *Appl. Math. Comput.* 181(2006) 609.
- [56] R. Cortell, Effects of a viscous dissipation and radiation on the thermal boundary layer over a nonlinearly stretching sheet, *Phys. Lett A* 372 (2008) 631.
- [57] R. Cortell, Viscous flow and heat transfer over a nonlinearly stretching sheet, *Appl. Math. Comput.* 184(2007) 864.
- [58] T. Hayat, Z.Abbas and T. Javed, Mixed convection flow of a micropolar fluid over a nonlinearly stretching sheet, *Phys. Lett A* 372 (2008) 637.
- [59] A. Raptis and C. Perdikis, Viscous flow over a non-linearly stretching sheet in the presence of a magnetic field, *Int. J. Non-linear Mech.* 41(2006) 527.
- [60] I. Pop and T. Y. Na, Unsteady flow past a stretching sheet, *Mech. Res. Comm.* 23 (1996) 413.
- [61] C. Y. Wang, Q. Du, M. Miklavcic and C. C. Chang, Impulsive stretching sheet in a viscous fluid. *SIAM. J. Appl. Math.* 1 (1997) 1.
- [62] S. J. Liao, A new branch of solutions of unsteady boundary layer flows over an impermeable stretched plate, *Int. J. Heat Mass Transfer* 48 (2005) 2529.

- [63] S. J. Liao, On the analytic solution of magnetohydrodynamic flows of non-Newtonian fluid over a stretching sheet, *Fluid Mech.* 488 (2003) 189.
- [64] A. A. Pahlavan and K. Sadeghy, On the use of homotopy analysis method for solving unsteady MHD flow of Maxwellian fluids above impulsively stretching sheets, *Comm. Nonlinear. Sci. Numer. Simulat.* 14 (2009) 1355.
- [65] M. Sajid, I. Ahmad, T. Hayat and M. Ayub, Unsteady flow and heat transfer of a second grade fluid over a stretching sheet, *Comm. Nonlinear. Sci. Numer. Simulat.* 14 (2009) 96.
- [66] R. Nazar, A. Ishak and I. Pop, Unsteady boundary layer flow over a stretching sheet in a micropolar fluid. *World Acadmey. Sci. Eng & Tech.* 38 (2008) 118.
- [67] C. Y. Wang, Liquid film on an unsteady stretching surface, *Quart. Appl. Math.* XLVIII (1990) 601.
- [68] H. I. Andersson, J. B. Aarseth and B. S. Dandapat, Heat transfer in a liquid film on an unsteady stretching surface, *Int. J. Heat Mass Transfer.* 43 (2003) 69 – 74.
- [69] R. Tsai , K. H. Huang and J. S. Huang, Flow and heat transfer over an unsteady stretching surface with non-uniform heat source. *Int. Commun. Heat Mass Transfer*, 35 (2008) 1340–1343.
- [70] M. S. Abel, N. Mahesha and J. Tawade, Heat transfer in a liquid film over an unsteady stretching surface with viscous dissipation in the presence of external magnetic field, *Appl. Math. Model.* 33 (2009) 3430.
- [71] S. Mukhopadhyay, Effect of thermal radiation on unsteady mixed convection flow and heat transfer over a porous stretching surface in a porous medium, *Int. J. Heat Mass Transfer* 52 (2009) 3261.

- [72] A. Ishak, R.Nazar and I.Pop, Heat transfer over an unsteady stretching permeable surface with prescribed wall temperature, *Nonlinear Analysis: Real World Applications* 10 (2009) 2909.
- [73] E. M. A. Elbashbeshy and M. A. A. Bazid, Heat transfer over an unsteady stretching surface, *Heat Mass Transf.* 41 (2004) 1.
- [74] Z. Abbas, T. Hayat, M. Sajid and S. Asghar, Unsteady flow of a second grade fluid film over an unsteady stretching surface. *Math. Comp. Model.* 48 (2008) 518.
- [75] C. Y. Wang, The three-dimensional flow due to a stretching flat surface, *Phys. Fluids* 27 (1984) 1915.
- [76] C. D. S Devi, H. S. Takhar, G. Nath, Unsteady three-dimensional, boundary layer flow due to a stretching surface, *Int. J. Heat Mass Transfer.* 29 (1986) 1996.
- [77] K. N. Lakshmisha, S. Venkateswaran, G. Nath, Three-dimensional unsteady flow with heat and mass transfer over a continuous stretching surface, *ASME J. Heat Transfer* 110 (1988) 590.
- [78] A.J. Chamkha, Hydromagnetic three-dimensional free convection on a vertical stretching surface with heat generation or absorption, *Int. J. Heat Fluid Flow.* 20 (1999) 84.
- [79] P. D. Ariel, Three-dimensional flow past a stretching sheet and the homotopy perturbation method, *Comp. Math. App.* 54 (2007) 920.
- [80] E. M. Aboeldahab, Hydromagnetic three-dimensional flow over a stretching surface with heat and mass transfer, *Heat and Mass Trans.* 41 (2005) 734.
- [81] E.M. Aboeldahab, G.E.D.A. Azzam, Unsteady three-dimensional combined heat and mass transfer free convective flow over a stretching surface with time-dependent chemical reaction, *Acta Mech.* 184 (2006) 121.

- [82] H. Xu, S.J. Liao, I. Pop, Series solutions of unsteady three-dimensional MHD flow and heat transfer in the boundary layer over an impulsively stretching plate, *Eur. J. Mech. B – Fluids*. 26 (2007) 15.
- [83] T. Hayat, M. Sajid, I. Pop, Three-dimensional flow over a stretching surface in a viscoelastic fluid, *Nonlinear Anal: Real World Appl.* 9 (2008) 1811.
- [84] R. Nazar, N. A. Latip, Numerical Investigation of Three-Dimensional Boundary Layer Flow Due to a Stretching Surface in a Viscoelastic Fluid, *Eur. J. Sci. Res.* 4 (2009) 509.
- [85] T. C. Chiam, Stagnation point flow towards a stretching plate, *J. Phys. Soc. Jpn.* 63 (1994) 2443.
- [86] T. R. Mahapatra and A. S. Gupta, Heat transfer in stagnation point flow towards a stretching sheet, *Heat and Mass transfer*, 38 (2002) 517.
- [87] R. Nazar, N.Amin, D. Filip and I. Pop, Stagnation point flow of a micropolar fluid towards a stretching sheet. *Int. J. Nonlinear Mech.* 39 (2004) 1227.
- [88] K. Sadeghy, H. Hajibeygi and S. M. Taghavi, Stagnation-point flow of upper-convected Maxwell fluid, *Int. J. Nonlinear Mech.* 41 (2006)1242.
- [89] A. Ishak, R. Nazar, N.Amin, D. Filip and I. Pop, Mixed convection of the stagnation-point flow towards a stretching vertical permeable sheet, *Malaysian. J. Math. Sci.* 2 (2007) 217 – 226.
- [90] T. Hayat, Z. Abbas, I. Pop and S. Asghar, Effects of radiation and magnetic field on the mixed convection stagnation-point flow over a vertical stretching sheet in a porous medium, *Int. J. Heat Mass Transfer* 53 (2010) 466.

- [91] T. R. Mahapatra, S. Dholey and A.S. Gupta, Oblique stagnation point flow of an incompressible viscoelastic fluid towards a stretching surface, *Int. J. Non-Linear Mech.* 42 (2007) 484.
- [92] F. Labropulu and D. Li, Stagnation-point flow of a second grade fluid with slip, *Int. J. Non-Linear Mech.* 43 (2008) 941.
- [93] R. Nazar, N.Amin, D. Filip and I. Pop, Stagnation point flow of a micropolar fluid towards a stretching sheet. *Int. J. Nonlinear Mech.* 39 (2004) 1227.
- [94] S. J. Liao, On the proposed homotopy analysis technique for non-linear problems and its applications. Ph. D. dissertation, Shanghai Jiao Tong University 1992.
- [95] S.J. Liao, *Beyond perturbation: Introduction to Homotopy Analysis Method*, Chapman & Hall, Boca Raton, (2003).
- [96] S. J. Liao and K. F. Cheung: Homotopy analysis of a nonlinear progressive waves in deep water, *J. Eng. Math.* 45 (2003) 105.
- [97] S. J. Liao, A new analytic algorithm of Lane-Emden type equations, *Appl. Math. Comp.* 142 (2003) 1.
- [98] S. J. Liao, On the homotopy analysis method for nonlinear problems. *Appl. Math. Comput.* 147 (2004) 499.
- [99] S.J. Liao and Y. Tan, A general approach to obtain series solutions of nonlinear differential equations, *Stud. Appl. Math.* 119 (2007) 297.
- [100] S. J. Liao, A uniformly analytic solution of 2D viscous flow past a semi-infinite flat plate, *J. Fluid. Mech.* 385 (1999) 101.
- [101] S. J. Liao, A new branch of solutions of boundary layer flows over a permeable stretching plate, *Int. J. Non-Linear Mech.* 42 (2007) 819.

- [102] S.J. Liao, Notes on the homotopy analysis method: Some definitions and theorems, *Commun. Nonlinear. Sci. Numer. Simulat.* 14 (2009) 983.
- [103] S.J. Liao, A general approach to get series solution of non-similarity boundary layer flows, *Commun. Nonlinear Sci Numer. Simulat.* 14 (2009) 2144.
- [104] J. Cheng, S. J. Liao, R. N. Mohapatra and K. Vajravelu, Series solutions of nano boundary layer flows by means of homotopy analysis Method, *J. Math. Anal. Appl.* 343 (2008) 233.
- [105] I. Hashim, O. Abdulaziz and S. Momani, The homotopy analysis method for Cauchy reaction–diffusion problems, *Phy. Lett. A*, 372 (2008) 613.
- [106] S. Abbasbandy, Soliton solutions for the 5th-order KdV equation with the homotopy analysis method, *Nonlinear Dyn.* 51 (2008) 83.
- [107] S. Abbasbandy, Homotopy analysis method for generalized Benjamin- Bona-Mahony equation, *ZAMP* 59 (2008) 51.
- [108] S. Abbasbandy, Solitary wave solutions to the Kuramoto–Sivashinsky by means of homotopy analysis method, *Nonlinear Dyn.* 52 (2008) 35.
- [109] S. Nadeem, S. Abbasbandy and M. Hussain, Series solutions of boundary layer flow of a micropolar fluid near the stagnation point towards a shrinking sheet, *Z. Naturforsch.* 64, (2009) 575.
- [110] S. Abbasbandy, Solitary wave solutions to the modified form of Camassa–Holm equation by means of the homotopy analysis method, *Chaos, Solitons and Fractals.* 39 (2009) 428.
- [111] S. Abbasbandy and E. Shivanian, Prediction of multiplicity of solutions of nonlinear boundary value problems: Novel application of homotopy analysis method, *Comm. Non-linear Sci. Num. Simul.* 15 (2010) 3830.

- [112] S. Abbasbandy and T. Hayat, Solution of the MHD Falkner-Skan flow by homotopy analysis method, *Comm. Nonlinear Sci. Num. Simulat.* 14 (2009) 3591.
- [113] A. S. Bataineh, M.S.M. Noorani and I. Hashim. The homotopy analysis method for Cauchy reaction–diffusion problems, *Phys. Lett. A* 372 (2008) 613.
- [114] A. S. Bataineh, M.S.M. Noorani and I. Hashim, Solutions of time-dependent Emden–Fowler type equations by homotopy analysis method, *Phy. Lett. A.* 371 (2007) 72.
- [115] A. S. Bataineh, M.S.M. Noorani and I. Hashim. Modified homotopy analysis method for solving systems of second-order BVPs. *Commun. Nonlinear. Sci. Numer. Simulat.* 14. (2009) 430.
- [116] I. Hashim, O. Abdulaziz and S. Momani, Homotopy analysis method for fractional IVPs, *Comm. Nonlinear Sci. Num. Simu.* 14 (2009) 674.
- [117] M. Ayub, A. Rasheed and T. Hayat, Exact flow of a third grade fluid past a porous plate using homotopy analysis method, *Int. J. Engg. Sci.* 41 (2003) 2091.
- [118] T. Hayat and M. Khan, Homotopy solution for a generalized second grade fluid past a porous plate, *Non-Linear Dynamics.* 42 (2005) 395.
- [119] T. Hayat and Z. Abbas, Heat transfer analysis on MHD flow of a second grade fluid in a channel with porous medium, *Choas, Soliton, and Fractals* 38 (2008) 556.
- [120] T. Hayat and M. Awais, Three-dimensional flow of upper-convected Maxwell (UCM) fluid, *Int. J. Numer. Meth. Fluids* doi: 10.1002/fld.2289.
- [121] M. Sajid and T. Hayat, The application of homotopy analysis method for thin film flow of a third order fluid, *Chaos, Solitons and Fractal* 38 (2008) 506.
- [122] M. Sajid, T. Javed and T. Hayat, MHD rotating flow of a viscous fluid over a shrinking surface, *Non-Linear Dyn.* 51 (2008) 259.

- [123] T. Hayat, Z. Abbas, M. Sajid, Heat and mass transfer analysis on the flows of a second grade fluid in the presence of chemical reaction, *Phys. Lett. A* 372 (2008) 2400.
- [124] T. Hayat and M. Nawaz, Hall and ion-slip effects on three-dimensional flow of a second grade fluid, *Int. J. Numer. Meth. Fluids* doi: 10.1002/fld.225.
- [125] T. Hayat, K. Maqbool and S. Asghar, Hall and heat transfer effects on the steady flow of a Sisko fluid, *Z. Naturforsch* 64 (2009) 769.
- [126] M. Subhas Abel, N. Mahesha and J. Tawade, Heat and transfer in a liquid film over an unsteady stretching surface with viscous dissipation in the presence of external magnetic field, *Appl. Math. Model.* 33 (2009) 3430.
- [127] T. Hayat, H. Mambili-Mamboundou, E. Momoniat and F. M. Mahomed. The Rayleigh problem for a third grade electrically conducting fluid in a magnetic field, *J. Nonlinear Math. Phys.* 15 (2008) 77.
- [128] T. Hayat, E. Momoniat and F. M. Mahomed, Axial Couette flow of an electrically fluid in an annulus, *Int. J. Modern Phys. B* 22 (2008) 2489.
- [129] M. B. Abd-el-Malek, N. A. Bardan and H. S. Hassan, Solution of the Rayleigh problem for a power law non-Newtonian conducting fluid via group method, *Int. J. Eng. Sc.* 40 (2002) 1599.
- [130] C. W. Soh, Invariant solutions of the unidirectional flow of an electrically charged power-law non-Newtonian fluid over a flat plate in the presence of transverse magnetic field, *Commun. Nonlinear Sci. Numer. Simulat.* 10 (2005) 537.
- [131] A. Ishak, R. Nazar and I. Pop. The effects of transpiration on the flow and heat transfer over a moving permeable surface in a parallel stream. *Chem. Eng. J.* 148 (2009) 63.

- [132] S. K. Jena and M. N. Mathur, Similarity solutions for laminar free convection flow of a thermo-micropolar fluid past a nonisothermal flat plate, *Int. J. Eng. Sci.* 19 (1981) 1431.
- [133] G. S. Guram and A. C. Smith, Stagnation flows of micropolar fluids with strong and weak interactions, *Comput. Math. Appl.* 6 (1980) 213.
- [134] G. Ahmadi, Self-similar solution of incompressible micropolar boundary layer flow over a semi-infinite flat plate, *Int. J. Eng. Sci.* 14 (1976) 639.
- [135] J. Peddieson, An application of the micropolar fluid model to the calculation of turbulent shear flow, *Int. J. Eng. Sci.* 10 (1972) 23.
- [136] M. M. Ali, T. S. Chen, B. F. Armaly, Natural convection-radiation interaction in boundary layer flow over horizontal surfaces, *AIAA J.* 22 (1984) 1797.
- [137] A. Chamkha, A. Al-Mudhaf and I. Pop, Effect of heat generation or absorption on thermophoretic free convection boundary layer from a vertical flat plate embedded in a porous medium, *Int. Commun. Heat Mass Transfer* 33 (2006) 1096.
- [138] S. L. Goren, The role of thermophoresis in laminar flow of a viscous and incompressible fluid, *J. Colloid. Interf. Sci.* 61 (1977) 77.
- [139] A. J. Chamkha and I. Pop, Effects of thermophoresis particle deposition in free convection boundary layer from a vertical flat plate embedded in a porous medium, *Int. Commun. Heat Mass Transfer*, 31 (2004) 421.
- [140] M. S. Aslam, M. M. Rahman and M. A. Sattar, Effects of variable suction and thermophoresis on steady MHD combined free-forced convective heat and mass transfer flow over a semi-infinite permeable inclined plate in the presence of thermal radiation. *Int. J. Thermal. Sci.* 47 (2008) 758.